ISSN 2518-170X (Online),
ISSN 2224-5278 (Print)

ҚАЗАҚСТАН РЕСПУБЛИКАСЫ
ҰЛТТЫҚ ҒЫЛЫМ АКАДЕМИЯСЫНЫҢ
Satbayev University

Х А Б А Р Л А Р Ы

ИЗВЕСТИЯ

НАЦИОНАЛЬНОЙ АКАДЕМИИ НАУК
РЕСПУБЛИКИ КАЗАХСТАН
Satbayev University

N E W S

OF THE ACADEMY OF SCIENCES
OF THE REPUBLIC OF KAZAKHSTAN
Satbayev University

SERIES
OF GEOLOGY AND TECHNICAL SCIENCES

1 (445)

JANUARY – FEBRUARY 2021

THE JOURNAL WAS FOUNDED IN 1940

PUBLISHED 6 TIMES A YEAR

ALMATY, NAS RK

NAS RK is pleased to announce that News of NAS RK. Series of geology and technical sciences scientific journal has been accepted for indexing in the Emerging Sources Citation Index, a new edition of Web of Science. Content in this index is under consideration by Clarivate Analytics to be accepted in the Science Citation Index Expanded, the Social Sciences Citation Index, and the Arts & Humanities Citation Index. The quality and depth of content Web of Science offers to researchers, authors, publishers, and institutions sets it apart from other research databases. The inclusion of News of NAS RK. Series of geology and technical sciences in the Emerging Sources Citation Index demonstrates our dedication to providing the most relevant and influential content of geology and engineering sciences to our community.

Қазақстан Республикасы Ұлттық ғылым академиясы "ҚР ҰҒА Хабарлары. Геология және техникалық ғылымдар сериясы" ғылыми журналының Web of Science-тің жаңаланған нұсқасы Emerging Sources Citation Index-те индекстелуге қабылданғанын хабарлайды. Бұл индекстелу барысында Clarivate Analytics компаниясы журналды одан әрі the Science Citation Index Expanded, the Social Sciences Citation Index және the Arts & Humanities Citation Index-ке қабылдау мәселесін қарастыруда. Webof Science зерттеушілер, авторлар, баспашылар мен мекемелерге контент тереңдігі мен сапасын ұсынады. ҚР ҰҒА Хабарлары. Геология және техникалық ғылымдар сериясы Emerging Sources Citation Index-ке енуі біздің қоғамдастық үшін ең өзекті және беделді геология және техникалық ғылымдар бойынша контентке адалдығымызды білдіреді.

НАН РК сообщает, что научный журнал «Известия НАН РК. Серия геологии и технических наук» был принят для индексирования в Emerging Sources Citation Index, обновленной версии Web of Science. Содержание в этом индексировании находится в стадии рассмотрения компанией Clarivate Analytics для дальнейшего принятия журнала в the Science Citation Index Expanded, the Social Sciences Citation Index и the Arts & Humanities Citation Index. Web of Science предлагает качество и глубину контента для исследователей, авторов, издателей и учреждений. Включение Известия НАН РК. Серия геологии и технических наук в Emerging Sources Citation Index демонстрирует нашу приверженность к наиболее актуальному и влиятельному контенту по геологии и техническим наукам для нашего сообщества.

«ҚР ҰҒА Хабарлары. Геология және техникалық ғылымдар сериясы».

ISSN 2518-170X (Online),
ISSN 2224-5278 (Print)

Меншіктенуші: «Қазақстан Республикасының Ұлттық ғылым академиясы» РҚБ (Алматы қ.).

Қазақстан Республикасының Ақпарат және қоғамдық даму министрлігінің Ақпарат комитетінде 29.07.2020 ж. берілген **№ KZ39VPY00025420** мерзімдік басылым тіркеуіне қойылу туралы куәлік.

Тақырыптық бағыты: ***геология және техникалық ғылымдар бойынша мақалалар жариялау.***

Мерзімділігі: жылына 6 рет.
Тиражы: 300 дана.

Редакцияның мекенжайы: 050010, Алматы қ., Шевченко көш., 28, 219, 220 бөл.,
тел.: 272-13-19, 272-13-18,
http://www.geolog-technical.kz/index.php/en/

Типографияның мекенжайы: «NurNaz GRACE», Алматы қ., Рысқұлов көш., 103.

«Известия НАН РК. Серия геологии и технических наук».

ISSN 2518-170X (Online),
ISSN 2224-5278 (Print)

Собственник: Республиканское общественное объединение «Национальная академия наук Республики Казахстан (г. Алматы).

Свидетельство о постановке на учет периодического печатного издания в Комитете информации Министерства информации и общественного развития Республики Казахстан **№ KZ39VPY00025420**, выданное 29.07.2020 г.

Тематическая направленность: ***публикация статей по геологии и технических наукам.***

Периодичность: 6 раз в год.
Тираж: 300 экземпляров.

Адрес редакции: 050010, г. Алматы, ул. Шевченко, 28, ком. 219, 220, тел.: 272-13-19, 272-13-18,
http://www.geolog-technical.kz/index.php/en/

Адрес типографии: «NurNaz GRACE», г. Алматы, ул. Рыскулова, 103.

News of the National Academy of Sciences of the Republic of Kazakhstan. Series of geology and technology sciences.

ISSN 2518-170X (Online),
ISSN 2224-5278 (Print)

Owner: RPA "National Academy of Sciences of the Republic of Kazakhstan" (Almaty).

The certificate of registration of a periodical printed publication in the Committee of information of the Ministry of Information and Social Development of the Republic of Kazakhstan **No. KZ39VPY00025420**, issued 29.07.2020.

Thematic scope: ***publication of papers on geology and technical sciences.***

Periodicity: 6 times a year.
Circulation: 300 copies.

Editorial address: 28, Shevchenko str., of. 219, 220, Almaty, 050010, tel. 272-13-19, 272-13-18,
http://www.geolog-technical.kz/index.php/en/

Address of printing house: «NurNaz GRACE», 103, Ryskulov str, Almaty.

N E W S
OF THE NATIONAL ACADEMY OF SCIENCES OF THE REPUBLIC OF KAZAKHSTAN
SERIES OF GEOLOGY AND TECHNICAL SCIENCES
ISSN 2224-5278
Volume 1, Number 445 (2021), 6 – 12 **https://doi.org/10.32014/2021.2518-170X.1**

UDC 621.396.93:614.8
IRSTI 47.09.53

Zh. S. Abdimuratov[1], Zh. D. Manbetova[1], M. N. Imankul[2], K. S. Chezhimbayeva[1], D. A. Davronbekov[4]

[1]Almaty University of Energy and Communications named after Gumarbek Daukeev, Almaty, Kazakhstan;
[2]Eurasian National University named after L.N.Gumilyov, Nur-Sultan, Kazakhstan;
[3]Tashkent University of Information Technologies named after Muhammad Al-Khwarizmi, Tashkent, Uzbekistan
E-mail: zh.abdymuratov@aues.kz, zmanbetova@inbox.ru, mimankul57@gmail.com, katipa67@yandex.ru, d.davronbekov@tuit.uz

ABSORBERS OF ELECTROMAGNETIC RADIATION BASED ON SHUNGITE SPECIES

Abstract. In recent decades, the industries have experienced rapid development of various technologies directly or indirectly related to the emission of electromagnetic energy into the environment. The number of emitting technical means in production and in everyday life is increasing. At present, there are different ways, methods and materials to reduce the effects of electromagnetic radiation.

The properties of absorbers of electromagnetic radiation (EMR), formed on the basis of domestic natural material of shungite species from the deposit of the mining company "Koksu", Almaty region, are considered. The results of the interaction of EMR with samples of materials of absorbers and the dependence of the transmission coefficients on the angle of incidence of electromagnetic waves (EMW) in the frequency range 5.3-10.6 GHz are obtained. Research in these frequency ranges is crucial and relevant with the development and transition in the future of systems and mobile cellular networks of promising generations to higher radio frequency ranges. The use of powdered shungite for the creation of EMR absorbers in ultra-high-frequency radiation (UHFR) range has not yet been studied enough.

Technological values of the selected EMR absorbers in comparison with other geomaterials: strength of stone-like shungite species, high indicators of density (for example, 2.61 g/cm^3 – "TS" brand; 2.49 g/cm^3 – "TK" brand) and mechanical resistance, high thermal and chemical stability, low cost, good mixing with binders. The test samples provide a decrease of EMR level due to the presence of absorption effects.

Key words: ultra-high frequency, electromagnetic radiation, absorber of electromagnetic radiation, shungite, reflection and transmission coefficients.

Introduction. Human exposure to anthropogenic EMF has increased to unprecedented levels, accompanied by an increase in various health problems. The proliferation of cellular antennas and other RF-generating devices in recent decades has led to increasing concern about potential consequences of EMR exposure to human health [1].

The solution to these problems can be found by weakening the level of EMR generated by electronic equipment by using EMR absorbers. Today, various materials and methods are applied to protect against EMR [2-4].

An important task to be solved by this work was to study the absorption properties of domestic species of shungite of two brands - finely dispersed carbonate taurite "TK-D" and shale finely dispersed taurite "TS-D" in order to establish the most efficient EMR absorbers of this class.

The main processes that lead to the weakening of EMW in EMR absorbers are reflection, absorption and multiple re-reflection of EMW from the interfaces of dissimilar media inside multilayer structures. Moreover, in most cases, it becomes necessary to reduce the value of the reflection coefficient, which is

implemented by such constructive solutions as multilayer structures, which can be a geometrically inhomogeneous structure with a gradient change in properties along the depth of the structure. The optimal version of the performance of wide-range EMR absorbers with reduced weight and size characteristics, not subject to corrosion, are structures based on carbon-containing fillers such as finely dispersed powdered shungite, fixed in a binder.

Shungite is a mineral of complex chemical composition with a carbon-silicate base represented by graphite-like globular carbon and silicon oxide, mainly in the form of quartz. Components such as silicon oxide and carbon usually have the largest share in the chemical composition of shungite. Other components of the mineral under consideration are oxides of aluminum, iron, titanium and some other elements, etc.

The trademarks of the Koksu shungite species "Taurit" are obtained by crushing and dry grinding operations that comply with the current regulatory requirements of the Kazakh company “GRK Koksu” LLP (ST 60-1907-23-TOO-001-2014). [5] When creating EMR absorbers in UHFR range, it is possible to use carbon-containing minerals shungite, the technological advantages of which are their low cost, chemical and thermal stability, good miscibility with binders, for which we used a silicone sealant.

The properties of shungite species are determined by two factors: properties of shungite carbon; the structure of the species and the relationship of carbon and silicates [5]. The complete chemical composition of two types of shungite from the Koksu deposit with the trademarks fine-dispersed carbonate taurite “TK-D” and fine-dispersed shale taurite “TS-D” are given in table 1 and table 2 respectively. Note that “TS-D” and “TK- D" represent a fine powder or granules from dark gray to black.

Table 1 – Chemical composition of fine- dispersed carbonate taurite "TK-D"

Determined components	C	SiO_2	CaO	MgO	Fe_2O_3	Al_2O_3	TiO_2	K_2O	Na_2O
Content of components in %	7.0-15.0	30,0-55,0	9,36	1,44	4,83	9,41	0,89	2,19	0,40

Table 2 – Chemical composition of fine-dispersed shale taurite “TS-D”

Determined components	C	SiO_2	CaO	MgO	Fe_2O_3	Al_2O_3	TiO_2
Content of components in %	4,0-8,0	72,0-85,0	0,35	0,67	3,67	12,8	0,78
Determined components	K_2O	Na_2O	MnO	P_2O_5	Co	Zn	Cu
Content %	2,0	0,25	0,014	<0,01	0,0025	0,006	0,001

Experimental part. Samples of materials based on shungite species, prepared for the experiment, were plates with a thickness of 3 mm and a size of 30*30 cm. The samples were sealed using a polymer film.

The experiment was carried out in November 2019 in the "Antenna-feeder devices" laboratory of the "Radio and mobile communications" department of Tashkent University of Information Technologies named after Mohammed Al-Khorezmi (Tashkent, Republic of Uzbekistan). An experimental setup was used, designed to study the phenomena of reflection and refraction of electromagnetic waves at the interfaces between media with different physical characteristics and reflection coefficient modules measurements as well as transmission of electromagnetic waves in the frequency range 5.3 ... 10.6 GHz.

The installation consists of a transmitting part, a receiving part, and a support on which plates based on shungite species are fixed (figure 1). The investigated shungite-based plate imitates the interface between two media.

The transmitting part of the antenna contains a UHFR generator (1) and a horn antenna (2) at a distance of 7-10 wavelengths from the horn antenna. Thus, a plane electromagnetic wave creates in a limited area of space. Falling at an angle φ onto the plate (7), depending on the material of the shungite plate and the type of polarization, the wave can:

a) be completely reflected;

b) partially pass through the plate and partially be reflected;

c) completely pass through the plate.

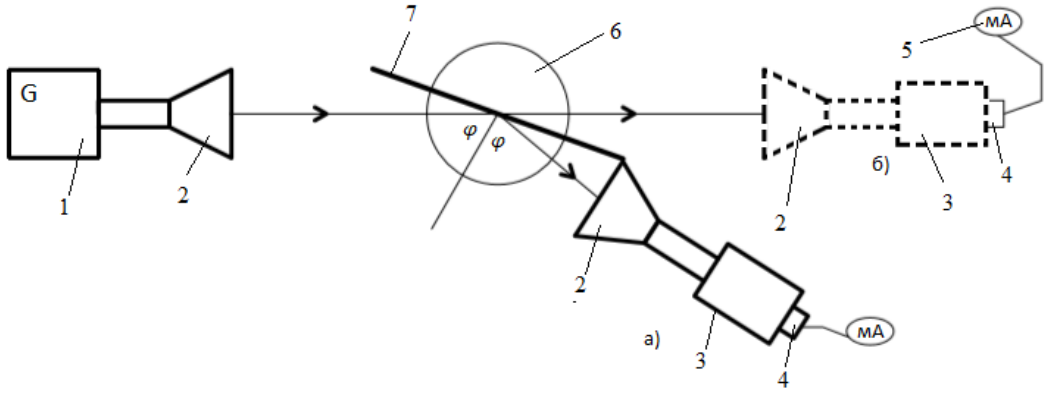

Figure 1 – Structural diagram of the measuring setup (1 - generator of UHFR range, 2 - horn antenna, 3 - variable attenuator, 4 - detector section, 5 - indicator device (microammeter), 6 - angle scale, 7 - investigated plate)

The receiving part consists of a horn antenna (2), a variable attenuator (3), a detector section (4) and a dial indicator (5). The variable attenuator is used to adjust the power supplied to the detector section from the horn antenna. The use of an attenuator allows avoiding the influence of the nonlinear characteristics of the detector on the measurement results.

The diode located in the detector section of UHFR rectifies the high frequency current. After rectification, the diode current is supplied to a DC microammeter (5). The receiving part of the installation is fixed on the platform that can move around a circle centered at point 0 (figure 1) and, consequently, can register both reflected (position a) and transmitted (position b) waves.

With direct connection of horn antennas (2) to the waveguide from the generator and the attenuator (3) in this installation, normal (relative to the plane of incidence of the wave) polarization is obtained. To obtain parallel polarization, the connection of horn antennas must be done through waveguide strands.

For experimental determination of the modules reflection coefficient and the transmission coefficient, an indirect method is applied by using a variable attenuator, graduated in decibels.

Reflection coefficient R – the ratio of the complex amplitudes of the electric field strengths of the reflected wave $\bar{E}^-$ and the incident wave $\bar{E}°$, i.e.

$$R = \bar{E}^-/\bar{E}°, \quad (1)$$

Transmission coefficient χ – the ratio of the complex amplitudes of the electric field strengths of the refraction of the wave $\bar{E}^-$ and the incident wave, $\bar{E}°$ i.e.

$$\chi = \bar{E}^-/\bar{E}°, \quad (2)$$

The reflection coefficient R and the *transmission coefficient* χ are generally complex quantities. Their modules characterize the ratio of the amplitudes of the corresponding waves, and the arguments characterize the phase shift between these fields at the interface.

Changing the weakening of the attenuator, achieving consistent microammeter readings, determine the ratio of the powers of the reflected and incident waves when determining the modulus of the reflection coefficient, and the ratio of the powers of the transmitted and incident waves when determining the modulus of the transmission coefficient.

When the receiving antenna is located in the field of the incident wave, the attenuation N_1 is introduced into the receiving path by the attenuator and the microammeter reading is recorded, which is about 5 μA. Then, by placing the antenna in the field of the reflected wave, the weakening of the attenuator is reduced to a value of N_2, at which the reading of the microammeter remains unchanged. The change in attenuation N_2-N_1 is equal to the ratio of the above powers, expressed in decibels. Since the power received by the antenna is proportional to the squares of the strengths of the corresponding electric fields, it can be written [6-7]:

$$N_2 - N_1 = 10lg\,|\bar{E}^-/\bar{E}°|^2 = 20lg\,|\bar{E}^-/\bar{E}°|, \quad (3)$$

where $\bar{E}°$ - vector of the electric field strength of the incident wave, perpendicular to the direction of propagation. $\bar{E}^-$ - vector of reflected wave. In general case, $\bar{E}°$ can be located in different ways relative to the plane of incidence and can always be represented as the sum of two mutually perpendicular vectors, therefore it is sufficient to consider two cases: vector $\bar{E}°$ lies in the plane of incidence of the wave and wave $\bar{E}°$ is perpendicular to the plane of incidence of the wave.

Hence, the modulus of the reflection coefficient is [6-7]:

$$|R_{сл}| = 10^{(N_2-N_1)/20} \quad (4)$$

The determination of the value of the transmission coefficient is carried out in the same way, and the modulus of the transmission coefficient is calculated by the formula

$$|\chi_{сл}| = 10^{(N_3-N_1)/20} \quad (5)$$

Experiment results. The tables 3.1-3.3 show the results of an experimental study in the absence of a media interface (without a sample), and when using sample plates based on finely dispersed powdered shungite of two brands - "TK-D", "TS-D".

At an oblique incidence of a plane electromagnetic wave to the interface between two media, it is sufficient to consider only two cases - normal and parallel polarization. Set the normal polarization of the incident wave. In this case, the vector $\bar{E}$ of the emitted wave should be perpendicular to the plane of incidence of the wave and the base of the laboratory model.

Table 3.1 – Experimental results in the absence of a sample

Incident wave polarization - normal				
Angle of wave incidence φ	Attenuation value N_1	Attenuation value N_2	Transmission coefficient	Reflection coefficient module
angle	dB	dB	–	–
20°	26,75	25,3	0,846	0,16
30°	26,75	24,8	0,799	0,3
40 °	26,75	24,4	0,763	0,24
50°	26,75	22,6	0,620	0,38
60 °	26,75	19,8	0,449	0,56
70 °	26,75	3,8	0,171	0,929

Table 3.2 – The experimental results for a sample of a plate made of carbonate taurite "TK-D"

Incident wave polarization - normal				
Angle of wave incidence φ	Attenuation value N_1	Attenuation value N_2	Transmission coefficient	Reflection coefficient module
angle	dB	dB	–	–
20°	26,75	19	0,410	0,6
30°	26,75	17,8	0,357	0,65
40 °	26,75	15,8	0,283	0,72
50°	26,75	14,2	0,236	0,77
60 °	26,75	9,3	0,134	0,87
70 °	26,75	4,5	0,077	0,923

Table 3.3 – The experimental results for a plate sample made of shale taurite "TS-D"

Incident wave polarization - normal				
Angle of wave incidence φ	Angle of wave incidence φ	Angle of wave incidence φ	Angle of wave incidence φ	Angle of wave incidence φ
angle	dB	dB	–	–
20°	26,75	21	0,516	0,49
30°	26,75	19,4	0,429	0,58
40 °	26,75	18	0,365	0,64
50°	26,75	14,7	0,250	0,76
60 °	26,75	11,5	0,173	0,83
70 °	26,75	5,3	0,085	0,92

As it can be seen from tables 3.2-3.3, the studied composites based on shungite species, namely shale taurite and carbonate taurite, can reduce the EMR level by an average of almost 2 times. Thus, a significant decrease in the coefficient for two samples of shungite has been established in comparison with the experiment "Without sample". The most effective weakening of EMR seen by the sample of carbonate taurite compared to shale taurite. But also, the sample "shale taurite" can be effectively used to quench the EMR level. The studies performed allow us to conclude that a composite material based on domestic shungite species has the ability to significantly attenuate electromagnetic waves in the UHFR range (figure 2).

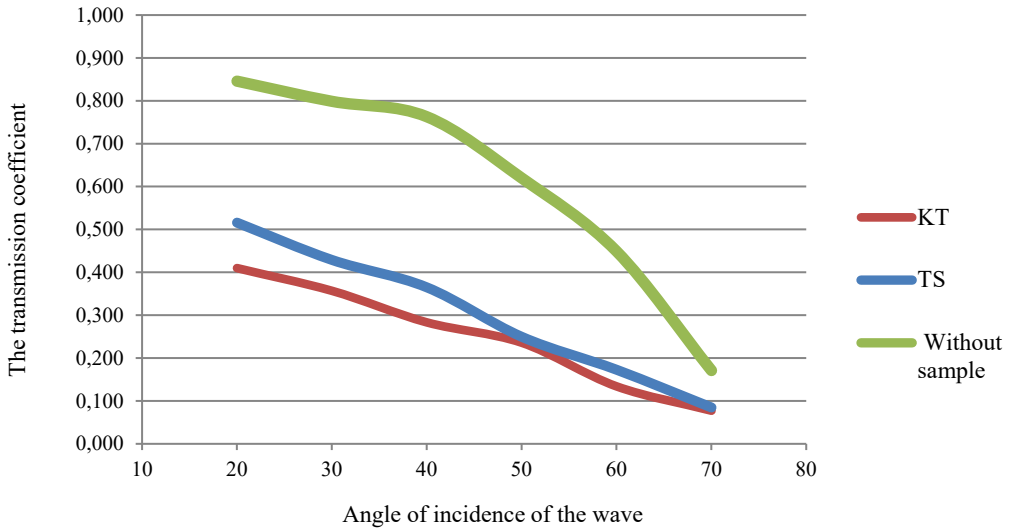

Figure 2 – Dependence of the transmission coefficient on the angle of incidence of the wave CT - carbonate taurite "TK-D"; ST - shale taurite "TS-D

Conclusion.

1. Composites based on shungite are able to withstand EMR attenuation in UHFR range.

2. A comparative analysis of the test samples has been carried out. The maximum attenuation is provided by a sample based on "TK-D" carbonate taurite. In the entire measured range, a change in the absorption coefficient is observed depending on the angle of incidence of electromagnetic waves on the examined object. The greater the degree of incidence, the lower the wave transmission coefficient. Experimental studies have shown that the level of negative radiation / effects of electromagnetic fields (EMF) when using materials based on shungite decreases, but is not completely neutralized. However, the obtained result can be considered effective, since when using plates based on shungite species, the level of EMR is significantly reduced, which negatively affects a person.

3. Taking into account the characteristics of taurite shungite species in UHFR range and the ability of these materials, separately or as part of composites, to weaken the EMR at UHFR, it is possible to create domestic wide-range EMR absorbers with controllable characteristics (for example, by selecting the type and concentration of the filler, binder, the order of alternation of layers with different electrical conductivities, and etc.), with predetermined values of the transmission and reflection coefficients.

Ж. С. Абдимуратов[1], Ж. Д. Манбетова[1], М. Н. Иманкул[2], К. С. Чежимбаева[1], Д. А. Давронбеков[3]

[1]Ғ.Дәукеев атындағы Алматы энергетика және байланыс университеті, Алматы, Қазақстан;
[2]Л.Н. Гумилев атындағы Еуразия ұлттық университеті, Нұр-Сұлтан, Қазақстан;
[3]М. Әл-Хорезми атындағы Ташкент ақпараттық технологиялар университеті, Ташкент, Өзбекстан

ШУНГИТ ТЕГІНЕ НЕГІЗДЕЛГЕН ЭЛЕКТРМАГНИТТІ СӘУЛЕЛЕНУ ЖҰТҚЫШТАРЫ

Аннотация. Соңғы онжылдықтарда салалар қоршаған ортаға электромагниттік энергия шығарумен тікелей немесе жанама байланысты әртүрлі технологиялардың қарқынды дамуын бастан кешіруде. Өндірісте және күнделікті өмірде эмиссиялық техникалық құралдардың саны артып келеді. Қазіргі уақытта электромагниттік сәулеленудің әсерін төмендетудің әртүрлі әдістері, әдістері мен материалдары бар.

Алматы облысы «Көксу» тау-кен компаниясының кен орындарынан алынған табиғи отандық шунгиттекті материал негізінде құрастырылған электрмагнитті сәулеленуді жұтқыш қасиеттерін қарастырамыз. ЭМӨ-нің сіңіргіш материалдар үлгілерімен өзара әрекеттесу нәтижелері және өткізу коэффициенттерінің 5,3-10,6 ГГц жиілік диапазонындағы электромагниттік толқындардың (ЭМҮ) құлау бұрышына тәуелділігі алынды. Жиіктің бұл дипазонында зерттеу өте маңызды және өзекті, өйткені келесі сатыдағы мобильді ұялы байланыс жүйелері мен желілері дамып, болашақта жоғары жиіліктік диапазондарға ауысуына байланысты болады. Ұнтақты шунгитті аса жоғары жиілік диапазонында электрмагнитті сәулеленудің жұтқыштары ретінде пайдалану жолдары әлі толық зерттелмеген.

Басқа геоматериалдармен салыстырғанда таңдалған электрмагнитті сәулелену жұтқыштарының технологиялық артықшылықтары мынадай: тас тәрізді шунгит тегінің беріктігі, жоғары тығыздық көрсеткіштері (мысалы, 2,61 г/ см^3 – марка «ТС» маркасына; 2,49 г/см^3 – «ТК» маркасына) және механикалық төзімділігі, жоғары термиялық және химиялық тұрақтылығы, бағасының арзан болуы, байланыстырғыштармен жақсы араласуы. Зерттелетін үлгілер жұту эффектінің болуына қарай электрмагнитті сәулелену деңгейінің төмендеуін қамтамасыз етеді.

Түйін сөздер: аса жоғары жиілік, электр магниттік сәулелену, электрмагнитті сәулеленуді жұтқыштар, шунгит, шағылысу және өту коэффициенттері.

Ж. С. Абдимуратов[1], Ж. Д. Манбетова[1], М. Н. Иманкул[2], К. С. Чежимбаева[1], Д. А. Давронбеков[3]

[1]Алматинский университет энергетики и связи им. Гумарбека Даукеева, Алматы, Казахстан;
[2]Евразийский национальный университет им. Л. Н.Гумилёва, Нур-Султан, Казахстан;
[3]Ташкентский университет информационных технологий им. М. Аль-Хоразмий, Ташкент,Узбекистан

ПОГЛОТИТЕЛИ ЭЛЕКТРОМАГНИТНОГО ИЗЛУЧЕНИЯ НА ОСНОВЕ ШУНГИТОВЫХ ПОРОД

Аннотация. В последние десятилетия отрасли промышленности переживают бурное развитие различных технологий, прямо или косвенно связанных с излучением электромагнитной энергии в окружающую среду. Увеличивается количество эмиссионных технических средств в производстве и в быту. В настоящее время существуют различные способы, методы и материалы для снижения воздействия электромагнитного излучения.

Рассмотрены свойства поглотителей электромагнитного излучения (ЭМИ), сформированных на основе отечественного природного материала шунгитовых пород месторождения горнорудной компании "Коксу" Алматинской области. Получены результаты взаимодействия ЭМИ с образцами материалов поглотителей и зависимость коэффициентов пропускания от угла падения электромагнитных волн (ЭМВ) в диапазоне частот 5,3-10,6 ГГц. Исследования в этих частотных диапазонах имеют решающее значение и актуальны при

разработке и переходе в будущем систем и мобильных сотовых сетей перспективных поколений на более высокие радиочастотные диапазоны. Применение порошкообразного шунгита для создания поглотителей ЭМИ в диапазоне сверхвысокочастотного излучения (УВЧ) до сих пор изучено недостаточно.

Технологические значения выбранных поглотителей ЭМИ по сравнению с другими геоматериалами: прочность камнеподобных пород шунгита, высокие показатели плотности (например, 2,61 г / см3 – марка “ТС"; 2,49 г / см3 – марка “ТК”) и механической стойкости, высокая термическая и химическая стабильность, низкая стоимость, хорошее смешивание со связующими. Исследуемые образцы обеспечивают снижение уровня ЭМИ за счет наличия эффектов поглощения.

Ключевые слова: сверхвысокая частота, электромагнитные излучения, поглотитель электромагнитных излучений, шунгит, коэффициенты отражения и прохождения.

Information about authors:

Abdimuratov Zhubanyshbay, candidate of technical sciences, associate professor, Almaty University of Energy and Communications named after Gumarbek Daukeev, Almaty, Kazakhstan; zh.abdymuratov@aues.kz; https://orcid.org/0000-0003-3403-456X

Manbetova Zhanat, PhD student, Almaty University of Energy and Communications named after Gumarbek Daukeev, Almaty, Kazakhstan; zmanbetova@inbox.ru; https://orcid.org/0000-0002-6716-4646

Imankul Manat, candidate of technical sciences, associate professor, Eurasian National University named after L.N. Gumilyov, Nur-Sultan, Kazakhstan; mimankul57@gmail.com; https://orcid.org/0000-0002-7123-1100

Chezhimbayeva Katipa, candidate of technical sciences, associate professor, Almaty University of Energy and Communications named after Gumarbek Daukeev, Almaty, Kazakhstan; Katipa67@yandex.ru; https://orcid.org/0000-0002-1039-1629

Davronbekov Dilmurod, PhD, associate professor, Tashkent University of Information Technologies named after Muhammad Al-Khwarizmi, Tashkent, Uzbekistan; d.davronbekov@tuit.uz; https://orcid.org/0000-0003-1193-7918

REFERENCES

[1] Vornoli A., Falcioni L., Mandrioli D., Bua L., Belpoggi F. The contribution of in vivo mammalian studies to the knowledge of adverse effects of radiofrequency radiation on human health // International Journal of Environmental Research and Public Health. September 2019.

[2] Krishtopova E.A., Lynkov L.M., Borbotko T.V. // Report. BGUIR. 2007. N 6. P. 3-7.

[3] Chung D.D. // Journal of Materials Engineering and Performance. 2000. N 9 (3). P. 350-354.

[4] Kozlovski V.V., Sofienko I.I. // Visnik ДУІКТ. 2009. 7(3). P. 233-246.

[5] Production. http://koksu.kz/produktsiya

[6] Volman V.I., Pimenov Yu.V, Technical electrodynamics. M.: Connection, 1971.

[7] Falkovski O.I. Technical electrodynamics. M.: Connection, 1978.

N E W S
OF THE NATIONAL ACADEMY OF SCIENCES OF THE REPUBLIC OF KAZAKHSTAN
SERIES OF GEOLOGY AND TECHNICAL SCIENCES
ISSN 2224-5278
Volume 1, Number 445 (2021), 13 – 21 **https://doi.org/10.32014/2021.2518-170X.2**

UDC 550.8.02
IRSTI 37.01.77

F. N. Abdoldina[1], A. B. Nazirova[1,2], Y. I. Dubovenko[3], G. K. Umirova[2]

[1]International IT University, Almaty, Kazakhstan;
[2]Satbayev University, Almaty, Kazakhstan;
[3]Institute of Geophysics NAS of Ukraine, Kiev, Ukraine.
E-mail: farida_mail@mail.ru, asem_berlibaeva@mail.ru, yuriiguy@gmail.com, gulmuha@mail.ru

SOLUTION OF THE GRAVITY EXPLORATION DIRECT PROBLEM BY THE SIMULATED ANNEALING METHOD FOR DATA INTERPRETATION OF GRAVITY MONITORING OF THE SUBSOIL CONDITIONS

Abstract. The long-term development of hydrocarbon reservoirs (HCR) in the geological environment, complex deformation processes occur. Gravity monitoring is carried out to evaluate the possible geodynamic risk and negative consequences from HCR. As a result, the interrelationships of the continuously changing field-geological situation (changes in production volumes, changes in reservoir pressure, processes of fluid injection into productive formations) are investigated. The main tool for solving the gravity inversion when determining areas of increased industrial hazard is the solution of the gravity direct problem. In these studies, proceeding from a given initial approximation of the environment, the problem is realized through successive approximations. To assess such distributions, the authors of the article recommend using the simulated annealing technique within the framework of stochastic optimization. It is aimed at fitting the optimal parameters of the medium provided that a minimal residual of the gravity field values occurs.

The approach is implemented using three simple mathematical models of the geological medium such as horizontal prism, homogeneous sphere, and vertical ledge. This technique allows fitting the media values simultaneously by a pair of its parameters. The operation of the algorithm is described and the simulation results are provided. The results showed acceptable accuracy of the algorithm for solving the direct gravity problem by the proposed method. The simulated annealing technique made it possible to increase the reliability of the HCR model while reduce the time for the analysis of the gravity field.

Key words: gravity direct problem, simulated annealing approach, gravity variations, gravity monitoring, hydrocarbon field.

1. Introduction. Complex geodynamic processes of a natural and technogenic nature always accompany the *forced deriving* of matter in the hydrocarbon reservoirs (HCR) in *natural mode*. These processes are especially acute in the HCR located within active faults. The reason for their activation may be *local* changes in the tectonic environment and the *geotechnical* effects (variations in reservoir pressure). They, in turn, are a consequence of the high modern tectonic activity of faults and the rock breaking disruptions [1]. Besides the local tectonic geodynamic phenomena (developed in various forms) geodynamic events of technogenic genesis during the exploitation of the HCRs are known in many oil and gas bearing basins such as seismic movements, abnormal subsidence of the ground surface, horizontal shifts of rock masses, and formation of the surface cracks. In this regard, the relevance of obtaining prompt and reliable information about the geodynamic state of the developed HCRs is indisputable.

An evaluation of the potential geodynamic risk and the possible negative consequences of a prolonged exploitation of HCRs is impossible without comprehensive geodynamic monitoring of the HCR [2], including the study of reservoir pressure dynamics. An optimal in accuracy and speed preset of

methods for evaluation the geodynamic processes combines strain monitoring (levelling, satellite interferometry, InSAR) with gravimetry. The latter method, as an inexpensive, fast and effective method of geophysics, has been successfully used in field development process when assessing the effect of fluid replacement in productive formations, studying reservoir compaction and zones of faults activation, identifying areas of increased industrial and geodynamic hazard, etc. [3]. Work [4] presents an example of a comprehensive assessment of geodynamic processes occurring during the development of HCR based on leveling and satellite observations.

For the successful solution the problems of geodynamic monitoring of the subsoil conditions by gravity measurements, a convenient data processing service (including the filtration, calculation and introduction of the necessary gravity corrections and reductions) as well as the interpretation unit for the calculated gravity variations are required. The main role in this service is assigned to solving the direct problems of gravimetry for various model assumptions on the structure of the studied geological medium [5-7]. Such a solution is the result of successive approximations, based on a pregiven initial approximation of the medium.

The logic of the serial computation algorithm for the direct gravimetry problem solution is simple: we select a certain set of *elementary* approximating bodies with a *simple* given geometry inside a *homogeneous* layered medium. Then we assume that these bodies are contained in a confined layer, which contains the *sources* of the studied gravity anomalies. The direct problem is solved by fitting the optimal parameters to obtain the minimal residual between the measured and calculated gravity values [8].

Traditional methods for solving the direct problems of gravimetry [6] do not meet the requirements for use them in singular conditions. In conditions of singularity, speed of decision making in conditions of confined initial data is crucial. Because of it, factor analysis is no longer effective due to a lack of time and the data. Heuristic models may provide a temporary solution, but we must to review them constantly while new information. Moreover, when you do not have enough basic data to build a hypothesis, and you have to correct them more and more, Bayesian methods are most effective, but with an eye to using machine learning (ML) for quick pattern recognition.

Among probabilistic methods, the so-called genetic algorithms, including the generative adversarial optimization techniques, meet the above criteria. In [8], it was shown that among the set of the genetic algorithms, *the simulated annealing approach* is the most acceptable for our purposes.

The purpose of the study is to demonstrate, using a number of simple mathematical models of the geological medium, the viability of the simulated annealing approach for the *stable* solution of the gravity direct problems.

2. Data acquisition. The realization of the geodynamic monitoring (GDM) of the state of bowels of the Earth in oil and gas fields is an obligatory measure at the development of HCRs. One cycle of measurements per year is enough to accumulate the data, based on which we can determine the presence of deformations in the bowels of a developed HCR [2]. During the gradual extraction of oil, it is replaced by water, which entails a change in the *total density* of the reservoir rocks. This results in the negative dynamics of gravity anomalies, which are recorded by high-precision *gravity monitoring* of the HCR. Its data allows us to prevent quickly the adverse processes in the HCR, providing the subsoil user with the significant retrenchment of supply and costs.

A special GIS GeoM was created [9,10] for storage and processing of the gravity monitoring data. PostgreSQL DBMS, PostGIS, GeoServer were used as free software to create GIS. GIS allows us to import the source files of records from gravimeters, to convert them, to filter the data, to make the necessary corrections, to extract the statistical information, to do the samplings and summary matrices, to average the data and to perform other linear transformations on them. The paper [10] describes the functional modelling of the main business processes for doing gravity monitoring at this HCR, and the implementation of the general subsystems of the mentioned GIS.

Figure 1 shows the DFD model of the “Solving the direct problem of gravity by simulating annealing method” business process. The process consists of the following sub-processes:

- selection of a mathematical model;
- selection of the starting point of the objective function f (x0);
- calculation of a new objective function f (x ');
- generation of a random number α;

– set E = E';
– calculation of the probability function;
– checking the stopping criterion;
– obtaining the minimal of the gravitational gravity field values.

To perform these processes, you need: processed data of gravimetric measurements, geological and lithological characteristics. At the output, we obtain the calculated value of the gravitational field of the gravity force, the minimum residual, the time of the calculation, the number of performed iterations, the optimal values of the sought parameters.

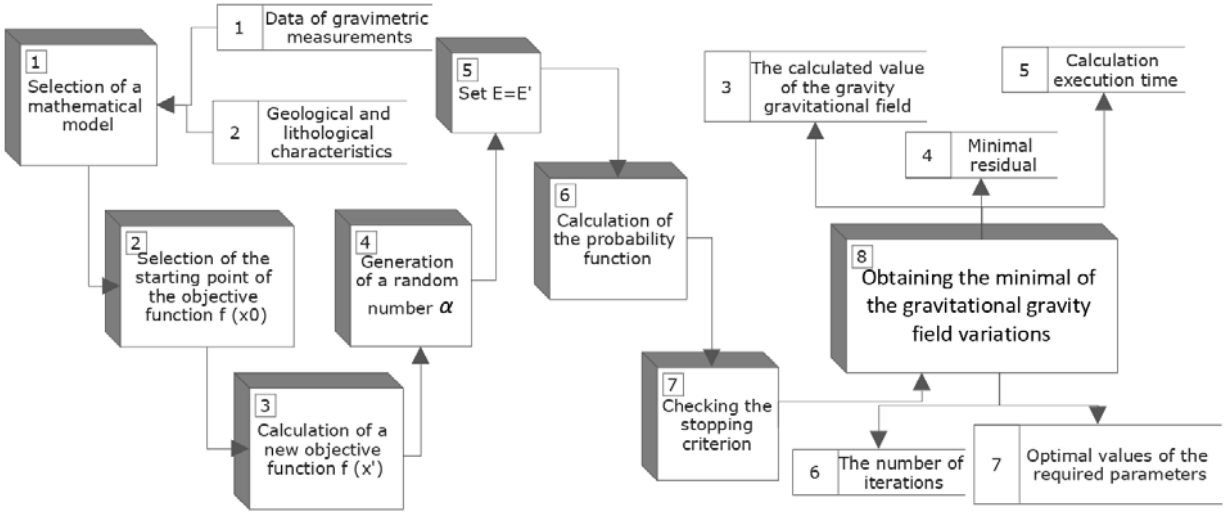

Figure 1 – DFD-model of the "Solving the direct problem of gravity by simulating annealing method" business process

The computational algorithm of this module is realized based on one of the modifications of the simulated annealing technique. Its primary testing on synthetic models was carried out earlier in [11]. In this case, it is necessary to verify the viability of the technique on real field data. For this purpose, the gravity observations made by one of the companies of the Republic of Kazakhstan, which has been engaged in this kind of research for a long time, is involved. The initial data are the digital records of the measurement of gravity variations within the gas-oil field, which is located within the Kzylkoginsky district of the Atyrau region of the Republic of Kazakhstan (it starts operation in 1995).

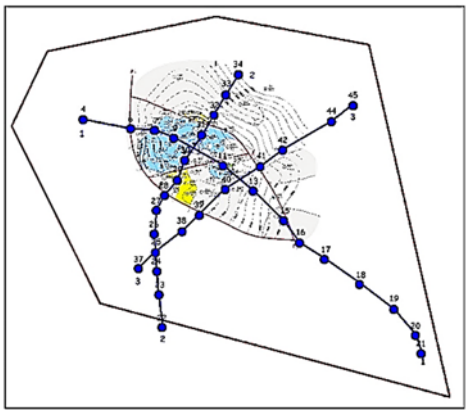

Figure 2 – The layout of points and profiles in the M reservoir

The gravity measurements at the M field are distributed through the long, almost linear profiles that intersect the general structural and tectonic features of the HCR: the arch part, faults, and boreholes pass in close proximity to the geological sections. The observation system with three profiles and 35 measurement points covers the entire territory of the field and the adjacent areas (see figure 2). The

profile 1-1 with a length of about 8000 m consists of 14 points, while the profile 2-2 with a length of 1500 m consists of 13 measurement points, and the profile 3-3 that has a length of 3500 m consists of 8 measurement points; the approximate step along the profile is 100 m. At each gravimetric point, several measurements were made with two gravimeters simultaneously, and then the data were averaged to increase the accuracy and the stability of the observations.

The preliminary processing of the data from the catalog (with spatio-temporal reference) included the filtering, averaging, and the calculation of root mean square errors. The correction for the intermediate layer (a Bouguer correction) was calculated by the formula $\delta g_B = -0.0418\sigma_c h$, where σ_c is the average density of the rocks of the intermediate layer (g/cm^3); h is the height of the observation point above the surface of the geoid (m). The obtained Bouguer anomaly Δg_B is the difference between the observed and synthetic gravity field: $\Delta g_B = g_{obs} - \gamma_0 + 0.3086h + \delta g_B$, where g_{obs} is the observed field, γ_0 is the normal value of the acceleration of gravity. The normal gravity was calculated for each profile point according to the formula $\gamma_0 = g_e \cdot (1 + 0.005302 \cdot \sin 2\phi - 0.000007 \cdot \sin^2 2\phi)$, where g_e is the average value of the normal acceleration of gravity at the equator of the Earth, and ϕ is the latitude of the observation point. In calculating the Bouguer anomalies, we took the average density of rocks of the intermediate layer in the core research area of ~ 2.65 g/cm^3.

3. Methods and models. Taking into account *a priori* geological information about the site structure for each specific profile, we solve the direct problem of gravimetry with the least-squares fitting approach for each profile. We solve the problem for various models of the geological medium containing the sources of gravity anomalies in a certain horizontal layer. We chose the fast simulated annealing approach [12,13] as the main solution technique while a compared algorithm is a solution of the gravity direct problem for the Poisson equation by the finite differences technique. To discretize the equation, we chose a "cross-like" difference scheme [14]. Besides, we took the same initial data and a *priori* restrictions for both methods.

Therefore, we tested the simulated annealing algorithm on the example of solving the one-dimensional (by profile) gravity direct problem for three common classes of sources: a horizontal prism (see Section 3.1), a sphere (see Section 3.2), and a vertical ledge (see Section 3.3). A horizontally layered model with a linear change in density inside the anomalous layer is accepted as the initial model of the medium. Outside the layer, we assumed a uniform enclosing medium, which is described by a monotonic density distribution having a constant predefined value. Accordingly, one of three states describes the mathematical model of the studied layer containing the sources of anomalies: a set of horizontal prisms (with different horizontal lengths and densities); a set of spherical bodies (with different radius and depth of the centre of mass); a set of vertical ledges (with different depths and lengths of steps).

In this work the simulation was carried out through the fitting of the objective function, sequentially choosing the location, size, shape, and the density σ of anomalous bodies in the application for calculating the gravity anomalies. The simulation results are presented below.

3.1. Horizontal prism. A horizontal prism as an elementary approximating body within a layer is a special case of a rectangular parallelepiped. At its base lies a regular rectangle, therefore its numerical parameters (length, width, height) we set as the difference of the coordinates of the corresponding points in the Cartesian coordinate system. To calculate the gravity impact of a horizontal prism confined by the planes $x = \xi_1$, $x = \xi_2$, $z = \zeta_1$, $z = \zeta_2$, we use the following expression:

$$U_z(0,0) = G\sigma\left[\begin{array}{c}\xi_1 \ln\left(\frac{\xi_1^2+\zeta_2^2}{\xi_1^2+\zeta_1^2}\right) - \xi_2 \ln\left(\frac{\xi_2^2+\zeta_2^2}{\xi_2^2+\zeta_1^2}\right) + 2\zeta_2\left(\operatorname{arctg}\left(\frac{\xi_1}{\zeta_2}\right) - \operatorname{arctg}\left(\frac{\xi_2}{\zeta_2}\right)\right) \\ +2\zeta_1\left(\operatorname{arctg}\left(\frac{\xi_2}{\zeta_1}\right) - \operatorname{arctg}\left(\frac{\xi_1}{\zeta_1}\right)\right)\end{array}\right], \quad (1)$$

where G is the gravity constant and σ is the density of the body.

For computing in a horizontal prism, the following initial parameters are set: the depth of the upper ζ_1 and lower ζ_2 edges of the anomalous body and the value of the gravity field Δg. For free parameters, we treat the values of the beginning ξ_1 and the end ξ_2 of the profile, and the sought parameter is the optimal density value σ.

3.2. Sphere. The gravity effect from a homogeneous spherical body of radius R and volume V, with excess density $\Delta\sigma$ located at depth h (see Figure 3(b)), in a one-dimensional version is calculated by the formula:

$$g_s = \frac{G\Delta\sigma Vh}{R^3} = \mathrm{GM}\frac{h}{(x^2+h^2)^{3/2}} \quad (2)$$

where $M = \Delta\sigma V = \Delta\sigma\frac{4}{3}\pi R^3$ - is the effective mass of a homogeneous spherical body, G is the gravity constant, h is the depth of the body, x is the center of the spherical body, R is the radius, and σ is the density.

We suppose to be known and fixed a pair of body parameters (the center of the sphere x, radius R). For a free parameter, we treat the *average* depth h of the anomalous body. The sought medium parameter to be optimized through the iterative improvement is the density σ of the sphere. If necessary (weak convergence, unsuccessful initial approximation, large residual, etc.), we free the parameters x and R and repeat the iteration cycle again.

3.3. Vertical ledge. We define a vertical ledge as a body of semi-infinite strike, confined by a pair of horizontal planes and a rectangular vertical one (see Figure 3 (c)). Its gravity impact is derived as a special case of the effect for a rectangular parallelepiped. The analytical expression for finding the gravity field Δg_{led} at the point x (along the x axis at $z = 0$, $y = 0$) is as follows:

$$g_{\mathrm{led}}(x) = G\Delta\sigma\left[x\ln\frac{x^2+h_2^2}{x^2+h_1^2} + \pi(h_2 - h_1) + 2h_2\mathrm{arctg}\frac{x}{h_2} - 2\mathrm{arctg}\frac{x}{h_1}\right] \quad (3)$$

where G is the gravity constant, σ is the density, x is the coordinate of the vertical discharge, h_1 is the depth of the lower horizontal plane and h_2 is the depth of the upper horizontal plane.

For this model, the initial parameters of the algorithm are set as follows: the vertical fault x, the depth of the lower horizontal plane h_1, and the measured gravity value Δg. For a free parameter, we treat the depth of the upper horizontal plane h_2, and the sought one is the density σ of the ledge. However, as we did in other models if necessary, free and fixed parameters can be mutually interchanged.

4. Results and discussions. First of all, we suppose a general condition for all the models mentioned: due to the small number of measurements and the significant distance between the observation points, we assume that the value of gravity at each separate point is the consequence of the integral impact of a separate modeled source of anomalies. That is, gravity at each point is a consequence of the effect of some *material point*, in the center of which is concentrated all of its gravitating mass. Then the conditions of the Poincaré lemma on the sweeping masses to the boundary of a convex region of a harmonic function are valid. Considering this condition, we present the simulated annealing simulation results with known initial parameters of the medium.

4.1. Horizontal prism. The calculations were performed with a step along the profile of 100 m, and the properties of rocks and their depth were taken into account. The charts of gravity anomalies from the model are obtained in the form of a series of horizontal prisms along three profiles (see figure 3). For this model, a solution was found in 6905 iterations at $T = 1000°$ and a cooling rate of 0.001 m/s^2, with a

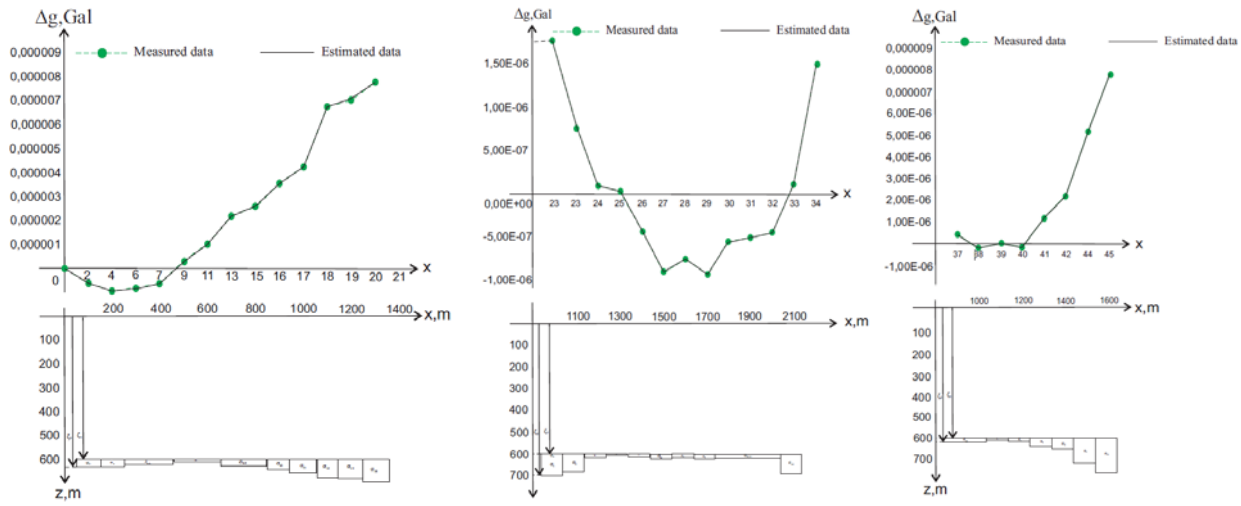

a) along the profile 1-1 b) along the profile 2-2 c) along the profile3-3

Figure 3 – Gravity anomaly from the model given as a series of horizontal prisms

relative error of 15% for ζ_1, ζ_2 and σ. We solve the problem with a constant step in the interval for the density σ and the depth of the spherical body, equal to 0.001. Such a step is defined in order to ensure the numerical stability of the algorithm: the smaller the iteration step, the more accurate the calculation.

In order to simulate the errors in the initial data, we solved the direct problem of gravimetry at a different level of measurement errors (5-20% of the maximum value of the anomaly). A pseudo-random number sensor with a Gaussian distribution (like AnyLogic or ArcGIS) simulates the errors. The average computation time is 3 s, which proves the speed of the algorithm for a small-dimensional data matrix. The relative error of calculations is 2.67% and indicates the accuracy of the approach.

4.2. Sphere. Calculations performed at a depth of 900 m along the profile 3-3 displayed that the solution (the right side of the chart of the gravity field, starting from point 41) has a significant residual of the gravity. We decided to carry out an additional iterative improvement for the entire profile while fitting by other free parameters of the model. This approach has resulted in a model with a good residual of gravity along the entire section (see figure 4). The calculations were performed at T = 1000°, a cooling rate 0.0001 m/s^2, with an error of 15% for ζ_1, x, and σ, with a step equal to 0.001. The relative error of the solution lies within acceptable limits, no more than 0.12%. The average computation time is 6 s. The solution is found at over 69,000 iterations.

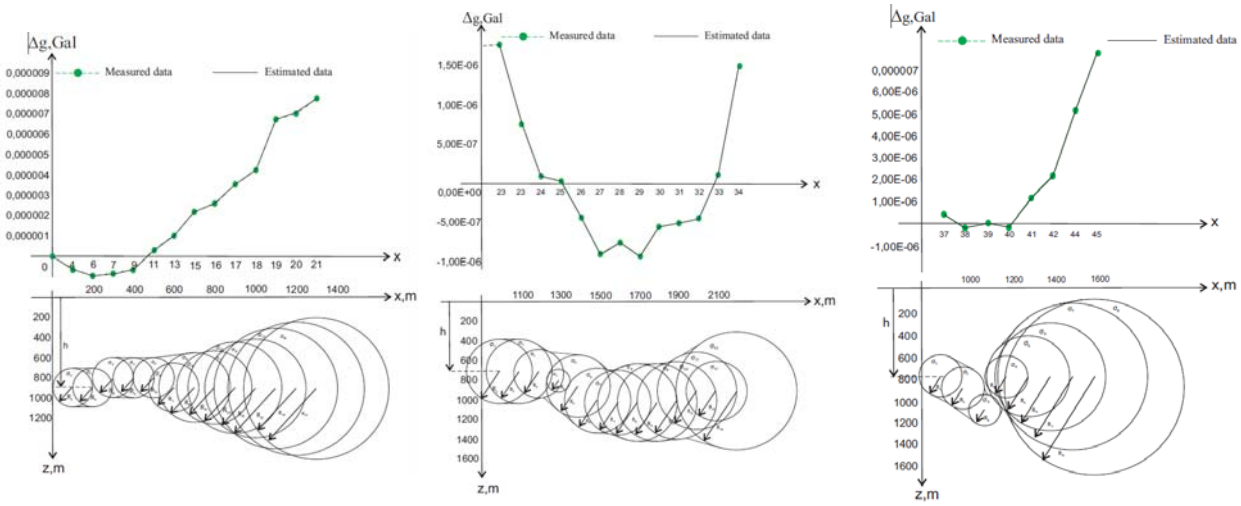

a) along the profile 1-1 b) along the profile 2-2 c) along the profile 3-3

Figure 4 – Gravity anomaly from the model given as a series of spherical bodies

4.3 Vertical ledge. Calculations for a vertical ledge started with a reference depth of 600 m along the profile. At the beginning of profile 1-1, a significant residual arose in the solution, and we subjected this part to additional calculations. The final solution (gravity effects from a set of vertical ledges) for all three profiles were obtained within the acceptable error (see figure 5). The relative measurement error lies within acceptable bounds, no more than 1.26%. The calculations were performed at T = 100° and a cooling rate of 00001. The average duration of computations is 17 s. Each solution was found at over 46,000 iterations.

In general, the results of calculations by simulating annealing approach showed a fairly *stable* solution provided that the initial data bulk is extremely limited. As part of a consistent fitting of parameters, we obtained the final models of the HCR medium under study that have the acceptable likelihood, with the accuracy of the solution by the gravity data is reached 10^{-11}. Thus, the simulated annealing approach allows us to fit quickly the options for suitable solutions for the express analysis of the internal structure of the geological medium within the boundaries of the studied HCR.

Due to the small amount of data, the simulation results have limited applicability and need to be verified using other geophysical methods or by solving the same problems using real field data of significantly larger dimensions.

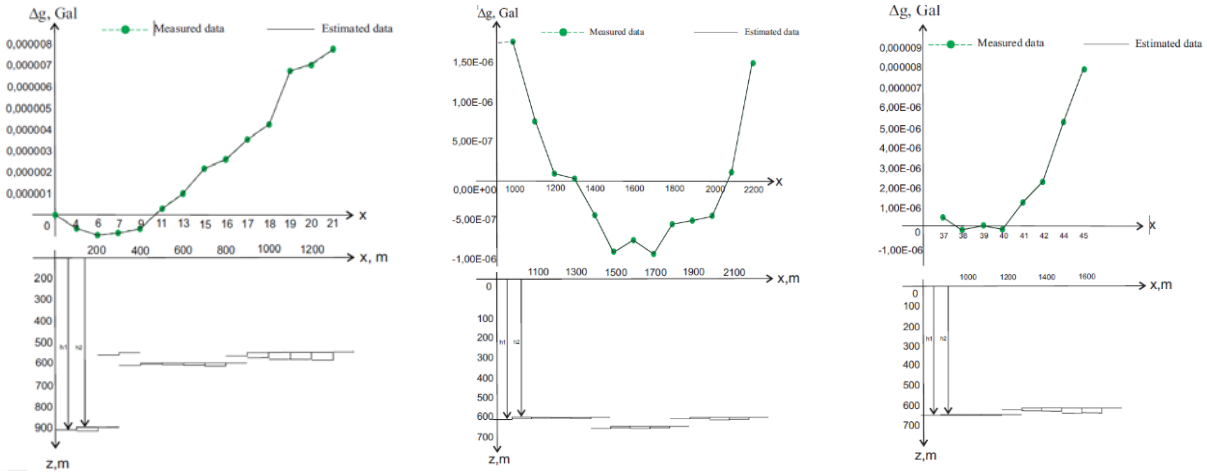

along the profile 1-1 along the profile 2-2 along the profile 3-3

Figure 5 – Gravity anomaly from the model given as a series of vertical ledges

5. Conclusions. The simulated annealing approach provides a solution to the direct problem of gravimetry for several mathematical models of the geological medium with *sufficient* accuracy. Given the number of iterations and the number of possible combinations of parameters, the technique allows to find quickly the optimal density and depth parameters for homogeneous bodies of regular geometric shape.

While comparing the solutions for different bodies with the same bulk of initial data, it was found that the calculation time depends on the choice of the initial temperature *T* and the cooling rate, i.e. the initial density approximation in the simulated annealing approach. The higher the temperature and the lower the cooling rate, the longer the calculation takes. Thus, for a vertical ledge, the average calculation duration was 17 s at a cooling rate of 0.0001 s. Nevertheless, such a dependence is a common property of all gradient-like solution search methods. Of all the above models, the model of horizontal prisms was calculated faster of all (3 s) at a cooling rate of 0.001 s.

A numerical module for GIS GeoM has been created, which allows you to fit the appropriate parameters of anomalous geological bodies by minimizing the residuals in gravity field trough the simulated annealing approach. Its testing on the example of various bodies and measured values of the gravity field allowed us to increase the reliability of the original HCR model at each profile. Thus, the implementation of this technique improves the accuracy, speed, and stability of solving the gravity direct problems for a multicomponent layered geological medium.

Acknowledgements. The paper was funded by grants No. AP05135158 of the Ministry of Education and Science of the Republic of Kazakhstan.

Ф. Н. Абдолдина[1], А. Б. Назирова[1,2], Ю. И. Дубовенко[3], Г. К. Умирова[2]

[1]Халықаралық ақпараттық технологиялар университеті, Алматы, Қазақстан;
[2] Сәтбаев университеті, Алматы, Қазақстан;
[3]Украина ҰҒА С.И. Субботин атындағы геофизика институты, Киев, Украина

ЖЕР ҚОЙНАУЫ ЖАҒДАЙЫНЫҢ ГРАВИМЕТРИЯЛЫҚ БАҚЫЛАУ ДЕРЕКТЕРІН ИНТЕРПРЕТАЦИЯЛАУ ҮШІН ИМИТАЦИЯЛЫҚ КҮЙДІРУ ӘДІСІМЕН ГРАВИБАРЛАУДЫҢ ТІКЕЛЕЙ МӘСЕЛЕСІН ШЕШУ

Аннотация. Көмірсутектер шоғырларын ұзақ игеру кезінде геологиялық ортада күрделі деформациялық процестер жүреді. Геодинамикалық қауіп-қатерді және теріс салдарын бағалау үшін гравитациялық мониторинг жүргізіледі. Нәтижесінде үздіксіз өзгеріп отыратын кәсіпшілік-геологиялық жағдайдың өзара байланысы зерттеледі (өндіру көлемінің өзгеруі, қаттық қысымның өзгеруі, флюидті өнімді қаттарға айдау процестері). Өнеркәсіптік қауіптілігі жоғары аймақтарды анықтау кезінде гравитациялық инверсияны шешудің негізгі құралы тікелей гравитациялық есепті шешу болып табылады. Бұл зерттеулерде ортаның

берілген бастапқы жақындауына сүйене отырып, тапсырма дәйекті жуықтау арқылы жүзеге асырылады. Мұндай үлестірімдерді бағалау үшін мақала авторлары стохастикалық оңтайландыру аясында модельдеу тазарту әдісін қолдануды ұсынады. Ол гравитациялық өріс мәндерінің минималды қалдығы болған жағдайда оңтайлы орта параметрлерін реттеуге бағытталған.

Тәсіл геологиялық ортаның үш қарапайым математикалық моделін қолдана отырып жүзеге асырылады: көлденең призма, біртекті сфера және тік проекция. Бұл әдіс қоршаған орта мәндерін оның параметрлерінің жұпына сәйкес бір уақытта реттеуге мүмкіндік береді. Алгоритмнің жұмысы сипатталған және модельдеу нәтижелері келтірілген. Алынған нәтижелер ұсынылған әдіспен тікелей гравитациялық есепті шешу алгоритмінің қолайлы дәлдігін көрсетті. Имитациялық тазарту әдісі гравитациялық өрісті талдау уақытын азайту кезінде ГАЖ моделінің сенімділігін арттыруға мүмкіндік берді.

Түйін сөздер: гравиметрияның тікелей мәселесі, имитациялық күйдіру, гравитациялық вариация, гравиметриялық бақылау, көмірсутегі кен орны.

Ф. Н. Абдолдина[1], А. Б. Назирова[1,2], Ю. И. Дубовенко[3], Г. К. Умирова[2]

[1]Международный Университет Информационных Технологий, Алматы, Казахстан;
[2]Satbayev University, Алматы, Казахстан;
[3]Институт геофизики НАН Украины им. С. И. Субботина, Киев, Украина

РЕШЕНИЕ ПРЯМОЙ ЗАДАЧИ ГРАВИРАЗВЕДКИ МЕТОДОМ ИМИТАЦИИ ОТЖИГА ДЛЯ ИНТЕРПРЕТАЦИИ ДАННЫХ ГРАВИМЕТРИЧЕСКОГО МОНИТОРИНГА СОСТОЯНИЯ НЕДР

Аннотация. При длительном освоении залежей углеводородов (УВ) в геологической среде происходят сложные деформационные процессы. Для оценки возможного геодинамического риска и негативных последствий от ГКР проводится гравитационный мониторинг. В результате исследуются взаимосвязи непрерывно меняющейся промыслово-геологической обстановки (изменения объемов добычи, изменения пластового давления, процессы закачки флюида в продуктивные пласты). Основным инструментом решения гравитационной инверсии при определении зон повышенной промышленной опасности является решение прямой гравитационной задачи. В этих исследованиях, исходя из заданного начального приближения среды, задача реализуется путем последовательных приближений. Для оценки таких распределений авторы статьи рекомендуют использовать метод имитационного отжига в рамках стохастической оптимизации. Она направлена на подгонку оптимальных параметров среды при условии, что происходит минимальный остаток значений гравитационного поля.

Подход реализуется с использованием трех простых математических моделей геологической среды: горизонтальной призмы, однородной сферы и вертикального выступа. Этот метод позволяет подгонять значения среды одновременно по паре ее параметров. Описана работа алгоритма и приведены результаты моделирования. Полученные результаты показали приемлемую точность алгоритма решения прямой гравитационной задачи предложенным методом. Метод имитационного отжига позволил повысить надежность модели ГКР при одновременном сокращении времени анализа гравитационного поля.

Ключевые слова: прямая задача гравиметрии, метод имитации отжига, вариации силы тяжести, гравиметрический мониторинг, месторождение углеводородов.

Information about authors:

Abdoldina F., Candidate of Technical Sciences, International Information Technology University, Almaty, Kazakhstan; farida_mail@mail.ru; https://orcid.org/0000-0003-1816-6343

Nazirova A., PhD student, Satbayev University, Almaty, Kazakhstan; asem_berlibaeva@mail.ru; https://orcid.org/0000-0002-3299-5108

Dubovenko Y, Candidate of Phys. and Math. Sciences, Institute of Geophysics NAS of Ukraine, Kiev, Ukraine; yuriiguy@gmail.com; https://orcid.org/0000-0002-8128-5989

Umirova G., PhD in Geology and Exploration of Mineral Deposits, Satbayev University, Almaty, Kazakhstan; gulmuha@mail.ru; https://orcid.org/0000-0001-5185-3132

REFERENCES

[1] Trofimov D.M. (2016) Modern micro-amplitude tectonic movements, remote methods for their study and importance for oil and gas geology // Infra Engineering, M. 80 p. (in Russ.).

[2] Shevelyova A. (2010) Integrated Geodynamic Monitoring and Risk Assessment of Occurrence of Seismic Deformation Processes Related to Development of Raw Hydrocarbon Deposits. SPE Caspian Carbonates Technology Conference, Atyrau, Kazakhstan, 8-10 November; Society of Petroleum Engineers. P. 1-8. https://doi.org/10.2118/139949-MS

[3] Nurpeisova M., Bekbassarov Zh., Kenesbayeva A., Kartbayeva K., Gabitova U. (2020) Complex evaluation of geodynamic safety in the development of hydrocarbon reserves deposits // News of NAS RK. Series of geology and technical sciences. Vol. 1, N 439. P. 90-98. https://doi.org/10.32014/2020.2518-170X.11

[4] Shlyahovskii V.A. (1984). The study of oil and gas prospective structures using a dialogue system for interpreting gravitational anomalies. Dissertation, Institute of Geophysics named after Subbotin S. I. (in Russ.).

[5] Hinze W., Von Frese R., Saad A. (2013) Gravity and Magnetic Exploration: Principles, Practices, and Applications, Cambridge University Press, Cambridge. https://doi.org/10.1017/CBO9780511843129

[6] Zhao L.S., Sen M., Stoffa P., Frohlich C. (2007) Application of Very Fast Simulated Annealing to the Determination of the Crustal Structure Beneath Tibet // Geophysical Journal International. Vol. 125, Issue 2. P. 355-370. https://doi.org/10.1111/j.1365-246X.1996.tb00004.x

[7] Chakravarthi V., Pramod Kumar M., Ramamma B., Rajeswara Sastry S. (2016) Automatic gravity modeling of sedimentary basins by means of polygonal source geometry and exponential density contrast variation: Two space domain based algorithms // Journal of Applied Geophysics. Vol. 124. P. 54-61. https://doi.org/10.1016/j.jappgeo.2015.11.007

[8] Abdelrahman E.M., Sharafeldin S.M. (1995) A least-squares minimization approach to depth determination from numerical horizontal gravity gradients // Geophysics. Vol. 60, Issue 4. P. 939-1278. https://doi.org/10.1190/1.1443857

[9] Nazirova A., Abdoldina F., Dubovenko Y., Umirova G. (2019) Application of the simulated annealing method for gravimetric monitoring data analysis of the bowels condition of oil and gas deposits // Bulletin of the Kazakh National Research Technical University after K.I. Satbayev. Vol. 3, N 133. P. 397-405 (in Russ.).

[10] Nazirova A., Abdoldina F., Aymahanov M., Umirova G., Muhamedyev R. (2016) An Automated System for Gravimetric Monitoring of Oil and Gas Deposits. First International Conference, DTGS 2016, St. Petersburg, Russia, June 22–24 2016, Published in: Communications in Computer and Information Science. Vol. 674. P. 585-595. https://doi.org/10.1007/978-3-319-49700-6_58

[11] Nazirova A., Abdoldina F., Dubovenko Y., Umirova G. (2019) Development of GIS subsystems for gravity monitoring data analysis of the subsoil conditions for oil and gas fields // Geoinformatics 2019, Kyiv, Ukraine, 13-16 May 2019; European Association of Geoscientists & Engineers. P. 1-5. https://www.earthdoc.org/content/papers/10.3997/2214-4609.201902099

[12] Sen M., Stoffa P. (2013) Simulated annealing methods. In Global Optimization Methods in Geophysical Inversion // Cambridge University Press, Cambridge. P. 81-118. https://doi.org/10.1017/CBO9780511997570.006

[13] Singh A., Biswas A. (2016) Application of global particle swarm optimization for inversion of residual gravity anomalies over geological bodies with idealized geometries // Natural Resources Research. Vol. 25. P. 297-314. https://doi.org/10.1007/s11053-015-9285-9

[14] Sheng Z., Xiaohong M., Minghua Z., Zhaoxi C., Chunxiao X., Yajie L. (2018) The improved residual node density based gravity forward method and its application // Journal of Applied Geophysics. Vol. 159. P. 765-772. https://doi.org/10.1016/j.jappgeo.2018.10.020

N E W S
OF THE NATIONAL ACADEMY OF SCIENCES OF THE REPUBLIC OF KAZAKHSTAN
SERIES OF GEOLOGY AND TECHNICAL SCIENCES
ISSN 2224-5278
Volume 1, Number 445 (2021), 22 – 28 **https://doi.org/10.32014/2021.2518-170X.3**

UDC 629.4.023.11
IRSTI 73.29.11

S. S. Abdullayev[1], I. S. Bondar[1], G. B. Bakyt[1],
G. K. Ashirbayev[1], A. M. Budiukin[2], Ye. Ye. Baubekov[1]

[1]Kazakh Academy of Transport and Communications named after M. Tynyshpayev, Almaty, Kazakhsta;
[2]Emperor Alexander I St. Petersburg State Transport University, Saint Petersburg, Russia.
E-mail: seidulla@mail.ru, i.bondar@kazatk.kz, gaba_b@bk.ru,
galimzhan_68@mail.ru, remont_ps21@mail.ru, baubekov3@mail.ru

INTERACTION OF FRAME STRUCTURES WITH ROLLING STOCK

Abstract. Need of use of mobile measuring computer systems when performing diagnostics of bridges is shown and also the analysis of amplitude-phase-frequency characteristics frame reinforced concrete and metal flying structures of railway bridges is provided at the movement of the train. This in turn allows to estimate conditions of span structures by width of ranges in points of half energy of spectral curve in the area of resonances. Assessment of technical condition and diagnostics of supported artificial structures is carried out according to dynamic parameters. According to this method frequency of natural oscillations is determined from peak values of averaged spectral densities of reduced power. Comparing width of the received ranges to ranges of the new (intact) flying structures it is possible to estimate degree of wear and a damage rate of elements of designs. Based on the results of the calculations, it has been confirmed that the inclusion of elements of the bridge web and the upper structure of the track in the joint work with the main bearing structures increases the accuracy of solving the problem of determining natural frequencies.

Key words: rolling stock, metal bridges, reinforced concrete bridges, railway track, locomotive, system "path - the crew", processes of oscillations, experimental oscillograms.

Introduction. On the high-level network of the railroads of Kazakhstan more than 9000 artificial constructions are operated: big bridges – 107 pieces, average bridges – 838 pieces, small bridges - 2430 pieces, water throughput pipes – 5342 pieces, including metal bridges – 219 pieces, reinforced concrete bridges – 3308 pieces Besides, are operated out-of-class big bridges through river. On the station Kapchagay and through the Urals River in Uralsk, a railway tunnel, antilandslide galleries and other constructions [1,2]. Today because of inadequate hardware of laboratory its employees conduct visual examinations of artificial constructions. In operation on the main railway directions there are constructions built more than a century ago at which construction the train loadings existing now were not considered. Due to the input of Technical regulations of the Customs Union of TR CU 003/2011 "About safety of infrastructure of railway transport", TR CU 001/2011 "About safety of the rolling stock" has arisen need of updating of the specifications and technical documentation regulating safe service conditions of the rolling stock and a railway track. Processing of the specifications and technical documentation is carried out taking into account requirements of the International union of the railroads (Union Internationale des Chemis de Fer) and the international standards [3-5].

Characteristics of perturbations acting on the rolling stock from the side of the track. The network of the railway of the republic covers a vast territory with various climatic and geological conditions, consists of separate sections with various conditions and freight traffic, along which a large and diverse fleet of rolling stock runs [6,7].

In the studies of the interaction of the track and the rolling stock, the influence of a wide variety of factors was studied:

- characteristics of the under-rail base: non-equal-elasticity, ballast type and rail-sleeper grid;
- roughness of the rail: butt roughness, unevenness of the welded seam, wave-like wear, random irregularities [8];
- condition and geometry of the path;
- properties of the rolling stock [9];
- wheel imperfections: potholes, imbalances, random irregularities [10,11];
- speed of movement [8];
- weather conditions [10,12].

The use of computers in the information and computing complex (CPI) presents a number of significant advantages:

1. As a result of increasing the speed of data processing, the efficiency of obtaining the necessary information is greatly increased, it becomes possible (in case of critical situations) to perform immediate actions;

2. The accuracy of results is significantly increased, the possibility of erroneous decisions is reduced, since the decisions taken on the basis of the CPI are based on reference data, and not on the subjective scenes of the researcher;

3. It becomes possible to obtain a characteristic of the irregularities of a given path segment;

4. Time and material expenses for data processing are significantly reduced;

5. It becomes possible to create a single data bank containing information that completely characterizes the test or controlled test site. The information of such a bank can be used both for organization of repair works, planning and carrying out dynamic-strength and running tests of new types of rolling stock, as well as for developing recommendations for the optimal use of rails of various types, etc.

To obtain characteristics informative for solving the problem of classification of vertical irregularities by their spectral characteristics, the methods of factor and variance analysis were used in the studies [13,14].

One of the methods of lowering the dimension of the original indicative space is the method of principal components, which provides a transition to a new system of attributes $Y=\{y_1 \ldots y_2\}$ each of the components y_i has the following properties:

1. y_i is a linear combination of the initial characteristics:

$$y_i \sum_{i=1}^{N} a_{ij} x_i \qquad j = \overline{1, N} \tag{1}$$

2. All γ_i are statistically independent of each other, i.e:

$$cov(y_l, y_k) = 0 \qquad l \neq k \tag{2}$$

3. All γ_i are ordered by their variance in the sample under study, with the first component γ_i having the greatest variance:

$$D(y_1) \geq D(y_2) \geq \ldots \geq D(y_N) \tag{3}$$

The transition to the system of principal components is a rotation of the coordinate system in such a way that the projection of the sampled sample on the first axis, γ_i, possesses the greatest possible variance for this sample. The second axis perpendicular to the first is directed in such a way that it is uncorrelated with the first and that the projection of the sample under study has the greatest variance on it. Similarly, the remaining axes of the main components are constructed. All of them are uncorrelated with each other and are arranged in descending order of variances.

Lowering the dimension of a characteristic space by the method of principal components is usually the rejection of those principal components to which the minimum variance of the original sample falls. However, the features with the greatest dispersion are not always the most informative for solving classification problems [15].

Figure 1 shows the images of two classes, described by two signs – x_1 and x_2. In the transition to the main components, the axis O_1, will have the greatest dispersion, however, the second component is the

most informative component for solving the classification problem. The above example shows the need to analyze the informativeness of components that do not have a large variance.

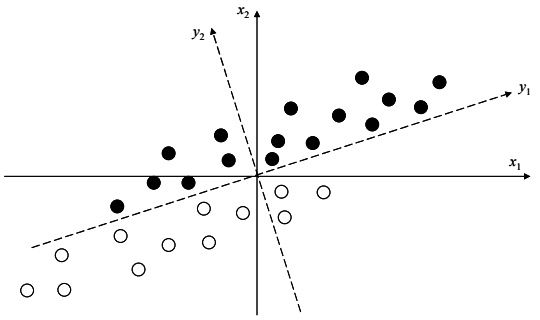

Figure 1 – Transformation of the original feature space inti the space of the main components

Using the spectral characteristics of the drawdown of the path stored in a bank of spectra, an estimate of the covariance matrix of the harmonic components C_x (table 2).

Table 2 – The matrix of component weights

Points	Frequency range (I/M)									
	I/60M-I/30M	I/30M-I/15	I/15M-I/10M	I/10M-I/7.5M	I/7.5M--I/6M	I/6M-I/5M	I/5M-I/4.5M	I/4.5M-I/3.7M	I/3.7M-I/3.3	I/3.3M-I/3M
y_1	0.783	-0.47	0.28	-0.28	-0.07	-0.03	-0.04	0.028	-0.016	-0.002
y_2	0.35	0.55	0.51	0.5	0.21	0.106	0.04	0.025	0.008	0.003
y_3	-0.31	-0.68	0.3	0.5	0.28	0.15	0.044	0.04	0.01	0.006
y_4	0.407	-0.08	-0.75	0.45	0.17	0.16	0.06	0.04	0.02	0.007
y_5	-0.03	0.076	-0.02	-0.464	0.783	0.35	0.16	0.14	0.016	0.015

The conducted studies showed that the first five components accounted for 99.7% of the variance of the initial characteristics - 76%, 13.2%, 5.4%, 3.5%, 1.6%, respectively. Figure 2 shows a graphical representation of the component weights that determine each of the five first components in the region of harmony of the spectra studied.

Thus, the space of the main components that are informative for solving the problem of classifying the state of the path in terms of the indicator of the probable initial conditions (the structure of the track, the type of rolling stock, the speed of 60 km / h) is constructed.

Modern methods for diagnosing bridges. One of the important tasks for the qualitative inspection and diagnostics of the existing state of span structures, supports, approach embankments, the upper structure of the track and other elements of artificial structures (ISSO) is the acquisition and use of modern devices of the latest generation. One of them is the latest generation Photometer PM-600/630 device from the Swiss company Proceq. The operation of the Photometer PM-600/630 is based on the principle of electromagnetic induction in determining the rods of the armature. The sensor coils induce a magnetic field, due to which eddy currents are formed on the surface of the electrically conductive material (rod of the armature). Eddy currents are formed on the surface of any electrically conductive material in magnetic fields. They induce a magnetic field in the opposite direction. The difference between the induced and received magnetic field is used by the device to obtain the results [15].

For example, the bridge monitoring system developed in Switzerland (Bridge Monitoring System "BRIMOS") [16] is based on the fact that the state of any design is reflected in the characteristics of its dynamic behavior. The so-called "dynamic autograph" (response) of the structure contains all the information that is necessary for a detailed assessment of its state. The technique used to assess the technical state of structures uses the method of estimation of random effects (Ambient Vibration Monitoring), which can be defined as a method of identification of bridge structures by dynamic response to a random effect, which can be considered wind, micro seismic activity or bridge-moving transport.

In Japan, the use of complex monitoring systems is quite common, for which special hardware and software systems have been developed and are constantly being improved. However, there are very few publications on the improvement of dynamic identification systems. Identification of a system is understood as the definition of the dynamic characteristics of a bridge or other engineering structure from information obtained by recording its oscillations.

Very simple and at the same time very effective is the method of selecting peak values of the parameters of oscillations of a bridge structure, based on the analysis of only output signals, connected with the determination of peak values. In accordance with this method, the natural oscillation frequency is determined from the peak values of the averaged reduced power spectral densities (SPM). These values are obtained by recalculating the measured values of vibration displacement, vibration velocities and vibration acceleration using a discrete Fourier transform. The coherence function, calculated for two simultaneously registered output signals, is close in magnitude to that for the natural frequencies. This pattern, in addition, helps to detect precisely those frequencies that can be considered as own frequencies. It is assumed that the dynamic response at resonance refers only to its own tone. The method of selecting peak values does not require the use of complex algorithms for its implementation. Within the framework of this method, various modifications of the fast Fourier transform are used to construct the graphical representation of the spectral density function, which are described in detail in the special literature [17-19]. The described method has been successfully tested in Austria and Switzerland on a large number of structures.

Experiment. The objects of the research described in the present work were beamed metal (built in 1952) and ferroconcrete (1972 built) span structures of the bridge across the Irtysh-Karaganda channel of the Erejmentau-Ekibastuz railway line in the Republic of Kazakhstan (km 257 PK 7 + 0) l = 27 m and 16 m.

Figure 3 show the schemes of a metal and reinforced concrete span structure with the arrangement of vibration sensors on structural elements.

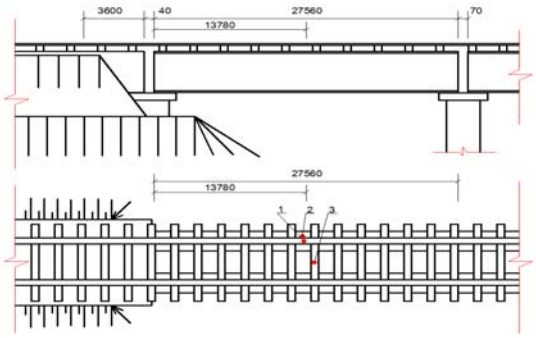

Figure 3 – Scheme of a metal span structure with the arrangement of vibration sensors on structural elements:
1 - middle of the beam span structure; 2- the sole of the rail; 3- middle of the wooden beam.

Of particular interest in the studies were frequency spectra of forced vertical oscillations of span structures, since they can be used to judge the causes that cause vibration of a bridge [14, 20]. To this end, a spectral analysis of the oscillograms of vertical vibro-displacement metal (figure 4, a) and reinforced concrete (figure 4, *b*) beams was performed during the movement of the rolling stock with velocities v = 41 to 98 km / h.

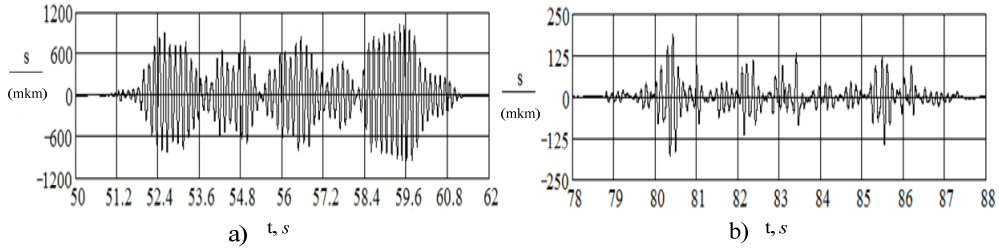

Figure 4 – Oscillograms of vertical vibro-displacement: *a - a metal beam with the passage of an electric train of 10 cars at a speed of 98 km / h, b - reinforced concrete beam at passage of an electric train from 8 cars at a speed of 62 km/h.*

The results of the spectral analysis for these processes are shown in figure 5 *a, b*.

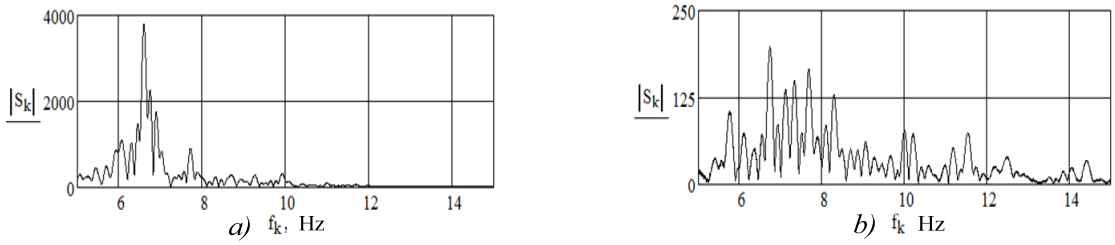

Figure 5 – Spectrum of oscillograms: *a - a metal beam; b - reinforced concrete beam*

Here, to each value of the frequency there corresponds a definite magnitude of the amplitude of the oscillations. The interaction of the metal beam span with the rolling stock occurs mainly in the case of disturbances whose frequencies are in the range $f = 5{,}34 \div 7{,}27$ *Hz*, and the reinforced concrete in the range $f = 5{,}26 \div 7{,}42$ *Hz*. These disturbances determine first of all the reaction of the span structures. The other perturbations, judging by the spectra, do not play a special role in the formation of the behavior of the span structures, since their amplitudes are very small and the energy they introduce into the system is insignificant [21].

By the "tails" of the experimental oscillograms (figure 6 a, b) and the spectra plotted from them (figure 7 a, b), the frequencies of free oscillations of the unloaded span structures were determined.

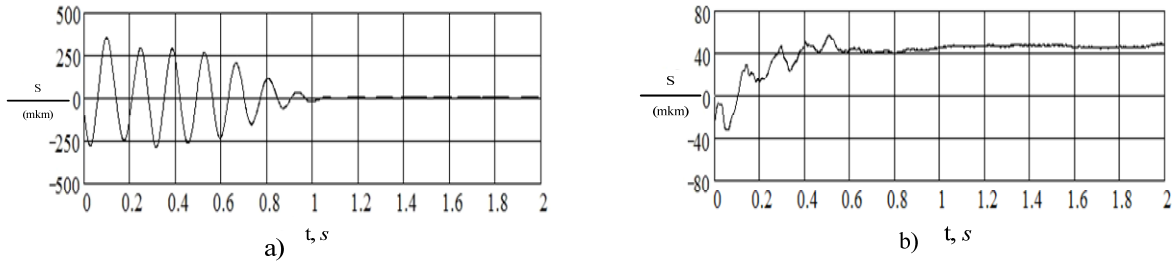

Figure 6 – Oscillograms of vibro-displacement after a load: *a - a metal beam; b - reinforced concrete beam*

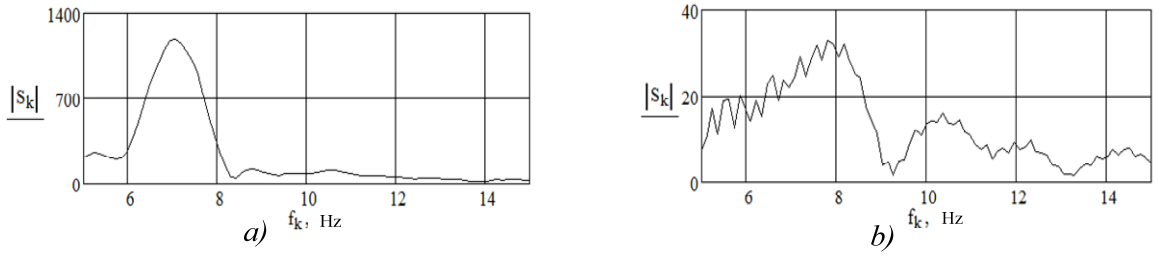

Figure 7 – Spectrum of oscillograms after the load is released: *a - a metal beam; b - reinforced concrete beam*

For metal and reinforced concrete beam girders, they are respectively equal to $f_{\text{m}} = 7{,}08$ Hz and $f_{\text{r.c.}} = 7{,}81$ Hz.

Conclusions. From the analysis of full-scale measurements of the processes of oscillations of beam span structures, it follows that the spectrum of oscillations of the span structures when interacting with a moving train is multimodal. In this case, the frequency of the individual components depends significantly on the speed of the train, and the main part of the energy of the oscillation process is in harmonics corresponding to the frequencies of the natural oscillations of the system "span structure - railway track - rolling stock".

To estimate the state of flying structures, one can use the width of the spectra at half-energy points of the spectral curve in the resonance region. Comparing the width of the obtained spectra with the spectra of the new undamaged flying structures, it is possible to estimate the degree of wear and the degree of damage to the structural elements.

The characteristics of the oscillations of the system "span structure - path - rolling stock" obtained during the measurements described in this work can serve as initial data in the calibration of the model of the structure and in the compilation of algorithms for the problem of detecting damage.

С. С. Абдуллаев[1], И. С. Бондарь[1], Ғ. Б. Бақыт[1],
Г. К. Аширбаев[1], А. М. Будюкин[2], Е. Е. Баубеков[1]

[1]М. Тынышбаев атындағы Қазақ көлік және коммуникациялар академиясы, Алматы, Қазақстан;
[2]І Александр императордың Петербург мемлекеттік теміржол көлігі университеті, Санкт-Петербург, Ресей

РАМАЛЫҚ ҚҰРЫЛЫМНЫҢ ЖЫЛЖЫМАЛЫ ҚҰРАММЕН ӨЗАРА ӘРЕКЕТІ

Аннотация. Көпір диагностикасын жүргізу кезінде ұтқыр өлшеу есептеу кешендерін пайдалану қажеттілігі көрсетілді, сондай-ақ поезд қозғалысы кезінде теміржол көпірлерінің қаңқалы темірбетон және металл аралық құрылыстарының амплитудалық-фазалық жиілік сипаттамаларына талдау жүргізілді. Бұл, өз кезегінде, резонанс аймағындағы спектрлік қисықтың жартылай энергия нүктелеріндегі диапазондардың ені бойынша аралық ғимараттардың жағдайын бағалауға мүмкіндік береді. Тірек жасанды құрылыстардың техникалық жай-күйін бағалау және диагностикалау динамикалық параметрлер бойынша жүзеге асырылады. Осы әдіске сәйкес табиғи тербелістердің жиілігі берілген қуаттың орташа спектрлік тығыздығының ең жоғары мәндерімен анықталады. Алынған спектрлердің енін жаңа зақымдалмаған жабынды құрылыс спектрлерімен салыстыра отырып, конструкция элементтерінің техникалық жай-күйін бағалауға болады. Есептеу нәтижелерінің негізінде көпір төсемі мен жолдың жоғарғы құрылысының негізгі көтергіш конструкциясының элементтерімен бірге жұмысына қосылуы меншікті жиілікті анықтау туралы міндетті шешудің дәлдігін жоғарылататындығы бекітілді.

Түйін сөздер: жылжымалы құрам, металл көпірлер, темірбетон көпірлер, теміржол табаны, локомотив, «экипаж-жол» жүйесі, тербеліс үдерістері, эксперименттік осцилограммалар.

С. С. Абдуллаев[1], И. С. Бондарь[1], Г. Б. Бакыт[1],
Г. К. Аширбаев[1], А. М. Будюкин[2], Е. Е. Баубеков[1]

[1]Казахская академия транспорта и коммуникаций им. М. Тынышпаева, Алматы, Казахстан;
[2]Петербургский Государственный университет путей сообщения императора Александра I, Санкт-Петербург, Россия

ВЗАИМОДЕЙСТВИЕ РАМНЫХ КОНСТРУКЦИЙ С ПОДВИЖНЫМ СОСТАВОМ

Аннотация. Показана необходимость использования мобильных измерительных вычислительных комплексов при проведении диагностики мостов, а также проведен анализ амплитудно-фазочастотных характеристик каркасных железобетонных и металлических пролетных строений железнодорожных мостов при движении поезда. Это, в свою очередь, позволяет оценить состояние пролетных строений по ширине диапазонов в точках полуэнергии спектральной кривой в области резонансов. Оценка технического состояния и диагностика опорных искусственных сооружений осуществляется по динамическим параметрам. Согласно этому методу частота собственных колебаний определяется по пиковым значениям усредненных спектральных плотностей приведенной мощности. Сравнивая ширину полученных диапазонов с диапазонами новых (неповрежденных) летательных аппаратов, можно оценить степень износа и степень повреждения элементов конструкций. По результатам проведенных расчетов подтверждено, что включение элементов полотна моста и верхнего строения пути в совместную работу с основными несущими конструк-циями повышает точность решения задачи определения собственных частот.

Ключевые слова: подвижной состав, металлические мосты, железобетонные мосты, железнодорожный путь, локомотив, система «экипаж-путь», процессы колебаний, экспериментальные осциллограммы.

Information about authors:
Abdullayev Seidulla Seidemetovich, Doctor of Technical sciences, Professor, Kazakh Academy of Transport and Communications named after M. Tynyshpayev, Almaty, Kazakhstan; seidulla@mail.ru; https://orcid.org/0000-0001-5028-8143

Bondar Ivan Sergeyevich, Candidate of Technical Sciences, Kazakh Academy of Transport and Communications named after M. Tynyshpayev, Almaty, Kazakhstan; i.bondar@kazatk.kz; https://orcid.org/0000-0002-0008-4043

Bakyt Gabit Bakytuly, Doctor of Philosophy (PhD), Kazakh Academy of Transport and Communications named after M. Tynyshpayev, gaba_b@bk.ru; https://orcid.org/0000-0001-5558-9316

Ashirbayev Galymzhan Kozhakhatovich, Candidate of Technical sciences, Associate Professor, Kazakh Academy of Transport and Communications named after M. Tynyshpayev, Almaty, Kazakhstan; galimzhan_68@mail.ru; https://orcid.org/0000-0002-7044-9968

Budiukin Alexey Mitrofanovich, Candidate of Technical Sciences, Associate Professor, Emperor Alexander I St. Petersburg State Transport University, Saint Petersburg, Russia; remont_ps21@mail.ru, https://orcid.org/0000-0003-3991-8372

Baubekov Yermek Yeltayevich, Doctor of Technical sciences, Professor, Kazakh Academy of Transport and Communications named after M. Tynyshpayev, Almaty, Kazakhstan; baubekov3@mail.ru, https://orcid.org/0000-0002-1134-5122

REFERENCES

[1] Khasenov S.S. Sovremennye metody diagnostiki mostov // Vestnik KazATK imeni M. Tynyshpaeva. 2014. Vol. 5. P. 10-14.

[2] Jiang H., Bian X., Cheng C. Simulating train moving loads in physical model testing of railway infrastructure and its numerical calibration // Acta Geotechnica. 2016. Vol. 11, N 2. P. 231-242.

[3] Markov D.P. Increase of hardness of rolling stock wheels (prerequisites and perspectives) // Scientific Research Institute of Railway Transport bulletin 1995. Vol. 3. P. 10-17.

[4] Solonenko V.G., Makhmetova N.M., Musayev J.S., Bekzhanova S.E., Kvashnin M.Ya. (2019) The method of limiting speed when passing turnouts of railway vehicles with bogies of model ZK1 // News of the National Academy of sciences of the Republic of Kazakhstan. Series of geology and technical sciences. Vol. 1, N 433 (2019). P. 151-162. https://doi.org/10.32014/2019.2518-170X.19 ISSN 2518-170X (Online), ISSN 2224-5278 (Print).

[5] Abdullayev, S., Tokmurzina, N., Bakyt, G. The determination of admissible speed of locomotives on the railway tracks of the republic of Kazakhstan // Transport Problems International Scientific Journal. 2016. Volume 11 Issue 1. PP.61-68.

[6] Sergienko A.B. Obrabotka tsifrovogo signala // St. Petersburg, Peter. 2011. 758 p.

[7] Fitzwilliam D. Track structure interactions for the Taiwan High Speed Rail project // In Track-Bridge Interaction on High-Speed Railways. 2008. CRC Press. P. 65-72.

[8] Saussine G., Allain E., Paradot N., Gaillot V. Ballast Flying Risk Assessment Method for High Speed Line // 9th World Congress on Railway Research. 2011. Paris, France. P. 37-43.

[9] Kvashnin M.Ya. Issledovanie mexanicheskih kolebanii zheleznodorozhnogo puti // Diss. ... cand. tekhnicheskih nauk. 2010. Almaty, 144 p.

[10] Daniel R. Effect of malfunctioning of the braking system on thermo-mechanical properties of freight train wheels // Dissertation – AAU. 2015. 89 p.

[11] Dyachenko1 L.K., Benin A.V. An assessment of the dynamic interaction of the rolling stock and the long-span bridges on high-speed railways // MATEC Web of Conferences. 2017. Vol. 107, N 14. P. 1-7.

[12] Zhang D., Hu H., Liu Yu., Dai L. Railway train wheel maintenance model and its application // Transportation Research Record: Journal of the Transportation Research Board. 2014. P. 28-36.

[13] Tarumi H. Activities Related to Testing and Research, Japan // Railway Technical Research Institute, Annual Report. 2010. P. 7-12.

[14] Chore1 H.S., Ingle R.K., Sawant V.A. Building frame - pile foundation - soil interaction analysis: a parametric study // Interaction and Multiscale Mechanics. 2010. Vol. 3, N 1. P. 55-79.

[15] Bondar N.G., Kozmin Yu.G., Roitburd Z.G., Tarasenko V.P., Yakovlev G.N. Vzaimodeistvie zheleznodorozhnyh mostov s podvizhnym sostavom // Moscow: Transport. 2009. 272 p.

[16] Ruge P., Birk C. Longitudinal forces in continuously welded rails on bridgedecks due to nonlinear track–bridge interaction // Computers and structures. 2007. Vol. 85, N 7-8. P. 458-475.

[17] Steffens D.M. Identification and Development of a Model of Railway Track Dynamic Behaviour // Queensland University of Technology. 2005. 317 p.

[18] Michal G., Nasir A., Yun S., Zong N., Lee W., Dhanasekar M. Crash Energy Management Systems for Australian rolling stock. Australia, 2013. 70 p.

[19] Xin L., Markine V.L., Shevtsov I.Y. Numerical analysis of the dynamic interaction between wheel set and turnout crossing using the explicit finite element method // Vehicle System Dynamics. 2016. Vol. 54, N 3. P. 301-327.

[20] Lyu Y., Zhu Y., Olofsson U. Wear between wheel and rail: A pin-on-disc study of environmental conditions and iron oxides // 2015. Wear 328. P. 277-285.

[21] Solonenko V.G., Makhmetova N.M., Musayev J.S., Bekzhanova S.E., Kvashnin M.Ya. (2019) Stresses in elements of metal railway bridges under the action of the crew // News of the National academy of sciences of the Republic of Kazakhstan. Series of geology and technical sciences. Vol. 2, N 434 (2019). P. 159-165. https://doi.org/10.32014/2019.2518-170X.50 ISSN 2518-170X (Online), ISSN 2224-5278 (Print).

N E W S
OF THE NATIONAL ACADEMY OF SCIENCES OF THE REPUBLIC OF KAZAKHSTAN
SERIES OF GEOLOGY AND TECHNICAL SCIENCES
ISSN 2224-5278
Volume 1, Number 445 (2021), 29 – 34 **https://doi.org/10.32014/2021.2518-170X.4**

IRSTI 30.19.31, 30.17.35, 30.51.23
UDC 519.677, 536.241

B. Alipova[1], B. Sapargaliyeva[2]

[1]International IT University, Almaty, Kazakhstan;
[2]Abai Kazakh National Pedagogical University, Almaty, Kazakhstan.
E-mail:b.alipova@edu.iitu.kz, bonya_sh@mail.ru

CREATION OF MATHEMATICAL AND COMPUTER MODELS OF THE DYNAMICS OF FLAME PROPAGATION OF AIR-SUSPENDED SOLIDS IN VARIOUS ROCKS USING MATLAB ENVIRONMENT

Abstract. The propagation of transient, air-suspended solids in a vented explosion chamber is numerically investigated by a dynamic formulation for the Concentration Limit of Flame Propagation (CLFP) with the GUI MATLAB environment. The geomechanics is modeled by a one-step overall reaction, which simulates the reaction of a stoichiometric propane– air-suspended solids. The CLFP modeling in the reaction rate model is numerically employed with mathematical models on basis Antoine's equation. This is based on an empirical correlation of the velocity fluctuations and implemented as interface with input-output data with graphic realization. The computer modeling show that the dynamic CLFP models provide superior results as general implementation of physical process of flame propagation and could be used for different rocks (f.e. granite, limestone, sandstone etc).

Key words: GUI MatLab, flame propagation, dynamic CLFP, air-suspended solids, equation of Antoine, rocks.

Introduction. Flame propagation investigation is widely used in different fields of industry as mining, tube construction, building construction and so on. In emergency gas explosions, the damage caused by pressure resulting from gas or air-suspended solids propagation and interaction with them depends on many conditions, such as the initial conditions, the operating environment, and the properties and mechanical, physical and chemical characteristics of the obstacles [1,2].

Computational fluid dynamics (CFD) and computer modeling using different special software can offer potentially cost-effective design solutions for such complex gas explosion scenarios. Such kind of scenario could be dangerous, time-limited, and expensive for experimental research. Many researches were bounded with classical approaches, e.g. such as research using the Reynolds-averaged Navier-Stokes method (RAEN). Such kinds of research were implemented by many authors [3,4]. We use here known approach based on equation of Antoine which describes flame propagation of different physical and chemical substances. It could be solved taking into consideration mechanical, physical and chemical properties of substances, in our case there are air-suspended solids in different rocks. It is supposed that the composition is known, and the user can use known set of definite rocks characteristics for calculation. Knowing them, and pressure and heat of combustion of definite air-suspended solids as well, created interface reproduce the graphical implementation and several numerical results using GUI MatLab interface. Thus, the graphical results of lower and upper concentration limits of flame propagation could be calculated, and the graphical representation is animated also. These studies confirmed the high accuracy of MatLab with a graphical interface in predicting the key characteristics of propagated flames.

Mathematicalmodel. In order to calculate certain processes of flame propagation for the construction of various structures of underground structures in different rocks (f.e. granite, limestone, sandstone etc.), the construction of pipelines or during the construction of gas storages, various storages of minerals and so

on, especially for construction in the rocks. Main combination of mechanical characteristics of rocks were taken from mining of Kazakhstan [5]. One of the most important characteristics of flame propagation is the calculations of the lower and upper concentration limits of flame propagation. In order to calculate them, the classical theories of the theory of heat transfer are used, in particular, one of the Antoine equation, which describes the dependence of the pressure of saturated vapors of liquids on atmospheric pressure and on the characteristics of the medium itself. Thus, the temperature can be calculated, that is, the heat of combustion and the lower and upper concentration limit of flame propagation. This research used several definite air-suspended of saturated vapors of liquids that propagate in different rocks (e.g. along a certain pipes). Here, the interface developed by the authors in the MatLab environment, provides the possibility of knowing certain input parameters, such as the characteristics and the A, B, C of the Antoine equation constants, knowing the atmospheric pressure in kPa, allows you to calculate the flame propagation temperature and thus calculate the lower and upper concentration limit of flame propagation. Naturally these limits depend on the heat of combustion in each specific environment.

The calculation of the lower concentration limit of the flame propagation of air suspensions.

The value of the lower concentration limit of the flame propagation (CLFP) of air-suspended particles (g/m3) for organic compounds (not applicable for calculating the combustion of metals):

$$CFLP = \frac{100 \cdot M}{a_1 \cdot \beta \cdot b_1 \cdot (\Delta H_i - \sum V_i \cdot \Delta H_{i1000})} \quad (1)$$

M – is the molecular weight of the dust; β – is the stoichiometric coefficient of oxygen in combustion reactions; ΔH_i – heat of combustion; V_i – is the stoichiometric coefficient of combustion products; ΔH_{i1000} – heat content of combustion products (enthalpy) when heated from 298 to *1000 K*; a_1 and b_1 are empirical coefficients for a given class of combustible materials.

Formula for calculating the lower concentration limit for organic compounds:

$$CFLP = a - \frac{b}{\Delta H_i} \quad (2)$$

where *a* and *b* are empirical coefficients.

$$CFLP = \frac{8 \cdot 10^5}{-\Delta H_{cm}^0} \quad (3)$$

Here H_{cm}^0 is heat combustion. The relative root-mean-square error of calculation by formula (3) is 15%.

Dynamic concentration limit of the flame propagation (CLFP) model.

To create certain mathematical models, the proposed dynamic formulation for the lower and upper concentration limits of flame propagation was used here. For this purpose, some experimental data obtained from measurements of flame propagation in various mixed mixtures were used to develop a conceptual model of the similarity of the lower concentration. The created application package has been successful in predicting the operation of certain industrial structures, where the contribution of mathematical and computer modeling is the simplest and most viable for numerical implementation.

Temperature limits of flame propagation of individual liquid substances.

If the dependence of the saturated vapor pressure of a liquid on temperature is known, then the value of the lower or upper temperature limit of flame propagation t_n (°C) can be calculated using the corresponding value

$$t_n = \frac{B}{A - \lg(\varphi_n \cdot P_0/100)} - C_A, \quad (4)$$

where *A, B, CA* – are the constants of the Antoine equation expressing the dependence of the pressure of saturated vapors of liquids, φ_n – the proportion of the gas phase.

Numerical procedure. In order to create mathematical models and construct corresponding models of the present study, the following tasks were performed [6-8]:

1. to calculate the Antoine equation and the upper concentration limits of the propagation of the flame of air-suspended of varying structures.

2. based on mathematical models developed by authors, computer models were developed. They were used for the corresponding parameters of the Antoine equation' constants and current atmospheric pressure, the known heat of combustion of air-suspensions.

3. a corresponding interface was created using the named input parameters, calculated the numerical values of the lower and upper concentration limits of flame propagation and the temperature. Flame concentration limits propagated by this definite temperature in certain directions. In this case, the corresponding built-in MatLab library was naturally used for calculations, the value of analytical and special functions of Bessel were displayed, the result was displayed both in numerical form and in graphical form (2D graphs). This plot represents the dependence of the lower concentration limit on time of flame propagation. Thus, a created interface was presented various structures of the flame beams of isopropyl alcohol, whose limit varies from 1 to 12%, while the corresponding Antoine's equation constants are taken as A = 7,5106, B = 1733,0, CA = 232,38. Concentration of atmospheric pressure is P0 =20 kPa.

The model described in this study is created using GUI MatLab. It solves fully compressible interdependent comparisons written in Cartesian coordinates and discretized and using the finite element method. Discretization is based on the formulation of the control volume of a homogeneous Cartesian grid. The first-order central difference approximation is used for the diffusion terms pulse pressure for the gradient in the pressure correction equation. The equation advances in time is fractional steps. We take several iterations of linking the equations to each other. Used boundary conditions for compressible flow is used to prevent bolt pressure at this boundary. Model is implemented by setting a variable at the lower center of the chamber to achieve an initial quasi-laminar phase match most experiments.

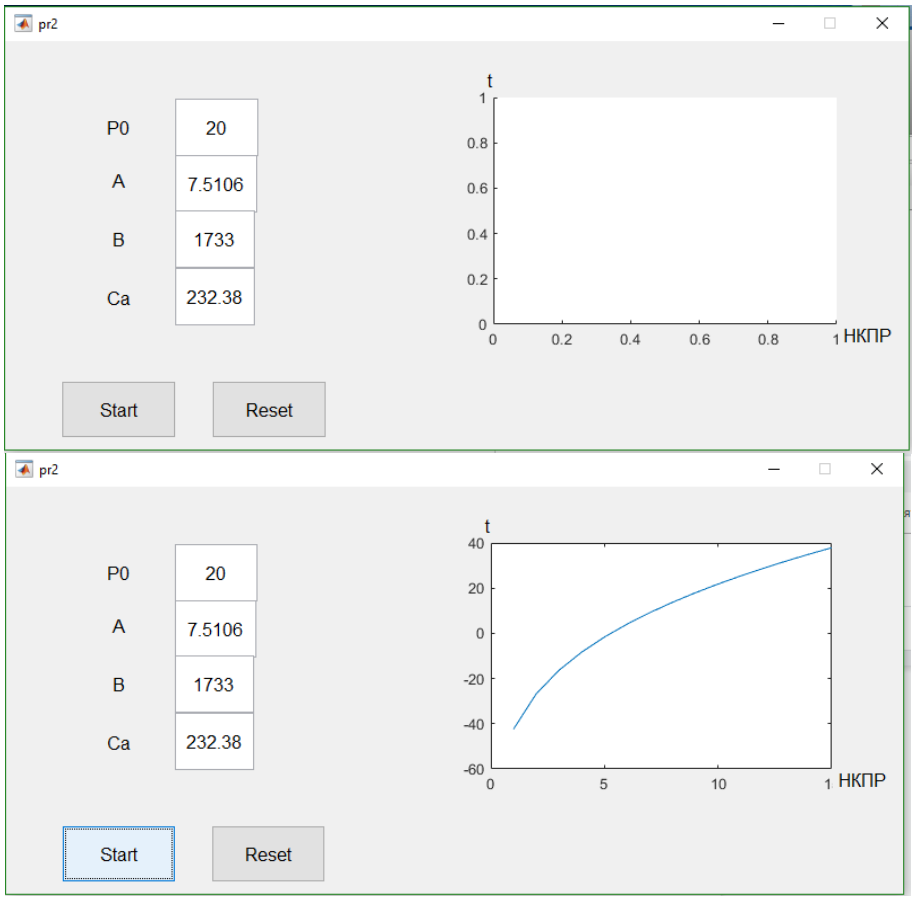

Modeling in the MatLab environment at start screen presents several forms with initial parameters and empty fields for answers. After entering the initial data, pressing the start button, the program starts calculating the unknown's values. Here is a code snippet that allows you to calculate and see how the lower boundary limits of certain substances were set.

When launched, the user sees several forms with initial parameters and an empty chart.

After you have entered the values and clicked on the “Start” button, the program will calculate the value of the unknowns and build a graph.

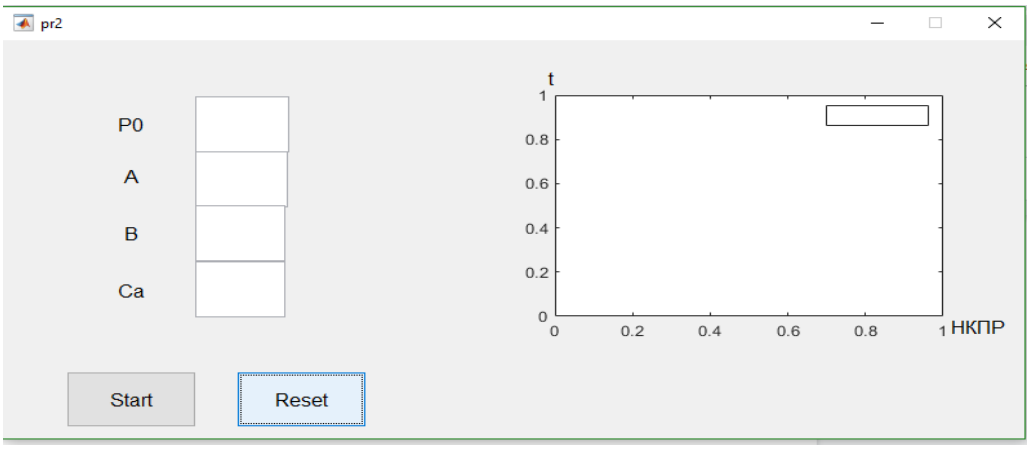

After pressing Reset, the program deletes the values of the variables and the graph.

```
p=get (handles.edit1,’string’); % value PO
p= str2double (p);
a=get (handles.edit2,’string’); % constant value A
a= str2double (a);
b=get (handles.edit3,’string’); % value B
b= str2double (b);
c=get (handles.edit4,’string’); % value Ca
c= str2double (c);
n=1:1:15;% CFLP
t=b./(a-log(n*p./100) ) | ¯c
plot (t)
```

Code snippet is responsible for the operation of the 'start' button, calculations and for the construction of the graph.

```
set(handles.edit1,'string', '');
set(handles.edit2,'string', '');
set(handles.edit3,'string', '');
set(handles.edit4,'string', '');
axes(handles.axes1)
cla;
legend('');
```

Thus, the interface in GUI MatLab was created and it helps to model several simple calculations and demonstrate the numerical calculation of CLFP for different rocks.

Conclusion. Predictions of possible explosions or fires in the combustion chamber can be presented for different models of the rate of mechanical and chemical reactions. Here, as we have already noticed, a dynamic model of the lower and upper concentration limits of flame propagation on base of Antoine’s equation was used. This task was carried out using an empirical model and a dynamic model, and the finite element method was used in MatLab modeling [9-13]. A close comparison of the existing model by the existing developed model by other models was not carried out due to the lack of data in the existing one, if, however, the created dynamic model in the form of an interface can be used for general prediction of turbulent and weakly turbulent air-suspensions showing a clear interaction between the air flow of

suspensions and possible solid obstacles. The animation interface will show the time of the peak pressure occurrence, which can probably improve the errors associated with the calculation and modeling of flame propagation in various media, in pipes. Further studies are planned to evaluate the predictability of this model over a wide range of flow configurations.

Б. Алипова[1], Б. Сапаргалиева[2]

[1]Халықаралық ақпараттық технологиялар университеті, Алматы, Қазақстан;
[2]Абай атындағы Қазақ Ұлттық педагогикалық университеті, Алматы, Қазақстан

MATLAB ОРТАСЫНДА ӘРТҮРЛІ ҚАТТЫ ТАУ ЖЫНЫСТАРЫНАН БӨЛІНЕТІН ГАЗ ҚАЛҚЫМАЛАРЫНЫҢ ЖАЛЫНЫ ТАРАЛУЫНЫҢ МАТЕМАТИКАЛЫҚ-КОМПЬЮТЕРЛІК МОДЕЛЬДЕРІН ЖАСАУ

Аннотация. MATLAB GUI графикалық ортасында жалынның концентрациялық таралу шегіне (CLFP) динамикалық тұжырымды қолдану арқылы желдетілетін жарылыс камерасында ауада тоқтатылған өтпелі бөлшектердің таралуы сандық тұрғыда зерттелді. Геомеханикалық және стехимиялық үдерістер стехиометриялық пропан-ауа арқылы тоқтатылған қатты денелер реакциясын имитациялайтын біратылы жалпы реакциямен модельденеді. Реакция жылдамдығы моделіндегі CLFP моделі Антуан теңдеуіне негізделген математикалық модельдермен сандық түрде қолданылады. Бұл жылдамдық ауытқуының эмпирикалық корреляциясына негізделген және графикалық іске асырумен енгізу-шығару деректерімен интерфейс ретінде жүзеге асырылады. Компьютерлік модельдеу CLFP динамикалық модельдері жалын таралуының физикалық үдерісінің жалпы жүзеге асыру арқылы жақсы нәтиже беретіндігін және түрлі тау жыныстарына қолдануға болатындығын көрсетті.

Түйін сөздер: MATLAB, графикалық интерфейс, жалынның таралуы, динамикалық CLFP, ауа-өлшенген зат, Антуан теңдеуі, жартас.

Б. Алипова[1], Б. Сапаргалиева[2]

[1]Международный университет информационных технологий, Алматы, Казахстан;
[2]Казахский национальный педагогический университет им. Абая, Алматы, Казахстан

СОЗДАНИЕ МАТЕМАТИЧЕСКО-КОМПЬЮТЕРНЫХ МОДЕЛЕЙ ДИНАМИКИ РАСПРОСТРАНЕНИЯ ПЛАМЕНИ АЭРОВЗВЕСЕЙ ТВЕРДЫХ ВЕЩЕСТВ В РАЗЛИЧНЫХ ГОРНЫХ ПОРОДАХ В СРЕДЕ MATLAB

Аннотация. Распространение переходных, взвешенных в воздухе твердых веществ в вентилируемой взрывной камере численно исследуется с помощью динамической формулировки для концентрационного предела распространения пламени (CLFP) в среде GUI MATLAB. Геомеханика моделируется одностадийной общей реакцией, которая имитирует реакцию стехиометрического пропан – воздух– взвешенные твердые вещества. Моделирование CLFP в модели скорости реакции численно используется с математическими моделями на основе уравнения Антуана. Это основано на эмпирической корреляции флуктуаций скорости и реализовано в виде интерфейса с данными ввода-вывода с графической реализацией. Компьютерное моделирование показало, что динамические модели CLFP дают превосходные результаты в качестве общей реализации физического процесса распространения пламени и могут быть использованы для различных горных пород (например, гранита, известняка, песчаника и др.).

Ключевые слова: MATLAB, графический интерфейс, распространение пламени, динамический CLFP, воздух-взвешенные вещества, уравнение Антуана, скалы.

Information about authors:

Bakhyt Alipova, PhD in Applied Mathematics, Associate Professor, International IT University, Almaty, Kazakhstan; b.alipova@edu.iitu.kz; https://orcid.org/0000-0003-0915-2759

Bayan Sapargaliyeva, PhD, Senior Lecturer of Abai Kazakh National Pedagogical University, Almaty, Kazakhstan; bonya_sh@mail.ru; https://orcid.org/0000-0001-7119-2466

REFERENCES

[1] Morachevsky G., Smirnova N.A., Piotrovskaya E.M. et al. Thermodynamics of liquid-vapor equilibrium. L.: Chemistry, 1989. 344 p. 3020 copies. ISBN 5-7245-0363-8.

[2] Lindstedt R.P., Sakthitharan V. Time Resolved Velocity and Turbulence Measurements in Turbulent Gaseous Explosions, Combust. Flame 114, 469-483 (1998).

[3] Masri A.R., Ibrahim S.S., Nehzat N., Green A.R. “Experimental Study of Premixed Flame Propagation over Various Solid Obstructions”, Exp. Therm. Fluid Sci. 21, 109-116 (2000).

[4] Makarov D.V., Molkov V.V. “Modeling and LargeEddy Simulation of Defagration Dynamics in a Closed Vessel”, Fiz. Goreniya Vzryva 40 (2), 13-23 (2004) [Combust., Expl., Shock Waves 40 (2), 136-144 (2004)].

[5] Physical properties of rocks and minerals (Petrophysics). Handbook of Geophysics under the editorship of Doctor of geological and mineral sci. N.B. Dortman., M., Nedra,527 (1976).

[6] Gubba S.R., Ibrahim S.S., Malalasekera W., Masri A.R. “GUI MATLAB Modelling of Premixed Defagrating Flames in a Small Scale Vented Explosion Chamber with a Series of Solid Obstructions”, Combust. Sci. Technol. 180, 1936-1955 (2008).

[7] Sapargalieva B., Naukenova A., Alipova B., Illari J.R., Shapalov Sh. “The Analysis of Heat And Mass Properties of the Fire Extinguishing Powder in Effectiveness Criteria” // Bulletin of the National Academy of Sciences of the Republic of Kazakhstan // Kazakh National Research Technical University K. I. Satpayeva, Series of Geology and Technical Sciences, 4 (430) July - August 2018. Almaty. P. 51-61.

[8] Sapargaliyeva B., Alipova B., Naukenova A. “Mathematical and Computer Modeling of Flame Attenuation in Narrow Channels”, International depository of copyright works No. EC-01-001884 dated 15.08.2018 (Berlin, Germany).

[9] Sapargaliyeva B., Alipova B., Naukenova A., Ilarri Javier Rodrigo, “Computer Modeling of Process of Flame Distribution and Attenuation in Narrow Channels”, 2018 IEEE International Conference"Management of Municipal Waste as an Important Factor of Sustainable Urban Development" (WASTE), St. Petersburg, 2018. P. 42-45. https://doi: 10.1109/WASTE.2018.8554152

[10] Sapargaliyeva Bayan, Naukenova Aigul, Alipova Bakhyt, Ilarri Javier Rodrigo. “Flame distribution and attenuation in narrow channels using mathematical software”, Advances in Science // Technology and Engineering Systems Journal, Special Issue on Advancement in Engineering and Computer Science, www.astesj.com, (2019). Vol. 4, N 3. P. 53-57. https://www.researchgate.net/publication/333245419

[11] Sapargaliyeva B., Naukenova A., Ilarri J.R., Shapalov Sh., Kerimbekova Z., Kenzhaliyeva G. “Investigation of Endothermic Properties of Industrial Wastes” // Reports of the National Academy of sciences of the Republic of Kazakhstan. Vol. 3, N 325 (2019). P. 19-26. ISSN 2224-5227, https://doi.org/10.32014/2019.2518-1483.67

[12] Naukenova A., Sapargaliyeva B., Shapalov Sh., Alipova B., Illari J.R. “Environmental Disposal of Large-Tonnage Industrial Waste for the Production of Fire Extinguishing Powders” // Reports of the National Academy of sciences of the Republic of Kazakhstan. Vol. 3, N 325 (2019). P. 35-42. ISSN 2224-5227, https://doi.org/10.32014/2019.2518-1483.69

[13] Shapalov Sh., Naukenova A., Sapargaliyeva B., Ilarri J.R. “Determination of the Fire Extinguishing Effectiveness of Pulverized Industrial Wastes” // Reports of the National Academy of sciences of the Republic of Kazakhstan. Vol. 3, N 325 (2019). P. 43-50. ISSN 2224-5227, https://doi.org/10.32014/2019.2518-1483.70

N E W S
OF THE NATIONAL ACADEMY OF SCIENCES OF THE REPUBLIC OF KAZAKHSTAN
SERIES OF GEOLOGY AND TECHNICAL SCIENCES
ISSN 2224-5278
Volume 1, Number 445 (2021), 35 – 38 **https://doi.org/10.32014/2021.2518-170X.5**

УДК 662

Б. К. Алияров[1], А. А. Кибарин[1], Р. К. Орумбаев[1], Б. Т. Ермағамбет[2]

[1]Алматинский университет энергетики и связи, Казахстан;
[2]Институт химии угля и технологии, Нур-Султан, Казахстан.
E-mail: aliyarov_b@mail.ru

УГЛЮ В ЭНЕРГЕТИКЕ БЫТЬ!

Аннотация. В статье обосновывается необходимость и возможность сохранения угля в энергетике в качестве топлива будущего при применении соответствующей технологии, основанного, в значительной степени, на использовании слоевой технологии его сжигания. Анализируются достоинства и недостатки сжигания угля в слое. Отмечена необходимость перехода на факельное сжигание угля для увеличения единичной мощности котла. Указана универсальность этого метода сжигания угля по отношению к его теплотехническим свойствам. Приведены источники проблем с выбросами в атмосферу при факельном сжигании угля. Показана произошедшая подмена понятия «грязная технология» понятием «грязное топливо» по отношению к угольному топливу. Указаны пути возврата к слоевому сжиганию угля с обеспечением требуемой мощности энергетического объекта через установку увеличенного количества котлов с меньшей производительностью. Отмечается возможность использования горючих летучих, содержащегося в угле для растопки котла и для стабилизации воспламенения угольного факела. Рассмотрена возможность снабжения жителей отдаленного поселка собственным газообразным топливом для приготовления пищи. Указывается возможность использования этого газообразного вещества для генерации электрической энергии с установкой газотурбинных установок малой мощности на котле со слоевым сжиганием угля. На основе такого комплексного анализа достоинств и недостатков угля сделан вывод о длительном сохранении угля в энергетике.

Ключевые слова: топливо, сжигание, экология, полнота преобразования.

Если сформулировать наиболее важные характеристики, по которым следует определять топливо будущего, то они могут быть следующими:

– запасов этого топлива должно хватить на несколько столетий;

– топливо должно быть пригодно для использования в качестве технологического сырья для получения неэнергетических продуктов.

Первому требованию удовлетворяют по крайней мере 4 вида первичной энергии: возобновляемые источники энергии, атомная энергия, термоядерная энергия (запасы этих трех топлив практически неисчерпаемы) и уголь. Второму требованию удовлетворяет только уголь.

Уголь можно считать первым после дров топливом, которое было освоено человеком. Уже первый опыт его применения выявил многие его достоинства: удобное хранение достаточно большого количества – на открытом воздухе просто на любой плоской горизонтальной поверхности, способность гореть долго одной порции угля (при слоевом сжигании), более высокая теплота сгорания и другие.

Первые котельные агрегаты, по сути, повторяли технологию сжигания, принятую для индивидуальных печей – размещение определенного количества угля на решетке (названа колосниковой), удерживающей определенное количество угля и создающей приемлемые условия для горения. Однако эта технология не смогла удовлетворить требованию интенсивного развития роста потребления тепловой и электрической энергии и соответственно – увеличению единичной производительности. Следует отметить, что в этот период развития сжигания угля охрана окружающей среды сводилась к хранению образующегося объема золы и шлака. Для улавливания

летучей золы было достаточно применения циклонов – уловителей со степенью улавливания на уровне 90 процентов и менее. Образование окислов азота и/или серы практически не рассматривалось.

Потребность в увеличении мощности котла привела к использованию технологии сжигания угля в виде факела, т.е. уголь сжигался так же, как и газ. Эта технология потребовала применения специального оборудования для подготовки угля к сжиганию – измельчения до уровня, сопоставимого с обычной мукой, называемого угольной пылью. Именно использование факельного сжигания позволило достичь мощности котлов на уровне нескольких тысяч тонн пара в час.

При своей несомненной привлекательности факельное сжигание угольной пыли создало существенные проблемы в области охраны окружающей среды, которые к тому времени стали намного жестче: трудности по улавливанию очень мелкой золы, высокий уровень образования окислов азота, сложное оборудование для очистки дымовых газов от окислов серы. Именно высокая степень загрязнения при сжигании угля в виде факела измельченного угля и трудности по его снижению перевели угольное топливо в разряд экологически недружелюбного топлива.

Следует отметить, что именно на этом этапе произошла подмена понятий «экологически грязное топливо», которого на самом деле не было, и понятия «экологически грязная технология сжигания». Результатом такой подмены было повсеместное ограничение в строительстве угольных ТЭС. Но наша страна сохранила приверженность к угольной энергетике – около 70 процентов электрической и 40 процентов тепловой энергии производится на угле.

Однако резкий рост единичной мощности агрегатов, такой же рост мощности объекта заметно усложнили приведение выбросов в атмосферу к приемлемому уровню. Устройства по улавливанию летучей золы и связыванию окислов серы по габаритам начали превосходить сам котельный агрегат. Некаталическое снижение уровня образования окислов азота быстро подошли к предельным значениям, за которыми наступало заметное ухудшение топочного процесса. Именно эти факторы привели к выводу, что использование угля в качестве топлива для генерации тепловой и электрической энергии практически неприемлемо.

В связи с этим, одним из путей сохранения угля (как отмечалось ранее – топливо будущего) в энергетике вполне может быть «возврат» к модернизированному слоевому сжиганию угля.

В наиболее общем случае этот возврат может быть реализован несколькими путями. Один из них почти очевидный – обеспечивать требуемую мощность объекта установкой увеличенного числа котлов со слоевыми топками. Однако при этом параметры пара – давление и температура – оказались несколько ниже значений, привычных для факельного сжигания.

В Алматинском университете энергетики и связи имени Гумарбека Даукеева под руководством академика Алиярова Б.К. уже много лет проводятся исследования по разработке технологии сжигания угля с приемлемыми экологическими показателями. При этой технологии выбросы в атомосферу снижаются до приемлемого уровня и обеспечивается достижение требуемых параметров пара (достижение которых, при традиционной схеме сжигания в слое не всегда возможно). При предлагаемой технологии сжигания угля концентрация основных загрязнителей атмосферы в дымовых газах снижаются до уровня, требуемого по Европейским стандартам, при использовании существующего оборудования. Например, специальные опыты, проведенные на одном из котлов, конструкции Орумбаева Р.К., при сжигании угля в слое (с выдерживанием гранулометрического состава и при подборе требуемой толщины слоя топлива, со специальной системой подачи воздуха под слой и другие) показали, что уровень образования окислов азота приближается к уровню, характерному для случая сжигания природного газа.

Самая большая привлекательность разрабатываемой в Казахстане технологии сжигания угля заключается в минимальной модернизации действующих котлов. Более того, при предлагаемой технологии заметно снижаются затраты энергии на измельчение топлива, так как по этой технологии основная масса угля сжигается в виде дробленного угля.

Экспертные оценки показали, что при предлагаемой технологии, даже при эффективности улавливания золы с существующим оборудованием на уровне 98 процентов, содержание золы в дымовых газах будет соответствовать уровню улавливания на уровне 99,5 процентов при факельном сжигании (что соответствует Европейским стандартам). Как уже отмечалось, уровень образования окислов азота может приблизиться до уровня сжигания природного газа. Сжигание

основной части угля по слоевой технологии заметно упрощает связывание серы топлива с известняком, вносимым вместе с углем в слой.

Эта технология по производительности котла приближается к факельному сжиганию. При этой технологии уголь сохраняет свои известные достоинства: развитую технологию добычи с высокой полнотой извлечения (недоступную для извлечения нефти, газа и урана), широкую доступность по цене, удобство транспортирования и хранения и другие при заметном снижении воздействия на окружающую среду.

Перевод одного из котлов на сжигание угля по предлагаемой технологии, несомненно, сделает Казахстан мировым лидером в области сжигания углей.

Можно также рассмотреть возможность использования угля для снабжения населенных пунктов (удаленных от основных магистральных сетей) различными видами энергии.

Давно известно, что в угле присутствует газообразная часть, называемая горючими летучими веществами, содержание которой меняется от 8 процентов для антрацита до 50 процентов для некоторых бурых углей. В принципе эта газообразная часть вполне может быть извлечена и может храниться в отдельной емкости. В Казахстане показана возможность использования этого газообразного вещества (топлива) в различных направлениях:

- использование в качестве растопочного топлива для котлов с факельным сжиганием;
- использование для генерации электрической энергии на газосжигающих агрегата;
- использование в качестве газового топлива для приготовления пищи.

Следует отметить, что уголь, из которого извлечена часть горючих летучих, вполне пригоден для сжигания в обычных топках. Такой подход, с учетом сложившейся доступности угля для любого населенного пункта, позволяет реализовать снабжение конкретного населенного пункта от собственного локального источника по своим локальным сетям:

- тепловой энергией;
- электрической энергией;
- газовым топливом для приготовления пищи.

Производство этих видов энергии на локальном источнике позволит снабжать населенный пункт с удаленным относительно магистральных сетей расположением практически всеми видами энергии, которыми пока пользуются в основом жители городов. Вместе с этим, несомненно, такое применение угля несколько снизит нагрузку на снабжение природным газом. Генерация электрической энергии непосредственно на месте потребления позволит заметно снизить неизбежные потери при транспортировании малого количества электрической энергии на заметные расстояния.

Применение предлагаемой технологии восстановит заслуженное место угля в области тепловой энергетики или иначе говоря – угольной энергетике быть!

Б. К. Алияров[1], А. А. Кибарин[1], Р. К. Орумбаев[1], Б. Т. Ермағамбет[2]

[1]Алматы энергетика және байланыс университеті, Қазақстан;
[2]Көмір химиясы және технология институты, Нұр-Сұлтан, Қазақстан

КӨМІР ЭНЕРГЕТИКАДА САҚТАЛАДЫ!

Аннотация. Мақалада көмірді қабаттап жағудың артықшылықтары мен кемшіліктері талданған. Қазанның жеке қуатын арттыру жолында көмірді қабаттап жағудан жалындатып жағу қажеттілігі көрсетілген, жалындатып жағудың жағылатын көмірдің жылу техникалық қасиеттеріне талғамсыздығы аталған. Көмірді жалындатып жағуға көшкенде атмосфераға шығатын қалдық көлемінің көбеюіне байланысты қоршаған ортаны қорғау мәселесінің артатыны анықталған. Осы себептен көмірге байланысты «лас технология мен лас отын» ұғымдарының орын ауыстыратыны келтірілген. Энергетика нысанының қажет қуатына орнатылатын жеке қуаты аз көмірді қабаттап жағатын қазан санын өсіру арқылы жетуге болатыны айтылған. Осымен брге Алматының Ғұмарбек Даукеев атындағы энергетика мен байланыс университетінде көмір жағудың жаңа технологиясы зерттелетіні аталған. Көмірдегі жанар ұшар заттарды қазанды жүргізерде немесе көмір жалынының тұтануын тұрақтандыруға болатыны келтірілген. Осы газтектес отынды алшақ орналасқан мекен тұрғындарына ас дайындауға қолдануға болатыны көрсетілген. Газтектес отынды қуаты

аздау газтурбиналық қондырғыларда қолданып, электр өндіру және қалған көмірді қазан ошағында қабаттап жағу негізінде жылу өндіру мүмкіндігі анықталған. Осылай көмірдің артықшылықтары мен кемшіліктерін жан-жақты қарастыру негізінде көмірдің энергетикада ұзақ жылдар бойы сақталатыны көрсетілген.

Түйін сөздер: отын, жағу, экология, өзгерту толықтығы.

B. Aliyarov[1], A. Kibarin[1], R. Orumbaev[1], B. T. Yermagambet[3]

[1]Almaty University of Power Engineering and Telecommunications, Kazakhstan;
[2]Institute of chemistry coal and technology, Nur-Sultan, Kazakhstan

COAL MUST BE AT THE ENERGY SECTOR!

Abstract. The article substantiates the necessity and possibility of preserving coal in the power industry as a fuel of the future, using the appropriate technology, based, to a large extent, on the use of layered combustion technology.

The advantages and disadvantages of coal combustion in a layer are analyzed. The need to switch to flaring coal combustion to increase the unit capacity of the boiler is noted. The universality of this method of coal combustion in relation to its thermal properties is indicated. The sources of problems with emissions into the atmosphere during coal flaring are given. Shown is the substitution of the concept of "dirty technology" with the concept of "dirty fuel" in relation to coal fuel.

The ways of returning to the layered combustion of coal are indicated, with the provision of the required capacity of the power facility through the installation of an increased number of boilers with lower productivity. It is noted that at the Almaty University of Energy and Communications named after Gumakrbek Daukeev, a coal combustion technology with reduced disadvantages is being developed

The possibility of using flammable volatiles contained in coal for kindling a boiler and for stabilizing the ignition of a coal flame is noted. the possibility of supplying residents of a remote village with their own gaseous fuel for cooking was considered.

The possibility of using this gaseous substance for the generation of electrical energy with the installation of low-power gas turbine units on a boiler with coal layer combustion is indicated. Based on such a comprehensive analysis of the advantages and disadvantages of coal, a conclusion was made about the long-term preservation of coal in the power industry.

Key words: fuel, combustion, ecology, completeness of transformation.

Information about authors:

Aliyarov Birlesbek, doctor of technical sciences, Academy National Academy of the Sciences, Prize – winner of the State premium of the Republic of Kazakhstan, professor; aliyarov_b@mail.ru; https://orcid.org/0000-0002-4772-1310

Andrey Kibarin, candidate of technical sciences, professor, Almaty University of Energy and Communications named after Gumarbek Daukeev, Kazakhstan

Orumbaev Rakhimzhan, doctor of technical sciences, honored inventor, professor, Almaty University of Energy and Communications named after Gumarbek Daukeev, Kazakhstan

Yermagambet Bolat Toleuhanuly, doctor chemical sciences, Institute of Coal Chemistry and Technology, Nur-Sultan, Kazakhstan; bake.yer@mail.ru; https://orcid.org/0000-0003-1556-9526

REFERENCES

[1] Aliyarov B.K. Technologies of oil-free kindling of boilers and stabilization of ignition of a pulverized coal flame at TPPs // Plenary report at the 7th International Conference on Plasma and Combustion. Almaty, 2019.

[2] Aliyarov B.K., Mergalimova A.K. Coal combustion technology with reduced environmental impact // Abstracts of the scientific-practical conference "Coal heat power engineering in Kazakhstan: problems, solutions, development prospects". Nur-Sultan, 2020.

N E W S
OF THE NATIONAL ACADEMY OF SCIENCES OF THE REPUBLIC OF KAZAKHSTAN
SERIES OF GEOLOGY AND TECHNICAL SCIENCES
ISSN 2224-5278
Volume 1, Number 445 (2021), 39 – 45 **https://doi.org/10.32014/2021.2518-170X.6**

UDC 621. 391. 837:621.397. 13

M. Amreev[1], R. Safin[2], T. Pavlova[1], E. Temyrkanova[1], Y. Garmashova[1]

[1]Almaty University of Power Engineering and Telecommunication, Almaty, Kazakhstan;
[2]Kazakh University Ways of Communications, Almaty, Kazakhstan.
E-mail: max.amreev@gmail.com

AMPLIFIER DESIGN FOR MODELING THE TRANSMISSION OF A DIGITAL VIDEO SIGNAL OVER A DATA TRANSMISSION CHANNEL

Abstract. The use of video surveillance systems is used in the areas of security, law and order, in the territories of protected objects, in monitoring the movement of road vehicles and in other areas.

The main disadvantage of a video surveillance system is its susceptibility to weather influences (rain, fog, snowfall, etc.), which degrades the quality of the video system by reducing the signal level.

Therefore, the urgency of finding new ways and possibilities to improve the quality of video signals is one of the priority areas of signal processing. The main task of this work was to determine the main parameters, simulate the transmission line and amplifier, and select the schematic diagram of the transmitting and receiving path with the voltage and current ratings.

Both the receiver and the cable video transmitter have different means of adjusting to different transmission line lengths. The signal at the output of each receiver should be in the range from 0.9 to 1.1 V, and the spread of the total ohmic resistance of the wires of the video transmission line at the input of the receiver should be no more than 2 – 3%. Based on these parameters, the equipment is configured for transmitting video over the channel. The magnitude of the mismatch is regulated by potentiometers, which allow smooth adjustment of the video transmission equipment [1].

As a rule, video transmission over the channel is carried out at a distance of 50 to 1500 m. If it is necessary to transmit video at distances less than 50 m, additional resistances are connected in series at the receiver input so that the total line resistance is 30 - 50 Ohm [1].

Key words: data transmission channel, video surveillance, television signal, operational amplifier.

Video surveillance systems are used in the sphere of law enforcement, on the territories of protected facilities, for monitoring the movement of vehicles and in other areas.

The main disadvantage of a video surveillance system is its vulnerability to weather conditions (rain, fog, snowfall, etc.), which degrades the quality of the video system by reducing the signal level.

Therefore, the urgency for finding new ways and possibilities of improving the quality of video signals is one of the priority directions of signal processing. The main task of this article is to determine the main parameters, to model the transmission line and amplifier, and to select a basic circuit of the receiving and transmitting path with voltage and current ratings.

Both video cable transmitter and receiver have different settings for various transmission line lengths. The signal at the output of each receiver should be in the range from 0.9 to 1.1 V, and the value deviations of the total ohmic impedance on the video transmission line cables at the receiver input should not exceed 2 – 3 %. Based on these parameters, the equipment is configured to transmit video over the channel. The magnitude of the mismatch is regulated by a potentiometer that allows performing a smooth hardware configuration of the video transmission [1].

As a rule, video transmission over the channel is carried between 50 and 1500 m. If it is necessary to transmit video over distances less than 50 m, additional impedances are sequentially turned on at the receiver input so that the total line impedance becomes 30 – 50 Ohms [1].

The stray capacitance of the line is compensated by special jumpers in the receiver. The level of compensation for the stray capacitance of the video transmission line is selected individually for each transmission line based on the video picture on the test monitor. Also, using a test monitor or an oscilloscope, the receiver is configured according to the amplitude of the output signal.

Using a multi-channel video receiver to improve the parameters of the received signal, it is sometimes advisable to connect monitors to the receiver outputs via an impedance series of 51- 82 Ohms.

In addition to interference from radio apparatus and power lines, sometimes the video transmission line is affected by electromagnetic interference received as a result of a lightning discharge. Such interferences can be quite strong, as a result of which the equipment for transmitting video through a twisted pair will fail. To avoid damage, it is necessary to use lightning protection on the video channel transmission lines.

Figure 1 shows a typical circuit for switching on a differential amplifier. It can be used as a video signal booster. In this circuit, the amplification factor is calculated using the formula:

$$K = \frac{V_{OUT}}{V_{IN}} = \frac{R_F}{R_G},$$

where V_{OUT} is the output voltage, V; V_{IN} – input voltage, V; R_F – feedback impedance, Ohm; R_G – input impedance of the circuit, Ohm.

Resistors R_0 help keep the amplifier in a stable state. It is recommended to select resistors with at least a nominal accuracy of no more than 0.1 %.

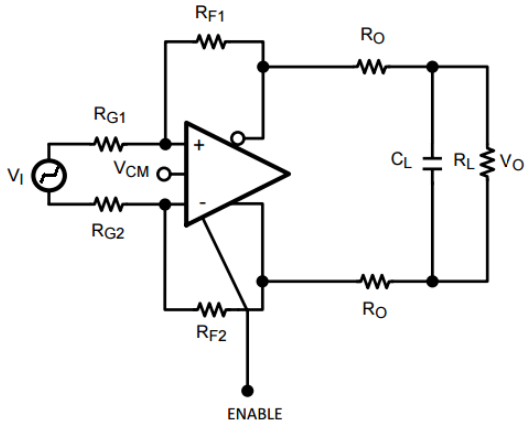

Figure 1 – A typical circuit of the amplifier switching

A high-speed broadband amplifier is the main component for transmitting a video signal over a data transmission channel. As a digital signal amplifier, the MAX403 OP-amp from the "Maxim Integrated Products, Inc" was selected, which was chosen as the most suitable for all requirements after careful analysis with analogues of this type of OP-amp.

Modeling the amplifier and transmission line.

The simulation results in OrCAD 9.1 for resistor impedances and long line values on a twisted pair are shown in figure 2.

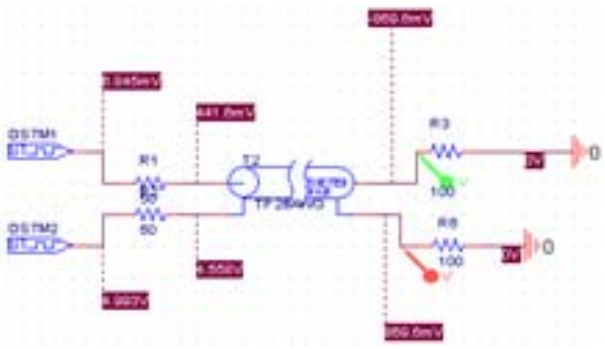

Figure 2 – Transmission line modeling

With a line length of 100 meters, figure 3 clearly shows signal delays of 0.62 μs. The signal is clear, its amplitude is about 1.5 V.

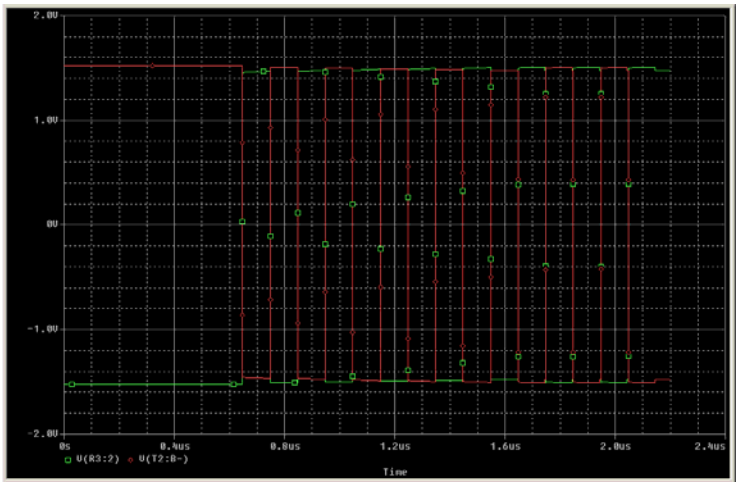

Figure 3 – Diagrams of antiphase signals U(R3; 2) and U(T2; B-) at the output of a long line of 100 meters on the same scale

There is the second signal in the opposite phase after the amplifier, which is clearly visible on the oscillogram. Figure 4 shows the signals transmitted through a 200-meter line.

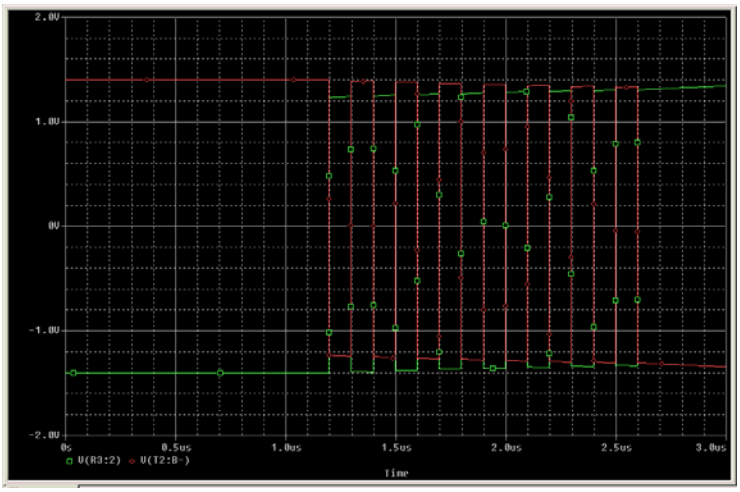

Figure 4 – Diagrams of antiphase signals U(R_3; 2) and U(T_2; B-) at the output of a long line of 200 meters on the same scale

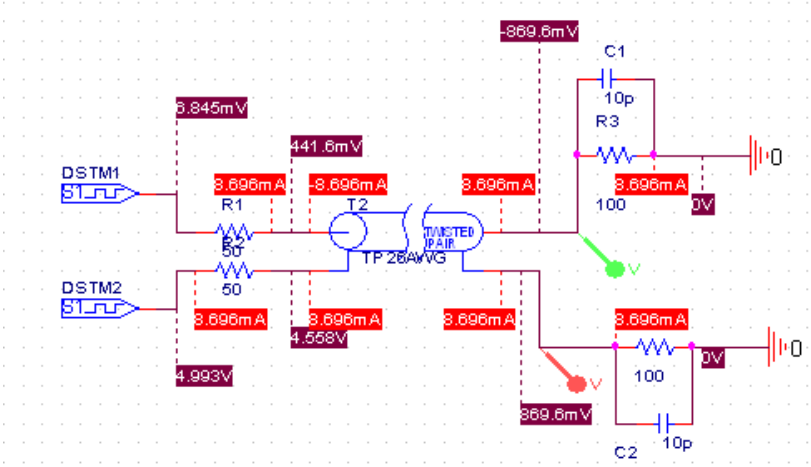

Figure 5 – Voltage and current ratings of circuit components

On a 200-meter line, we would like to note that the signal delay had increased to 1.2 μs. The signal amplitude had decreased to 1.4 V. Each pulse is distinct, but it is noticeably declining.

Figure 6 shows peaks in the signals U (R_3; 2) and U (T_2; B , which occur when a 10 pF capacitors are inserted to load the circuit. Small bursts (peaks) are noticeable at 0.75, 1.85, and 2.05 μs for the U (R3; 2) signal and for the U (T2; B-) signal at 0.75, 0.8, 1.75, 1.95, and 2.15 μs.

Similar measurements were also made for lines from 300 to 1000 meters with 100 m increments.

After receiving the simulation measurement data, the following results were obtained at a speed of 10 Mbit/s and a speed of 100 Mbit/s; it is summarized in tables 1 and 2.

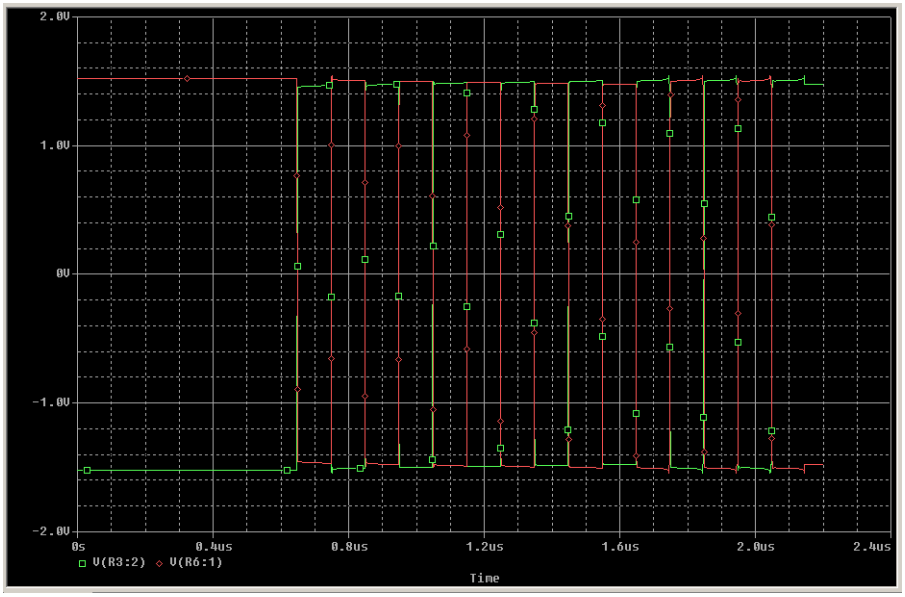

Figure 6 – Diagrams of antiphase signals U(R3; 2) and U(T2; B-) at the output of a long line of 100 meters with capacitive parameters on the same scale

Table 1 – Video signal transmission performance at 10 Mbit/s

Characteristics	Measurement data									
Line length, m	100	200	300	400	500	600	700	800	900	1000
Signal amplitude, V	1,5	1,3	1,2	1	0,9	0,8	0,7	1,2	1,1	1
Signal delay, μs	0,65	1,2	1,75	2,3	2,85	3,4	3,95	4,5	5,2	5,59

Table 2 – Video signal transmission performance at 100 Mbit/s

Characteristics	Measurement data		
Line length, m	100	500	1000
Signal amplitude, V	1,5	0,9	1
Signal delay, μs	559	2750	5490

Devices that use fully differential amplifiers have certain specifications. The main requirements are high linearity and the necessary signal amplitude. Linearity is achieved by using a well-chosen feedback line and setting the amplification factor by means of resistors, as well as appropriate supply voltage. The signal amplitude can be adapted using the appropriate amplification factors. The MAX403 operational amplifier, which was selected for the simulation, requires the installation of bypass capacitors of 0.01 and 0.1 μF. All capacitors must be grounded. Sinusoidal noise output can lead to loss of dynamic range and

increased distortion. In addition, capacitive loads must be isolated from the amplifier output by small-value resistors. This is particularly true when the load has a resistive component that exceeds 500 Ohms. A typical A/D converter has a capacitive element of about 10 pF, and the component can be resistive for over 1000 Ohms. During transmission over a data channel, such as a coaxial one, the resistive component will be 50 Ohms; over a twisted pair it will be 100 Ohms. The usage of appropriate resistors will be sufficient to isolate any subsequent capacitance [5]. The supply voltage is set to +12 V and – 12 V, the general output mode is 0 V [4]. The basic circuit of the receiving and transmitting path is shown in figure 7.

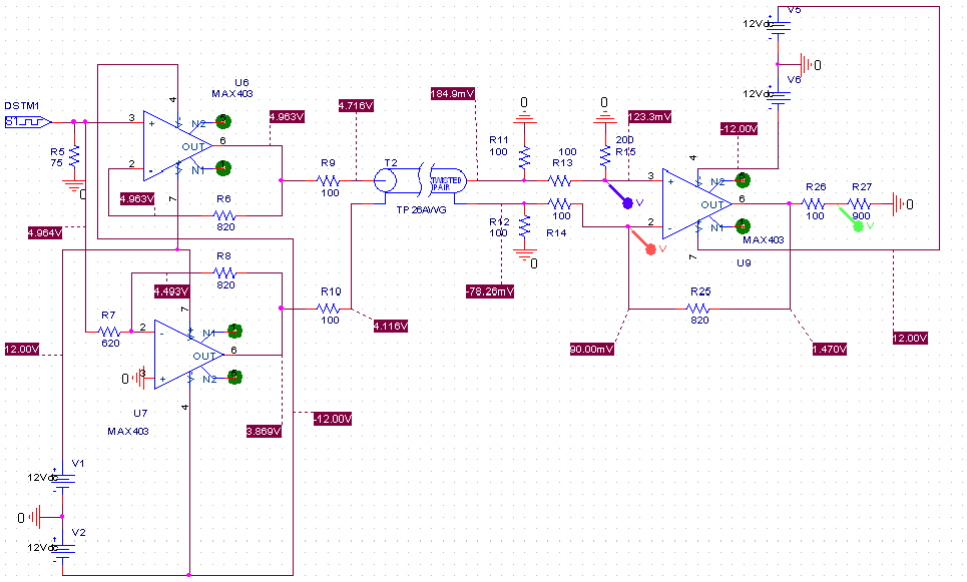

Figure 7 – Basic circuit of the receiving and transmitting path with voltage and current ratings

One of the simulation results is shown in the figure 8.

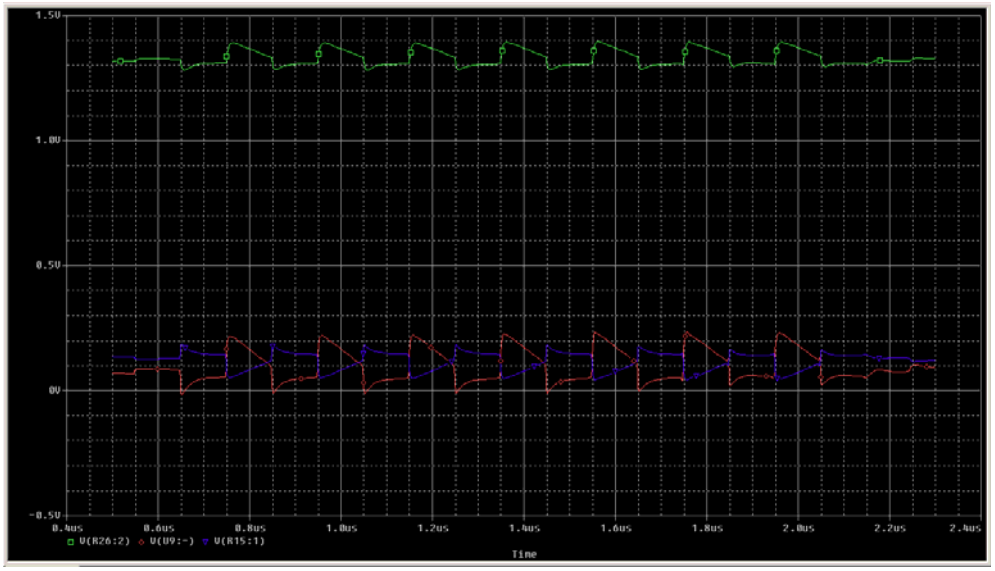

Figure 8 – Diagrams of antiphase signals U(U_9; N) and U(R_{15}; 1) at the output of a long line of and output signal U(R_2; 2) at 100 Mbit/s on the same scale

During a change of the data transfer rate over the TP26AWG twisted pair cable, there was a noticeable variation in the signal level and delay. With an increase in the signal transmission rate

compared to 10 Mbit/s, no significant changes in the amplitude were noticeable, but the signal delay was significantly reduced up to 10^{-3} seconds.

Conclusions. The long line based on a twisted pair TP26AWG and MAX403 operational amplifier was selected. The signal delay was reduced to 10^{-3} seconds. The signal amplitude became about 1 V, which allowed us to completely restore the received signal at the reception. Data transmission was simulated at 10 Mbit/s and 100 Mbit/s, which fully allowed transmitting a digital signal over a distance of more than half a kilometer with acceptable distortion.

М. Амреев[1], Р. Сафин[2], Т. Павлова[1], Э. К. Темырканова[1], Ю. Гармашова[1]

[1]Ғұмарбек Даукеев атындағы Алматы энергетика және байланыс университеті, Алматы, Қазақстан;
[2]Қазақ қатынас жолдары университеті, Алматы, Қазақстан

ҚАУІПСІЗДІК ТЕЛЕДИДАРЫНДАҒЫ БАЙЛАНЫС АРНАСЫ АРҚЫЛЫ КАМЕРА МЕН МОНИТОР АРАСЫНДАҒЫ САНДЫҚ СИГНАЛ КҮШЕЙТКІШІН ЖОБАЛАУ

Аннотация. Бейнебақылау жүйелерін пайдалану қауіпсіздік, заңдылық, құқық қорғау орындарында, күзетілетін нысандар аумағында, жол көлік құралдарының қозғалысын бақылау кезінде және басқа жерлерде қолданылады.

Бейнебақылау жүйесінің басты кемшілігі – ауа райының әсеріне бейімділігі (жаңбыр, тұман, қар, т.б.) әрі бұл сигнал жүйесін азайту арқылы бейне жүйесінің сапасын төмендетеді.

Сондықтан бейне сигналдар сапасын жақсартудың жаңа жолдары мен мүмкіндіктерін іздеудің өзектілігі – сигнал өңдеудің басым бағыттарының бірі болып саналады. Жұмыстың негізгі міндеті –негізгі параметрлерді анықтау, электр беру желісі мен күшейткішті имитациялау және кернеу мен ток көрсеткіштері арқылы беру және қабылдау жолының түбегейлі схемасын таңдау.

Қабылдағыштың да, кабельдік бейне таратқыштың да тарату желісінің әр түрлі ұзындығына арналған әртүрлі реттеу құралдары бар. Әрбір қабылдағыштың шығысындағы Сигнал 0,9-дан 1,1 В-қа дейінгі диапазонда болуы тиіс, ал қабылдағыштың кіреберісіндегі бейне беру желісі сымдарының жиынтық омдық кедергісінің шашырауы 2-3% - дан аспауы тиіс. Осы параметрлерге сүйене отырып, жабдық бейнені арна арқылы жіберуге бейімделеді.

Сәйкессіздік потенциометрлермен реттеледі, бұл бейне сигнал беру жабдықтарының жұмысын біркелкі реттеуге мүмкіндік береді [1].

Әдетте, канал арқылы бейне беру 50-ден 1500 м-ге дейінгі қашықтықта жүзеге асырылады. Егер бейнені 50 м-ден аз қашықтықта жіберу қажет болса, ресивер кірісінде қосымша кедергілер тізбектей қосылады, сонда жалпы сызық кедергісі 30 - 50 Ом болады [1].

Түйін сөздер: бейнебақылау, теледидарлық сигнал, жедел күшейткіш.

М. Амреев[1], Р. Сафин[2], Т. Павлова[1], Э. К. Темырканова[1], Ю. Гармашова[1]

[1]Алматинский университет энергетики и связи им. Гумарбека Даукеева, Алматы, Казахстан;
[2]Казахский университет путей сообщения, Алматы, Казахстан

ПРОЕКТИРОВАНИЕ УСИЛИТЕЛЯ ЦИФРОВОГО СИГНАЛА МЕЖДУ КАМЕРОЙ И МОНИТОРОМ ПО КАНАЛУ СВЯЗИ В ОХРАННОМ ТЕЛЕВИДЕНИИ

Аннотация. Применение систем видеонаблюдения применяется в зонах обеспечения безопасности, правопорядка, на территориях охраняемых объектов, при контроле за движением дорожных транспортных средств и в других зонах.

Основным недостатком системы видеонаблюдения является ее восприимчивость к погодным воздействиям (дождь, туман, снегопад и т.д.), что ухудшает качество работы видеосистемы за счет снижения уровня сигнала.

Поэтому актуальность поиска новых путей и возможностей повышения качества видеосигналов является одним из приоритетных направлений обработки сигналов. Основной задачей данной работы было опреде-

ление основных параметров, моделирование линии передачи и усилителя, а также выбор принципиальной схемы передающего и приемного тракта с номинальными напряжениями и токами.

И приемник, и кабельный видеопередатчик имеют различные средства настройки на различную длину линии передачи. Сигнал на выходе каждого приемника должен находиться в диапазоне от 0,9 до 1,1 В, а разброс суммарного омического сопротивления проводов линии видеопередачи на входе приемника должен составлять не более 2-3%. Исходя из этих параметров, оборудование настраивается на передачу видео по каналу. Величина рассогласования регулируется потенциометрами, которые позволяют плавно регулировать работу аппаратуры передачи видеосигнала [1].

Как правило, передача видео по каналу осуществляется на расстоянии от 50 до 1500 м. При необходимости передачи видеосигнала на расстояния менее 50 м на входе приемника последовательно подключаются дополнительные сопротивления так, чтобы общее сопротивление линии составляло 30-50 Ом [1].

Ключевые слова: видеонаблюдение, телевизионный сигнал, операционный усилитель.

Information about authors:

Amreyev M.B., doctor's degree, Almaty University of Power Engineering and Telecommunication, Almaty, Kazakhstan; max.amreev@gmail.com; https://orcid.org/0000-0002-4874-1161

Safin R.T., Senior lecturer of the Department «TCSS», Almaty University of Power Engineering and Telecommunication, Almaty, Kazakhstan; raf.safin@mail.ru; https://orcid.org/0000-0003-1583-0034

Pavlova T., Senior lecturer of the Department «TCSS», Almaty University of Power Engineering and Telecommunication, Almaty, Kazakhstan; t_sheh@mail.ru**;** https://orcid.org/0000-0002-3063-8094

Temyrkanova Elvira, PhD doctor, Associate Professor, Head of the Department of Telecommunications and Innovative Technologies»; https://orcid.org/0000-0003-4059-5996

Garmashova Y., MSc, docent of the Department «TCSS», Almaty University of Power Engineering and Telecommunication, Almaty, Kazakhstan; juliagarmashova@yandex.kz; https://orcid.org/0000-0003-4267-3839

REFERENCES

[1] Mamiy A.R. Operational amplifiers. Maykop: ASU, 2005.

[2] Efimov I.P. Operational amplifiers and their application. Ulyanovsk: UISTU, 2009.

[3] Efimov I.E. Radio frequency transmission lines. M.: Svyaz – the Press, 2007.

[4] Razevig V.D. ORCAD computer-automated design systems. M.: SOLON – the Press, 2003.

[5] Determination of the Eb/N0 Ratio and Calculation of the Probability of an Error in the Digital Communication Chanel of the IP-Video Surveillance System./Статья/. Conference Computer Science and Information Technologies. Armenia, Yerevan, September 25-29, 2017. P. 386-389. ISBN 978-5-8080-0797-0

[6] Study of a transmission-reception system of the voice signal of increased security on the basis of generator of chaotic oscillations.

[7] Research and comparative analysis of phaso-inverter Cascades with single-polar power supply. International conference on Information science and communications Technologies 4-6 November, TUIT Campus, Local Hotels, Tashkent Uzbekistan.

N E W S
OF THE NATIONAL ACADEMY OF SCIENCES OF THE REPUBLIC OF KAZAKHSTAN
SERIES OF GEOLOGY AND TECHNICAL SCIENCES
ISSN 2224-5278
Volume 1, Number 445 (2021), 46 – 51 **https://doi.org/10.32014/2021.2518-170X.7**

UDC 628.3 (574.54)

K. K. Anuarbekov[1], E. T. Kaipbayev[1], G. Mengdibayeva[2]

[1]Kazakh National Agrarian Research University, Almaty, Kazakhstan;
[2]Kazakh Research Institute of Plant Protection and Quarantine named after J. Zhiembaev, Almaty, Kazakhstan.
E-mail: kanat.anuarbekov@kaznau.kz, yerbolat.kaipbayev@yandex.ru, www.gulnaz87.kz@mail.ru

ASSESSMENT OF SOCIAL AND ENVIRONMENTAL DAMAGE CAUSED BY SEWAGE AND COLLECTOR-DRAINAGE WATER POLLUTION IN THE LOWER REACHES OF THE SYRDARYA RIVER

Abstract. The significant impact of irrigation on the natural and ecological situation in the zone of irrigated agriculture in Kazakhstan was determined by the concept of irrigation development in Central Asia and Kazakhstan.

The problem of reducing the existing environmental conditions on the irrigated lands of Kazakhstan, especially in the Southern and South-Eastern regions, and the normalization of the ecological and meliorative situation are directly related to various water management regions of Kyrgyzstan and Uzbekistan.

The Syrdarya river, which flows among these countries, comes to us with a water salinity of 1,75 g/l. They are also contaminated with pesticides, organochlorine pesticides – DDT (dichlorodiphenyltrichloroethane) and HCH (hexachlorocyclohexane), used on irrigated land. Water salinity is also increasing in the territories of Kazakhstan.

In general, on irrigated lands, as a result of salt intake from irrigation waters, there was an increase in salt reserves in soils and ground waters. Their intensity largely depends on the salinity of irrigation water and the volume of water intake. As a result of regulating the flow of the river. An irreversible soil-ecological process is taking place in the Syrdarya with great intensity, where the development of irrigated land and the volume of CDW (collector-drainage water) and wastewater discharged into the rivers in the upper reaches of the rivers has been widely developed.

Key words: mineralization, wastewater, irrigation system, salt balance, irrigation regime, collector-drainage water.

Introduction. Thus, as a result of anthropogenic impact in the natural environment of the river basin, in the Syrdarya, salt accumulates mainly in ground water, which can dramatically worsen the reclamation and environmental situation on irrigated lands and transfer it from the zone of controlled and accounted for consequences to the zone of uncontrolled and not accounted for, as in the Aral sea basin.

Therefore, the system of economic levers should include such management parameters as cost estimates of damage from water pollution. This will encourage the introduction of environmental and resource-saving technologies in agriculture, as well as compensation for damage caused to agriculture as a result of water pollution.

A full calculation of the damage to the national economy and the state caused as a result of the negative impact of economic activities on water resources is possible on the basis of an economic assessment and consideration of factors affecting the environmental situation of the region, which include economic, socio-economic and social damage.

Economic damage (*Ei*) – losses from product quality reduction (*Ep*), losses from product under-receipt (*Ec*), costs of restoring or maintaining the normal state of the natural environment (*Em*).

Socio-economic damage (*ESi*) – losses in health and social security related to the increase in morbidity (*Esm*), losses due to migration caused by the deterioration of the natural environment (*ESp*), the cost of additional recreation due to the unsatisfactory state of the natural environment (*ESr*).

Social damage (*Si*) – ecstatic losses due to the destruction of the natural environment (*Se*), psychological losses caused by the unsatisfactory state of recreation areas (*Sp*), losses caused by the deterioration of the environmental conditions of life of members of society (*Sl*). All this is the amount of transformable damage caused to the national economy from pollution of water sources and is defined as the sum of individual damages, i.e.:

$$\sum Di=Ei+ESi+Si=(Ep+Ec+Ea+Em)+(ESm+ESp+ESr)+(Se+Sp+Sl), \quad (1)$$

The economic damage caused by water sources pollution caused by water consumers who carry out various measures to restore lost products is determined by the formula:

$$Ep=(P_1-P_2)VP, \quad (2)$$

where $Ц_1$ and $Ц_2$ are the purchase price of agricultural products before and after contamination of the water source; ВП is the annual volume of agricultural production.

$$Ec=\Delta VP(C_2-C_1+K), \quad (3)$$

where C1 and C2 are the annual production costs, respectively, before and after source pollution and humus removal; Δ VP - decrease in annual production when a water source is polluted and soil fertility decreases; ΔK - increase in specific capital investments of a water consumer when a water source is polluted and loss of fertile soils.

The economic assessment of the annual damage from the annual discharge of pollutants into the water management area is determined by the formula:

$$Eai=144*б_к*M, \quad (4)$$

where $б_к$ is a constant that characterizes water management areas and river basins; M is the reduced mass of the annual discharge of impurities by this source of pollution into the water source, conditionally T/year and is determined by the formula:

$$M=\sum_{i=1}^{N} Ai*m_i, \quad (5)$$

where *i* - ordinal number of the discharged impurities; m_i is the total mass of the annual reset of the *i*-th impurity, T/year; *N* is the total number of impurities, discharged into the water source; *A* - the relative hazard of resetting the *i*-th substance in reservoirs, conditionally T/year, determined by the formula:

$$Ai= 1 / MPCp/x/, \quad (6)$$

where *MPCp /x/* is the maximum permissible concentration of the *i*-th substance in the water used for fisheries purposes, t/ m^2.

The A_i value for some common pollutants, depending on the type of wastewater, is shown in table 1.

Economic damage from the cost of restoring or maintaining the normal state of the natural environment is determined by the formula:

$$Em=(Cs_1-Cs_2)*W_i, \quad (7)$$

where Cs_1 *and* Cs_2 are the cost of treatment per 1m^3 of water before and after certain stages of water protection measures, tenge; *Wi* is the volume of contaminated water, m^3.

Methods. Socio-economic damage due to increased morbidity is determined by the direct counting method, which consists in comparing the incidence rates in the studied polluted and control (non-polluted) areas. In this case, the damage due to increased morbidity *(ESm)* is defined as the sum of the cost of "unexpected" products and treatment costs.

$$ESm=U+H_1+H_2, \quad (8)$$

where *U* is the cost of under-delivered products, tenge; H_1-funds spent on hospital treatment, tenge; H_2 - the same for medical examination of patients, tenge.

$$U=O*I_{wd}, \quad (9)$$

where O is the average output of one worker per day, tenge; I_{wd} is the number of working days lost due to disability due to increased morbidity.

$$H_1=K*D, \quad (10)$$

where K is the cost of hospital bed days, tenge: D is the number of days of hospital stay.

$$H_2=K_1*D_1, \quad (11)$$

where K_1 is the cost of one doctor's visit, tenge; D_1 is the duration of medical examination.

Losses due to migration caused by environmental degradation (*ESp)* and is defined as the sum of "non-produced products and compensation costs".

$$ESp=N_1+Cc=(Aa*St)+(Ce*P), \quad (12)$$

N_1 - the cost of non-produced products due to migration of personnel, tenge; *Aa* - average annual output of one employee, tenge; *St* - staff turnover due to deterioration of the natural environment, h; *Cc* - compensation costs due to migration caused by deterioration of the natural environment, tenge; *Ce* - the amount of compensation expense received due to migration; *P* - the number of people changing their residence due to deterioration of the natural environment, people.

The cost of additional recreation required due to the unsatisfactory state of the natural environment (*ESr*) is determined as the amount:

$$ESr=U+Sm=A*Nr+Hc*Hr, \quad (13)$$

where *Nr* is the number of working days lost for additional rest necessary due to the unsatisfactory state of the natural environment; *Hc* is the cost of bed days in holiday homes and resorts; *Hr* is the number of days spent in a holiday home and resort.

Results. The most difficult task was to determine the social damage received by the national economy from water pollution and depletion. Since the payment for social damage caused by environmental pollution has not been established, they can be estimated based on the standards for the cost of new land as a means of production in the national economy, i.e.

$$Si=(Sm+ Sp + Sl)=F(C_0+ Ces), \quad (14)$$

where F is the area of the recreation area in river basins, ha; C_0 - is the cost of land tenge/ha; *Ces* is the capital investment spent on restoring the ecological situation of the recreation area, tenge/ha.

Losses from water pollution are equated to the costs necessary to restore the quality of contaminated water to the required condition. The amount of losses is determined depending on the mass of discharged pollution *(Pi)*, specific values of losses, type of pollution *(i)* and categories of water body and is determined by the formula.

$$P_i=Q_i(K_{opi}-K_{hi})*t^i*10^{-6}, \quad (15)$$

where *Pi* - weight of *i*-th contaminated substances, taken into account when calculating the damages (m_i); Q_i - flow rate of return water exceeds the *i*-th pollutant, m^3/t; K_{opi} and K_{hi} - average for the reset period of the concentration of the *i*-th pollutant, respectively, the actual and permissible according to the standards and agreed with the authorities on regulation of use and protection of water, g/m^3; t^i - is the reset period of the *i*-th contaminated substances hour.

At this concentration, the amount of damage can be determined by the reduced cost of cleaning water from a contaminated source to the requirements of the "rules for the protection of surface water" using the formula:

$$D_i=P_i*C_s; \quad (16)$$

where Y_i is the damage caused by water pollution, tenge; C_s is the specific amount of losses caused to the national economy from the mass of discharged pollutants, tenge/t.

Table 1 – Estimated values for preventing economic damage when using wastewater for irrigation

Indicators of pollution	Reduced weight of annual discharge of impurities (mm) us, g/m	Pollution concentration, content in wastewater before irrigation, g/m^3	Degree of soil purification (MPC), g/m^3	Amount of dirt removed by the soil, m, g/m^3	Indicator for the dangerous discharge of impurity *i* of the substance (*Ai*)
Suspended solids	Municipal sewage	485,4	20,0	465,4	0,05
*BOC_5	23,3	120,0	3,0	117,0	0,33
**COD	38,6	152,0	6,0	146,0	0,17
Total nitrogen	24,8	13,4	–	3,4	0,10
Suspended solids	0,3	595,0	20,0	585,0	0,05
BOC_5	Poultry factories	1500,0	3,0	1497,0	0,33
COD	29,3	850,0	6,0	844,0	0,17
Total nitrogen	494,0	64,0	10,0	54,0	0,10
Suspended solids	143,5	1987,0	20,0	1967,0	0,05
BOC_5	5,4	–	–	–	–
COD	Animal and water complex runoff (cattle)	214,0	6,0	5208,0	0,17
Total nitrogen	98,4	805,0	10,0	795,0	0,10
Suspended solids	–	143,0	20,0	123,0	0,05
BOC_5	885,4	59,0	3,0	56,0	0,33
COD	79,5	313,0	6,0	307,0	0,17
Total nitrogen	Standard clean waters of industrial enterprises	29,0	10,0	19,0	0,10
Suspended solids	6,2	800,0	20,0	780,0	0,05
BOC_5	18,5	–	–	–	–
COD	52,2	144,2	6,0	1436,0	0,17
Total nitrogen	1,9	1288,0	10,0	1278,0	0,10
Suspended solids	Meat processing plant drains	328,0	20,0	308,0	0,05
BOC_5	39,0	–	–	–	–
COD	–	352	6,0	346,0	0,17
Total nitrogen	244,1	23	10,0	13,0	0,10
	Drains of the cotton mill	15,4	–	58,8	1,3
* - Biochemical oxygen consumption ** -Chemical oxygen demand					

Based on the use of hydrogeological and hydrochemical data. We have determined the amount of social and environmental damage from the mass of discharged wastewater and CDW, taking into account the type and chemical composition, as well as its specific features (table 2).

Table 2 – Socio-economic damage from Syrdarya river pollution with in the Republic of Kazakhstan

Source of pollution	Indicators		
	P_i, mln.t	C_y, tenge/t	Y_i, mln.tenge
Industry	0,25	130,14	32,535
Communal service	0,52	130,32	67,766
Agricultural industry	0,015	126,0	1,894
CDW from irrigated land	10,09	129,6	1297,3
Surface runoff from urban areas	0,20	128,7	25,74
TOTAL:	11,075	644,76	1425,235

As can be seen from table 2, huge social and environmental damage was caused by the South Kazakhstan and Kyzylorda regions in the basin of the river Syrdarya, where irrigated agriculture and industry are widely developed, which amount to 1425.235 million tenge.

Thus, today every sovereign state has the right to demand compensation for social and environmental damage that occurs when water resources are polluted by water users located in the upper reaches of rivers. To do this, it is necessary to develop an economic mechanism for nature management that would ensure the most complete coordination of individual, collective and state interests in the protection of the environment and the rational use of natural resources.

К. К. Ануарбеков[1], Е. Т. Кайпбаев[1], Г. Ж. Меңдібаева[2]

[1]Қазақ ұлттық аграрлық зерттеу университеті, Алматы, Қазақстан;
[2]Ж.Жиембаев атындағы өсімдік қорғау және карантин ғылыми-зерттеу институты

СЫРДАРИЯ ӨЗЕНІНІҢ ТӨМЕНГІ АҒЫСЫНДАҒЫ ТӨГІНДІ ЖӘНЕ КОЛЛЕКТОР-ДРЕНАЖ СУЫНЫҢ (КДС) ЛАСТАНУЫНАН КЕЛЕТІН ӘЛЕУМЕТТІК-ЭКОЛОГИЯЛЫҚ ЗИЯНЫН БАҒАЛАУ

Аннотация. Қазақстанның суармалы егіншілік аймағындағы табиғи-экологиялық жағдайға суарудың маңызды әсері Орта Азия мен Қазақстандағы ирригацияны дамыту тұжырымдамасы негізінде анықталды.

Қазақстанның суармалы жерлерінде, әсіресе, оңтүстік және оңтүстік-шығыс аймақтарында қалыптасқан экологиялық жағдайды азайту және экологиялық-мелиоративті жағдайды

Бізге осы елдерде ағып жатқан Сырдария өзені суының тұздылығы 1,75 г/л-мен келеді. Ол суармалы жерлерде қолданылатын пестицид, хлорорганикалық пестицидтермен – ДДТ (дихлордифенилтрихлорэтан) және НСН (гексахлорциклогексан) арқылы ластанған. Судың минералдануы Қазақстан аумағында да артып келеді.

Жалпы суармалы жерлерде тұздың суармалы сумен келуі нәтижесінде топырақта және жерасты суында тұз қорының көбейгені байқалды. Олардың қарқындылығы көбінесе суармалы судың тұздылығына және су алу мөлшеріне байланысты.

Сырдария өзенінің ағынды суын реттеу нәтижесінде суармалы жерлерді игеру және өзендерге құйылатын КДВ (коллекторлық-дренажды су) көлемі мен өзендердің жоғарғы ағысындағы ағынды су мөлшері кең дамыған қайтымсыз топырақтық-экологиялық үдеріс жүреді.

Түйін сөздер: минерализация, төгінді су, суғару жүйесі, тұз тепе-теңдігі, суғару режимі, коллектор-дренаж су.

К. К. Ануарбеков[1], Е. Т. Кайпбаев[1], Г. Ж. Мендибаева[2]

[1]Казахский национальный аграрный исследовательский университет, Алматы, Казахстан;
[2]Казахский научно-исследовательский институт защиты и карантина растений им. Ж. Жиембаева

ОЦЕНКА СОЦИАЛЬНО-ЭКОЛОГИЧЕСКОГО УЩЕРБА ОТ ЗАГРЯЗНЕНИЯ СТОЧНЫМИ И КОЛЛЕКТОРНО-ДРЕНАЖНЫМИ ВОДАМИ В НИЗОВЬЯХ РЕКИ СЫРДАРЬЯ

Аннотация. Значительное влияние ирригации на природную и экологическую обстановку в зоне орошаемого земледелия Казахстана было определено концепцией развития ирригации в Центральной Азии и Казахстане.

Проблемы снижения существующей экологической обстановки на орошаемых землях Казахстана, особенно в южных и юго-восточных регионах, и нормализации эколого-мелиоративной обстановки непосредственно связаны с различными водохозяйственными районами Кыргызстана и Узбекистана.

Река Сырдарья, протекающая между этими странами, приходит к нам с минерализацией воды 1,75 г/л. Они также загрязнены пестицидами, хлорорганическими пестицидами – ДДТ (дихлордифенилтрихлорэтан) и ГХГ (гексахлорциклогексан), используемыми на орошаемых землях. Минерализация воды и на территориях Казахстана.

В целом на орошаемых землях в результате поступления соли из оросительных вод наблюдалось увеличение запасов соли в почвах и грунтовых водах. Их интенсивность во многом зависит от минерали-

зации оросительной воды и объема водозабора. В результате регулировалось течение реки. Необратимый почвенно-экологический процесс с большой интенсивностью протекает в Сырдарье, где широко развито освоение орошаемых земель и объем сбросов ЦДО (коллекторно-дренажных вод) и сточных вод в верхних течениях рек.

Ключевые слова: минерализация, сточные воды, оросительная система, солевой баланс, режим орошения, коллектор-дренажные воды.

Information about authors:

Anuarbekov Kanat, PhD, associate professor of the Department of “Water resources and melioration”, Kazakh National Agrarian Research University, Almaty, Kazakhstan; kanat.anuarbekov@kaznau.kz; https://orcid.org/0000-0003-0832-6980

Kaipbayev Yerbolat, PhD, associate professor of the Department of “Water resources and melioration”, Kazakh National Agrarian Research University, Almaty, Kazakhstan; yerbolat.kaipbayev@yandex.ru; https://orcid.org/0000-0002-7931-7881

Mendibayeva Gulnaz, PhD, Kazakh Research Institute of Plant Protection and Quarantine named after J. Zhiembaev, Almaty, Kazakhstan; www.gulnaz87.kz; https://orcid.org/0000-0002-0929-061X

REFERENCES

[1] Mustafayev Zh.S. Soil-ecological justification of agricultural land reclamation in Kazakhstan. Almaty: "Gylym," 1997. 57 p.

[2] Shomantayev A.A. Hydrochemical regime of watercourses and agricultural use of wastewater and drainage in the lower reaches of the Syrdary. Kyzylorda, 2001.

[3] Aidarov M.P. Regulation of water-salt and nutrient regimes of irrigated land. M: Agropromizdat, 1985. 304 p.

[4] Anuarbekov K.K., Zubairov O.Z., Nusipbekov M.Z. Influence of the improvement of water-salt regime on the yield // Biosciences Biotechnology Research Asia. April 2015, Vol. 12 (1), 999-1006.

[5] Anuarbekov K.K and other. Exploitation of wastewater irrigation system (WWIS) // News of the National Academy of Sciences of the Republic of Kazakhstan, Series of Geology and Technical Sciences, Vol. 6, N 432 (2018). P. 129-136.

[6] Anuarbekov K., Zubairov O., Nusipbekov M. Improving water-salt regime in irrigated agriculture // Life Science Journal 2014; 11 (5): 459-464] (ISSN:1097-8135)

[7] Anuarbekov K.K and other. Water-saving technology of irrigation of corn // Journal News of the National Academy of Sciences of the Republic of Kazakhstan, Series of Geology and Technical Sciences, Vol. 2, N 428 (2018). P. 149-155.

N E W S
OF THE NATIONAL ACADEMY OF SCIENCES OF THE REPUBLIC OF KAZAKHSTAN
SERIES OF GEOLOGY AND TECHNICAL SCIENCES
ISSN 2224-5278
Volume 1, Number 445 (2021), 52 – 57 **https://doi.org/10.32014/2021.2518-170X.8**

UDC 595. 14 (574. 3 + 574. 2)

A. D. Baibotayeva, G. D. Kenzhalieva, K. T. Zhantasov,
M. K. Zhantasova, E. N. Kocherov

M. Auezov South Kazakhstan University, Shymkent, Kazakhstan.
E-mail: aigul_saraneo@mail.ru

STUDY OF THE EFFECT OF HEAVY METALS ON SOIL COVER AND METHODS OF THEIR BIOREMEDIATION CONTROL

Abstract. The article provides information on literature and patent information on the analysis of heavy metals formed during the extraction and processing of various types of raw materials for the production of non-ferrous metals and chemical products. The influence of heavy metals on the environment and living organisms, fauna and flora, as well as people living in different industrial regions of Kazakhstan is shown. Migration of heavy metals in the soil cover hydrosphere and atmosphere is shown. Based on the analytical review, the goals and objectives of the study are outlined, the chemical composition of raw materials for the main heavy metals formed in solid and dust - like production waste, and for technological processing in the production of lead and zinc in the East Kazakhstan and Turkestan regions is shown. Information is provided on the presence of heavy metals in the soil and their purification by various bioremediation methods. The data of soil analysis on the territory of the Turkestan region in recreation areas of people and in non-ferrous metallurgy enterprises nearby to the mining complex are presented. The dependence of the distribution of heavy metals and the chemical composition of the analyzed samples taken in various points of the Turkestan region and the city of Shymkent is shown. Data on the maximum content of heavy metals in the soil at which experimental worms die are established.

Key words: soil, heavy metals, worms, control, dust and gas mixture, maximum permissible concentrations, phytoremediation, cleaning.

Introduction. The problem of utilization, deep processing of technogenic waste and raw materials containing heavy and other metals in the industrial regions of the Republic of Kazakhstan, as well as cross-border countries of the world is an urgent task.

Soil cover is the most important formation of the globe, which is very important for the life of humanity and the environment. This is due to the fact that the soil cover is the main source of food. In the form of plant and animal origin, not only in the Republic of Kazakhstan, but also in other States. In addition, the most important property of the soil is its fertility, which ensures the quality and quantity of agricultural products. The natural fertility of the soil cover is regulated by the supply of nutrients, which can be affected by various factors - impurities and soil pollutants.

The authors ' work [1] established that lead pollution occurs mainly due to the burning of gasoline (60%) in motor transport, the production of non-ferrous metals (22%), iron, steel and ferroalloys (11%), as well as other factors.

According to the authors ' work [2], it is noted that in some soils the increase in chromium is almost 2 times, lead is 1.8 times, copper, vanadium and nickel is 1.4 times, and zinc is 1.2 times.

However, ongoing efforts to reduce heavy metals in oil-contaminated soils do not produce the desired results in terms of their content in the soil cover.

Anthropogenic sources of heavy metals are mining and processing of minerals and raw materials, the combustion of fuel of vehicles and technical means of agriculture, wastewater, and oil spill and oil, ferrous and nonferrous metallurgy [3-16]. Based on this the role of soil cover on the life and productivity of terrestrial ecological systems is of great importance.

For example, contamination of soil cover, which is an important component of photosynthetic processes in plants with heavy metals, has two negative features:

- intake from the soil to plants, from plants to the human and animal bodies, causing serious diseases and reducing vital activity, due to the toxicological effects of agricultural products containing harmful components;

- accumulating in the soil in large quantities, they change the physical, chemical, biological and other properties of the soil cover, violating its fertility and the main importance for the agro-industrial complex.

Therefore, the object of research is the ecological safety of densely populated territories of industrial regions, cities and localities with agricultural land to ensure the normal life of fauna and flora.

The subject of the study is soil contamination with such heavy metals as lead, arsenic, copper, cadmium, zinc, and the possibility of their bioassay by bioremediation method.

It is known that heavy metals have a significant impact on the deterioration of the structural and agrochemical properties of the soil. This leads to an increase in spore-bearing fungi, bacteria and, in many cases, to the death of plants. When heavy metals get into water, they cause irreparable damage and upset the balance of the ecological system, participating in redox processes, due to the variable valence, complexing properties change.

The danger of the influence of heavy metals on humans and animals is manifested not only in the direct impact of high concentrations and accumulation in the body, but also in the fact that they are difficult to remove and have a Toxicological effect with the possibility of abnormal diseases and poisoning.

Studies by a number of authors of scientific papers [5-7,14-16] revealed the environmental impact of metals such as Pb, Zn, Wi, Cu, W, Co, etc., carried away from the sources of formation by migration along with dust and gases.

For example, the Mangistau region of the Republic of Kazakhstan is one of the regions with a rather tense radioecological situation. This is due to the extraction and processing of radioactive raw materials used for energy, industrial, medical and research purposes. Radioecological conditions are determined by the degree of saturation of dangerous objects of natural and man-made origin. Dangerous man-made radioecological objects include sinkholes over the site of underground nuclear explosions Sayotes, Koshkar ATA tailings storage, places where radioactive waste is buried at Mangystau nuclear power plant industrial sites, uranium quarries and waste from the oil industry.

Soil analysis of these regions based on soil maps of the Mangistau region allowed us to establish that the main factors that affect the degree of their ecological disturbance are the prevailing types of soil pollution and salinization. Indicators for soil bonitet of the region are very low, which is due to the low content of humus in zonal soils and the presence of negative signs, such as salinity, salinity, crushed stone, and only in certain areas of the region used for irrigated arable land, the bonitet score is higher [17].

The analysis of literature and patent information finds that contamination of areas located close to industrial enterprises in the mining of non-ferrous metallurgy and processing them on lead and zinc, the value of heavy metals and degree of contamination they have different indicators. This is due, in our opinion, to the direction of the prevailing wind and the presence of the MPC level of heavy metals above acceptable standards, which is common for industrial regions and the soils of nearby cities and towns.

To reduce the content of heavy metals, patent information on methods for determining, disposing of, and cleaning contaminated soils from heavy metals was collected and analyzed [13-20]. The authors of [15] conducted research to determine heavy metals in the human body, from the influence of dust and gas emissions and wastewater from the enterprises of JSC Kazzinc (Ust - Kamenogorsk lead - zinc plant) and JSC UKTMP (Ust - Kamenogorsk titanium - magnesium plant), located within the city of Ust - Kamenogorsk, East Kazakhstan region of the Republic of Kazakhstan.

Based on the literature and patent analysis of the available information, studies were conducted to determine the contamination and presence of heavy metals in the soil on the territory of the former Shymkent lead plant and Achisay mining and processing plant located in the Turkestan region.

Analysis of soil contamination with heavy metals in industrial regions of the mining and processing complex of non-ferrous metallurgy enterprises was carried out by selecting point representative soil samples weighing at least 15 kg from the survey sites to a depth of 20 cm from a square hole.

Arsenic containing dusts of various stages of lead - zinc production formed during the operation of non-ferrous metallurgy enterprises were studied.

The average chemical composition of raw dusts from different production stages and sampling points is shown in tables 1, 2 and 3.

Table 1 – Average chemical composition of raw materials of the Achisayskoye field

Name of the object	Pb	Zn	Cu	Cd	Bi	As	Sb	Ag	Al_2O_3
Achisayskoe field	18,87	116	3,5	0,041	н/о*	0,64	0,2	615,0	3,5
Note*: n/a detected									

Table 2 – Average chemical composition of dusts of various stages of lead - zinc production

Name of the material	Content of components in %, %							
	Pb %	Zn %	Cu %	Fe %	S %	Sb %	As %	CaO %
Fine dust	39,79	15,19	10,94	3,2	8,3	0,51	1,0	n/d*
Dry cleaning dust	39,9	8,88	2,06	7,87	14,37	0,34	0,37	н/о
Cyclone dust of the mine furnace	32,37	7,987	2,32	9,84	–	0,19	0,65	1,62
Cyclone dust of the sinter shop	38,68	7,32	2,69	9,2	11,74	0,16	0,404	2,54
Converter dust	63,33	3,47	1,82	0,23	n/d	0,66	7,08	n/d
Converter dust from: 6	29,9	1,79	40,82			5,51	n/d	
Note*: n/d not detected								

In the course of the research, the content of the studied heavy metal components exceeded the MPC standards.

Table 3 – analysis of samples from various points of the industrial region of the Turkestan region of the Republic of Kazakhstan

№	Objects	Component content, mg/kg					Method of testing
		Pb	Cd	Zn	Cu	As	
1	Dendro Park Shymkent	4,0	1,0	10,0	0	0	МУ.08-47/203
2	Achisay (Turkestan region)	1287	37	871	344	0,64	
3	Internal overburden generated during mining of brown coals of the Lenger Deposit (Tolebi district)	461	10	871	62	0,59	
4	Industrial Corporation Yuzhpolymetal JSC, Shymkent	1287	37	7164	344	0,68	
	MPC	32,0	0,5-1,0	23	23	2,0	

The elemental and morphological composition of the selected presented samples of point samples from various locations of research objects obtained using the JSM-6490LV electron scanning microscope is shown in figures 1, 2, 3 and 4.

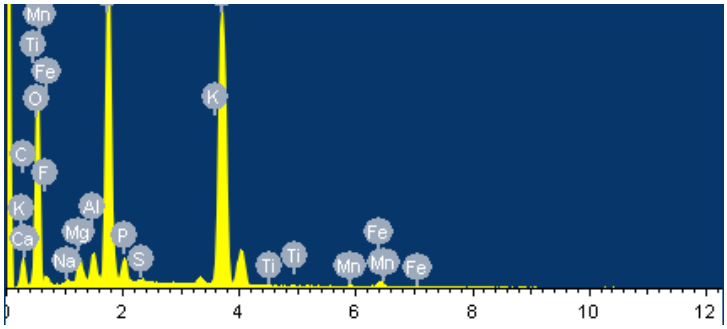

Figure 1 – Chemical composition of spot samples of soil of the Achisai State Production Complex, with content in (%)

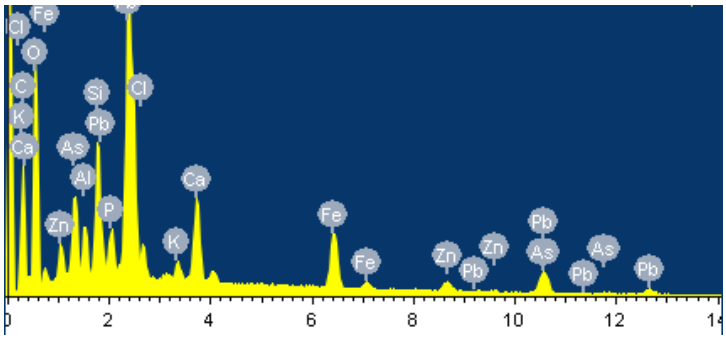

Figure 2 – Chemical composition of spot soil samples, internal overburden rocks formed during the extraction of brown coal from the Lenger deposit (Tolebi district), with a content in (%)

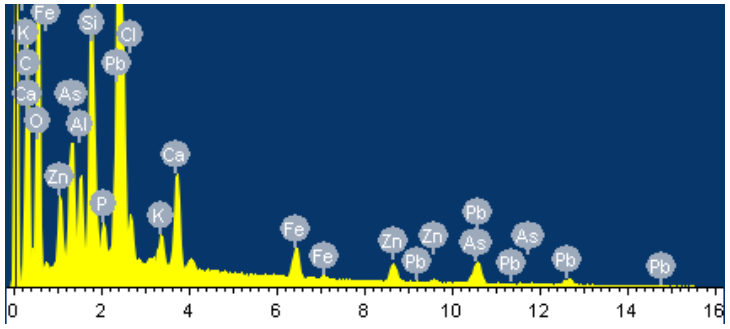

Figure 3 – Chemical composition of point soil samples "Yuzh - polymetal", with content in (%)

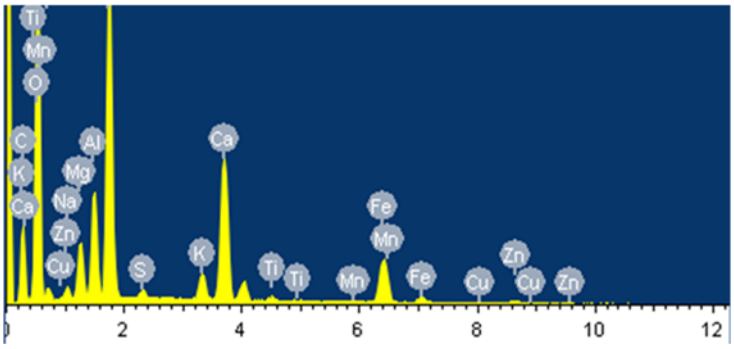

Figure 4 – Chemical composition of spot soil samples (control) Dendropark of Shymkent, with content in (%)

On the basis of the obtained analyzes of point samples using a JSM-6490LV scanning electron microscope, it was revealed that in the soils of the territory of the industrial enterprises under study, the content of heavy metals is above the MPC (Pb - 32.0 g / cm^3, Cd - 0.5 - 1.0 g / cm^3 , Zn - 23 g / cm^3, Cu - 23 g / cm^3, As - 2.0 g / cm^3), which causes irreparable damage to the fauna and flora of the studied regions of the Turkestan region and requires the development of methods for phytoremediation soil control and a method for cleaning soil from heavy metals.

Conclusion. 1. The analysis of patent information on soil cover contamination with heavy metals, such as lead, copper, zinc, vanadium, Nickel, arsenic, cadmium, etc. was carried out in Russian and foreign literature.

The sources of the formation of heavy metals in the Aktobe region have been established - the plants of TNK Kazchrome JSC, in the East Kazakhstan region - 2 enterprises, in the Turkestan region - 2 enterprises of the Achisai State Production Complex and Yuzhpolymetal JSC, excluding motor vehicles.

2. Point samples were taken of land contamination from the plant territory.

The analysis of the morphological and chemical composition of the selected soils was also carried out. Revealed the content of heavy metals in the samples on a scanning electron microscope company JSM-6490LV, the content of heavy metals is above the maximum permissible concentration Pb - 32,0 g/cm^3, Cd - 0,5 – 1,0 g/cm^3, Zn – 23 g/см^3, Cu – 23 g/cm^3, As - 2,0 g/см^3, which requires the use of cardinal solutions for bioremediation. A method for cleaning soil from heavy metals is shown.

А. Д. Байботаева, Г. Д. Кенжалиева, К. Т. Жантасов, М. К. Жантасова, Е. Н. Кочеров

М. Әуезов атындағы Оңтүстік Қазақстан университеті, Шымкент, Қазақстан

АУЫР МЕТАЛДАРДЫҢ ТОПЫРАҚ ЖАМЫЛҒЫСЫНА ӘСЕРІН ЗЕРТТЕУ ЖӘНЕ ОЛАРДЫ БИОРЕМЕДИАЦИЯЛЫҚ БАҚЫЛАУ ӘДІСТЕРІ

Аннотация. Бұл мақалада түрлі-түсті металдар мен химия өнімдерін өндіруге арналған шикізаттың алуан түрлерін алу және өңдеу кезінде пайда болған ауыр металдарды талдау туралы әдебиеттер мен патенттік мәліметтер келтірілген. Ауыр металдардың қоршаған ортаға және тірі организмдерге, фауна мен флораға, сондай-ақ Қазақстанның түрлі өндірістік аймағында тұратын адамдарға әсері көрсетілген. Ауыр металдардың топырақ жамылғысындағы, гидросферадағы және атмосферадағы миграциясы көрсетілген. Аналитикалық шолу негізінде зерттеудің мақсаттары мен міндеттері көрсетілген, қатты және шаңды өндіріс қалдықтарында пайда болатын негізгі ауыр металдарға қатысты Шығыс Қазақстан мен Түркістан облыстарында қорғасын мен мырыш өндірісі кезінде технологиялық қайта бөлу үшін шикізаттың химиялық құрамы көрсетілген. Топырақта ауыр металдардың болуы және оларды түрлі биоремедиация әдістерімен тазарту туралы мәліметтер келтірілген.Түркістан облысының аумағында адамдардың демалу аймақтарындағы және тау-кен кешеніне жақын түсті металлургия кәсіпорындарындағы топырақты талдау мәліметтері келтірілген. Түркістан облысы мен Шымкент қаласының түрлі нүктесінен алынған ауыр металдардың таралуы мен талданатын үлгілердің химиялық құрамының тәуелділігі көрсетілген. Тәжірибелік құрттар өлетін топырақтағы ауыр металдардың максималды құрамы туралы мәліметтер анықталды.

Түйін сөздер: топырақ, ауыр металдар, құрт, бақылау, шаң мен газ қоспасы, шекті рұқсат етілген концентрация, фиторемедиация, тазарту.

А. Д. Байботаева, Г. Д. Кенжалиева, К. Т. Жантасов, М. К. Жантасова, Е. Н. Кочеров

Южно-Казахстанский университет им. М. Ауэзова, Шымкент, Казахстан

ИССЛЕДОВАНИЕ ВЛИЯНИЯ ТЯЖЕЛЫХ МЕТАЛЛОВ НА ПОЧВЕННЫЙ ПОКРОВ И МЕТОДЫ ИХ БИОРЕМЕДИАЦИОННОГО КОНТРОЛЯ

Аннотация. В статье приводятся сведения по литературным и патентным данным по анализу тяжелых металлов, образующихся при добыче и переработке различных видов сырья для производства цветных металлов и химической продукции. Показано влияние тяжелых металлов на окружающую среду и живые организмы, животный и растительный мир, а также на людей, проживающих в различных промышленных регионах Казахстана. Показана миграция тяжелых металлов в гидросфере и атмосфере почвенного покрова. На основе аналитического обзора намечены цели и задачи исследования, показан химический состав сырья для основных тяжелых металлов, образующихся в твердых и пылевидных отходах производства, а также для технологической переработки при производстве свинца и цинка в Восточно-Казахстанской и Туркестанской областях. Приводятся сведения о наличии тяжелых металлов в почве и их очистке различными методами биоремедиации. Представлены данные почвенного анализа на территории Туркестанской области: в зонах отдыха населения и на предприятиях цветной металлургии, расположенных вблизи горнорудного комплекса. Показана зависимость распределения тяжелых металлов и химического состава анализируемых проб, взятых в различных точках Туркестанской области и города Шымкента. Установлены данные о максимальном содержании тяжелых металлов в почве, при котором подопытные черви погибают.

Ключевые слова: почва, тяжелые металлы, черви, контроль, пылегазовая смесь, предельно допустимые концентрации, фиторемедиация, очистка.

Information about authors:

Baybotaeva Aigul Dikhanbaevna, post degree of the Department of Life Safety and Environmental Protection of the M. Auezov South Kazakhstan University; aigul_saraneo@mail.ru; https://orcid.org/0000-0001-8560-9218

Kenzhalieva Gulmira Duisenbaevna, Associate Professor of the Department of Life Safety and Environmental Protection, M. Auezov South Kazakhstan University, Candidate of Technical Sciences, Associate Professor; nursara@mail.ru; https://orcid.org/0000-0003-0200-7145

Zhantasov Kurmanbek Tazhmakhanbetovich, Professor of the Department of Chemical Technology of Inorganic Substances, M. Auezov Kazakhstan University; k_zhantasov@mail.ru; https://orcid.org/0000-0001-6867-1204

Zhantasova Madina Kurmanbekovna, Teacher of school-gymnasium Titov № 20; zhantasova84@bk.ru; https://orcid.org/0000-0002-2705-4063

Kocherov Erkebulan Nurgalyievich, Associate Professor of the Department of Life Safety and Environmental Protection, M. Auezov South Kazakhstan University, Candidate of Technical Sciences, Associate Professor; erkebulan083@mail.ru; https://orcid.org/0000-0001-6652-7954

REFERENCES

[1] Bychinsky V.A. Ecological biochemistry: Heavy metals in soils in the zone of influence of an industrial city. Irkutsk, 2008. 189 p. (in Russ.).

[2] Ishangaliyev A.A., Urynbayeva G.N. (2015). Methods of reducing of phytotoxicity of heavy metals Bulletin of the Kazakh-Russian International University // Bulletin of the Kazakh-Russian International University, Aktobe, 2015. P. 14-16.

[3] Amrin M.K., Yermukhanova G.T., Mashyrykov K.S., Nurly R.B., Zhumazhanova A.B. The environment of the regions of the Mangistau region in the light of their possible impact on the dental status of children // Scientific-Practical Journal of Medicine. 2019. [Bulletin of the KRIU], 3. P. 142-148 (in Russ.).

[4] Amosova Ya.M. i dr. Protection of soils from chemical pollution. M.: Moskovskiy universitet, 1989. 94 p. (in Russ.).

[5] Buvalets D.Yu., Kapustin O.E. (2015) Contamination of industrial cities with zinc and other heavy metals // Bulletin of the KRIU, 49 (1158). P. 33-34 (in Russ.).

[6] Chernykh N.A., Ovcharenko M.M., Popovicheva L.P., Chernykh I.N. (1995) Methods for reducing the phytotoxicity of heavy metals // Agrokhimiya. 2000. P. 101-107 (in Russ.).

[7] Methodical guidelines for the determination of heavy metals in agricultural soils and crop products M.: TSINAO, 1992. P. 13-15 (in Russ.).

[8] Approximately permissible concentrations (APC) of heavy metals and arsenic in soils. Hygienic standards GN 2.1.7.020.94. M.: Goskomsanepidnadzor Rossii, 1994 (in Russ.).

[9] Zhantasov K.T. and other (2016) Method for removing arsenic from lead-zinc production dust. Innovative patent of the Republic of Kazakhstan № 22051. 2009 (in Russ.).

[10] Zhantasov K.T. and other. Method for removing arsenic from lead-zinc production dust Innovatsionnyy patent RK № 24266. 2017 (in Russ.).

[11] Postnikov D.A. Method for cleaning the soil of heavy metals. Patent RU2365078S1. 2017 (in Russ.).

[12] Lukatkin A.S., Bashmakov D.I. Method for biological treatment of soils. Patent RU2231944C. 2004 (in Russ.).

[13] Kostenko Ye.A., Lysenko I.O. Assessment of the content of heavy metals in the agro-industrial zone of Stavropol // KubGAU. 2012. 80(06). 112 p. (in Russ.).

[14] Pereslegina I.A, Sirotkina M.V, Gabina S.V and etc. Method for determining heavy metals in the human body. Opubl. 16.01.2012, biol. N 1 (in Russ.).

[15] Sychev V.G., Stupakov G.A., Pankratova K.G. and other. Method of manufacturing standard samples of soil contaminated with heavy metals. Patent RU 2660861 C1. 2018. (in Russ.).

[16] Pavlichenko L.M., Yespolayeva A.R., Iztayeva A.M. The content of heavy metals in the soil of Mangystau region // International Journal of Applied and Basic Research. 2016. 2-1. P. 53-58 (in Russ.).

[17] Morozova N.A., Prokhorova N.V. Accumulation of heavy metals in soils and plants of the urban environment // University named after V. I. Vernadsk. 2007. Vol. 1, N 4 (10). P. 77-81 (in Russ.).

[18] Ragimov A.O., Mazirov M.A., Zinchenko S.I. (2015) Environmental assessment of soil and snow cover of the Vladimir region // Electronic scientific and production magazine "AgroEkoInfo". 2015. 6 (12): 47 (in Russ.).

[19] Shchelkunov L.F., Dudkin M.S., Korzun V.N. Food and ecology. Odessa: TSSP Optimum, 2000. P. 49-53 (in Russ.).

[20] Sychev V.G., Stupakov G.A., Pankratova K.G. and other. A method for preparing standard samples of oil contaminated with heavy metals. Patent RU 2660861 C1. 2018 (in Russ.).

[21] State Standart 17. 4. 3. 06 – 83. Protection of Nature. Soils. General requirements for sampling. Kazakhstan, 2017 (in Russ.).

[22] State Standart 17. 4. 02 – 84 Methods for sampling and preparation of samples for chemical, bacteriological, helminthological analysis. Kazakhstan, 2017 (in Russ.).

[23] State Standart 17.4.3.01 - 83 Methodical recommendations for conducting ionic and laboratory compliance of copper, lead, cadmium and zinc ions. Kazakhstan, 2017 (in Russ.).

[24] State Standart 29269 – 91 Soils general requirements for analysis. Russia, 1991 (in Russ.).

[25] State Standart R 56157 – 2014 The soil. Techniques (methods) for analyzing the composition and properties of soil samples. General development requirements. Russia, 2014 (in Russ.).

[26] MU.08-47/203 The soil. Methods for measuring the mass concentrations of zinc, cadmium, lead, copper, manganese, nickel, cobalt, iron, arsenic, selenium and rutile stripping voltammetry method. Russia, 2008 (in Russ.).

N E W S
OF THE NATIONAL ACADEMY OF SCIENCES OF THE REPUBLIC OF KAZAKHSTAN
SERIES OF GEOLOGY AND TECHNICAL SCIENCES
ISSN 2224-5278
Volume 1, Number 445 (2021), 58 – 65 **https://doi.org/10.32014/2021.2518-170X.9**

UDC 678.4:539.3
IRSTI 67.11.59

A. F. Bulat[1], A. S. Kobets[2], V. I. Dyrda[1], V. A. Lapin[3], S. M. Grebenyuk[4], M. I. Lysytsia[1], M. H. Marienkov[5], H. M. Ahaltsov[1], Ye. V. Kalhankov[2]

[1]Institute of Geotechnical Mechanics named by N. Poljakov
of National Academy of Sciences of Ukraine, Dnipro, Ukraine;
[2]Dnipro State Agrarian and Economic University, Dnipro, Ukraine;
[3]Kazakh Research and Design Institute of Construction and Architecture, Almaty, Kazakhstan;
[4]Zaporizhzhya National University, Zaporizhzhya, Ukraine;
[5]State Enterprise "State Research Institute of Building Constructions", Kyiv, Ukraine.
E-mail: gtm.bulat@gmail.com, info@dsau.ua, vita.igtm@gmail.com, lapin_1956@list.ru, gsm1212@ukr.net, lisitsa.n.i@gmail.com, n.maryenkov@ndibk.gov.ua, ag.gena@gmail.com, kalhankov.ye.v@dsau.dp.ua

VIBROSEISMIC PROTECTION OF BUILDINGS AND STRUCTURES AGAINST NATURAL AND TECHNOGENEOUS DYNAMIC IMPACTS

Abstract. In this article, the authors analyze results of their long-term researches on protection of buildings and structures against dynamic loads caused by the nature and/or human activities. They also give the grounds for necessity to provide vibration insulation of buildings, and show how to choose and calculate proper parameters for rubber vibroseismic insulators. Specifics of finite element method applied for static calculating the vibroseismic insulators is also described. In order to take into account weak compressibility of rubber, a moment finite element scheme was used, which assumes a triple approximation of the displacement vector components consisting of strain tensor and volume change function. Stress-strain state of the shock absorbers was determined for different standard sizes and diameters. The authors also describe two variants of calculation depending on the method of fixing the insulator's ends. In the first case, the ends are vulcanized to the metal plates. In the second variant, the ends are free and can move in a horizontal plane. Influence of ratio of the shock absorber height and radius to the strain state of a structure was also analyzed. In order to determine factual levels of the soil and pile vibration (in two horizontal and one vertical directions), vibrodynamic studies were carried out. The obtained vibration signals were registered by the one-component vibration transducers 731A (vibration sensors) produced by the Wilcoxon Research company (the USA). Then, the vibration records were processed by the specialized program "Seismic Monitoring". Based on the results of these studies, numerical calculations were performed in order to determine whether the predicted levels of the residential building vibrations are in compliance with the existing sanitary standards when exposed to real technogeneous loads. Vibrodynamic tests on vibration acceleration levels of the vibration-insulated reinforced concrete slabs and floors in residential building confirmed high effectiveness of the used vibroseismic insulation system with the rubber elements: the registered vibration acceleration levels in the residential building on all floors did not exceed acceptable levels set by the sanitary standards, and ensured comfortable living conditions under different dynamic impacts. The results of this work make it possible to design buildings with anti-seismic protection by using the designed rubber elements in accordance with the local conditions of the city of Almaty.

Key words: shock absorber, vibroseismic isolation, finite element method, sanitary standards.

Preface. The considered system of vibroseismic insulation consists of non-linear elements with high dissipative properties; it includes structures, which limit drift of the upper part of the building, and is resistant to wind loads.

The vibroseismic insulation significantly reduces not only dynamic loads, but also horizontal interstorey drift (wraps), and, therefore, significantly diminishes damage of the building supporting structures, cuts economic losses and provides comfortable living conditions for people. As a rule, all these

advantages are provided at the design stage in accordance with national regulations. For example, according to the Ukrainian norms [1], when designing buildings with vibroseismic insulation, in addition to spectral calculation, it is also necessary to calculate dynamics by accelerograms obtained at the construction site. Similar provisions are fixed in the building codes of the Republic of Kazakhstan, which are also based on the European standards.

The authors of this work were among those who developed a lot of national regulatory documents among which is the National Construction Standard ДБН В.1-12:2014 “Construction in Seismic Regions of Ukraine”, which is harmonized with Eurocode 8 “Design of Structures for Earthquake Resistance (EN 1998–1: 2004 Eurocode 8). These documents include the section “Design of Seismoinsulation Systems” enabling to design vibroseismic-resistant structures with a specified level of safety.

The purpose of this work was to calculate and validate parameters of the vibration insulation system for buildings and structures under dynamic effects caused by the nature and human activities. For the conditions of the city of Almaty, this technical solution of seismic insulation based on the rubber elements is innovative.

Grounds for necessity in vibroseismic protection of buildings under natural and technogeneous dynamic impacts. Let's consider vibroseismic insulation of a residential complex in the city of Lviv (Ukraine) at the address: Pid Dubom street, 26, located in a zone with dynamic impact of freight and passenger trains. This residential complex consists of three sections (6, 10 and 13 floors), each section is built on its own vibration-proof pile foundation. In order to resist to the dynamic impacts of the railway trains, foundations of the buildings were made in the form of monolithic reinforced concrete grillages on a pile foundation (cross section of the piles is 350×350 mm); thickness of the pile foundation grillages in the six-storey section is 600 mm and 800 mm in the rest sections.

Results of the full-scale dynamic studies at the construction site at a distance of 15-22 m from the railway showed the following: in case of no anti-vibration protection system, predicted excess of permissible vibration acceleration levels of the building floors was from 6 dB to 12 dB (2-4 times higher than the sanitary standards) in the octaves of 8 Hz, 16 Hz, 31.5 Hz, 63 Hz. In order to ensure comfortable living of people, normalization of vibration acceleration levels is given in the norms described in [1].

For reducing vibration levels of the buildings, an anti-vibration protection system was installed: a rubber vibroseismic insulator with diameter of 340 mm and thickness of 50 mm was installed on the head of each pile before concreting the slab of the grillage. In order to protect the structures of the grillage and cellars of the buildings against horizontal and vertical vibrations of soil, the designed system for vibration insulation consisting of polystyrene plates with thickness of 100 mm is installed between the external surfaces of the foundation slab, walls of the underground storeys and backfill soil.

These innovative anti-vibration systems are very effective for buildings: the calculated frequency of the building intrinsic vertical vibrations is 3.8-4.7 Hz, which is 3-12 times less than the frequency of the soil forced oscillations (15-80 Hz) when exposed to effects of the railway trains; levels of the floor vibration do not exceed permissible sanitary norms for the residential buildings [1] under seismic overloads (determined at 6 points); the calculated safety factor against overturning of the buildings is from 5.4 to 16.5, and at wind loads, the safety factor is from 101.6 to 196.6.

Experimental studies and calculation of elements for anti-vibration protection of buildings and structures. The solid cylindrical rubber elements made of natural caoutchouc were used as components of the system for anti-vibration and anti-seismic protection of buildings and structures. In view of practical use, calculations were performed, design and method of the elements installation were patented, design documentation was developed, and four types of samples – with diameter of 340 mm, 400 mm, 420 mm and 500 mm and height of 50 mm – were manufactured and tested. The following tests were carried out: static testing of their compressive and shear stiffness at various loads; and dynamic testing of stiffness and dissipative characteristics. The test procedure is presented in details in [2].

Both analytical and numerical methods are used for calculating the vibroseismic insulators. Among the numerical methods, method of finite element stands out due to its universality and adequate accuracy.

Let’s consider specific aspects of applying this method for static calculation of the vibroseismic insulators. In order to take into account the rubber weak compressibility and to eliminate some other disadvantages of the traditional finite element method, a moment finite element scheme was proposed for weakly compressible materials [3]. Its effectiveness for calculating rubber shock absorbers is shown in [4].

Let's consider a spatial hexagonal finite element with a linear approximation of displacements.

According to the moment scheme for weakly compressible material, stiffness matrix for each separate element will be represented in the global Cartesian coordinate system $O'z_{1'}z_{2'}z_{3'}$ in the form of [5]:

$$\left[K^{k'm'}\right]=\left[K_D^{k'm'}\right]+\left[K_S^{k'm'}\right], \quad (k',m'=1,\ldots,3) \tag{1}$$

where we have shearing component

$$\left[K_D^{k'm'}\right]=[A]\left[F_{ij}^{k'}\right]^T\left[H_D^{ijkl}\right]\left[F_{kl}^{m'}\right][A]^T \tag{2}$$

and spherical component of the stiffness matrix

$$\left[K_S^{k'm'}\right]=[A]\left[F_\theta^{k'}\right]^T\left[H_S\right]\left[F_\theta^{m'}\right][A]^T, \tag{3}$$

where matrices of elastic constants, which take into account metric of finite element and describe shearing and bulk properties of the material, are determined, respectively, as:

$$\left[H_D^{ijkl}\right]=\int_{-1}^{1}\int_{-1}^{1}\int_{-1}^{1}2\mu g^{ik}g^{jl}\{\psi\}^T\{\psi\}\sqrt{g}\,dx_1dx_2dx_3, \tag{4}$$

$$\left[H_S\right]=\int_{-1}^{1}\int_{-1}^{1}\int_{-1}^{1}\lambda\{\psi\}^T\{\psi\}\sqrt{g}\,dx_1dx_2dx_3, \tag{5}$$

where $\{\psi\}=\{1,x_1,x_2,x_1x_2,x_3,x_1x_3,x_2x_3,x_1x_2x_3\}$ is vector of power functions, g^{ij} and g are components and determinant of metric tensor of the finite element coordinate system $Ox_1x_2x_3$, $(i,j=1,\ldots,3)$, and μ,λ are the Lamé constants.

Let's determine matrix [A] in the relations (2) and (3) by using various representations of the displacement vector components in the global coordinate system. On the one hand, according to the moment scheme, we have the expansion of displacements in a series of power functions:

$$u_{k'}=\{\psi\}\{\omega_{k'}\}^T, \tag{6}$$

where $\{\omega_{k'}\}=\left\{\omega_{k'}^{(000)},\omega_{k'}^{(100)},\omega_{k'}^{(010)},\omega_{k'}^{(110)},\omega_{k'}^{(001)},\omega_{k'}^{(101)},\omega_{k'}^{(011)},\omega_{k'}^{(111)}\right\}$ is vector of displacement expansion coefficients.

On the other hand, displacements of any point of the body are determined through the shape functions and values of nodal displacements:

$$u_{k'}=\{N_L\}\{u_{k'}^L\}^T, \tag{7}$$

here $\{u_{k'}^L\}=\left\{u_{k'}^{(1)},u_{k'}^{(2)},u_{k'}^{(3)},u_{k'}^{(4)},u_{k'}^{(5)},u_{k'}^{(6)},u_{k'}^{(7)},u_{k'}^{(8)},\right\}$ is vector of nodal displacements, $\{N_L\}=(N_1,N_2,N_3,N_4,N_5,N_6,N_7,N_8)$ is vector of shape functions. The shape functions for the hexagonal finite element are described in the local coordinate system by the relations:

$$N_L(x_1,\,x_2,\,x_3)=\frac{1}{8}\left(1+x_1x_1^L\right)\left(1+x_2x_2^L\right)\left(1+x_3x_3^L\right), \tag{8}$$

where x_i^L is the i-th coordinate of the L-th node in the coordinate system of the finite element; i = 1, 2, 3; L = 1, …,8.

By comparing expressions (6) and (7) with allowance for (8), we can express matrix of transition [A] from power functions $\{\psi\}$ to the shape functions $\{N_L\}$, so that the following relation can be realized:

$$\{\omega_{k'}\}=[A]^T\{u_{k'}^L\}. \tag{9}$$

Matrix $F_{ij}^{k'}$ should be formed in such a way that, when constructing the stiffness matrix (2), components of the strain tensor can be represented as an expansion in a power series in the following form:

$$\varepsilon_{11}=e_{11}^{(000)}+e_{11}^{(010)}\psi^{(010)}+e_{11}^{(001)}\psi^{(001)}+e_{11}^{(011)}\psi^{(011)},$$
$$\varepsilon_{22}=e_{22}^{(000)}+e_{22}^{(100)}\psi^{(100)}+e_{22}^{(001)}\psi^{(001)}+e_{22}^{(101)}\psi^{(101)},$$
$$\varepsilon_{33}=e_{33}^{(000)}+e_{33}^{(100)}\psi^{(100)}+e_{33}^{(010)}\psi^{(010)}+e_{33}^{(110)}\psi^{(110)},$$

$$\varepsilon_{12} = e_{12}^{(000)} + e_{12}^{(001)}\psi^{(001)},$$
$$\varepsilon_{23} = e_{23}^{(000)} + e_{23}^{(100)}\psi^{(100)}, \quad (10)$$

where $e_{ij}^{(pqr)}$ are the coefficients of deformation decomposition determined by $\omega_{k'}^{(\mu\nu\eta)}$.

Matrix $F_{\theta}^{k'}$, which is part of the (3), is formed in a similar way. According to the moment scheme, the volume change function is determined by the relation:

$$\{\theta\} = \{\xi\}^T \{\psi\}, \quad (11)$$

where expansion coefficients of the vector $\{\xi\}$ are determined

$$\xi^{(\alpha\beta\gamma)} = \left. \frac{\partial^{(\alpha+\beta+\gamma)} \varepsilon_{ij} g^{ij}}{(\partial x_1)^{\alpha} (\partial x_2)^{\beta} (\partial x_3)^{\gamma}} \right|_{x_1=x_2=x_3=0}. \quad (12)$$

through the strain expansion coefficients

$$\xi^{(\alpha\beta\gamma)} = e_{11}^{(\alpha\beta\gamma)} g^{11} + e_{22}^{(\alpha\beta\gamma)} g^{22} + e_{33}^{(\alpha\beta\gamma)} g^{33}. \quad (13)$$

In the end, we can represent vector $\{\xi\}$ through the vector of displacement expansion coefficients $\omega_{k'}$:

$$\{\xi\} = \{F^{k'}\}\{\omega_{k'}\}. \quad (14)$$

Based on the described approach, a study of the stress-strain state of a number of sizes of shock absorbers of different diameters was performed.

Dimensions of the shock absorbers were: height $h = 0.05$ m, radius $R = 0.17$ m; 0.20 m; 0.21 m; 0.25 m; mechanical characteristics of rubber: elastic modulus $E = 5.38$ MPa, Poisson's ratio $\nu = 0.49$. Subsidence for all shock absorbers was accepted as $\Delta = 0.005$ m. Here, two calculation options are presented depending on the method of fixing the absorber's ends. In the first case, the ends are vulcanized to the metal plates. In the second variant, the ends are free and can move in a horizontal plane.

The maximum buckling of the shock absorber's lateral surface is shown in figure 1. While analyzing this characteristic, one can see manifestation of the rubber weak compressibility. With a greater h/R ratio, axial strain is compensated by radial deformation, the maximum value of which is greater in the case of the fixed ends than with free ends. In case of the free ends, shape of the deformed lateral surface is close to cylinder, and with the fixed ends it takes a barrel-like shape. This is true for any h/R ratios; though, in the second case, the less is this ratio the more pronounced is the barrel-like shape.

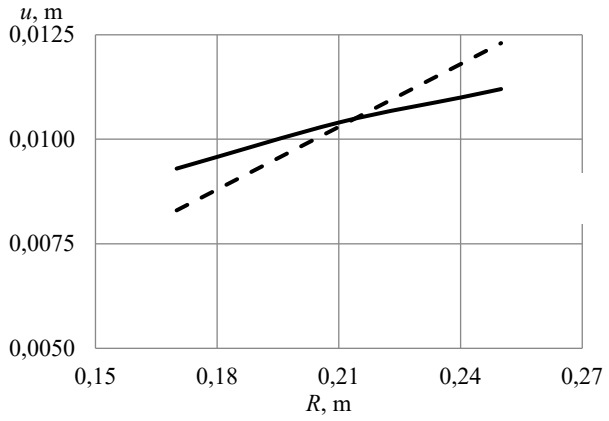

——— – fixed ends, ------- – free ends

Figure 1 – Buckling of the shock absorber's lateral surface

Technical solution and installation of the VSB. The designed vibroseismic insulating blocks are made in the form of solid or hollow rubber or rubber-metal elements, usually, base of the rubber is natural caoutchouc. In Ukraine, the VSB with diameter from 340 mm to 500 mm and height of 40-50 mm are used. In this research, their geometric parameters, as well as compressive and shear stiffness, were

determined by the results of the calculation of the vibroseismically-insulated building. Rubber with maximum damping characteristics was chosen; when analyzing the rubber compounding, special ingredients were used (protective groups, antiagers, modifiers, etc.), which increase the VSB resistance to aging.

There are two ways for insulating buildings from vibration: to install the VSB at the level of the pile grillage (figure 2); or to install them in the basement of the building. In both cases, the upper part of the building, being under dynamic loads of natural and technogeneous character, is separated from the soil by the vibration insulators.

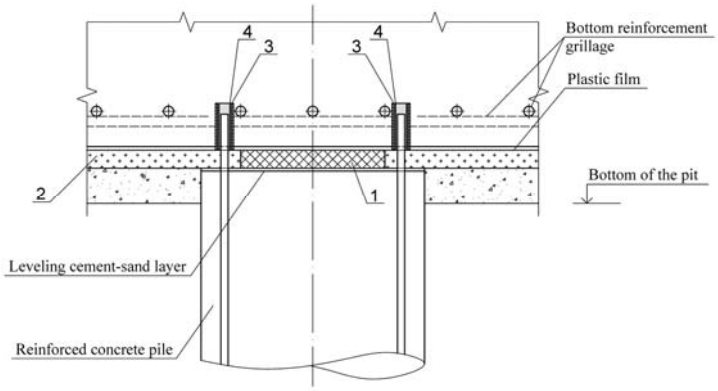

Figure 2 – Installation of the VSB at the level of pile grillage

One of the variants of the VSB installation on the pile is shown in figure 2: 1 – rubber VSB mounted on top of the pile head; 2 – a layer of expanded polystyrene; 3 – steel pipe; 4 – O-type rubber inserts placed between the reinforcing bars and the pipe: they improve damping characteristics of the vibroinsulation system and facilitate the grillage plate to drift relative to the pile.

This system for vibroseismic insulation of buildings and structures [6] has a number of important advantages: no resonance vibrations of the buildings are occurred during earthquakes or dynamic impacts of technogeneous character with spread or narrow-band acceleration spectrum; dynamic loads on the building are double less and even more; upper part of the building is protected from uneven subsidence of the foundation; natural frequency of the building's vibrations is 5-7 Hz at vertical oscillations and less than 1.0 Hz at horizontal ones; high damping ability of the protection system makes it possible to filter harmful vibrations in the wide frequency range; installation of vibroinsulators at the grillage level does not require additional fire protection and creates favorable conditions for making process of the rubber aging essentially longer.

Future trends of constructing buildings and structures with anti-vibration protection system. The main reasons for growing use of seismic insulation in the high-rise buildings is the necessity to reduce seismic loads (up to twice, i.e., by one point by the Ukrainian and EU seismic scales), to minimize relative horizontal interstorey drifting (wraps of the storey slabs) and, as consequences, to reduce consumption of materials, extent of structural damages and economic losses and to provide comfortable conditions for people during the earthquakes or under the effects of surface and underground transport (railway, subway, vehicles, vibrointensive equipment, etc.).

These factors present significant interest for investors and customers. According to the calculated data of departments for seismic resistance and economic researches in the State enterprise "State research institute of building constructions", it is possible to save from 35 thousand to 50 thousand US dollars per multi-storey (9-27 floors) residential house equipped with the seismic insulation due to the less consumption of concrete and reinforcement steel.

According to the State enterprise "State research institute of building constructions" and other literary sources, vibro- and seismic insulation allows to:

– prevent destruction of buildings and structures during earthquakes and under industrial impacts;

– cut the estimated costs of construction by 3-6 %;

– reduce material consumption for buildings and structures up to 10 %;

– reduce labour-intensiveness of construction by 4-6 %;

– expand the scope of typical series through developing regions with high seismic risk and increase height of the buildings with using the same structures.

In Ukraine, sixteen buildings were built and commissioned, including in Kiev: a ten-storey complex in Kikvidze street consisting of ten buildings with the system of vibroseismic protection against the impacts of trains of shallow-bedded underground railway, and complex of three twenty-storey buildings with the system of vibroseismic protection against the impacts of underground trains and surface transport in the Obolonskiy avenue (figure 7); in Lviv: a complex of three buildings with vibroseismic protection against railway transport in the Pid Dubom street. Construction of two 27-storey buildings with protection against the earthquakes has launched in Odessa, in the Genoese street (Odessa is located in the prone-to-earthquake zone due to the proximity to the Vrancea zone in Romania).

The test results indicate that the system of the building's vibroseismic protection against vertical vibrations in the whole and horizontal vibrations (at the level of the pile grillage) provides comfortable living conditions under dynamic impacts of subway trains, wind loads and microseismic vibrations. The results of this research can be used for designing high-rise buildings in the city of Nur-Sultan to protect them against excessive wind effects, and in designs of high-rise buildings in the city of Almaty with location near tectonic faults. For calculating seismically insulated systems with considering regional specificity, the calculation method [7,8] can be used. It is also recommended to arrange stations of engineering-seismometric service in the high-rise buildings [9,10].

The designed seismic insulation can also be used for reconstruction and reinforcement of buildings and historical and architectural monuments located in seismic hazard zones. In this case, the following advantages are obvious:

Use of the seismic insulation in the basement of the building preserves appearance of the building without destroying its architectural features;

Volume of works on reinforcing the upper isolated part of the building is significantly reduced: just the minimum design measures are to be performed in the aboveground part of the building, according to the requirements of the standard DBN B.1.1-12:2014;

When exposed to a calculated earthquake, reliability of the seismically insulated building is much higher than of buildings with traditional reinforcement; this is due to the fact that seismically insulated building stands significant deformation without structural damages during the seismic impact, while in building with traditional reinforcement, it is impossible to avoid crack formation and structural damages.

The designed vibration and seismic insulation is also recommended for repairing and restoration of historical monuments, hospitals, banks and other critical structures erected ages ago [11].

А. Ф. Булат[1], А. С. Кобец[2], В. И. Дырда[1], В. А. Лапин[3], С. Н. Гребенюк[4], Н. И. Лисица[1], Н. Г. Марьенков[5], Г. Н. Агальцов[1], Е. В. Калганков[2]

[1]Украина Ұлттық ғылым академиясының Геотехникалық механика институты, Днепр, Украина;
[2]Днепр мемлекеттік аграрлық-экономикалық университеті, Днепр, Украина;
[3]«Қазақ құрылыс және сәулет ғылыми-зерттеу және жобалау институты» АҚ, Алматы, Қазақстан;
[4]Запорожье ұлттық университеті, Запорожье, Украина;
[5]«Құрылыс құрылымдары мемлекеттік ғылыми-зерттеу институты» РМҚК, Киев, Украина

ҒИМАРАТТАР МЕН ҚҰРЫЛЫСТАРДЫ ДІРІЛДІ СЕЙСМИКАЛЫҚ ТАБИҒИ ЖӘНЕ ТЕХНОГЕНДІК СИПАТТАҒЫ ДИНАМИКАЛЫҚ ӘСЕРДЕН ҚОРҒАУ

Аннотация. Мақалада ғимараттар мен құрылыстарды табиғи және техногендік сипаттағы динамикалық жүктемелерден қорғау жөніндегі көпжылдық зерттеулердің нәтижелері қарастырылады. Ғимараттардың діріл оқшаулау қажеттілігінің негіздемесі, параметрлерді таңдау және резеңке діріл оқшаулағыштарын есептеу ұсынылған. Дірілді сейсмикалық изоляторларды статикалық есептеу үшін ақырлы элемент әдісін қолдану ерекшеліктері келтірілген. Резинаның әлсіз қысылуын ескеру үшін штамм тензоры мен көлемнің өзгеру функциясын құрайтын орын ауыстыру векторының құрамдас бөліктерін үш есе жақындатудан тұратын ақырлы элементтің момент схемасы қолданылды. Түрлі диаметрдегі амортизаторлардың бірқатар стандартты өлшемдерінің кернеулі-деформацияланған күйі анықталды. Шеттерін бекіту әдісіне байланысты екі есептеу

әдісі ұсынылған. Бірінші жағдайда, ұштары металл плиталарға вулканизацияланған. Екіншіден, ұштары бос және көлденең жазықтықта қозғалуы мүмкін. Амортизатордың биіктігі мен оның радиусының арақатынасы құрылымның деформацияланған күйіне әсері талданады. Топырақ пен қадалардың нақты діріл деңгейін анықтау үшін (екі көлденең және бір тік бағытта) вибродинамикалық зерттеулер жүргізілді. Діріл сигналдарын тіркеуді «Wilcoxon Research» (АҚШ) компаниясынан 731А маркалы бір компонентті дірілдеткіштер (діріл датчиктері) жүргізді. Діріл жазбалары мамандандырылған «Сейсмономониторинг» бағдарламасын пайдалану арқылы өңделді. Осы зерттеулердің нәтижелері бойынша нақты техногендік жүктемелер әсерінен тұрғын үй-жайлардағы болжамды діріл деңгейінің қолданыстағы санитарлық нормаларға сәйкестігін анықтау үшін сандық есептеу жүргізілді. Дірілмен оқшауланған темірбетон плитасы мен тұрғын үй едендерінің дірілүдеткіш сынамалары резеңке элементтерін қолдана отырып, діріл-сейсмикалық оқшаулау жүйесінің тиімділігін дәлелдеді: түрлі қабаттардағы тұрғын үй-жайлардағы тіркелген діріл үдеуінің деңгейі қажетті деңгейден аспайды, бұл динамикалық әсердің болуы жағдайында жайлы өмір сүруді қамтамасыз етеді. Жұмыс нәтижелері Алматы қаласының жергілікті жағдайына байланысты резеңке элементтерін қолдана отырып, сейсмикалық оқшауланған ғимараттарды жобалауға мүмкіндік береді.

Түйін сөздер: амортизатор, дірілді оқшаулау, ақырлы элемент әдісі, санитарлық нормалар

А. Ф. Булат[1], А. С. Кобец[2], В. И. Дырда[1], В. А. Лапин[3], С. Н. Гребенюк[4], Н. И. Лисица[1], Н. Г. Марьенков[5], Г. Н. Агальцов[1], Е. В. Калганков[2]

[1]Институт геотехнической механики Национальной академии наук Украины, Днепр, Украина;
[2]Днепровский государственный аграрно-экономический университет, Днепр, Украина;
[3]Акционерное общество «Казахский научно-исследовательский и проектный институт строительства и архитектуры», Алматы, Казахстан;
[4]Запорожский национальный университет, Запорожье, Украина;
[5]Государственное предприятие «Государственный научно-исследовательский институт строительных конструкций», Киев, Украина

ВИБРОСЕЙСМОЗАЩИТА ЗДАНИЙ И СООРУЖЕНИЙ ОТ ДИНАМИЧЕСКОГО ВОЗДЕЙСТВИЯ ПРИРОДНОГО И ТЕХНОГЕННОГО ХАРАКТЕРА

Аннотация. В статье рассмотрены результаты многолетних исследований по защите зданий и сооружений от динамических нагрузок природного и техногенного характера. Представлено обоснование необходимости вибросейсмоизоляции зданий, выбор параметров и расчёт резиновых вибросейсмоизоляторов. Представлены особенности применения метода конечных элементов для статического расчёта вибросейсмоизоляторов. Для учёта слабой сжимаемости резины использовалась моментная схема конечного элемента, которая заключается в тройной аппроксимации компонентов вектора перемещений, составляющих тензора деформаций и функции изменения объёма. Определено напряженно-деформированное состояние ряда типоразмеров амортизаторов различных диаметров. Представлено два варианта расчёта в зависимости от способа закрепления торцов. В первом случае торцы привулканизированы к металлическим пластинам. Во втором торцы свободны и могут перемещаться в горизонтальной плоскости. Проанализировано влияние соотношения между высотой амортизатора и его радиусом на деформированное состояние конструкции. Для определения фактических уровней вибраций почвы и свай (по двум горизонтальным и одному вертикальному направлениям) были проведены вибродинамические исследования. Регистрация вибросигналов осуществлялась однокомпонентными вибропреобразователями (датчики вибрации) марки 731А фирмы «Wilcoxon research» (США). Обработка записей колебаний проводилась с использованием специализированной программы «Сейсмомониторинг». По результатам этих исследований выполнены численные расчёты для определения соответствия прогнозируемых уровней вибраций в жилых помещениях существующим санитарным нормам при воздействии реальных техногенных нагрузок. Вибродинамические испытания уровней виброускорений виброизолированной железобетонной плиты и перекрытий жилого дома подтвердили эффективность системы вибросейсмоизоляции с применением резиновых элементов: зарегистрированные уровни виброускорений в жилых помещениях на разных этажах не превышают допустимых уровней по санитарным нормам, что обеспечивает комфортные условия проживания при наличии динамических воздействий. Результаты работы позволяют проектировать сейсмоизолированные здания с применением резиновых элементов применительно к местным условиям города Алматы.

Ключевые слова: амортизатор, вибросейсмоизоляция, метод конечных элементов, санитарные нормы.

Information about authors:

Bulat Anatolii Fedorovych, Academician of the National Academy of Science of Ukraine, Doctor of Technical Sciences (D.Sc.), Professor, Director of the Institute, Institute of Geotechnical Mechanics named by N. Poljakov of National Academy of Science of Ukraine, Dnipro, Ukraine; gtm.bulat@gmail.com; https://orcid.org/0000-0002-6541-2140

Kobets Anatolii Stepanovych, Doctor of Public Administration, Professor, Rector, Dnipro State Agrarian and Economic University, Dnipro, Ukraine; agro@dsau.ua; https://orcid.org/0000-0002-2507-7763

Dyrda Vitalii Illarionovych, Doctor of Technical Sciences (D.Sc.), Professor, Head of Department of Elastomeric Component Mechanics in Mining Machines, Institute of Geotechnical Mechanics named by N. Poljakov of National Academy of Science of Ukraine, Dnipro, Ukraine; vita.igtm@gmail.com; https://orcid.org/0000-0002-2113-816X

Lapin Vladimir Alekseevich, Candidate of Technical Sciences (Ph.D.), Director of Center for Scientific Research in Building Industry, Corresponding Member of International Engineering Academy and National Engineering Academy of the Republic of Kazakhstan, Kazakh Research and Design Institute of Construction and Architecture, Almaty, Kazakhstan; vlapin@kazniisa.kz; http://orcid.org/0000-0002-1669-5332

Grebenyuk Serhii Mykolaiovych, Doctor of Technical Sciences (D.Sc.), Head of the Department of Mathematical Analysis in Zaporizhzhya National University, Zaporizhzhya, Ukraine; gsm1212@ukr.net; https://orcid.org/0000-0002-5247-9004

Lysytsia Mykola Ivanovych, Candidate of Technical Sciences (Ph.D.), Senior Researcher, Senior Researcher in Department of Elastomeric Component Mechanics in Mining Machines, Institute of Geotechnical Mechanics named by N. Poljakov of National Academy of Science of Ukraine, Dnipro, Ukraine; vita.igtm@gmail.com; https://orcid.org/0000-0001-6364-8937

Marienkov Mykola Hryhorovych, Doctor of Technical Sciences (D. Sc.), Head of the Department, State Enterprise "State Research Institute of Building Structures", Kyiv, Ukraine; n.maryenkov@ndibk.gov.ua; https://orcid.org/0000-0002-7246-845X

Ahaltsov Hennadii Mykolaiovych, Master of Science, Junior Researcher of Department of Elastomeric Component Mechanics in Mining Machines, Institute of Geotechnical Mechanics named by N. Poljakov of National Academy of Science of Ukraine, Dnipro, Ukraine; ag.gena@gmail.com; https://orcid.org/0000-0001-6296-7573

Kalhankov Yevhen Vasylovych, Master of Science, Senior Lecturer of Department "Reliability and repair of machines", Dnipro State Agrarian and Economic University, Dnipro, Ukraine; kalhankov.ye.v@dsau.dp.ua; https://orcid.org/0000-0002-4759-6687

REFERENCES

[1] SBC B.1.1-12:2014. Construction in seismic areas of Ukraine [DBN B.1.1-12:2014. Budivnytstvo u seysmichnykh rayonakh Ukrayiny]. Kyiv, Ukraine, 2014 (in Ukr.).

[2] Bulat A.F., Dyrda V.I., Lysytsia N.I., Ahaltsov H.M., Nemchinov Yu.I., Marienkov N.G., Lapin V.A., Kobets A.S., Nemchenko V.V. (2018) Some problems of ensuring vibrational and seismic safety of buildings and structures [Nekotoryye problemy obespecheniya vibratsionnoy i seysmicheskoy bezopasnosti zdaniy i sooruzheniy]. The herald JSC "KazRDICA" 10(86): 13-19 (in Russ.).

[3] Kirichevskii V.V. (2002) The finite element method in the mechanics of elastomers [Metod konechnykh elementov v mekhanike elastomerov]. Naukova dumka, Kyiv, Ukraine ISBN 966-00-0101-0

[4] Bulat A.F., Dyrda V.I., Lysytsya M.I., Grebenyuk S.M. (2018) Numerical Simulation of the Stress-Strain State of Thin-Layer Rubber-Metal Vibration Absorber Elements Under Nonlinear Deformation, Strength of Materials, 3 (50): 387-395, https://doi.org/10.1007/s11223-018-9982-9

[5] Kirichevskii V.V., Dokhniak B.M., Kozub Yu.G., Gomeniuk S.I., Kirichevskii R.V., Grebeniuk S.N. (2005) Finite Element Method in the MIRELA+ Computer Complex [Metod konechnykh elementov v vychislitelnom komplekse "MIRELA+"], Naukova dumka, Kyiv, Ukraine. ISBN 966-00-0234-3

[6] Bulat A.F., Kobetc A.S., Dyrda V.I., Kalgankov E.V., Lysytsia M.I., Marienkov M.H., Lapin V.A. (2019) Vibro seismic support [Vibroseismoopora]. Patent UA 141011, МПК F16F 1/00, E02D 31/08, E04B 1/98 (In Ukr.)

[7] Lapin V.A., Yerzhanov S.E., Aldakhov Y.S. (2020) Statistical modeling of a seismic insulation object under random seismic exposure // Journal of Physics: Conference Series 1425 012006. https://doi.org/10.1088/1742-6596/1425/1/012006

[8] Kabylbekov K.A., Dasibekov A.D., Abdrakhmanova Kh.K., Saidakhmetov P.A., Issayev E.B., Urmashev B.A. Calculation and visualization of oscillating systems // News of the national academy of sciences of the republic of Kazakhstan. Series of geology and technical sciences. Vol. 5, N 431 (2018). P. 110-119. ISSN 2518-170X (Online), ISSN 2224-5278 (Print) https://doi.org/10.32014/2018.2518-170X.41

[9] Yerzhanov S.Y., Lapin V.A., Aldakhov Y.S. (2020) Monitoring the changes of dynamic characteristics of a high building // Journal of Physics: Conference Series 1425 012008. https://doi.org/10.1088/1742-6596/1425/1/012008

[10] Shepetov A.L., Sadykov T.Kh., Mukashev K.M., Zhukov V.V., Vil'danova L.I., Salikhov N.M., Muradov A.D., Argynova A.Kh. Seismic signal registration with an acoustic detector at the tien shan mountain station // News of the national academy of sciences of the republic of Kazakhstan. Series of geology and technical sciences. Vol. 3, N 429 (2018). P. 47-56. ISSN 2518-170X (Online), ISSN 2224-5278 (Print) http://www.geolog-technical.kz/images/pdf/g20183/47-56.pdf

[11] Mikhailova N.N., Uzbekov A.N. Tectonic and technogenic earthquakes in central Kazakhstan // News of the national academy of sciences of the republic of Kazakhstan. Series of geology and technical sciences. Vol. 3, N 429 (2018). P. 146-155. ISSN 2518-170X (Online), ISSN 2224-5278 (Print) http://www.geolog-technical.kz/images/pdf/g20183/146-155.pdf

N E W S
OF THE NATIONAL ACADEMY OF SCIENCES OF THE REPUBLIC OF KAZAKHSTAN
SERIES OF GEOLOGY AND TECHNICAL SCIENCES
ISSN 2224-5278
Volume 1, Number 445 (2021), 66 – 72 **https://doi.org/10.32014/2021.2518-170X.10**

UDC 502(470.67)

N. S. Faiz[1], M. I. Satayev[1], J. I. Satayeva[2],
A. A. Berdaliyeva[3], A. M. Azimov[1], O. Ya. Nikonov[4]

[1]Non-profit JSC «M.Auezov South Kazakhstan University», Shymkent, Kazakhstan;
[2]«Saken Seifullin Kazakh Agrotechnical University», Nursultan, Kazakhstan;
[3]JSC «South Kazakhstan Medical Academy», Shymkent, Kazakhstan;
[4]Kharkiv National automobile and highway university, Kharkiv, Ukraine.
E-mail: nursultan_90faiz@mail.ru, maratsatayev@mail.ru, julduz.kaynar@mail.ru,
aydin_01@mail.ru, azimov-78@mail.ru, nikonov.oj@gmail.com

VISUALIZATION OF GEODATA OF SEASONAL FLUCTUATIONS OF MAGNETIC FIELDS BASED ON ESRI ARCGIS

Abstract. Energy objects, installations of high and ultra-high voltage, are considered man-made, dangerous objects in terms of the intensity of the electric and magnetic field distribution, which create ion shells in high-altitude zones and spread a certain radius on the territory of a residential area. In this regard, during the construction and commissioning of low-frequency power facilities, it is necessary to conduct a specific environmental analysis on the selected territory. One of the main sanitary and epidemiological requirements for the construction and commissioning of high – voltage power lines is to take into account changes in the daily and seasonal distribution of electrical loads along high-voltage power lines, which have a continuous dynamic characteristic that increases the level of electric and magnetic field strength. In turn, the development of information support for environmental problems of the territory based on GIS technologies makes it possible to record information about the ecological state of the territory at a specific time and present this state with a set of thematic environmental maps of various territorial or district entities.

It should be noted that the above characteristics increase the advantage of geoinformation technologies as an information platform of the database, which will make it possible to obtain data for processing operational analyses and conclusions about the state of the environment around high-voltage power lines.

Key words: remote monitoring, geoinformation technology, dynamics of changes in electrical loads, dynamics of changes in current loads, digital maps of the area.

Introduction. The interaction of physical agents, the intensity of the distribution of electric and magnetic fields produced by high-voltage power lines with biological systems depends on the frequency, amplitude of the fields, and exposure time [1]. It can be assumed that the interaction of electromagnetic radiation with a living organism will depend on the amount and parameters of the transmitted energy, as well as on the type of irradiated tissue [2]. In the article [3], the specific goal was to determine the safe distance from the electromagnetic field created by high-voltage overhead power lines in the immediate vicinity of the specified section. Measurements were made for both electric and magnetic fields in different months in order to detect the highest levels of electromagnetic field fluctuations during peak loads. In the article [4], the measurement of electric and magnetic field fluctuations was carried out for 48 hours. The measurements were carried out six times at each site at intervals of about two months, in the period from January to December. For each measurement, the cross section of the magnetic flux density was determined in the middle of the span from nine measurement points in the range of 80 m. Technical data for both lines, as well as data on load flow during measurement periods, were provided by grid operators. These data were used to calculate the 48-hour average absolute values of the magnetic flux density and compare them with the simulated values. The results of the electromagnetic field estimation near a high-voltage substation are presented [5]. Electric and magnetic fields were measured depending on

the distance to high - voltage equipment, while others were measured depending on the time change. The main goal was to verify compliance with specific limits and, if necessary, to identify protective measures. Finally, safe exposure times were determined for personnel working at these facilities. In the future, detailed maps of electromagnetic field variations will be available to energy companies. The article [6,7] noted the importance of conducting an environmental survey around high-and ultra-high-voltage power lines, which are potentially dangerous, low-frequency objects in the anthropogenic environment.

The level of change in the intensity of electric and magnetic fields is continuously dynamic, which requires constant monitoring of the course of disturbing events. Therefore, when conducting environmental monitoring, it is necessary to be guided by methods and means that can be used to extract reliable and accurate data on certain man-made objects, in our case, energy objects that directly affect the ecological system [8-10].

There are a number of environmental monitoring methods for obtaining reliable results about the state of the environment, which are influenced by the intensity of the electric and magnetic field distribution. One of these methods is the method of mathematical modeling or the method of data visualization through the use of new generation information technologies [11,12].

The geographic information system (GIS) is a powerful information platform that allows you to develop digital maps of various topologies, graphically visualize spatial GEODATA, and obtain additional necessary data about the objects under study [12-15].

The use of the GIS program in assessing the level of electromagnetic pollution generated by a high voltage power line allows you to solve the following problems:

- get the dependence of the distribution of the electric and magnetic fields generated by a high-and ultra-high-voltage power line, which allows you to accurately assess the electromagnetic situation in the selected local area;
- develop a geo-information database and a layer-by-layer electronic map of the location of high-and ultra-high-voltage power lines on the map of the selected territory;
- create user interfaces in the form of an integrating shell, which provides an electronic map of electromagnetic pollution zones for a specific radius of the selected territory;
- get calculated forecasts for the electromagnetic environment over large territories from a radiating, low-frequency object [8, 12-14].

These functions make it possible to create a unified system for monitoring electromagnetic pollution (analysis of the state of the environment located in the zone of the electromagnetic field, make forecasts based on the data obtained, as well as evaluate the selected environmental zone for carcinogenic risks of various types of adverse conditions).

Materials and methods of research. Residential areas Nursat and Kazygurt of Shymkent city, which are located in the zone of active influence of the electromagnetic field, were taken as the studied objects. According to these residential areas, high-voltage power lines, 110 and 220 kV, which originate from the Nursat 110/10 kV and Shymkent 220/110/10 kV substations, have been laid.

In the course of conducting environmental surveys, together with specialists of the regional power grid company "Ontustik Zharyk Transit" LLP, measurements were taken of daytime and evening maximum electric loads of high-voltage power lines in summer and winter periods.

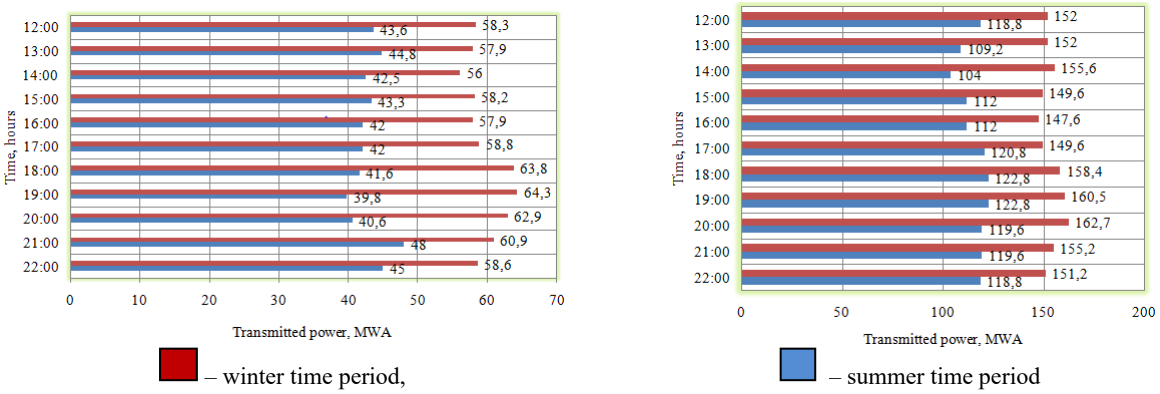

Figure 1 – Dynamics of changes in electrical loads in 110 and 220 kV high-Voltage power line

Figure 1 shows that the peak values of electrical loads on high-voltage transmission lines, 110 kV in the summer time periods was 48 MVA, and in the winter time periods is 64.3 MVA. For high-voltage, 220 kV transmission lines, the peak values of electrical loads were 123 and 163 MVA, respectively, in the summer and winter time periods. It should be noted that the growth of electrical loads increases in the evening, in summer time, evening maxima in 110 kV high-voltage power lines occur at the time from 21:00-22:00 (48-45 MVA), and in winter time at 18:00-21:00 (63.8 – 60.9 MVA). In high-voltage 220 kV transmission lines, the peak values of electrical loads in summer periods fall on the evening time of day at 17:00-21:00 (120.8 -119.6 MVA), in winter periods at 18:00-20:00 (158.4-162.7 MVA).

The dynamics of changes in current loads has a similar characteristic. When calculating current loads, correction factors were introduced that take into account the dependence of current loads on the ambient temperature. The correction coefficients in summer time periods are k_c = 0.8, in winter time periods they are k_c = 1.2. Data on current loads in 110 and 220 kV high-voltage power lines are shown in figure 2.

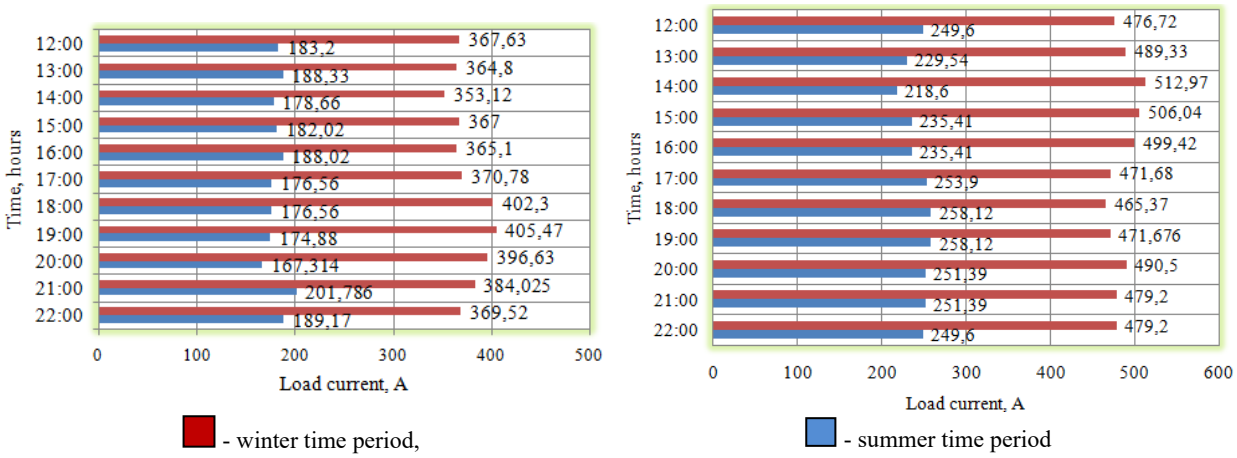

Figure 2 – Dynamics of changes in electrical loads in 110 and 220 kV high-Voltage power line

Figure 2 shows that the peak values of current loads on high-voltage power lines, 110 kV in the summer time periods was 201.786 A, in the winter time periods is 405.47 A. For high-voltage power lines, 220 kV peak current loads were 258.12 and 512.97 A, respectively, in the summer and winter time periods. It should be noted that the growth of electrical loads increases in the evening, in summer, evening maxima in 110 kV high-voltage power lines occur at times with 21:00 22:00 (201,786-189,17 A), in winter time periods at 18:00-21:00 (402,3 – 384,025 A). In high-voltage, 220 kV transmission lines, the peak values of electrical loads in summer periods fall on the evening of 17:00-21:00 (253.9 -251.39 A), in winter periods at 18:00-20:00 (499.42-512.97 A).

The dependence of the intensity of the magnetic field distribution generated by a high-voltage power line on the dynamics of changes in current loads is described by the mirror image method using the following formula:

$$\mathrm{HI(I)} = \frac{I \cdot \gamma}{2 \cdot \pi}\left(\sqrt{(2k1 - k3 - k2)^2 + 3(k3 - k5)^2 + (2k3 - k4 - k6)^2 + 3(k4 - k6)^2}\right) \qquad (1)$$

The dynamics of changes in the magnetic field strength in high-voltage power lines, 110 and 220 kV of the measurements carried out in the Nursat and Kazygurt microdistricts, with maximum current loads in summer and winter periods are shown in figures 3 and 4.

Figure 3 shows that during winter periods, the impact of the magnetic field in 110 kV high-voltage power lines on the ecosystem is almost 2 times higher compared to summer periods. The critical values of the magnetic field strength per day in the summer time periods were 5,225 A/m, in the winter time periods 10,476 A/m.

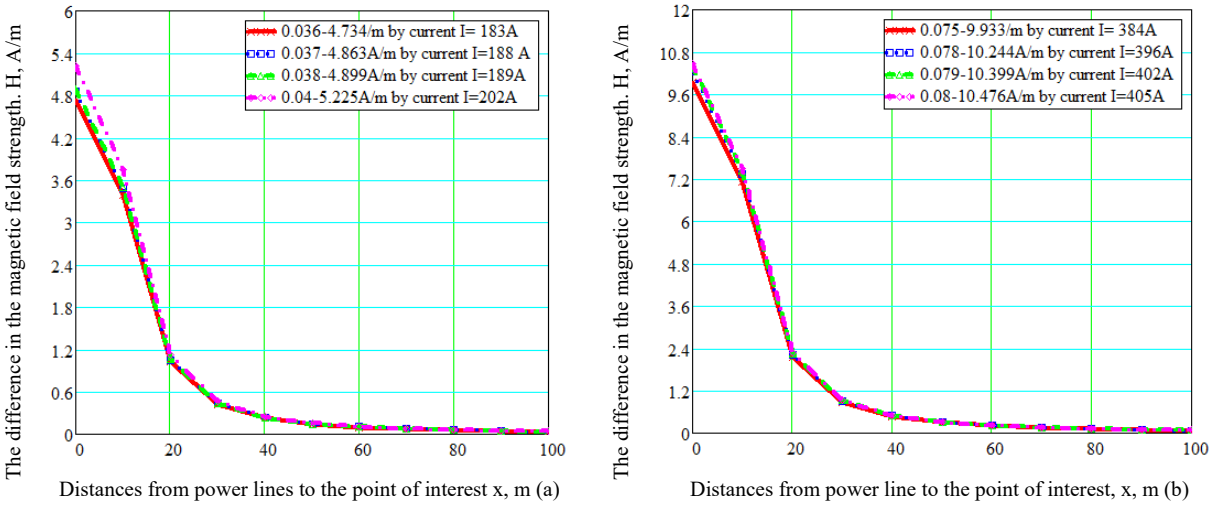

Figure 3 – Dynamics of daily changes in the magnetic field in the summer (a) and winter (b) periods in 110 kV power lines carried out in the Nursat microdistrict

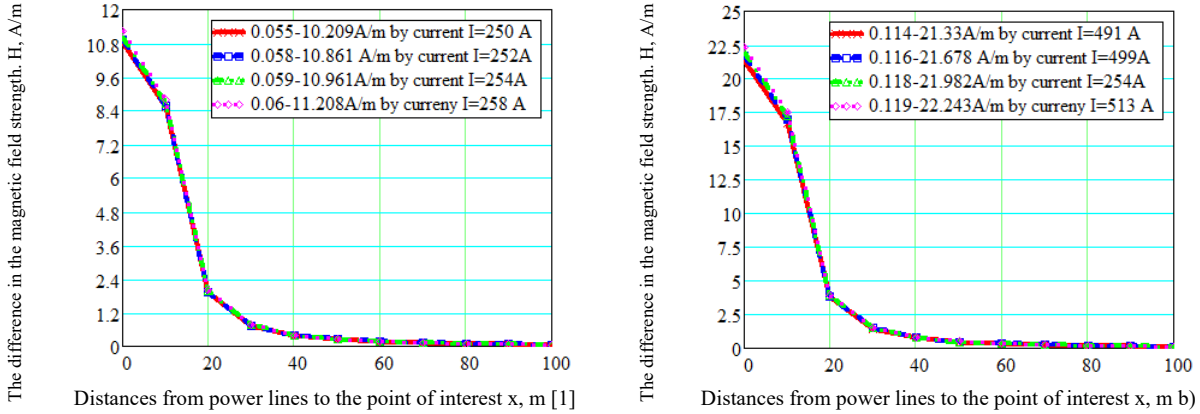

Figure 4 – Dynamics of daily changes in the magnetic field in the summer (a) and (b) winter periods in power lines with a voltage of 220 kV, carried out in the Kazygurt microdistrict.

Figure 4 shows that during winter periods, the impact of the magnetic field in 220 kV high-voltage power lines on the ecosystem is almost 2 times higher compared to summer periods. The critical values of the magnetic field strength per day in the summer time periods were 11.208 A/m, and in the winter time periods 22.243 A/m.

Results and discussion. As a result, digital maps of the area were built based on the ESRI ArcGIS application program, which visually showed the intensity of the distribution of magnetic fields generated by 110 and 220 kV high-voltage power lines in the residential areas of Nursat and Kazygurt in the summer and winter periods of the day. Statistics that describe the effects of characteristic magnetic field distribution zones on the environment are constructed using a magnetic field distribution buffer. To construct the buffer, we used the method of interpolation of inversely weighted distances (IDW) with an interval of 10 m. During the construction of digital maps, the maximum values of magnetic fields produced by low-frequency energy objects in the summer and winter periods of the day were taken.

Digital maps of the area describing the dynamics of changes in the magnetic field generated by a high-voltage power line, 110 and 220 kV, in the residential areas of Nursat and Kazygurt are shown in figures 5, 6.

From figure 5, it can be seen that the shift in the distance of propagation of magnetic pollution in winter compared to summer is 8 m. In turn, the distance shift increases the level of magnetic pollution and, in comparison, has an increased risk of carcinogenic phenomena.

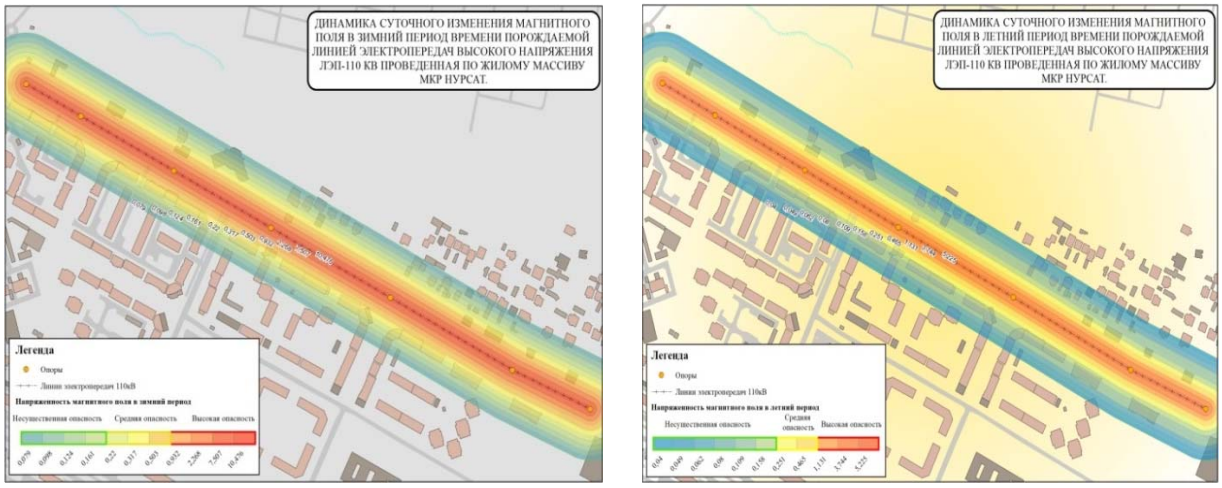

a) b)

Figure 5 – GIS map describing the dynamics of changes in the magnetic field in 110 kV high-voltage power lines in the summer (a) and winter (b) periods of time in the residential area of Nursat

a) b)

Figure 6 – GIS map describing the dynamics of changes in the magnetic field in 220 kV high-voltage power lines in the summer (a) and winter (b) periods of time in the residential area of the Kazygurt microdistrict

From figure 6, it can be seen that the shift in the distance of propagation of magnetic pollution in winter compared to summer is 15 m. In turn, the distance shift increases the level of magnetic pollution and, in comparison, has an increased risk of carcinogenic phenomena.

Conclusion. The use of geoinformation technologies made it possible to build a digital map of the area. In our case, the values of the intensity of the electromagnetic field distribution and the degree of its impact on the environment were taken as input data. The output data was obtained by constructing an interpolation of the inversely weighted distance. According to statistical data, as well as according to the literature review and the regulations of sanitary and epidemiological requirements, the radius of coverage of the spread of magnetic pollution in the Nursat residential area in summer is 0 -18 m, and in winter it reaches up to 26 meters. In the environment of the Kazygurt residential area, where high-voltage power lines, 220 kV, are installed, the radius of coverage of the spread of magnetic pollution in summer periods is 0-25 m, in winter periods it reaches up to 40 meters. By introducing local data, as well as by ranking the level of impact of the electromagnetic field on the environment, zones of residential areas that are under increased exposure to the electromagnetic field were identified. The data obtained show that the level of impact of the magnetic field on the environment is transient, which indicates a decrease or increase in the number of residential objects that are exposed to the emergence of a carcinogenic risk in the ecosystem.

Н. С. Файз[1], М. И. Сатаев[1], Ж. И. Сатаева[2], А. А. Бердалиева[3], А. М. Азимов[1], О. Я. Никонов[4]

[1]«М. Әуезов атындағы Оңтүстік Қазақстан университеті» КЕАҚ, Шымкент, Қазақстан;
[2]С. Сейфуллин атындағы Қазақ агротехникалық университеті, Нұр-Сұлтан, Қазақстан;
[3]«Оңтүстік Қазақстан медицина Академиясы» АҚ, Шымкент, Қазақстан;
[4]«Харьков Ұлттық автомобиль және жол университеті», Харьков, Украина

МАУСЫМДЫҚ МАГНИТ ӨРІСІНІҢ ГЕОМӘЛІМЕТТЕРІН ESRI ARCGIS БАЗАСЫНДА ВИЗУАЛДАУ

Аннотация. Энергетикалық объектілер, жоғары және аса жоғары кернеулі қондырғылар биік аймақтарда иондық қабықтар жасайтын және аудан аумағы бойынша белгілі бір радиуспен таралатын электр және магнит өрістерінің таралу қарқындылығы тұрғысынан техногендік, қауіпті объектілер болып саналады. Осыған байланысты, төмен жиілікті энергетика объектілерін салу және пайдалануға беру кезінде таңдалған аумақта нақты экологиялық талдау жүргізу қажет. Жоғары вольтты электр беру желілерін салу және пайдалануға беру кезіндегі негізгі санитарлық-эпидемиологиялық талаптардың бірі электр және магнит өрістерінің кернеу деңгейін арттыратын үздіксіз динамикалық сипаттамасы бар жоғары вольтты электр беру желілері бойындағы электр жүктемелерінің тәуліктік және маусымдық таралуының өзгеруін есепке алу болып табылады. Өз кезегінде, ГАЖ-технологиялар негізінде аумақтың экологиялық проблемаларын ақпараттық қамтамасыз етуді дамыту белгілі бір уақытта аумақтың экологиялық жағдайы туралы ақпаратты тіркеуге және осы жағдайды әртүрлі аумақтық немесе аудандық құрылымдардың тақырыптық экологиялық карталарының жиынтығымен ұсынуға мүмкіндік береді.

Жоғарыда аталған сипаттамалар деректер базасының ақпараттық платформасы ретінде геоақпараттық технологиялардың артықшылығын арттыратынын атап өткен жөн, бұл жоғары вольтты электр беру желілерінің айналасындағы қоршаған ортаның жай-күйі туралы жедел талдаулар мен қорытындыларды өңдеу үшін деректер алуға мүмкіндік береді.

Түйін сөздер: қашықтықтан басқару мониторингі, геоақпараттық технологиялар, электр жүктемелерінің өзгеру динамикасы, ток жүктемелерінің өзгеру динамикасы, жергілікті жерлердің сандық картасы.

Н. С. Файз[1], М. И. Сатаев[1], Ж. И. Сатаева[2], А. А. Бердалиева[3], А. М. Азимов[1], О. Я. Никонов[4]

[1]НАО «Южно-Казахстанский Университет им. М. Ауэзова», Шымкент, Казахстан;
[2]Казахский агротехнический университет им. С. Сейфуллина, Нурсултан, Казахстан;
[3]АО «Южно-Казахстанская Медицинская Академия», Шымкент, Казахстан;
[4]Харьковский Национальный автомобильно-дорожный университет, Харьков, Украина

ВИЗУАЛИЗАЦИЯ ГЕОДАННЫХ СЕЗОННЫХ КОЛЕБАНИЙ МАГНИТНЫХ ПОЛЕЙ НА БАЗЕ ESRI ARCGIS

Аннотация. Энергетические объекты, установки высокого и сверхвысокого напряжения считаются техногенными, опасными объектами с точки зрения интенсивности распределения электрического и магнитного полей, которые создают ионные оболочки в высотных зонах и распространяются определенным радиусом по территории жилого района. В связи с этим при строительстве и вводе в эксплуатацию объектов низкочастотной энергетики необходимо провести конкретный экологический анализ на выбранной территории. Одним из основных санитарно-эпидемиологических требований при строительстве и вводе в эксплуатацию высоковольтных линий электропередачи является учет изменений суточного и сезонного распределения электрических нагрузок вдоль высоковольтных линий электропередачи, имеющих непрерывную динамическую характеристику, повышающую уровень напряженности электрического и магнитного полей. В свою очередь, развитие информационного обеспечения экологических проблем территории на осно-ве ГИС-технологий позволяет фиксировать информацию об экологическом состоянии территории в конкретный момент времени и представлять это состояние набором тематических экологических карт различных территориальных или районных образований.

Следует отметить, что вышеперечисленные характеристики повышают преимущество геоинформационных технологий как информационной платформы базы данных, которая позволит получать данные для обработки оперативных анализов и выводов о состоянии окружающей среды вокруг высоковольтных линий электропередачи.

Ключевые слова: дистанционный мониторинг, электромагнитные поля, геоинформационные технологии, динамика изменение электрических нагрузок, динамика изменение токовых нагрузок, цифровые карты местности.

Information about the authors

Faiz Nursultan Saparulu, Master of technical science, third - year doctoral student, Non-profit JSC «M. Auezov South Kazakhstan University», Shymkent, Kazakhstan; nursultan_90faiz@mail.ru; https://orcid.org/0000-0002-7491-4281

Satayev Marat Isakovich, Doctor of technical science, Professor, Non-profit JSC «M. Auezov South Kazakhstan University», Shymkent, Kazakhstan; maratsatayev@mail.ru; https://orcid.org/0000-0002-5819-4480

Satayeva Zhulduz Isakovna, senior teacher, «Saken Seifullin Kazakh Agrotechnical University», Nur-Sultan, Kazakhstan; julduz.kaynar@mail.ru; https://orcid.org/ 0000-0001-8327-3474

Berdaliyeva Aydin Abdullaevna, Candidate of technical science, JSC «South Kazakhstan Medical Academy», Shymkent, Kazakhstan; aydin_01@mail.ru; https://orcid.org/0000-0003-2423-500X

Azimov Abdugani Mutalovich, Phd Doctor, Non-profit JSC «M. Auezov South Kazakhstan University», Shymkent, Kazakhstan;azimov-78@mail.ru; https://orcid.org/0000-0002-1316-5854

Nikonov Oleg Yakovlevich, Doctor of technical science, professor, Kharkiv National automobile and highway university, Kharkiv, Ukraine; nikonov.oj@gmail.com; https://orcid.org/0000-0002-8878-4318

REFERENCES

[1] Di Nallo A.M., Strigari L., Giliberti C. et al. (2008) Monitoring of people and workers exposure to the electric, magnetic and electromagnetic fields in an Italian national cancer Institute // *J Exp Clin Cancer Res*, 27, 16. https://doi.org/10.1186/1756-9966-27-16.

[2] Wdowiak A., Mazurek P.A., Wdowiak A., Bojar I. Effect of electromagnetic waves on human reproduction // Ann Agric Environ Med. 2017; 24 (1): 13-18. DOI: 10.5604/12321966.1228394

[3] Al-Bassam E., Elumalai A., Khan A. *et al.* (2016) Assessment of electromagnetic field levels from surrounding high-tension overhead power lines for proposed land use // *Environ Monit Assess,* 188, 316. https://doi.org/10.1007/s10661-016-5318-z.

[4] Bürgi A., Sagar S., Struchen B., Joss S, Röösli M.(2017) Exposure Modelling of Extremely Low-Frequency Magnetic Fields from Overhead Power Lines and it is Validation by Measurements // International Journal of Environmental Research and Public Health, 14, 949. https://doi.org/10.3390/ijerph14090949.5

[5] Iliasa M.F., Baloi F.I., Iliasa F.M.F., Simo A., Musuroi S., Andea P. (2020) Health-Related Electromagnetic Field Assessment in the Proximity of High Voltage Power Equipment // Mihaela Frigura-Iliasa. *Appl. Sci*., 2020, 10, 260. https//doi.org/10.3390/ app10010260

[6] Faiz N.S., Satayev M.I., Berdaliyeva A.A., A.M.Azimov. Assessment of the level of electromagnetic pollution generated by power lines to high voltage on the north and north central parts of the city Shymkent // Bulletin of AUPET.2019. N 4. P. 220-229.

[7] Faiz N.S., Satayev M.I., A.M.Azimov., Berdaliyeva A.A., Nikonov O.Ya. Carcinogenic risk of an electric field on the example of high-voltage power devices power line // Bulletin of PSU. 2020. N 2. P. 448-460.

[8] Duisebayev M.K. Ensuring environmental safety in the operation of electrical equipment of power lines and high-voltage substations. Almaty. JSC «AUPET», 2014. 102 p.

[9] Camilla Pedersen, Elvira V. Brauner, Naja H. Rod, VannaAlbieri, Claus E. Andersen, KaareUlbak, Ole Hertel, Christoffer Johansen, Joachim Schuz, Ole Raaschou-Nielsen. Distance to High-Voltage Power Lines and Risk of Childhood Leukemia – an Analysis of Confounding by and Interaction with Other Potential Risk Factors. PLOS ONE, 2014. Vol. 9. P. 1-7. DOI:10.1371/journal.pone.0107096

[10] GIS Solutions for Environmental Management. www.esri.com.environment.

[11] Michael Zipf, Samarth Kumar, Hendrik Scharf, Christoph Zöphel, Constantin Dierstein and Dominik Möst. Multi-Criteria High Voltage Power LineRouting An Open Source GIS-Based Approach. International journal of Geo – Information, 2019. P. 1-24. DOI:10.3390/ijgi8080316.

[12] Enrique A. Navarro-Camba., Jaume Segura-García and Claudio Gomez-Perretta. Exposure to 50 Hz Magnetic Fields in Homes andAreas Surrounding Urban Transformer Stations in Silla (Spain): Environmental Impact Assessment. Sustainability, 2018. P. 1-11. DOI: 10.3390/su10082641.

[13] Antonio Heredia-Rojas, Abraham Octavio Rodríguez-De la Fuente, Ricardo Gomez-Flores, Omar Heredia-Rodríguez, Laura E. Rodríguez-Flores, Michaela Beltcheva and Ma. Esperanza Castañeda-Garza. In Vivo Cytotoxicity Induced by 60 Hz Electromagnetic Fields under a High-Voltage Substation Environment. Sustainability. 2018. DOI:10.3390/su10082789.

[14] Mukhamediev R.I., Mustakayev R., Yakunin K.O., Kuchin Y.I., Kiseleva S.V., Gopejenko V.I. Decision support system for optimization of RES generators placement based on geospatial data // News of the National Academy of Sciences of the Republic Kazakhstan. Series of geology and technical science. Vol. 1, N 439 (2020). P. 81-89. https://doi.org/10.32014/2020.2518-170X. ISSN 2518-170X (Online), ISSN 2224-5278 (Print)

[15] Samigulina G.A., Nyusupov A.T., Shayakhmetova A.S. Analytical review of software for multi-agent systems and their applications // News of the National Academy of Sciences of the Republic Kazakhstan. Series of geology and technical science. Vol. 3, N 429 (2018). P. 173-181. ISSN 2518-170X (Online), ISSN 2224-5278 (Print)

N E W S
OF THE NATIONAL ACADEMY OF SCIENCES OF THE REPUBLIC OF KAZAKHSTAN
SERIES OF GEOLOGY AND TECHNICAL SCIENCES
ISSN 2224-5278
Volume 1, Number 445 (2021), 73 – 81 **https://doi.org/10.32014/2021.2518-170X.11**

UDC 628.32

S. Jakovlevs

Latvia University of Agriculture, Jelgava, Latvia
E-mail: sjakovlevs5603@tanu.pro

A MODEL FOR CALCULATING THE COLLECTION AND PUMPING OF RAIN AND MELT WATER IN THE DESIGN OF MULTIFUNCTIONAL BUILDINGS FOR PUBLIC AND INDUSTRIAL PURPOSES

Abstract. In drainage systems, it is often necessary to raise polluted rain and melt water to a low height. For example, pumping wastewater from one gravity collector to another, raising wastewater by several meters in order to reduce the deepening of the collecting sewer collector and, as a result, reduce capital costs for its construction. In such places, it may be more economically feasible to reduce such deepening. The novelty of the study is that the development of a drain can be fulfilled only if the filling of the throughput of the collectors is sufficiently ensured. The study shows that the possibilities of expanding collectors can be achieved based on compensation for energy consumption. The study outlined the necessity of allocating the device of a high-pressure pumping station with the subsequent laying of a pressure sewage collector to a common collector, or to the main sewer network, which in turn supplies rain and melt water to the main collector. The practical significance of the study is the widespread introduction of intermediate pumps of low pressure in sewerage networks is constrained by the lack of a sufficient range of reliable and economical low pressure pumps for contaminated liquids.

Key words: pumps, heads, treatment system, rain and melt water.

Introduction. Special purpose-made centrifugal pumps are mainly used for pumping wastewater. They are distinguished by the fact that they do not require preliminary wastewater treatment [1]. Due to the complexity of adjustment, the centrifugal blades of the discs operate most of the time with excess heads, which leads to waste of energy [2]. In order to reduce the likelihood of clogging, centrifugal impellers are made with fewer blades than pumps for clean water (most often 1-3 blades per disc) [3]. Fewer blades result in lower efficiency [4]. A centrifugal pump with a head up to 10 metres of water column for certain flow rates is hard to find these days [5]. The need to raise water to this height often occurs during the operation of sewage collection systems [6-9]. Therefore, these tasks require the use of pumps operating with excess heads. These excess heads then have to be extinguished by throttling or by building special extinguishing chambers (additional capital costs). Screw pumps can be used to raise rain and melt water to low heights (up to 8–10 meters) [10].

At the wastewater system, it becomes necessary to pump sludge from primary sedimentation tanks, as well as fine-grained sand from secondary sedimentation tanks. The lack of high speeds inside the screw pumps makes them promising for use as dredging pumps that drain rainwater into the collection network [11-14]. However, these pumps have not been widely used in the sewer industry [15-19]. This is due to the fact that traditional designs of screw pumps have a number of disadvantages that hinder their widespread adoption [20].

Materials and methods. One of the main characteristics of any pump is its flow – the volume of liquid that the pump lifts per unit of time [21-25]. The main equation for determining the theoretical water transmission is the following (1)

$$Q_{teor} = Wan \quad (1)$$

where W – the volume of water in the interblade space of the pump, m^3; a – number of rotations; n – rotational velocity of the screw, min^{-1}.

A complex task is to determine the volume of water in the interblade space of the screw. It depends not only on the design of the screw, but also on the operating characteristics of the pump, such as the rotational speed of the screw, its angle of inclination, and the like. Consider a simplified diagram of a screw pump, which consists of a hub, on the cylindrical surface of which a tube of infinitely small cross-section is coiled along the helix. Let us choose two coordinate systems with a common origin at point O, located on the axis of the screw hub. The first system with traditional coordinate axes x, y, z is tied to the horizon, the second – α, β, γ (2) is tied to the axis of the screw hub. A line A-A is drawn so that it would be a line of the horizontal surface of the liquid in the space between turns. The parametric equation of the helix in coordinates α, β, γ is written as

$$\alpha = r_{zil}\cos\varphi, \beta = r_{zil}\sin\varphi, \gamma = \frac{h}{2\pi}\varphi \quad (2)$$

where h – lead of helix, cm.

Performing the transition from one coordinate system to another, determine the difference between points lying on this line over the horizontal surface passing through the origin of the coordinate system x, y, z. This difference is determined by the equation (3)

$$x = r_{zil}\cos\lambda\,(\varphi tg\lambda tg\varepsilon r_{zil} + \cos\varphi) \quad (3)$$

where r_{zil} – radius of the cylindrical surface of the hub, cm; φ – helical line angle; λ – angle of the screw above the horizon; $tg\varepsilon r_{zil}$ – tangent of an angle of helix pitch.

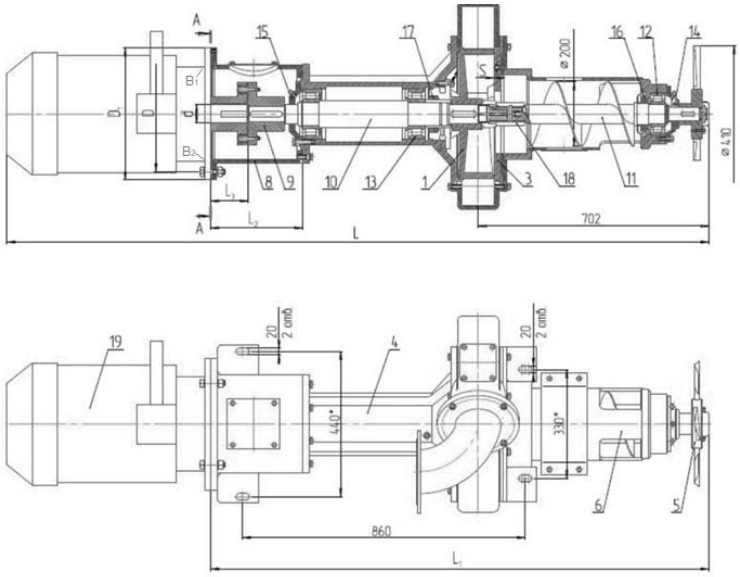

Figure 1 – Typical drawing of a screw pump

On a tube of infinitely small diameter, forming a helical line, there are two points B_1 and B_2, which have the same ordinates x_1 and x_2 of sections with the horizon line A-A. The point B_1 is determined by the helical line angle φ_1, point B_2 – by the rotational angle φ_2. Let there be a certain volume of liquid between these points. The point B_1 is the top bend point of the tube. In the case when the horizon line A-A rises above the point B_1, the liquid will begin to flow into the lower annular space. Therefore, this point is decisive for the liquid level when the maximum filling of the interblade space is observed. Since the point B_1 is a knick point, its coordinate x_1 has a maximum value over a certain interval. Taking this into account, from formula (3), the helical line angle φ_1 can be determined by equating the derivative (3) to zero (5–6)

$$dx = r_{zil}\cos\lambda\,(\varphi tg\lambda tg\varepsilon r_{zil} + \cos\varphi) = 0 \quad (4)$$

From which

$$tg\lambda tg\varepsilon r_{zil} - sin\,\varphi_1 = 0,\ sin\,\varphi_1 = tg\lambda tg\varepsilon r_{zil} \tag{5}$$

In order for the angle φ_1 to take positive values, it is necessary that the condition was met (6–7)

$$tg\lambda tg\varepsilon r_{zil} \leq 1 \tag{6}$$

or

$$\lambda + \varepsilon r_{zil} \leq 90^0 \tag{7}$$

Equation (7) determines the maximum tilt angle of the screw pump, at which it can work. When the angle is exceeded, the liquid will completely flow from the upper interblade space to the lower one. At the same time, the bigger the angle of elevation of the helical line εr_{zil}, the smaller should be the angle of installation of the auger to the horizon λ. Let us find the angle φ_2. The coordinates of the points B_1 and B_2 along the axis x are expressed by the equations (8–9)

$$x_1 = r_{zil}\,cos\,\lambda\,(\varphi_1 tg\lambda tg\varepsilon r_{zil} + cos\,\varphi_1) \tag{8}$$

$$x_2 = r_{zil}\,cos\,\lambda\,(\varphi_2 tg\lambda tg\varepsilon r_{zil} + cos\,\varphi_2) \tag{9}$$

Taking into account their congruence (10)

$$r_{zil}\,cos\,\lambda\,(\varphi_1 tg\lambda tg\varepsilon r_{zil} + cos\,\varphi_1) = r_{zil}\,cos\,\lambda\,(\varphi_2 tg\lambda tg\varepsilon r_{zil} + cos\,\varphi_2) \tag{10}$$

from which (11)

$$\frac{cos\,\varphi_1 - cos\,\varphi_2}{\varphi_1 - \varphi_2} = tg\lambda tg\varepsilon r_{zil} \tag{11}$$

The length of the arc holding water in the interblade space can be expressed by the equation (12)

$$S = \frac{r_{zil}(\varphi_1 - \varphi_2)}{cos\,\lambda} \tag{12}$$

In order to find the volume of liquid that is placed in the coil of the helical tube, it is necessary to multiply the length of the arc by the cross-sectional area of the tube. In a real pump, the pitch angles of the helical line at the inner and outer radius of the helical blade are different. The relationship between them can be expressed by the equation (13)

$$\frac{\lambda_r}{\varepsilon_R} = arctg\,\frac{r}{R} \tag{13}$$

where r – inner radius of the helical blade, cm; R – outer radius of the helical blade, cm. It can be seen that the angle of ascent of the blade along the inner radius is greater than along the outer one.

Calculating the volume of liquid in the interturn space, using the equation (14)

$$V = \int_{\varphi_1}^{\psi_1}\int_{r}^{r_{zil}} \Delta\gamma r_{zil} dr_{zil} d\varphi + \int_{\psi_1}^{\varphi_2}\int_{r}^{R} \Delta\gamma r_{zil} dr_{zil} d\varphi + \int_{\varphi_2}^{\psi_2}\int_{r}^{r_{zil}} \Delta\gamma r_{zil} dr_{zil} d\varphi \tag{14}$$

where ψ_1, ψ_2 – rotation angles of the helical line of the outer contour of the screw blade to the points of intersection with the horizon line A-A; r_{zil} – function (15) which can be found from equation (13), taking $\Delta\gamma = 0$

$$r_{zil} = \frac{tg\lambda}{cos\,\varphi}\left(\frac{x_1}{sin\,\lambda} - tg\varphi\right) \tag{15}$$

Results and Discussion. Conventional screw pumps are single or multi-sided screws that rotate at low frequency in a specially designed open tray, or in a closed tube. The screw pump has the following performance characteristics: Q – feed; H – height of liquid rise (water head); N – power consumption; η – efficiency. The design and operating characteristics of the pump: D – screw diameter (outer diameter of the blades); d – diameter of the screw shaft (screw hub); S – helix pitch distance of screw; L – length of the screw; a – number of rotations; a – angle of inclination to the horizon; δ – the gap between screw and

tray; c – distance along the axis of the screw between two adjacent blades [26-28]. Based on the calculated data, the study proposes the following model for installing a screw pump. It is proposed to manufacture two screws with external diameters $D = 0.39m$ and $0.5m$ and the length $L = 4.6m$, and the ratio of diameters $d/D = 0.5$ each. The installation will make possible to change the angle of inclination of the screw a, its rotation frequency n, water level in the channel in front of the screw, as well as the gap between the screw and the tray in which it rotates δ. It is known that the total pump efficiency η_{povn} consists of its mechanical η_{mex}, hydraulic η_{gidr} and volumetric efficiency η_{obemn} and is determined by the equation (16)

$$\eta_{povn} = \eta_{mex}\eta_{gidr}\eta_{obemn} \tag{16}$$

Mechanical efficiency depends on the design of the pump. In the experimental setup, an electric drive with a single-stage reduction unit is used. For this design, the mechanical efficiency is determined at the level of $\eta_{mex} = 0.85$. The author does not recommend determining the volumetric and hydraulic efficiency separately, considering it a difficult task. It is proposed to find experimentally the product of the volumetric and hydraulic efficiency (23), calling it the general hydraulic efficiency.

$$\eta_{povn} = \eta_{gidr}\eta_{zag.gidr} \tag{17}$$

Then the total efficiency can be determined by the equation (18)

$$\eta_{povn} = \eta_{gidr}\eta_{zag.gidr} \tag{18}$$

The value $\eta_{zag.gidr}$ is found by determining the power developed by the pump and the power consumed by it minus mechanical losses (determined by the mechanical efficiency). At high speeds, splashing losses become significant. It is proposed to theoretically determine the amount of overflows through the gaps according to known equations. Partly as the flow rate during the outflow through a small hole in a thin wall at a constant pressure, and partly as the flow rate when flowing out through a large rectangular hole. For this, another method is proposed for determining the flows through the gaps, as well as another method for determining η_{gidr} and η_{obemn} of the pumps, then comparing it with the experimental Q_{dosl} under the same conditions, that was determined experimentally. The pump lifts the liquid in portions, the volume of which is equal to the volume of the section between adjacent blades of the screw. The section can be considered as a cylinder with a generatrix and oblique, but parallel to each other, bases [29-31].

Then the volume of liquid in one section of the pump, subject to its maximum filling, can be determined by the formula (19)

$$W = W_1 - W_2 \tag{19}$$

where W_1 – volume forming a cylindrical tray in which the auger and adjacent auger blades rotate, cm^3; W_2 – volume forming the submerged part of the inner shaft (hub) of the screw, cm^3.

These volumes can be determined by the equations (20–21)

$$W_1 = \frac{F_1+F_2}{2}c \tag{20}$$

$$W_1 = \frac{f_1+f_2}{2}c \tag{21}$$

where F_1,F_2 – the area of the wetted surface of the lower and upper blades, respectively, cm^2, f_1,f_2 – area of the conditionally wetted surfaces of the screw hub sections in the lower and upper parts of the section, cm^2.

Let us express the area F_1 and f_1 through the filling of the screw section in its lower part of H_1 and h_1. Taking into account the fact that at the maximum filling of the pump section we will obtain the ratio (22–23),

$$H_{max} = \frac{D+d}{2} \tag{22}$$

$$h_{max} = d \tag{23}$$

where H_{max},h_{max} – maximum filling of the section along the screw diameter and the diameter of the hub, respectively; D,d – screw and hub diameters, cm.

Taking into account equation (23) obtain (24–25)

$$\frac{2H_{max}}{D} - 1 = \frac{2(D+d)}{2D} = \frac{d}{D} \tag{24}$$

$$\frac{2h_{max}}{d} - 1 = 1 \tag{25}$$

Let us express the areas included in equations (20–21) through the diameters of the screw and hub, as a result obtain (26–27), the areas F_2 and f_2 are expressed by equations (30–31)

$$F_1 = \frac{D^2}{8}\left[2\pi - 2arccos\left(\frac{2H_1}{D} - 1\right)\right] + \frac{D^2}{8} sin\left[2arccos\left(\frac{2H_1}{D} - 1\right)\right] \tag{26}$$

$$f_1 = \frac{d^2}{8}\left[2\pi - 2arccos\left(\frac{2h_1}{d} - 1\right)\right] + \frac{d^2}{8} sin\left[2arccos\left(\frac{2h_1}{d} - 1\right)\right] \tag{27}$$

Considering that the functional connections between the fillings in the upper and lower parts of the screw section have the form (28-29),

$$H_2 = H_1 - c\,tg\alpha \tag{28}$$

$$h_2 = h_1 - c\,tg\alpha \tag{29}$$

$$F_2 = \frac{D^2}{8}\left[2\pi - 2arccos\left(\frac{2(H_1 - c\,tg\alpha)}{D} - 1\right)\right] + \frac{D^2}{8} sin\left[2arccos\left(\frac{2(H_1 - c\,tg\alpha)}{D} - 1\right)\right] \tag{30}$$

$$f_2 = \frac{d^2}{8}\left[2\pi - 2arccos\left(\frac{2(h_1 - c\,tg\alpha)}{d} - 1\right)\right] + \frac{d^2}{8} sin\left[2arccos\left(\frac{2(h_1 - c\,tg\alpha)}{d} - 1\right)\right] \tag{31}$$

The theoretical pump feed Q_{teor}, defined as the product of the volume of one section at its maximum filling W_{max} by the number of sections N (32–33), raising water per unit of time

$$Q_{teor} = W_{max}N \tag{32}$$

$$N = an' \tag{33}$$

where a – number of blades in the screw, n' – its rotation frequency (c^{-1}).

Then the losses of the pumped liquid, for overflow through the gaps between the screw blades and the cylindrical tray, as well as overflow over the edge of the screw, will be determined by the equation (34)

$$Q_{peretik} = Q_{teor} - Q_{dosl} \tag{34}$$

The volumetric efficiency is determined by the equation (35)

$$\eta_{obemn} = \frac{Q_{dosl}}{Q_{teor}} \tag{35}$$

The proposed model makes possible to determine the flow rate of the screw pump Q^1_{dosl} with the following parameters: screw diameter $D^1 = 0.39m$, crew hub diameter $d^1 = 0.195m$, screw filling $\frac{h^1}{D^1} = 0.75$, angle of inclination to the horizon $\alpha^1 = 30^0$, gap between the screw and the tray $\delta^1 = 5.2\,mm$. The screw rotation frequency was changed in the range $n = 75 \div 120$ rpm (min^{-1}). Calculating the volumetric η_{obemn} and hydraulic η_{gidr} efficiency of this pump at different speeds, using equations (25–41) and the experimental values of its delivery. The calculation will be carried out for all flow rates in litres per second for speeds from 75 to 120 min^{-1} at 5 min^{-1} intervals (table 1).

First, express the screw speed in rotations per second $n'(c^{-1})$. The number of emptying sections during the operation of the screw in one second for a speed of $75min^{-1}$ will be $N_{(390)75} = 3 \times 1.25 = 3.75pc$. For other speeds, look at the value $N_{(390)}$ in the table 1.

Table 1 – Components of the efficiency of a screw pump with a screw diameter of 390 mm

n (min^{-1})	$n'(s^{-1})$	N $(sekz/s)$	Q_{teor} (l/s)	Q_{dosl} (l/s)	$Q_{peretik}$ (l/s)	η_{obemn}	η_{gidr}	$\eta_{zag\ gidr}$	η_{povn}
75	1.25	3.75	28.12	15.0	13.12	0.53	0.96	0.51	0.43
80	1.33	3.99	29.93	17.0	12.93	0.57	0.93	0.53	0.45
85	1.42	4.26	31.95	19.0	12.95	0.59	0.92	0.54	0.46
90	1.5	4.5	33.75	20.0	13.75	0.59	0.93	0.55	0.47
95	1.58	4.74	35.55	21.5	14.05	0.60	0.88	0.53	0.45
100	1.67	5.01	37.58	22.5	15.08	0.60	0.85	0.51	0.43
105	1.75	5.25	39.38	24.0	15.38	0.61	0.82	0.50	0.42
110	1.83	5.49	41.18	25.5	15.68	0.62	0.76	0.47	0.40
115	1.92	5.76	43.2	27.0	16.2	0.63	0.68	0.43	0.37
120	2.0	6.0	45.0	28.0	17.0	0.62	0.61	0.38	0.32

To determine the volume of one section of the pump, calculate the necessary areas of the wetted walls of the section using equations (32-37):

$$F_{2(390)} = \frac{0.39^2}{8}\left[2 \times 3.14 - 2arccos\ (\frac{2\times(0.2925-0.13tg30°}{0.39} - 1)\right]+$$

$$+\frac{0.39^2}{8} sin\left[2arccos\ (\frac{2\times(2925-0.13tg30°)}{D} - 1)\right] = 0.0684(m^2) \quad (36)$$

$$f_{1(390)} = \frac{0.195^2}{8}\left[2 \times 3.14 - 2\text{arccos}\ (\frac{2 \times 0.195}{0.195} - 1)\right] +$$

$$+\frac{0.195^2}{8} sin\left[2arccos\left(\frac{2\times 0.195}{0.195} - 1\right)\right] = 0.0298(m^2) \quad (37)$$

$$f_{2(390)} = \frac{0.195^2}{8}\left[2 \times 3.14 - 2arccos\left(\frac{2 \times (0.195 - 0.13tg30^0)}{0.195} - 1\right)\right] +$$

$$\frac{0.195^2}{8} sin\left[2arccos\left(\frac{2\times(0.195-0.13tg30^0)}{0.195} - 1\right)\right] = 0.0192(m^2) \quad (38)$$

Determine the volume of one section, subject to the maximum filling by the equations (20–21):

$$W_{1(390)} = \frac{0.096+0.0684}{2} 0.13 = 0.0107(m^3) \quad (39)$$

$$W_{2(390)} = \frac{0.0298+0.0192}{2} 0.13 = 0.0032(m^3) \quad (40)$$

$$W_{max(390)} = 0.0107 - 0.0032 = 0.0075(m^3) \quad (41)$$

Determine the theoretical pump flow for a speed of 75 $min^{-1}$by the equation (32)

$$Q_{teor(390)75} = 7{,}5 \times 3{,}75 = 28{,}12(l/s) \quad (42)$$

The value of overflows through the gaps for the screw rotation frequency of 75 min^{-1}, determined by the equation (34), will be (Table 1):

$$Q_{peretik(390)75} = 28.12 - 15 = 13.12(l/s) \quad (43)$$

The volumetric efficiency determined by equation (35), will be:

$$\eta_{obemn(390)75} = \frac{15}{28.12} = 0.53 \quad (44)$$

The obtained data and the overall hydraulic efficiency are written in the Table 1, that is, η_{obemn} x η_{gidr}, from where the hydraulic efficiency from the equation (17) is determined:

$$\eta_{gidr(390)75} = \frac{\eta_{zag\ gidr(390)75}}{\eta_{obemn(390)75}} = \frac{0.51}{0.53} = 0.96 \quad (45)$$

The total pump efficiency, calculated by equation (22), will be:

$$\eta_{povn(390)75} = \eta_{obemn(390)75} \times \eta_{gidr(390)75} \times \eta_{mex} = 0.53 \times 0.96 \times 0.85 = 0.43 \quad (46)$$

At high rotational speeds (more than $115\ min^{-1}$) the amount of liquid increases, the filling of the pump sections is splattered and decreases through the dynamic curvature of the free surface of the liquid, and the volumetric efficiency decreases. The hydraulic efficiency is sufficiently high at the low speeds.

Conclusion. The expediency of using screw pumps for pumping rain and melt water and recirculating activated sludge at treatment facilities has been substantiated, which ensures operation without significant excess heads, as well as without significant dynamic loads. A mathematical model of the pump operation has been developed and an improved method for calculating the components of the efficiency of screw pumps has been proposed, on the basis of which the structure of energy forms is shown. The constructive improvements to increase the overall efficiency of the pump have been developed. Based on predictive calculations, it is shown that it is possible to pump rain and melt water, and activated sludge with an efficiency that exceeds existing analogues by 30% without reducing the pump's performance.

С. Яковлевс

Латвия ауылшаруашылығы университеті, Елгава, Латвия

ҚОҒАМДЫҚ ЖӘНЕ ӨНДІРІСТІК МАҚСАТТАҒЫ КӨПФУНКЦИОНАЛДЫ ҒИМАРАТТАРДЫ ЖОБАЛАУ КЕЗІНДЕГІ ЖАУЫН ЖӘНЕ ЕРІГЕН СУДЫ ЖИНАУ МЕН СОРУДЫ ЕСЕПТЕУГЕ АРНАЛҒАН ҮЛГІ

Аннотация. Су тарту жүйелерінде ластанған жаңбыр мен еріген суды шамалы биіктікке көтеру қажет. Мысалы ретінде ағын суды өздігінен ағатын бір резервуардан басқасына айдау, резервуар тереңдігін азайту және соның салдарынан құрылысына кететін шығынды азайту мақсатында ағынды суды бірнеше метрге көтеруді атап өтуге болады. Мұндай аудандарда тереңдікті азайту экономика тұрғысынан тиімді болуы мүмкін. Зерттеудің ғылыми жаңалығы су қоймаларын жеткілікті деңгейде толтыру арқылы қалыптастыруға болатындығымен айқындалады. Зерттеу жұмысы коллекторларды кеңейту мүмкіндігі энергия компенсациясы негізінде қолжетімді болатындығын көрсетті. Зерттеу қысымды сорғы станциясының жалпы коллектормен немесе негізгі кәріз желісіне кәріз қысымын төсеу арқылы таралу қажеттігін көрсетті әрі бұл жаңбыр мен еріген суды негізгі коллекторға айдауды қамтамасыз етеді. Зерттеудің практикалық маңыздылығы кәріз желілеріне төмен қысымды аралық сорғыларды кеңінен енгізу болып есептеледі, бұл ластанған сұйықтық үшін сенімді және үнемді төмен қысымды сорғылардың жеткілікті ассортиментінің болмауымен шектеледі.

Түйін сөздер: сорғы, тегеурін, тазарту жүйесі, жауын-шашын және қар суы.

С. Яковлевс

Латвийский сельскохозяйственный университет, Елгава, Латвия

МОДЕЛЬ РАСЧЕТА СБОРА И ПЕРЕКАЧКИ ДОЖДЕВЫХ И ТАЛЫХ ВОД ПРИ ПРОЕКТИРОВАНИИ МНОГОФУНКЦИОНАЛЬНЫХ ЗДАНИЙ ОБЩЕСТВЕННОГО И ПРОМЫШЛЕННОГО НАЗНАЧЕНИЙ

Аннотация. В дренажных системах часто приходится поднимать на небольшую высоту загрязненные дождевые и талые воды. Например, перекачивание сточных вод из одного гравитационного коллектора в другой, подъем сточных вод на несколько метров с целью уменьшения углубления коллектора коллекторной канализации и, как следствие, снижения капитальных затрат на его строительство. В таких местах экономически более целесообразно уменьшить такое углубление. Новизна исследования заключается в том, что разработка дренажа может быть выполнена только при условии достаточного обеспечения заполнения пропускной способности коллекторов. Исследование показывает, что возможности расширения коллекторов могут быть достигнуты на основе компенсации энергопотребления. В исследовании обозначена необходи-

мость выделения устройства насосной станции высокого давления с последующей прокладкой напорного канализационного коллектора к общему коллектору или к магистральной канализационной сети, которая в свою очередь подает дождевую и талую воду в магистральный коллектор. Практическая значимость исследования заключается в том, что широкое внедрение промежуточных насосов низкого давления в канализационные сети сдерживается отсутствием достаточного ассортимента надежных и экономичных насосов низкого давления для загрязненных жидкостей.

Ключевые слова: насосы, напоры, система очистки, дождевая и талая вода.

Information about the author:

Jakovlevs S., Department of Architecture and Building, Faculty of Environmental and Civil Engineering, Latvia University of Agriculture, Jelgava, Latvia; sjakovlevs5603@tanu.pro; https://orcid.org/0000-0001-7737-0569

REFERENCES

[1] Kamei-Ishikawa N.D., Yoshida A.I., Umita T. (2016) Cesium and strontium loads into a combined sewer system from rainwater runoff // Journal of Environmental Management, 183: 1041-1049. https://doi.org/10.1016/j.jenvman.2016.09.067 (in Eng.).

[2] Feng C.M., Cai Z.W., Mi N., Zhang Y.J., Qian H.L. (2016) Translocation and transformation of phosphorus in rainwater runoff in the bio-retention system // Journal of Ecology and Rural Environment, 32 (4): 639-644. https://doi.org/10.11934/j.issn.1673-4831.2016.04.019 (in Eng.).

[3] Gan L., Zuo J., Xie B., Li P., Huang X. (2012) Zeolite (Na) modified by nano-Fe particles adsorbing phosphate in rainwater runoff // Journal of Environmental Sciences (China), 24 (11): 1929-1933. https://doi.org/10.1016/S1001-0742(11)61035-8 (in Eng.).

[4] Zhang B., Xie G., Zhang C., Zhang J. (2012) The economic benefits of rainwater-runoff reduction by urban green spaces: A case study in Beijing, China // Journal of Environmental Management, 100: 65-71. https://doi.org/10.1016/j.jenvman.2012.01.015 (in Eng.).

[5] Speak A.F., Rothwell J.J., Lindley S.J., Smith C.L. (2013) Rainwater runoff retention on an aged intensive green roof // Science of the Total Environment, (461–462): 28-38. https://doi.org/10.1016/j.scitotenv.2013.04.085 (in Eng.).

[6] Markovič G., Zeleòáková M. (2014). Measurements of quantity of rainwater runoff from roof in experimental conditions // World Applied Sciences Journal, 31 (14): 24-27. DOI: 10.7862/rb.2014.53 (in Eng.).

[7] Kutsova V.Z., Kovzel M.A., Shvets P.U., Grebeneva A.V., Prutchykova V.V. (2018) Structure, phase composition of supercooled austenite, and kinetics of its decomposition in perlite temperature range of chromium-manganese cast iron // Metallofizika i Noveishie Tekhnologii, 40 (4): 551-560 (in Eng.).

[8] Akbayeva L., Mamytova N., Beisenova R., Tazitdinova R., Abzhalelov A., Akhayeva A. (2020) Studying the self-cleaning ability of water bodies and watercounts of Arshalyn district of Akmola region // Journal of Environmental Management and Tourism, 11 (5): 1095-1104 (in Eng.).

[9] Beisenova R., Tulegenova S., Tazitdinova R., Kovalenko O., Turlybekova G. (2020) Purification by ketoconazole adsorption from sewage // Systematic Reviews in Pharmacy 11 (6): 550-554 (in Eng.).

[10] Ren B., Liu K., Ma H., Zhou H., Zheng X. (2014) SWAT model for analysis of pollution load of manganese in rainwater runoff in a manganese mine // Journal of Chemical and Pharmaceutical Research, 6 (7): 1922-1928. https://doi.org/10.1155/2015/163163 (in Eng.).

[11] Blocken B., Carmeliet J. (2012) A simplified numerical model for rainwater runoff on building facades: Possibilities and limitations // Building and Environment, 53: 59-73. https://doi.org/10.1016/j.buildenv.2012.01.010 (in Eng.).

[12] Ryndin V.V. (1980) Mathematical modeling of the process of filling an engine through an inlet manifold. Izvestia vyssih ucebnyh zavedenij // Masinostroenie, 2: 71-75 (in Eng.).

[13] Rabat O.Zh., Absametov D., Kunelbayev M.M., Hasanov E.L., Mykhalevskiy D.V., Abdrashitova R.N., Salnikova Y.I. (2018) Performance calculation of solar water heating unit at a petrol filling station // Periodico Tche Quimica, 15 (30): 589-598 (in Eng.).

[14] Bulatov N.K., Sarzhanov D.K., Elubaev S.Z., Suleymenov T.B., Kasymzhanova K.S., Balabayev O.T. (2020) Engineering and experimental testing of prototypes of biogas equipment. Renewable Energy, 160: 278-287 (in Eng.).

[15] Blocken B., Derome D., Carmeliet J. (2013) Rainwater runoff from building facades: A review // Building and Environment, 60: 339-361. https://doi.org/10.1016/j.buildenv.2012.10.008 (in Eng.).

[16] Nadirov R.K., Nadirov K.S., Esimova A.M., Nadirova Zh.K. (2014) Electrochemical synthesis of amino derivatives of biflavonoids // Chemistry of Natural Compounds, 50: 735-736 (in Eng.).

[17] Ryndin V.V. (2020) Application of the postulate of nonequilibrium to calculate the nonequilibrium of systems of dissimilar gases and liquids // Periodico Tche Quimica, 17 (34): 998-1011 (in Eng.).

[18] Kunelbayev M.M., Kadyrov M.A., Ponomarev A.A., Bulatov N.K., Mukhamadeyeva R.M. (2017) Resources of obtaining biogas in the Republic of Kazakhstan. Ecology, Environment and Conservation, 23 (4): 2090-2095 (in Eng.).

[19] Montayev S.A., Montayeva A.S., Adilova N.B., Shinguzhiyeva A.B., Montayeva N.S., Taskaliyev A.T. (2018) Prospects of creating the technology of composite adsorbent for water purification based on the composition of siliceous and clay rocks of Kazakhstan // International Journal of Mechanical Engineering and Technology, 9(1): 805-813 (in Eng.).

[20] Zhang B., Xie G.D., Li N., Wang S. (2015) Effect of urban green space changes on the role of rainwater runoff reduction in Beijing, China // Landscape and Urban Planning, 140: 8-16. https://doi.org/10.1016/j.landurbplan.2015.03.014 (in Eng.).

[21] Xu T., Peng L., Yang X., He Y., Jiang Z. (2019) Assessing the rainwater runoff reduction effects of typical green roofs in a humid subtropical city. Shengtai Xuebao / Acta Ecologica Sinica, 39 (20): 7557-7566. https://doi.org/10.5846/stxb201808281837 (in Eng.).

[22] Alekseev O.M., Lazarenko M.M., Puchkovs'ka G.O., Bezrodnaya T.V., Sendzyuk A.A. (2010) Peculiarities of the thermal motion in crystals formed by cetyltrimethylammonium bromide molecules // Ukrainian Journal of Physics, 55 (9): 973-979 (in Eng.).

[23] Privalko V.P., Dinzhos R.V., Rekhteta N.A., Calleja F.J.B. (2003) Structure-diamagnetic susceptibility correlations in regular alternating terpolymers of ethene and propene with carbon monoxide // Journal of Macromolecular Science – Physics, 42B (5): 929-938 (in Eng.).

[24] Nadirov R.K., Nadirov K.S., Bimbetova G.Zh., Nadirova Zh.K. (2016) Synthesis and cytotoxic activity of new flavopiridol analogs // Chemistry of Natural Compounds, 52: 499-500 (in Eng.).

[25] Moldabayeva G.Z., Metaxa G.P., Alisheva Z.N. (2019) Theoretical bases for the implementation of the processes to reduce viscosity in the conditions of natural reservation // News of the National Academy of Sciences of the Republic of Kazakhstan, Series of Geology and Technical Sciences, 5 (437): 138-143 (in Eng.).

[26] Metaksa G.P., Moldabayeva G.Z., Alisheva Z.N. (2019) Mechanism of structure formation in fluid-bearing minerals // Mining Informational and Analytical Bulletin, 2019 (2): 78-84 (in Eng.).

[27] Savon D.Y., Aleksakhin A.V., Skryabin O.O., Goodilin A.A. (2019) Occupational health and safety digitalization in the coal industry. Eurasian Mining, 2019 (2): 70-72 (in Eng.).

[28] Koval Yu.M., Kutsova V.Z., Kovzel M.A., Shvets P.Yu. (2020) Features of structure formation, kinetics of phase transformations, mechanical and tribological properties of the Fe-based Cr–Mn–Ni alloys. Progress in Physics of Metals, 21 (2): 180-248 (in Eng.).

[29] Shamshedenova S., Beisenova R., Rakhymzhan Z., Zhaznaeva Z., Syzdykova N., Tazitdinova R., Khanturin M. (2019) Ecological characteristics of groundwater in rural areas of the Karaganda region // Journal of Ecological Engineering, 20 (11): 67-75 (in Eng.).

[30] Montaev S.A., Zharylgapov S.M., Montaeva N.S., Shakeshev B.T. (2020) Research of possibility of producing ceramic paving stones by vibrocompression with the purpose of using them in the improvement of urban areas. IOP Conference Series: Materials Science and Engineering, 775 (1): 012118 (in Eng.).

[31] Skydan O., Sheludchenko B., Kukharets S., Medvedskyi O., Yarosh Y. (2019) Analytical study of multifractal invariant attributes of traffic flows // Eastern-European Journal of Enterprise Technologies, 3 (3-99): 22-29 (in Eng.).

N E W S
OF THE NATIONAL ACADEMY OF SCIENCES OF THE REPUBLIC OF KAZAKHSTAN
SERIES OF GEOLOGY AND TECHNICAL SCIENCES
ISSN 2224-5278
Volume 1, Number 445 (2021), 82 – 90 **https://doi.org/10.32014/2021.2518-170X.12**

UDC 541.13

G. Kalimbetov[1], A. Toigozhinova[1], W. Wojcik[2]

[1]Kazakh Academy of transport and communications named after M. Tynyshpaev, Almaty, Kazakhstan;
[2]Lublin technical University, Poland.
E-mail: gala_84_11@mail.ru

DEVELOPMENT OF STRUCTURAL SCHEMES AND OPERATION ALGORITHMS FOR THE AUTOMATIC CONTROL SYSTEM OF A MULTIFUNCTIONAL ENERGY COMPLEX

Abstract. Among the promising automatic control systems, logical-dynamic control systems that change both the structure and parameters of the control device using switches formed on the basis of a certain logical algorithm have proven themselves well. The use of logical algorithms as part of MACS subsystems for complex technical objects makes it possible to increase the static and dynamic accuracy of control due to purposeful qualitative and quantitative changes in the control signal. This approach will give the control system fundamentally new properties that allow to fully take into account the nature and dynamics of the movement of the control object. When developing existing logical control algorithms, the issues of their application for multi-connected and multi-functional objects control were not considered. Common to existing logical algorithms is that when switching the structure and/or changing parameters, only the dynamics of its own subsystem is taken into account, which is unacceptable in the case of multi-connected dynamic object control, since cross-links have a significant impact on the quality of control. Thus, the problem of synthesis of logical algorithms for multi-connected objects control is an actual theoretical and applied problem. Despite the considerable amount of research conducted in this area, the application of logical algorithms for complex multidimensional objects control is not sufficiently considered, and there is no unified design concept for this type of MACS, taking into account the required quality of functioning in various operating modes. In this regard, there is a need to synthesize algorithms for logical multi-connected control that form control signals in order to coordinate the actions of all separate MACS subsystems in accordance with new external conditions and operating modes. The problem under consideration determined the purpose of this work and the research objectives.

Key words: structural scheme, algorithm, model, multifunctional energy complex, automatic control system, object, automation, research methods.

Introduction. Automation of various technological processes and industries, in the modern digital world, is very relevant in all industrial circles and areas, and this is one of the decisive factors in increasing productivity and improving working conditions in heavy industrial conditions. All existing and under construction industrial facilities are equipped with technical and software automation at one level or another. The development and widespread implementation of computer technology opens up new opportunities for control of various objects and allows the use of new technologies, including in automatic regulation systems (ARS) and automatic control systems (ACS). It becomes quite realistic to automate the control process, using the professional knowledge and experience of a specialist in the relevant field for the operation of the object in various conditions and technological modes. This formulation allows to speak about the creation of qualitatively new systems for the automation of energy complex facilities. Such systems are based not on a complex mathematical description, but on a management strategy developed on the basis of the production experience of a specialist in the relevant field [1].

The main functional blocks of ACS, elements of structural schemes. Information aspect of control.

The object of the research is the MFEC control systems operating in conditions of unpredictability and changing external environment. MFEC - as a control object is non-stationary - during its operation, changes in the dynamic parameters of both energy subsystems and cross-links are possible, which is caused by a change in operating modes or changes in external conditions of functioning [1]. Such parametric changes lead to a significant change in the dynamics of transient processes in all subsystems, which cannot be fully compensated by linear controllers. For complete and adequate control of such a complex technical object, it is required to develop automatic control systems in the class of multi-connected ACS, which are a set of subsystems interconnected through natural cross-links in the control object and interacting with each other in order to achieve a common goal of functioning.

The proposed algorithms for creating an ACS controller for maintaining the level are not highly specialized and can be used in almost any field of technology, and the outlined methodological foundations allow to create an ACS using fuzzy logic to maintain any parameter, taking into account the specifics of a particular unit.

The subject of the research is the control processes of technological complexes, the peculiarities of their dynamics, methods and technical means of implementing control algorithms based on the theory of fuzzy sets.

The goal of the work is to increase the efficiency of using energy-saturated objects by introducing automation systems, creating control algorithms using fuzzy logic methods, researching new capabilities of the ACS and solving practical problems in choosing the structure and parameters of such systems.

In order to achieve the goal of the work, the following tasks were set and solved:

- there was carried out the analysis of tasks arising in the control of dynamic objects; studied the technical base, methods and tools used to solve the tasks;
- there were synthesized the structure and control algorithm of the MFEC system, carried out a detailed analysis of the influence of the parameters of the system itself and external conditions on the dynamics of the control system;
- there was investigated the possibility of using the apparatus of fuzzy logic for the synthesis of control algorithms, revealed the features of the dynamics of these systems;
- there was synthesized an adaptive control algorithm for automatic adjustment of system parameters to changing external conditions;
- there was considered the possibility of implementing diagnostic algorithms for control systems to warn about possible accidents and proposed algorithms for conducting diagnostic tests;
- there was developed a methodology for creating control algorithms based on fuzzy logic and for choosing the parameters of a fuzzy controller;
- based on the analysis of domestic and foreign experience, there was generalized and concretely implemented the approach to the creation of an automatic control system in the hopper of the hydraulic classifier of a mining dredger using the theory of fuzzy sets;
- there was showed the effectiveness of the selected algorithm.

The theoretical and methodological basis of the work consists of approaches and tools of the theory of nonlinear dynamical systems, the theory of fuzzy sets and a computational experiment.

Structural scheme of the investigated class of MACS of complex technical objects. In this work, the P-canonical structure is chosen as the considered class of MACS. With the chosen structure, the interaction between the set of one-dimensional ACS is carried out through natural connections in the control object. Let us consider in more detail the selected structure of object description as a multi-connected control object. Let elements with transfer functions $W_{ii}(s)$, $(i = 1,2)$ be the main ones, and elements with transfer functions $W_{ij}(s)$ $(i \neq j, i, j = 1,2)$ - communication elements. Figure 1 shows the P-canonical structure on the example of a two-connected object, where $u_i(s)$ $(i = 1, 2)$ are control signals that are input relative to a multiply connected control object, $y_i(s)$ $(i = 1, 2)$ are output signals from a multi-connected control object.

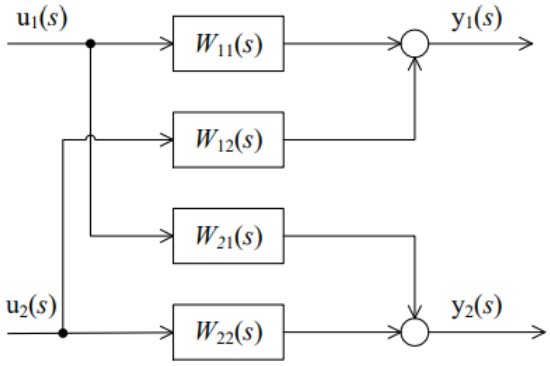

Figure 1 – P-canonical structure on the example of a two-connected object

P-canonical multi-connected objects are described by the following formula:

$$\begin{bmatrix} y_1(s) \\ y_2(s) \end{bmatrix} = \begin{bmatrix} W_{11}(s) & W_{12}(s) \\ W_{21}(s) & W_{22}(s) \end{bmatrix} \begin{bmatrix} u_1(s) \\ u_2(s) \end{bmatrix},$$

or in a generalized form:

$$Y(s) = W(s)U(s).$$

This structure makes it possible to more clearly assess the influence of cross-links on the dynamics of the subsystem and to form a control signal adequate to the current state of the entire MACS [2].

Research methods. The considered method defines an object using the individual characteristics of the subsystems and the characteristics of the connections between them. Multi-connected automatic control systems (figure 2), in which all connections between subsystems are carried out through a multidimensional object, are described by the following equations:

$$\begin{cases} \mathbf{Y}(t) = \mathbf{W}_{OY}(p)[\mathbf{U}(t) + \mathbf{F}(t)], \\ \mathbf{U}(t) = \mathbf{W}_{PE\Gamma}(p)[\mathbf{G}(t) - \mathbf{Y}(t)]. \end{cases}$$

where G(t), Y(t), U(t), F(t) – vector of the set, controllable, and disturbing coordinate, ε(t) – own control error vector, p – differentiation operator.

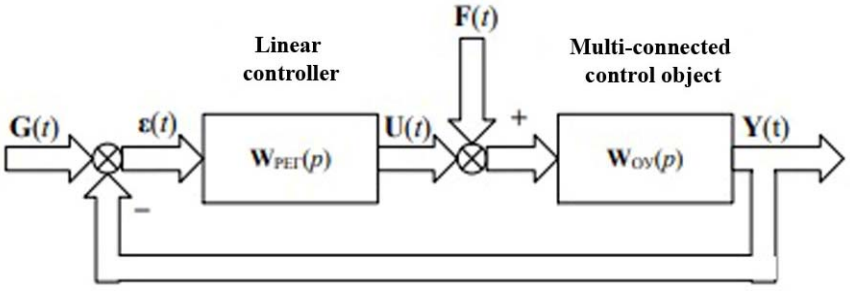

Fugure 2 – Structural scheme of MACS

As an individual characteristic of a subsystem, there is used such a characteristic of a diagonal element of a multi-connected control object, which would fully reflect the studied properties of this element of the MACS. An example of such a characteristic is the transfer function of the subsystem in the control mode:

$$\Phi_i(s) == \frac{Y_i(s)}{G_i(s)} = \frac{W_{PE\Gamma ii}(s)W_{OYii}(s)}{1 + W_{PE\Gamma ii}(s)W_{OYii}(s)}, \quad i = 1,\ldots,n,$$

where for each i-th subsystem, $W_{РЕГii}(s)$ – the transfer function of the linear controller, $W_{ОУii}(s)$ – the transfer function of the control object

In the general case, the connection between a group of subsystems is characterized using the determinants of matrices of the corresponding dimensions $||W_{ОУ}ij(s)\gamma ij||$, where γij - a discrete function:

$$\gamma_{ij} = \begin{cases} 1, & i \neq j, \\ 0, & i = j. \end{cases}$$

This characteristic reflects the integral connection between a group of subsystems. In general case, the function H(s) characterizes both the sign and the magnitude ("strength"), as well as the nature of the connections in the group of subsystems that are connected by this multi-connected connection element. An important feature of this approach is that when describing cross-links between subsystems, their number does not matter. The work gives preference to a systematic approach to describing MACS based on decomposition into subsystems and multidimensional communication elements between them.

Mathematical model of the investigated class of MACS of complex technical objects. Another important aspect of the creation of MACS is the way of creating a mathematical model of a multi-connected control object, which describes the dynamics of its transient processes. One of the very first ways to describe MACS is based on the description of the behavior of the system under study in the state space, which are expressed as a system of differential equations in the Cauchy form. In the context of this approach, for a description in a dynamic system, there is created a matrix mathematical model that includes matrices of input control parameters (Bn×r), of output parameters (Cm×n), of a system (An×n) and of a direct connection (Dm×n).

In general, for multi-connected stationary dynamical systems, the linearized equations of state in the Cauchy normal form have the following form:

$$\begin{cases} \dot{X}(t) = AX(t) + BU(t), \\ Y(t) = CX(t) + DU(t), \end{cases}$$

where X(t)1×n –vector of states, U(t)1×r – vector of control (input) coordinates, Y(t)1×m – vector of controlled (output) coordinates. The state space is determined by the smallest set of phase coordinates that fully characterize the investigated complex technical object at any moment of time [5].

This approach makes it possible to develop unified methods for developing control algorithms regardless of the physical nature of the control object. However, the use of this approach in practice is mathematically complex and requires significant computational resources. Moreover, the abstractness of the vector of states and the difficulty of measuring lead to the loss of "physicality." All MACS parameters are mixed, and it is problematic to analyze the influence of the parameters on the MACS stability margins [5].

However, despite all the positive qualities, these control means are also characterized by significant disadvantages, which include:

- small variation of the parameters of the configured regulator, which does not allow to ensure the required quality of operation in all modes of operation,
- limited possibilities of applicability in MACS due to the fact that parametric changes in the control system can not always compensate the qualitative changes in the control object,
- the need to comply with the adequacy of the reference model and the presence of significant a priori information about the control object.

All of this greatly complicates the synthesis and subsequent analysis of such systems, which leads to a rather high complexity of the application of this approach in engineering practice. Also, adaptive control systems imply preliminary parameterization of the object. But often a priori information is not enough to create a model of an object with an accuracy of a parameter, since the dynamics of an object is nonlinear, which greatly complicates the creation of an accurate mathematical model of an object. In connection with the above problems, it becomes expedient to use robust control methods, which not only allow maintaining the stability of the MACS within certain limits, but are also characterized by less sensitivity to changes in the parameters of the control object compared to optimal systems [7].

Neural network control systems are characterized by a number of properties that make it possible to create highly efficient ACS on their basis:

- the ability to train n example and to generalize data,
- the adaptation to structural and parametric changes, both of the control object and the external environment,
- the possibility of synthesis of regulators that form a control signal based on nonlinear laws, as well as the high stability of its structure [10].

Results of the study of the effectiveness of MACS with a double logic control algorithm. In modern MACS, complex multidimensional technical objects in different modes of operation undergo significant changes in the properties and parameters of a multi-connected control object, which lead to a change in the quality of control. Let us consider a homogeneous three-connected ACS without logic controllers, the structural scheme of which is shown on figure 3.

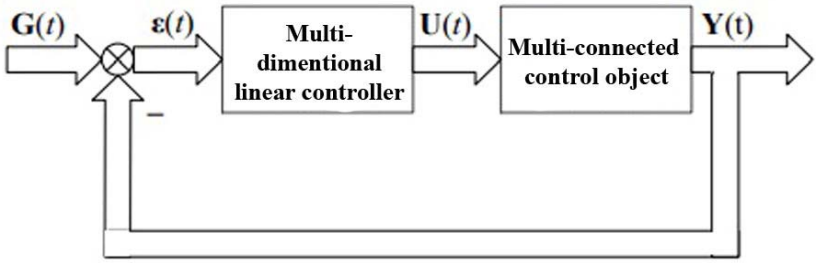

Figure 3 – Structural scheme of the investigated MACS

In the study of homogeneous MACS, it is proposed to use an individual characteristic of a subsystem, reflecting its properties in the control mode, and a multidimensional communication element, reflecting the strength and nature of cross-links between subsystems. Since the considered MACS is homogeneous, the individual characteristics of all subsystems are identical to each other and have the following form:

$$\Phi_i(s)=\frac{W_{OY_{ii}}(s)W_{PEG_{ii}}(s)}{1+W_{OY_{ii}}(s)W_{PEG_{ii}}(s)},\quad i=1,2,3,$$

where $W_{OYii}(s)$, $W_{PEGii}(s)$ – transfer functions of the control object and linear regulator as part of the i-th subsystem, respectively. As a control object as part of the autonomous i-th subsystem, let us consider the serial connection of the aperiodic link and the oscillatory link, which is described by the following given transfer function $W_{OYii}(s)$:

$$W_{OY_{ii}}(s)=\frac{K_{IM}}{(T_{IM}s+1)(T_{OY}^2s+2\xi_{OY}T_{OY}s+1)},\quad i=1,2,3,$$

where T_{IM} –time constant of the actuator, K_{IM} – transfer coefficient of the actuator, T_{OY} – time constant of a multi-connected control object, ξ_{OY} – damping coefficient of a multi-connected control object. In the design mode, the actuator does not change the amplitude of the control signal (K_{IM} = 2), but is characterized by inertia (T_{IM} = 0,1 sec.). The control object is characterized by significant inertia (T_{OY} = 1 sec.) And a high damping coefficient (ξ_{OY} = 0.9). Thus, in the design mode, the parameters of the control object have the following preset values: K_{IM} = 2, T_{IM} = 0.1 sec., T_{OY} = 1 sec., ξ_{OY} = 0.9. A multi-connected control object in the design mode is characterized by the presence of both stabilizing and destabilizing connections. The multidimensional connection element K_{OY}, corresponding to this nature of cross-links, in the design mode, is described by the following given matrix:

$$\mathbf{K}_{OY}=\begin{bmatrix}K_{11} & K_{12} & K_{13}\\ K_{21} & K_{22} & K_{23}\\ K_{31} & K_{32} & K_{33}\end{bmatrix},$$

where Kij – cross-links transfer coefficient from the j-th subsystem to the i-th subsystem. In the design mode, the elements of the multidimensional connection element K_{OY} have the following values: K11 = K22 = K33 = 1, K12 = -0.4, K13 = 0.5, K21 = 0.7, K23 = -0.3, K31 = 0, 5, K32 = -0.6. As a linear regulator in the i-th subsystem, let us consider a given isodromic link with the following transfer function WРЕГii(s):

$$W_{PEГ_{ii}}(s) = K_{PEГ}\frac{\tau_{PEГ}s+1}{s}, \quad i = 1, 2, 3,$$

where for each i-th subsystem $K_{РЕГ}$ - the transfer coefficient of the linear controller, τРЕГ - the forcing constant of the linear controller.

Let us synthesize the parameters of a linear regulator that provides the required stability margins (by the amplitude $\theta_{ТРЕБ} \geq 6$, by the phase $\varphi_{ТРЕБ} \geq 50°$) and control quality (regulation time t <10 sec., overregulation $\delta \approx 0\%$) in each subsystem, taking into account the influence of cross-links in MACS. Since the studied MACS is homogeneous, it is advisable to use the generalized characteristic of a multi-connected communication element, which is described and determines the nature and strength of cross-links communication between a group of subsystems:

$$H_2 = h_{12} + h_{13} + h_{23} = 0{,}28 - 0{,}25 - 0{,}18 = -0{,}15, \quad H_3 = h_{123} = -0{,}15.$$

It can be seen that in the design mode, a local stabilizing negative feedback is formed between the first and second subsystems (h12> 0), however, in the studied system as a whole, a destabilizing positive feedback is formed (H2 <0, H3 <0).

Based on the obtained characteristics H2 and H3, we create a characteristic connection equation that allows to estimate the stability margins in MACS [5]:

$$D(x, H) = 1 + \sum_{i=2}^{n} H_i x^i = 1 - 0{,}15x^2 - 0{,}15x^3 = 0.$$

Investigation of stability margins for both closed and open systems are discussed in detail in [27]. The roots x_j(j = 1,2,3) of the characteristic connection equation allow to evaluate the stability of the system by the amplitude-phase frequency response of the closed system, and the modified roots x_j*(j = 1,2,3) - by the amplitude-phase frequency response of the closed system.

$$x_i^* = \frac{x_i}{(1 - x_i)}.$$

The value of the roots xi and modified roots xi* are presented in table.

Roots x_i and modified roots x_i* of the studied MACS in the design mode

i	*Root* , x_i		*Modified root* , x_i*	
1	1,6	1,6	-2,66	$2{,}66e^{-j180°}$
2	-1,3-*j*1,57	$2e^{-j129{,}6°}$	-0,7-*j*0,2	$0{,}73e^{-j164°}$
3	-1,3+*j*1,57	$2e^{j129{,}6°}$	-0,7+*j*0,2	$0{,}73e^{j164°}$

Let us calculate the parameters of the linear controller that provides the required stability margins both by the phase and by the amplitude relative to the calculated modified roots. In order to do this, we calculate the parameters of the linear controller, which provides for each subsystem the phase stability margin $\varphi = \gamma - 90°$, where γ – the smallest argument among the modified roots xi* (in the context of the example under consideration: γ = 164 °).

The graphs of transient processes Y(t) in the investigated MACS in the design mode without a logic controller are shown on figure 4. The simulation results show that the synthesized linear regulator provides the required quality of control as part of the investigated MACS in the design mode.

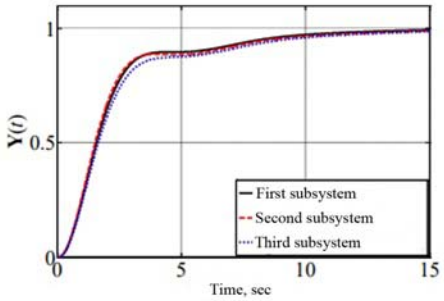

Figure 4 – Graphs of transient processes Y(t) in the investigated MACS in the design mode without logic algorithms

However, there is some "deflection" in the dynamics of the output coordinate due to the presence of an oscillatory link, as well as some difference in the tempo of the subsystems. Based on the simulation results, it can be concluded that the proposed logical controller corrects the dynamics of the output coordinates and approves the rates of each subsystem while maintaining the required performance. Thus, in the design mode, MACS, both without logic controllers, and with them, ensures the specified performance indicators.

The discussion of the results. Based on the results of simulation, it has been established that the proposed logical control algorithm, due to the formation of additional connections between subsystems, allows stabilizing the characteristics of the studied MACS with parametric changes in the cross-links of a multi-connected control object and ensuring high quality control at (H2 <0, H3> 0), (H2> 0, H3> 0).

The scientific novelty of the evaluation results of the effectiveness of the MACS with a double logical control algorithm is to confirm the effectiveness of using the proposed logical control algorithm as part of the MACS with parametric changes, the presence of pure delay and the action of various disturbances by the method of simulation.

Conclusions. In the course of the conducted scientific research, the purpose of which is to improve the quality of multi-connected control of a complex technical object based on logical algorithms, all the tasks were solved and the following results were obtained:

1. Developed the research concept and structure of MACS with a two-channel logic controller based on the decomposition method. The proposed concept consists in the integration of a linear controller that implements linear control laws and a two-channel logical corrector that analyzes both the nature of subsystems and the influence on their dynamics of cross-links in order to improve the quality of control of a multi-connected object in off-design modes. On the basis of the proposed concept, the structure of a two-channel logic controller has been developed as part of the i-th subsystem of the MACS, which forms the main correcting signal for controlling its own subsystem (based on the analysis of its current state and dynamics) and an additional coordinating signal (based on a comparative analysis of the dynamics of all subsystems as part of the MACS). The scientific novelty of the proposed concept of creating an MACS structure with a two-channel logic controller is the formation of a control signal ui*(t) based on the integration of the main signal ui(t) for controlling its own subsystem and an additional coordinating signal $\bar{u}i(t)$, which takes into account the influence of cross-links.

2. Conducted the synthesis of a double logical algorithm for controlling the subsystem as part of the MACS. In the context of solving this problem, there was developed a logical algorithm for controlling an autonomous subsystem as part of a multi-connected control object, which generates a correcting error εi*(t) based on the analysis of both the current state and the predicted dynamics of its own i-th subsystem based on control error signals εi(t) and its derivative εi'(t), respectively. Also, a logical algorithm for the control of the subsystem was developed, taking into account the influence of cross-links, which forms an artificial coordinating connection $\bar{u}i(t)$ based on the signal $\bar{y}i'(t)$ obtained on the basis of a logical comparative analysis of the dynamics yi'(t) of its own i-th subsystem with the dynamics of yj' (t) of other j-th subsystems. The scientific novelty of the double logical algorithm lies in the correction of the dynamics of the subsystems together with the formation of additional artificial cross-links for the coordination of all subsystems of the MACS.

Ғ. П. Қалымбетов[1], А. Ж. Тойгожинова[1], W. Wojcik[2]

[1]М. Тынышбаев атындағы Қазақ көлік және телекоммуникациялар академиясы, Алматы, Қазақстан;
[2]Люблин техникалық университеті, Польша

КӨПФУНКЦИОНАЛДЫ ЭНЕРГЕТИКАЛЫҚ КЕШЕННІҢ АВТОМАТТЫ БАСҚАРУ ЖҮЙЕСІ ЖҰМЫСЫНЫҢ АЛГОРИТМДЕРІ МЕН ҚҰРЫЛЫМДЫҚ ДИАГРАММАЛАРЫН ДАМЫТУ

Аннотация. Перспективалы автоматты басқару жүйелерінің ішінде белгілі бір логикалық алгоритм негізінде қалыптасқан ажыратқыш арқылы басқару құрылғысының құрылымын да, параметрлерін де өзгертетін логикалық-динамикалық басқару жүйелері жақсы танылды. Логикалық алгоритмдерді АБКЖ ішкі жүйелерінің бөлігі ретінде күрделі техникалық объектілерге қолдану басқару сигналының мақсатты сапалы және сандық өзгеруіне байланысты басқарудың статикалық және динамикалық дәлдігін арттыруға мүмкіндік береді. Бұл тәсіл басқару жүйесінің табиғаты мен динамикасын толығымен ескеруге мүмкіндік беретін басқару жүйесіне принципиалды жаңа қасиеттер береді. Қолданыстағы логикалық басқару алгоритмдерін әзірлеу кезінде оларды көп байланыстырылған және көпфункционалды нысанды басқаруға қолдану мәселелері қарастырылмаған. Қолданыстағы логикалық алгоритмдерге тән нәрсе – құрылымды ауыстыру және/ немесе параметрлерді өзгерту кезінде тек өзіндік ішкі жүйенің динамикасы ескеріледі, бұл көп байланысқан динамикалық объектіні басқару жағдайында қолайсыз, өйткені айқас сілтемелер басқару сапасына айтарлықтай әсер етеді. Осылайша бірнеше байланыстырылған объектілерді басқарудың логикалық алгоритмдерін синтездеу мәселесі өзекті теориялық және қолданбалы мәселе болып саналады. Осы салада жүргізілген зерттеулердің едәуір көлеміне қарамастан, күрделі көпөлшемді объектілерді басқарудың логикалық алгоритмдерін қолдану жеткілікті деңгейде қарастырылмаған және түрлі жұмыс режимінде қажетті жұмыс сапасын негізге ала отырып, АБКЖ-ның осы типіне арналған бірыңғай жобалық тұжырымдама жоқ. Осыған байланысты АБКЖ барлық жеке ішкі жүйелерінің әрекеттерін жаңа сыртқы жағдайлар мен жұмыс режиміне сәйкес үйлестіру үшін басқару сигналдарын тудыратын, логикалық көбейтілген байланысты басқару алгоритмдерін синтездеу қажет болады. Қарастырылып отырған мәселе жұмысымыздың мақсатын айқындайды.

Түйін сөздер: блок-схема, алгоритм, модель, көпфункционалды энергетикалық кешен, автоматты басқару жүйесі, нысан, автоматика, зерттеу әдістері.

Г. П. Калимбетов[1], А. Ж. Тойгожинова[1], W. Wojcik[2]

[1]Казахская академия транспорта и коммуникаций им. М. Тынышпаева, Алматы, Казахстан
[2]Люблинский технический университет, Польша

РАЗРАБОТКА СТРУКТУРНЫХ СХЕМ И АЛГОРИТМОВ РАБОТЫ СИСТЕМЫ АВТОМАТИЧЕСКОГО УПРАВЛЕНИЯ МНОГОФУНКЦИОНАЛЬНЫМ ЭНЕРГЕТИЧЕСКИМ КОМПЛЕКСОМ

Аннотация. Среди перспективных систем автоматического управления хорошо зарекомендовали себя логико-динамические системы управления, изменяющие как структуру, так и параметры устройства управления с помощью переключателей, сформированных на основе определенного логического алгоритма. Использование логических алгоритмов в составе подсистем МСАУ для сложных технических объектов позволяет повысить статическую и динамическую точность управления за счет целенаправленного качественного и количественного изменения управляющего сигнала. Такой подход придаст системе управления принципиально новые свойства, позволяющие в полной мере учитывать характер и динамику объекта управления. При разработке существующих логических алгоритмов управления не рассматривались вопросы их применения для управления многосвязным и многофункциональным объектом. Общим для существующих логиических алгоритмов является то, что при переключении структуры и / или изменении параметров учитывается только динамика собственной подсистемы, что недопустимо в случае управления многосвязным динамическим объектом, поскольку перекрестные связи оказывают существенное влияние на качество управления. Таким образом, задача синтеза логических алгоритмов управления многосвязными объектами является актуальной теоретической и прикладной задачей. Несмотря на значительный объем исследований, проводимых в этой области, применение логических алгоритмов управления сложными многомерными объектами недостаточно рассмотрено, и отсутствует единая концепция проектирования данного типа МСАУ, учитывающая требуемое качество функционирования в различных режимах эксплуатации. В связи с этим возникает необходимость синтеза алгоритмов логического многосвязного управления, формирующих

управляющие сигналы для координации действий всех отдельных подсистем МСАУ в соответствии с новыми внешними условиями и режимами работы. Рассматриваемая проблема определила цель данной работы и задачи исследования.

Ключевые слова: структурная схема, алгоритм, модель, многофункциональный энергетический комплекс, система автоматического регулирования, объект, автоматизация, методы иследования.

Information about authors:

Kalimbetov G.P., doctoral student of the Kazakh Academy of Transport and Communications named after M. Tynyshpaev, Master of Engineering Sciences, Almaty, Kazakhstan; gala_84_11@mail.ru; https://orcid.org/0000-0001-9397-0978

Toigozhinova A.Zh., Head of the Department of "Automation and Control" of the Kazakh Academy of Transport and Communications named after M. Tynyshpaev; PhD, associate professor of KazATC, Almaty, Kazakhstan; aynur_t@mail.ru; https://orcid.org/0000-0002-0305-2776

Waldemar Wójcik, Director of the Institute of “Digitalization and Computational Technology” of Poland, Doctor of Technical Sciences, Head of the Department of Electronics, Lublin Technical University, Poland; waldemar.wojcik@pollub.pl; https://orcid.org/ 0000-0002-0843-8053

REFERENCES

[1] Analysis of periodic motions in multi-connected systems with fuzzy controllers in separate subsystems / B.G. Ilyasov, R.A. Munasypov, G.A. Saitova et al. // Mechatronics, automation, control: Theoretical and applied research journal. 2004. N 8. P. 24-29.

[2] Analysis of the stability of automatic control systems: textbook / B.G. Ilyasov et al; ed. B.G. Ilyasova; Ufa State Aviation Technical University. Ufa: USATU, 2006. 204 p.

[3] Antipin A.F. Basic principles of creating a universal programming system for a logic controller based on clear terms / A.F. Antipin // Electrotechnology, electric drive and electrical equipment of enterprises: collection of all-russian scientific and technical conference in 2 volumes / editorial board: Yu. G. Matveev et al. Ufa: Publishing house USNTU, 2007. Vol. 2. P. 10-12.

[4] Beloglazov D.A. Analysis of methods of stability of fuzzy control systems / D.A. Beloglazov, E.Yu. Kosenko // Proceedings of the SFU. Technical science. 2013. N 2 (139). P. 127-133.

[5] Bogdanov A.V. Multidimensional clear logic regulator with the development of production rules in situational subprograms / A. V. Bogdanov, E. A. Muravyova, T. V. Sazonova // Bulletin of the Orenburg State University. 2012. N 5. P. 248-252.

[6] Ilyasov B.G. Analysis of multi-connected control systems with nonlinear correction of subsystems / B.G. Ilyasov, G.A. Saitova, I.I. Sabitov // Problems of Control and Modeling in Complex Systems: Mat. 13th Int. conf. Samara: SamSC RAS, 2011. P. 127-130.

[7] Wójcik W., Kotyra A., Smolarz A., Komada P. Application of vavelet transform in detection of burned fuels in energetic boilers, Proceedings on International Conference on Optoelektronic Information Technologies PHOTONICS-ODS 2000, Vinnytsia (Ukraine) 2000, 182 p.

[8] Kim D.P. Theory of automatic control. Vol. 2: Multidimensional, nonlinear, optimal and adaptive systems / D.P. Kim. M.: Fizmatlit, 2007. 440 p.

[9] Leonenko A.V. Fuzzy modeling in MATLAB and fuzzyTECH / A. V. Leonenko. SPb: BHV-Petersburg, 2005. 736 p.

[10] Sabitov I.I. Application of logical controllers in the channels of a multi-connected system / I.I. Sabitov // Mavlyut readings: collection of scientific articles of 7th All-Russia youth scientific conf. Ufa: USATU, 2013. Vol. 3. P. 282-283.

[11] Kvyetnyy R.N., Sofina O.Y., Lozun A.V. Modification of fractal coding algorithm by a combination of modern technologies and parallel computations // In 16th Conference on Optical Fibers and Their Applications (pp. 98161R-98161R). International Society for Optics and Photonics, 2015. P. 181-195.

[12] Moskvina S.M., Yukhymchuk M.S. Evaluation of the impact of uncontrolled parametric perturbations on stability of automatic systems with logical control units // 16th Conference on Optical Fibers and Their Applications. International Society for Optics and Photonics, 2015. P. 18-25. 98161X-98161X-7.

[13] Wójcik W., Smolarz A., Kotyra A. Optical fibre system for flame monitoring in power boilers, Proceedings on 2-nd International Symposium on Microelectronics Technologies and Microsystems, Lviv 1998. P. 102-108.

[14] Kalimbetov G.P., Toygozhinova A.Zh. Analysis of energy sorces using the force of the wind and methods of increasing their efficiency // Bulletin of KazNRTU named after K. Satpayev. 2020. 6 (142). P. 265-271.

N E W S
OF THE NATIONAL ACADEMY OF SCIENCES OF THE REPUBLIC OF KAZAKHSTAN
SERIES OF GEOLOGY AND TECHNICAL SCIENCES
ISSN 2224-5278
Volume 1, Number 445 (2021), 91 – 97 **https://doi.org/10.32014/2021.2518-170X.13**

UDC 621.311.21:628

Zh. K. Kassymbekov[1], G. Zh. Kassymbekov[2]

[1]Satbayev University, Almaty, Kazakhstan;
[2]Kazhydro, Almaty, Kazakhstan.
E-mail: jkk2004 @ mail.ru, a_k-82@mail.ru

DEVELOPMENT AND TESTING OF A HYDROCYCLONE SAND TRAP FOR MINI HPP

Abstract. The goal of the project is to develop and use a hydrocyclone sand trap to improve the operation of a mini hydroelectric power station. In contrast to the existing design of a similar type of hydroelectric power station, a bulky sump for water purification has been replaced with an efficient hydrocyclone device. Due to this, a simplification of the design of the HPP is achieved, an increase in the degree of sand collection from the composition of the water used.

Research methods. The initial data for the calculation were taken: the flow rate of water passing through the hydrocyclone and the pressure drop at the inlet and outlet of the hydrocyclone. Computer simulation of the process was carried out using the SolidWorks software (flow simulation). The main technological parameters and a rational mode of operation were established by testing experimental samples both in laboratory and in production conditions.

Research results. In the established mode, the density of clarified water is equal to 1.009 ... 1.050 t / m^3, and the degree of purification is 91 ... 97%. Replacing a bulky reinforced concrete sump with hydrocyclone sand traps of a simplified design reduces the cost of building a water treatment unit from 30% (existing) to 7%. This makes it possible to expand the volume of development of small hydroelectric power plants, especially in mountainous conditions.

Key words: mini hydroelectric power station, development, hydrocyclone sand trap, process modeling, experimental stand, tests.

Introduction. It is well known that hydropower is the most widespread in practice and technologically advanced industry in renewable energy sources [1-6].

Unlike other ecologically safe renewable sources such as the sun, wind, small hydropower practically does not depend on weather conditions and capable to provide steady supply of the cheap electric power to the consumer.

Articles [7-9] show that broad prospects are revealed before small (100 - 1000 kW) and mini-hydroelectric plants (up to 100 kW), especially when using them in foothill and mountain regions. The efficiency of such a power plant can significantly increase if it is used in conjunction with other types of renewable sources, for example, wind power or solar power plants.

As operation experience of a hydroelectric power station demonstrates, the technical condition and reliability of hydroturbine equipment affect the efficiency of their operation, especially the power characteristic [9-12]. In the presence of mechanical impurities in the feed water, hydraulic units are often subjected to abrasive wear. Abrasive wear of turbines leads to a significant drop in their efficiency, and consequently, to a decrease in the power and power output of a hydroelectric power station, to a reduction in the service life of hydro turbine equipment [13-18].

In the widespread derivational schemes of hydroelectric power stations, the protection of hydraulic units from bottom and bottom sediments is carried out in water receivers, and purification of water from hazardous fractions of mechanical impurities is carried out in sedimentation tanks.

In common HES derivation schemes, the protection of hydraulic units from bottom and bottom sediments is carried out in water intakes, and the water is cleaned from dangerous fractions of mechanical impurities in septic tanks [5,19].

However, the cost of the construction of the sump, due to its cumbersome design, are very significant and sometimes make up 20-35% of the investment in the construction of a hydropower plant [19].

These problems to reduce capital investments in construction and the cost of operating a hydropower plant, in our opinion, can be eliminated by using the energy of the watercourse through the diversion channel (pipeline) to separate mechanical impurities from water using hydrocyclones. In this case, the construction of bulky settlers is no longer necessary [2].

Description of the development and research methods. The developed mini hydroelectric power station (HPP) includes a hydrocyclone sand trap, a water treatment unit, a diversion unit, a canal, a hydroelectric power station, a hydro turbine, a generator, a hydrocyclone and a suction pipe (figures 1 and 2) [19].

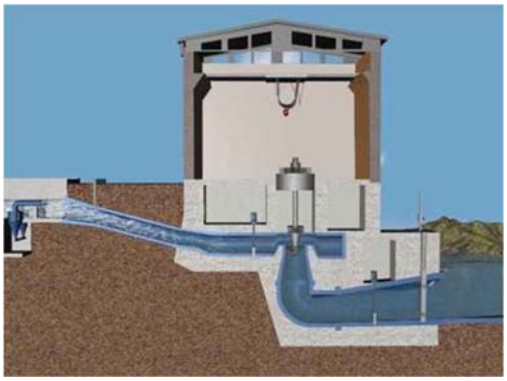

Figure 1 – Technological scheme of mini HPP with hydrocyclone

Figure 2 – General view of the developed hydrocyclone sand trap

The sand collection unit (figure 2) consists of hydrocyclones with receiving chambers and a drain pipe, a viewing well, a viewing channel pan, a sand pipe and a ladder. The threshold, installed inside the diversion channel, is provided in order to ensure the complete flow of water with mechanical impurities into the inlet chamber of the hydrocyclone.

When a hydropower plant is in operation, water with mechanical impurities, moving at the expense of the velocity head in the channel, gets tangentially into the hydrocyclone and is cleared of solid components. Purified water through the upper drain pipe, located in the direction of flow of fluid, flows back into the channel and is fed to the working nozzles of the turbine. Mechanical impurities captured in a hydrocyclone, mainly in the form of fine sand with diameters greater than 0.05 mm, are ejected into a heap by a sand extraction pipe.

The height of the sand mass accumulation at the sand hole within 1/3 of the height of the conical part of the hydrocyclone and the opening of the sand removal line is adjusted using an automatic controller of a simple action.

The initial data for the calculation of a hydro-cyclone unit of a small hydroelectric station are taken: the flow of water passing through the hydro-cyclone - Qn and the pressure drop at the entrance to the hydro-cyclone and its output - Nn, as well as the content of suspended particles before cleaning - γ. [21].

Based on the results of the analysis, it was revealed that in order to use computer simulation data, the numerical model must be verified by a physical experiment. Therefore, numerical analyzes of the processes were carried out on the basis of the STAR CCM + 6.04 software package using the results of experimental studies.

This study includes the calculation of the flow lines of the velocity of particles of a liquid in a hydrocyclone, the trajectory of movement of solid particles, pressure drop, and the efficiency of separation of liquid and solid particles.

For the numerical calculations of this problem, the geometry was chosen with the following characteristics:

1. Dimensions of the hydrocyclone: the area of the entrance area is 0.075 m^2, the area of the output area is 0.0153386 m2, height is 1.1 m, the area of waste particles is 0.007 m2.

2. The grid is selected according to a multifaceted scheme to provide a balanced solution to complex.

Surface meshes are a discrete representation of the geometry of the individual areas that will be used to generate volumetric meshes. It consists of faces (triangles) and vertices and connects all surfaces of the geometry. A total of 70898 cells and 397585 surfaces are used to implement the calculation.

In the three-dimensional motion simulation under consideration, it was assumed that the flow is stationary, i.e. does not depend on time, the density of water and particles of contaminated liquid are constant, and the flow of water is incompressible.

In the simulation of turbulence, the Navier-Stokes differential equation is used, where the averaging process can be considered as temporary for stationary states and averaging the set for repeated transition situations and the continuity equation. The boundary and initial conditions were selected on the basis of experimental data.

At the inlet of the hydrocyclone, the velocity of the supplied suspension was 0.38 m / s, and the initial pressure was 1100 kPa. The results of pressure on a symmetric section of a hydrocyclone show that the outlet pressure drops to 550 kPa. This is in the permissible errors coincide with the subsequent experimental data.

The ratio of the amount of water and particles of contaminated liquid in the calculation is in the order of 3: 1. Figure 3 shows the proportion of particles and their distribution in the hydrocyclone by weight. It turned out that the maximum fraction of particles is at the entrance (0.35) and approximately 0.05 at the exit.

Due to the fact that during the operation of a hydrocyclone, centrifugal forces exert a significant effect on mechanical particles and the difference in the densities of the components considered the position of the particles under various possible modes of operation. The established features are to a certain extent characterized by the model solution shown in figure 4.

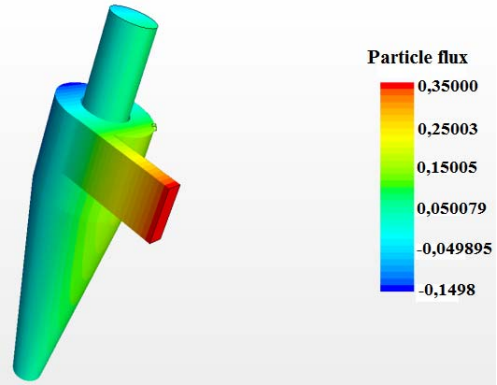

Figure 3 – Mass fraction of mechanical particles

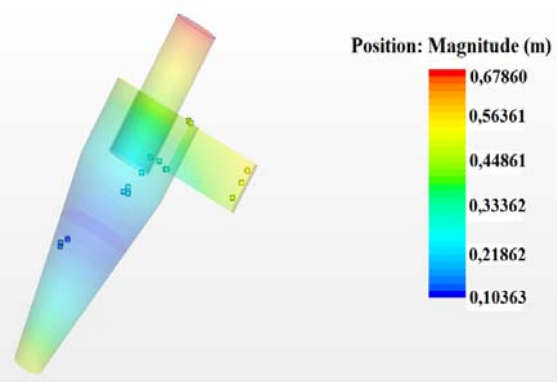

Figure 4 – Location of sand in a hydrocyclone

In the future, it is planned to consider models for establishing the optimal operating modes of a hydrocyclone with changes in the properties and states of the studied phases of the medium.

The main technological parameters and the rational mode of operation of the proposed water treatment unit were established according to the results of tests on a specially constructed laboratory installation (figure 5).

On the first table the main part of the research facility was located, based on the centrifugal pump 1.5KM with step-by-step power control, parameters of the pressure hydrocyclone and a hydroturbine.

On the second table was installed a personal computer with a program for monitoring the work of the bench installation and a communication cabinet with controls and measurements, as well as a module for connecting sensors to a personal computer.

A hydrocyclone with a cylindrical part diameter of 170 mm and a height of 480 mm was adopted for testing. The diameters of the inlet and outlet nozzles are the same and are 60 mm, and the diameters of the sand hole are 40 mm.

Figure 5 – Laboratory stand (a) and a hydraulic turbine with a generator (c)

Results of the investigation. As the data obtained under laboratory conditions show, when the pump is operating with a capacity of up to 250 l / min, the dependence of the water supply Q on the pressure at the inlet to the hydrocyclone P1 occurs in the same way as in ordinary centrifugal pumps. The pressure loss is 10-20%. In this case, due to the supply of purified water after the hydrocyclone to the water intake tank directly, the indicators of the electronic sensor at the inlet of the hydraulic turbine P2 and at the outlet P3 are insignificant

In order to establish the energy characteristics of the installation, the "hydroturbine-generator" unit was specially studied. In this case, three modes were considered: the operation of the unit at maximum load (P1), at average load (P2), and at minimum load (P3).

The results obtained for establishing the generated power are shown in figure 6. They show that the value of the generated power (energy) directly depends on the pressure on the line and on the rotational speed of the generator shaft.

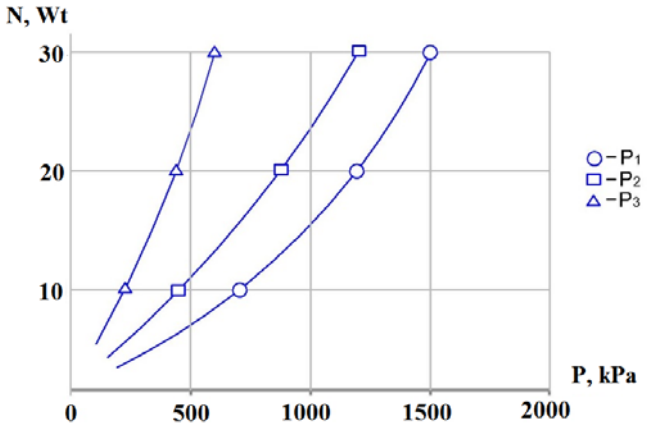

Figure 6 – Results of testing the unit "hydro turbine - generator"

As a result of the production test, it was found that when the pressure at the inlet of the prototype hydrocyclone changes within Pin = 25 - 45 kPa, there is an increase in the flow rate of liquid through the drain pipe Q in from 5.78 l / s to 57.5 l / s, and through sand hole Qp.o. - up to 4.42 l / s.

As can be seen from the graphical dependences Qout = f (Pout) and Qin = f (Pin) (figure 7), the maximum flow rate of the hydrocyclone through the drain (57.5 l / s) is provided at an inlet pressure of 45 kPa, when the valve on the pressure line is open to the full cross section. The pressure loss in the hydrocyclone chamber at the same time is 2,2 ... 3,5 kPa.

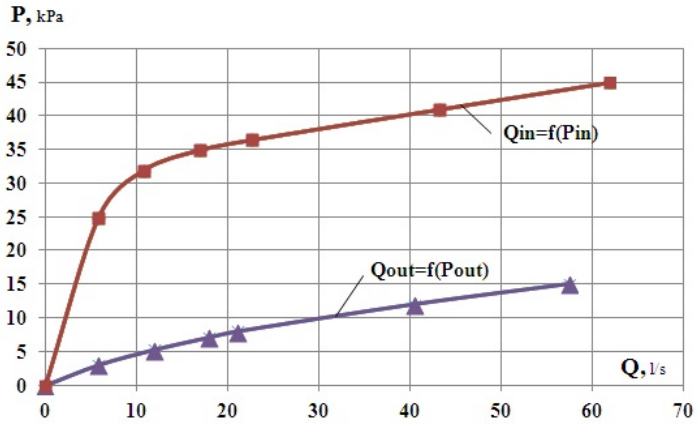

Figure 7 – Graphic dependences Qout = f (Pout) and Qin = f (Pin)

During the tests, by changing the diameter dp from 10 to 25 mm, the concentration of the ground mass was reached with a ground weight consumption of 0.73 ... 0.77 kg / s and a density of up to 1.843 t / m3) significantly increases the density of the condensed mass, however, this leads to clogging of the discharge opening.

In the established mode, the clarified water density was equal to 1.009 ... 1.05 t / m^3, and the degree of purification - 91 ... 97%. The minimum particle size was 0.05 mm, and the maximum particle size was 3.75 mm.

It has been established that the required type of hydrocyclone in the design should be adopted on the basis of a technical and economic comparison of the construction and operational indicators of the water treatment unit, taking into account the presence of a sufficient hydraulic slope of the water supply path and free water flows necessary for separating a two-phase liquid.

For the calculation and design of hydrocyclone sanding units, the same parameters for water and pollution should be specified as for sedimentation tanks. The hydraulic size of particles, which must be isolated to provide the required cleaning effect, is determined at the required height of water layer. The main design value of the hydrocyclones is capacity for purified water and degree of purification. Water productivity Qout *(Qhc)* can be calculated by the formula taking into account the diameter of hydrocyclone *Dhc:*

$$Q_{hc} = 0{,}785 q_{hc} D_{hc}^2 \quad (1)$$

Based on the total amount of water Qw supplied, the number of hydrocyclone working units is determined: N = Qw / Qhc. After the designation of the devise diameter and determination of their quantity, basic parameters of the hydrocyclone were established.

The angle of inclination of the generatrix conical part of the hydrocyclones in each specific case is set depending on the properties of the precipitate being precipitated. The main components and parts of hydrocyclones can be made of steel and plastic materials.

In view of the fact that hydrocyclones of considerable diameter (700-1000 mm) are analogous to ours, they are installed in those nodes of the technological scheme in which it is necessary to process volumes of contaminated water at the size of the boundary grain separation 0.4-0.5 mm, within these limits. With low productivity and the need to separate sand of small size (0.2-0.4 mm), as in the case of cooling water in the node of technical water supply of hydroelectric power stations, hydrocyclones with diameters within 350-500 mm are recommended.

Conclusions. Tested in production conditions, prototypes of a hydrocyclone sand trapping unit with a diameter of 700 mm showed the degree of water purification from mechanical impurities up to 91-97%. The installed capacity of one hydropower plant in use is 3-10 MW. Annual power generation reaches 4.0 - 5.0 million kWh.

Replacing the bulky reinforced concrete sedimentation tank of the existing hydroelectric power plants with hydrocyclone sand traps of a simplified design reduces the costs of building a water treatment unit from 30% (existing) to 7%.

The economic effect from the use of the developed technology of water supply for the hydroelectric unit of a small hydroelectric power station is achieved by simplifying the sand collection unit and thereby reducing capital investments for construction and operating costs.

Achieving a stable operating mode of the hydroelectric unit and its accompanying main units of the hydroelectric power station without special stops allows reducing losses in electricity supply to 15-20%.

The originality and effectiveness of the solution was awarded a certificate and medal of the World Intellectual Property Organization (WIPO). The basic version of the proposed hydroelectric power station was demonstrated at EXPO-2017 (Astana, Kazakhstan) and received expert approval.

The considered option of the hydroelectric power plant was additionally studied within the framework of the target program "Creation of the basis for the serial production of renewable energy sources in Kazakhstan of the world level" (BR05236263, National Academy of Sciences, Kazakhstan).

Ж. Қ. Қасымбеков[1], Ғ. Ж. Қасымбеков[2]

[1]Satbayev University, Алматы, Қазақстан;
[2]«Қазгидро» ЖШС, Алматы, Қазақстан

МИНИ ГЭС-ке АРНАЛҒАН ГИДРОЦИКЛОНДЫҚ ҚҰМТҰТҚЫШ ЖАСАУ ЖӘНЕ СЫНАҚТАН ӨТКІЗУ

Аннотация. Жобаның мақсаты – шағын (мини) гидроэлектрстанция жұмысын жетілдіру үшін гидроциклонды құмтұтқыш жасау және пайдалану. Жасалған технологияның бұрынғы ұқсас түрінен айырмашылығы – суды тазартуға арналған көлемді тұндырғыш тиімді гидроциклон қондырғысымен ауыстырылғандығында. Соның нәтижесінде су электр станциясын жобалауды оңайлатуға, пайдаланылған су құрамынан құм алу дәрежесінің жоғарылауына қол жеткізеді.

Зерттеу әдістері. Есептеу үшін мынадай мәліметтер алынды: гидроциклон арқылы өтетін су шығыны және гидроциклон кірісі мен шығысындағы қысымның төмендеуі. Үдерісті компьютерлік модельдеу SolidWorks бағдарламалық жасақтама (ағынды модельдеу) арқылы жүзеге асырылды. Негізгі технологиялық параметрлер мен рационалды жұмыс режимі тәжірибелік үлгілерді зертханалық және өндірістік жағдайда сынау арқылы белгіленді.

Зерттеу нәтижелері. Белгіленген режимде тазартылған су тығыздығы 1,009 ... 1,050 т / м^3, ал тазарту дәрежесі 91 ... 97% құрайды. Ірі темірбетонды тұндырғышты жеңілдетілген гидроциклонды құмтұтқышқа ауыстыру, су тазарту қондырғысын салуға кететін шығынды 30%-дан (қолданыстағы) 7%-ға дейін төмендетеді. Бұл таулы аймақтардағы шағын су электр станцияларының даму жағдайын арттыруға мүмкіндік береді.

Түйін сөздер: мини ГЭС, жасау, гидроциклондық құмтұтқыш, үдерісті модельдеу, тәжірибелік стенд, сынақтар.

Ж. К. Касымбеков[1], Г. Ж. Касымбеков[2]

[1]Satbayev University, Алматы,Казахстан;
[2]«Казгидро», Алматы,Казахстан

РАЗРАБОТКА И ИСПЫТАНИЕ ГИДРОЦИКЛОННОЙ ПЕСКОЛОВКИ ДЛЯ МИНИ ГЭС

Аннотация. Целью проекта является разработка и использование гидроциклонной песколовки для улучшения работы мини-гидроэлектростанции. В отличие от существующей конструкции гидроэлектростанции аналогичного типа, громоздкий отстойник для очистки воды был заменен эффективным гидроциклонным устройством. За счет этого достигается упрощение конструкции ГЭС, увеличение степени сбора песка из состава используемой воды.

Методы исследования. Исходными данными для расчета были взяты: расход воды, проходящей через гидроциклон, и перепад давления на входе и выходе гидроциклона. Компьютерное моделирование процесса проводилось с использованием программного обеспечения SolidWorks (flow simulation). Основные технологические параметры и рациональный режим работы были установлены путем испытаний экспериментальных образцов как в лабораторных, так и в производственных условиях.

Результаты исследований. В установленном режиме плотность осветленной воды равна 1,009 ... 1,050 т/м^3, а степень очистки – 91 ... 97%. Замена громоздкого железобетонного отстойника гидроциклонными песколовками упрощенной конструкции снижает стоимость строительства установки очистки воды с 30% (существующей) до 7%. Это дает возможность расширить объемы освоения малых гидроэлектростанций, особенно в горных условиях.

Ключевые слова: мини ГЭС, разработка, гидроциклонная песколовка, моделирование процесса, экспериментальный стенд, испытания.

Information about authors:

Kassymbekov Zh.K., Professor of the Department of "Engineering systems and networks" of the Kazakh National Research Technical University named after K. I. Satpayev, doctor of technical sciences, Professor, academician of NIA RK; jkk2004@mail.ru; https://orcid.org/0000-0001-6445-3584

Kassymbekov G.Zh., Chief specialist of LLP "Kazhydro", engineer-hydropower; a_k-82@mail.ru; https://orcid.org/0000-0001-6591-2519

REFERENES

[1] IEA (2010) Energy Technology Perspectives 2010, OECD/IEA, Paris.

[2] Zhurinov M.Zh., Kassymbekov Zh.K., Kassymbekov G.Zh. (2019) Mastering and development hydropower in Kazakhstan // News of the National Academy of Sciences of the Republic of Kazakhstan. Series of Geology and Technical Sciences. Vol. 3, N 435. P. 219-224. https://doi.org/10.32014/2019.2518-170X.88.

[3] European Small Hydropower Association ESHA (2004). "Guide on How to Develop a Small Hydropower Plant" Brussels, Belgium.

[4] Central Asia Energy and Water Development Program (2015) The World Bank. 2015. URL: http://www.worldbank.org/content/dam/Worldbank/Brief/Europe.

[5] Vilkovisky I.Ya. (2007) Hydropower of Kazakhstan // Current status and prospects. Almaty: Kazhydro LLP. 13 p.

[6] Kassymbekov Zh.K. (2018) Vacuum cleaning of sewer wells using tractor exhaust gas energy // Water and Ecology: Problems and Solutions, N 2 (74). P. 25-31.

[7] Grigorash O.V. Kvitko A.V., Popuchieva M.A. (2015) Prospects for small hydroelectric power plants in foothill and mountain rivers // Scientific journal Cube GAU, Krasnodar. 2015. N 112 (08). P. 1-13.

[8] Vasiliev I.E., Klyuev R.V., Dolganov A.A. (2011) Research and calculation of the sustainability of high-mountain small hydroelectric power plants // International scientific journal "Sustainable Development of Mountain Territories", Vladikavkaz. N 3 (9).

[9] Belash I.G. (2010) Problems of reliability and efficiency of hydro-turbine equipment of hydroelectric power plants // Proceedings of the conference "Improving the reliability and efficiency of operation of power plants and energy systems", MPEI, www.energy2010.mpei.ru.

[10] Shervarli D.E. (2006) Development of methods for ensuring the reliability of the equipment of a hydroelectric power station // Avtoref. dis. ... for Candidate of Engineering Sciences - Novosibirsk. 17 p.

[11] Marence M., Milicevic D., Vucina S., 2003. Hydro Power Plant Mostarsko blato-A multi-purpose project in karst. HYDRO 2003, Dubrovnik, Croatia.

[12] Brekke Hermod (2002) Design of hydraulic machinery working in sand laden water. Abrasive erosion and corrosion of hydraulic machinery, London.

[13] Neopane Hari P., Ole G. Dahlhaug, and Thapa Bhola (2009) Experimental examination of the effect of particle size and shape in hydraulic turbines. Waterpower XVI, Spokane, Washington, USA.

[14] Padhy M. K. and R. P. Saini (2008). A review on silt erosion in hydro turbines // Renewable and Sustainable Energy Reviews, 12 (7).

[15] Thapa Bhola and Brekke Hermod(2004) Effect of sand particle size and surface curvature in erosion of hydraulic turbine. IAHR symposium on hydraulic machinery and systems, Stockholm.

[16] Bergeron S.Y., Vu T.C., Vincent A.P. (2002) Silt erosion in hydraulic turbines: The need for real-time numerical simulations.

[17] Doby M.J., Nowakowski A.F., Nowak E., Dyakowski T. (2007) Numerical and experimental examination of swirl flow in a cylindrical container with rotating lids // Minerals Engineering, 20 (4): 361-367.

[18] Forder A., Thew M., Harrison D. (1998). A numerical investigation of solid particle erosion experienced within oilfield control valves. Wear, 216 (2): 184-193.

[19] Kassymbekov Zh.K., Kasymbekov G.Zh. (2011) Small derivative hydroelectric power station with hydrocyclone water treatment plants // Bulletin of KazNTU named after K.I. Satpayev. Almaty. N 6 (88). P. 42-45.

[20] Kassymbekov,Zh.K., Ni,N.P., Botantaeva, B.S. (2014) Testing of the water-pipe centrifugal vent valve- pressure damper in laboratory conditions // Water and Ecology, 2 (58): 39-44.

[21] Zhurinov M., K. Kassymbekov Zh.K.,, Dyussembekova N., Siemens E., Kassymbekov G. Zh. (2020) Testing of the prototype of mini-hydro power plants of hydrocyclone type in production conditions // News of The National Academy of Sciences of the Republic of Kazakhstan. Series of Geology and Technical Sciences. Vol. 1, N 439. P. 48-55.

N E W S
OF THE NATIONAL ACADEMY OF SCIENCES OF THE REPUBLIC OF KAZAKHSTAN
SERIES OF GEOLOGY AND TECHNICAL SCIENCES
ISSN 2224-5278
Volume 1, Number 445 (2021), 98 – 105 **https://doi.org/10.32014/2021.2518-170X.14**

UDC 621.878/879.06

R. A. Kozbagarov[1], M. V. Taran[2], K. A. Zhussupov[2],
A. E. Kanazhanov[1], N. S. Kamzanov[2], A. V. Kochetkov[3]

[1]Satbayev University, Almaty, Kazakhstan;
[2]Kazakh Academy of Transport and Communications named after M. Tynyshpayev, Almaty, Kazakhstan;
[3]Yuri Gagarin State Technical University of Saratov, Saratov, Russia.
E-mail: ryctem_1968@mail.ru

INCREASING THE EFFICIENCY OF MOTOR GRADERS WORK ON THE BASIS OF WORKING ELEMENTS PERFECTION

Abstract. The research considers methods of motor graders rise of efficiency by perfecting constructions of cutting elements and working organs on the basis of rise of a resource of their work.

The work contains a research of interdependence of parameters of motor graders working organs by statistical methods with the purpose of detection of the basic tendencies of their development. The basic directions of designing of motor graders working organs and most perspective constructions are detected by a method of analysis of patent solutions. The formulas for account of resistance of ground to cutting by a knife with one direct and two sloping cutting edges with allowance for an angle of declination of a knife and its wear are deduced. The regularities of a wear of the cutting elements of a blade are investigated, its influence to efficiency of work and on parameters of working organs design is detected. The maximum size of wear is determined.

The requirements to motor graders working equipment are defined on the basis of conducted researches, the new constructions of multiple use knives and order of their sequential replacement are developed in correspondence with the research work. It ensures the raise of efficiency of the machine by 10…15 per cent and it increases resource of knives in comparison with a traditional construction 3…4 times as much.

Key words: grader, cutting element, wear, soil, blade, cutting, working body.

Introduction. Earthworks in the total volume of construction have a significant share. Over 15 billion m^3 of earthworks is carried out annually in the CIS, including over 800 million m^3 in the Republic of Kazakhstan.

Studies [1,2] have shown that 70...80% of the ETM fleet, including motor graders, work with unacceptably worn-out CE. At the same time, the performance of motor graders is provided by the engine power reserve, although they operate in an economically unprofitable mode, with an excess load on components and parts in comparison with the optimal one, with an increase in fuel consumption, which ultimately increases the cost of soil development.

The wear allowed in practice of the CE ETM causes an increase in the cutting force by 3...4 times, the energy intensity of the cutting process by 1,4...3 times, the cost of soil development by 8...15% with a decrease in productivity by 10...30%. This leads to an increase in the stress state of the entire machine and reduces its operational reliability. Excessive wear of the CE leads to the economic impracticability or practical impossibility of further operation of the machines.

The above-mentioned intensive wear of CE ETM [6], which leads to an increase in the energy intensity of ground cutting, requires frequent replacement, in which most of the expensive scarce metal goes to scrap. Therefore, one of the main ways to improve the efficiency of ETM is to improve CE structures by reducing their metal consumption by making the wear part of the tool removable, reducing the energy consumption of the cutting process and increasing the wear resistance.

The above-mentioned areas of research on the productive use of machines, identification and creation of promising designs of working bodies have determined the task of further improving the efficiency of motor graders by improving the working elements, taking into account their wear resistance, and this determines the relevance of the work.

Methods. Theoretical research has been carried out to identify the most significant parameters of the working bodies of motor graders by the method of correlation analysis.

By processing an information databank on a PC which includes more than 5600 parameter values of 282 grader models, the following results are obtained:

– pair correlation equations are derived, while the main parameter is the power of the installed engine, which is most correlated with the other parameters;

– a regression equation is obtained that relates seven parameters of the blade [8], changing simultaneously, with the engine power:

$$N = -1.84 \cdot 10^{-11} + 1.21 \cdot 10^{-15} Bo - 1.27 \cdot 10^{-16} Ho - 1.81 \cdot 10^{-15} Hz + \\ +4.67 \cdot 10^{-14} Hr - 4.92 \cdot 10^{-16} Zv + 0.002 Po - 1.26 \cdot 10^{-15} C. \quad (1)$$

The obtained regression equations showed that from the studied parameters of the damp, the decisive factor is the force pressing the blade (force in the hydraulic cylinders of the blade), i.e. force providing cutting of the ground, the value of which is closely related to the wear of the CE.

This confirms the importance of studying the patterns of CE wear and their use in the design and operation of dumps.

The results of the analysis of patent information on CE of motor graders are considered. A morphological classification of patent information was developed [3], which allowed it to be systematized.

A PC was used to process the patent information collected and systematized by the classifier, in particular to obtain regression equations to determine the rate of patenting for each classification feature.

Based on the processing of information arrays, mathematical models of patenting dynamics for motor grader knives, the method and structures of their attachment are obtained, which are shown in table 1, which allow us to identify the main trends in improving the working bodies of motor graders and their prospects, as well as the prospects and significance of individual design solutions.

Table 1 – Mathematical models of the dynamics of patenting motor grader knives, methods and structures of their attachment (according to morphological classification

Cipher	Classification features	Code	Regression equation
P_1	For the purpose of knives	1	$N_i = \exp[0.347 + 0.028(t - 87.500)]$
P_2	By the shape of the knife	2	$N_i = \exp[0.396 + 0.037(t - 88.286)]$
P_3	By the profile of the knife	3	$N_i = \exp[0.719 + 0.093(t - 88.667)]$
P_4	The rows of fastening of the knife	4	$N_i = \exp[0.358 + 0.124(t - 88.600)]$
P_5	By the number of cutting edges	5	$N_i = \exp[0.914 + 0.102(t - 88.286)]$
P_6	By the location of the cutting edges	6	$N_i = \exp[0.783 + 0.101(t - 87.000)]$
P_7	By the shape of the cutting edges	7	$N_i = \exp[0.099 + 0.030(t - 87.857)]$
P_8	Increased wear resistance, durability, rigidity, reliability	8	$N_i = \exp[1.090 + 0.129(t - 88.091)]$
P_9	By the method of fastening the knife	9	$N_i = \exp[0.896 + 0.028(t - 87.250)]$
P_{10}	By the shape of the bolt heads	10	$N_i = \exp[0.173 + 0.044(t - 86.875)]$
P_{11}	By bolt bar shape	11	$N_i = \exp[0.497 - 0.079(t - 90.000)]$
P_{12}	By the shape of the holes on the knife and base plate	12	$N_i = \exp[0.717 - 0.070(t - 89.000)]$
P_{13}	By the design of the tightening elements	13	$N_i = \exp[1.169 - 0.049(t - 87.833)]$
P_{14}	Digging process intensifiers	14	$N_i = \exp[0.277 + 0.078(t - 89.400)]$

It is established that one of the most promising directions in the design of dump knives is their multiple use, i.e. execution of several cutting edges on one knife [7.9].

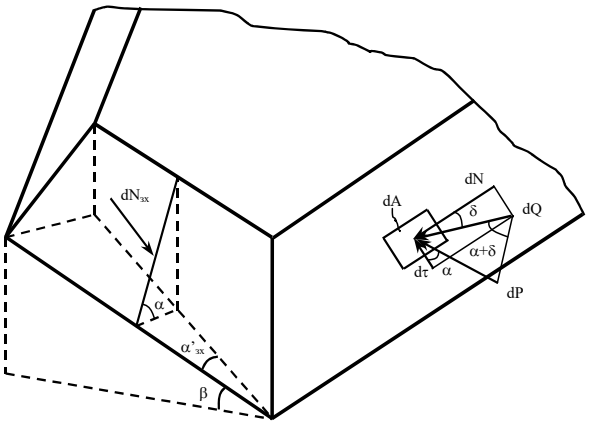

Figure 1 – Diagram of forces acting on the working cutting edges of the knife

Results. One of the most significant design solutions is a rectangular knife with four cutting edges. This design is taken as a basis for further improvement. The development of this direction is possible by using polygonal knives with more than four edges.

Theoretical developments of the main stages of ground cutting with reusable polygonal knives are considered, taking into account the possibility of simultaneous direct and oblique cutting with three or two adjacent cutting edges. A diagram of the knife operation is shown in figure 1, and on its basis formulas are derived that allow to characterize the change in the ground resistance to cutting depending on a number of factors that can affect the design of the CE blade, i.e. its knives.

It is established that the main parameter influencing the resistance of the ground to cutting by knives [4,5], which make up the cutting part of the motor grader blade, is the angle of capture of the side working face of the knife α'_{zh}, depending on its design.

The highest efficiency of cutting soil in a straight position of the damp (when its capture angle $\delta_{zh}=90^0$) corresponds to the capture angles of the side working face of the knife $\alpha'_{zh}=25\ldots35^0$.

The angle of inclination of the knife β also affects the amount of ground resistance to cutting. As it grows, this value decreases. However, the β parameter is not constructive, but depends on the technology of the motor grader.

A formula is derived for calculating the resistance P of the soil to cutting with a knife with one straight and two inclined cutting edges, taking into account the angle of the knife. A formula is also obtained for calculating the coefficient of reducing the cutting resistance of the soil when using such a knife in comparison with the work of one straight edge.

A formula is derived for calculating the resistance of the soil to cutting with a knife, taking into account its wear:

$$P_{Pk}=B_n\cdot\left[(h-S)\cdot\left(1+f\cdot\sqrt{\frac{1}{\sin^2\alpha}-1}\right)+\frac{r}{\cos45^0}\cdot\left(1+f\times\sqrt{\frac{1}{\sin^2(\varphi+45^0)}-1}\right)+a\cdot\left(1+f\cdot\sqrt{\frac{1}{\sin^2\varphi}-1}\right)\right]\times$$

$$\times\frac{1-\sin\rho\cdot\cos2\varphi_n}{1+\sin\rho\cdot\cos2\varphi_n}\left\{3\cdot C_o\cdot\cos\rho+\gamma_n\cdot\left[\frac{h-S}{2}+\frac{r\cdot\sin(\varphi+45^0)}{2\cdot\cos45^0}+\frac{a\cdot\sin\varphi}{2}\right]\right\}+2\cdot\left[K_z\cdot B_k\cdot h\cdot\mu+\varepsilon\cdot B_k\cdot h\cdot\mu\cdot\upsilon^2\right], \quad (2)$$

which shows that the formation of wear areas significantly increases the cutting resistance. However, in order to use this formula effectively, it is necessary to study the patterns of blade wear.

The width of the knife and its edges primarily affect the ability to regulate the process of working off the blade, in particular, the process of its wear. Production observations were made that showed uneven wear of the dumb blade along the length. A method of sequential change of the most worn-out sections of the blade is proposed. The width of the knives should ensure the most optimal division of the blade into such sections. In this case, the criterion is the cost of working out knives. It is established that the optimal number of knives on the blade corresponds to 20...25. Accordingly, the width of the knife edge should be within 120...150 mm, and the ratio of the width of the main working edge and the width of the side working edge of the knife $B_k/B_n=0.4..0.6$.

To the geometrical elements of wear of the blade of the wedge profile include: the blunting area «*a*», oriented at a negative angle «*φ*» to the cutting plane and the rounding of the front edge of the blade, characterized by a radius «*r*». In various specific cases, any of these elements can be of decisive importance. Identifying the significance of each of them and establishing its critical values is an extremely difficult task, which, along with this, does not make it possible to obtain sufficiently reliable results due to the multi-planned process of cutting soil and a large number of random factors affecting it. Therefore, the complex dimension «*S*», including all of the above, was taken as the defining wear element.

The study of the regularities of changes in the geometric wear elements that form the reduced size «*S*» had two goals:

1. Establish their relationship and on this basis derive the minimum number of formulas that characterize the given size and are convenient for practical use;

2. Determine the impact of CE wear on the efficiency of cutting the ground and identify the maximum permissible amount of CE during the operation of the motor grader.

$$S = bc + cd + de = r \cdot \cos\alpha + r \cdot \cos\varphi + a \cdot \sin\varphi \text{ or } S = r(\cos\alpha + \cos\varphi) + a \cdot \sin\varphi. \quad (3)$$

As a result of production tests, regularities of changes in geometric parameters of wear of motor grader dumps in various soils were established. The corresponding equations are obtained.

Taking into account the established dependencies, formula (3) for the most common soils of the Republic of Kazakhstan can be transformed as follows:

– for sandy loam:

$$S = (2.7 + 0.026V)(2.13 + \cos\alpha), \quad (4)$$

– for clay-containing soils:

$$S = (2.7 + 0.030V)(1.66 + \cos\alpha). \quad (5)$$

The results of calculations using the obtained formulas give satisfactory convergence with the results of measurements.

On the basis of the carried out experiments, the dependences of the wear elements «*r*» and «*a*» on «*S*» were also obtained, which made it possible to clarify and concretize the General formulas for determining the forces of ground resistance to cutting. The calculation showed a significant impact of wear growth on the increase in ground cutting resistance (figure 2).

Comparison of the regularities of changes in the reduced size «*S*» and performance of motor graders showed their close relationship. It was found that an increase in the given size to the value $S = 30mm$ causes a decrease in productivity in soils of categories II and III by more than two times. At the same time, as mentioned above, most dumps are operated with significant wear of the knives, i.e. the greatest amount of ground is produced by heavily worn blades.

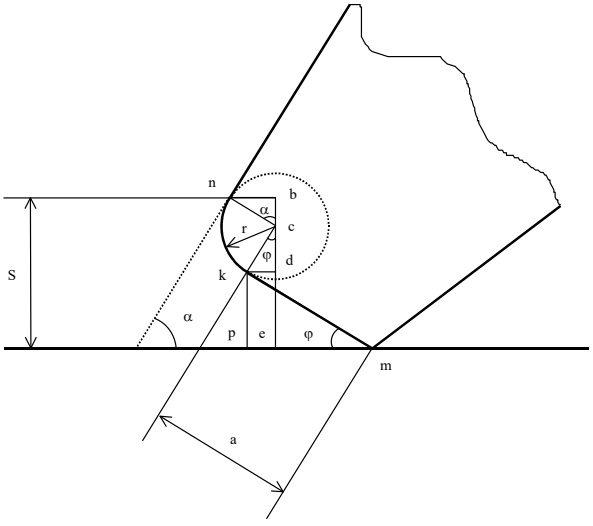

Figure 2 – Geometric diagram for determining the reduced size of wear

The study of changes in the cost of soil development depending on the value of the reduced size of the blade wear «*S*» and the amount of ground running at the corresponding wear showed that there are values of «*S*» corresponding to the minimum cost. Acceptance of such values as the maximum permissible will optimize the workflow of motor graders.

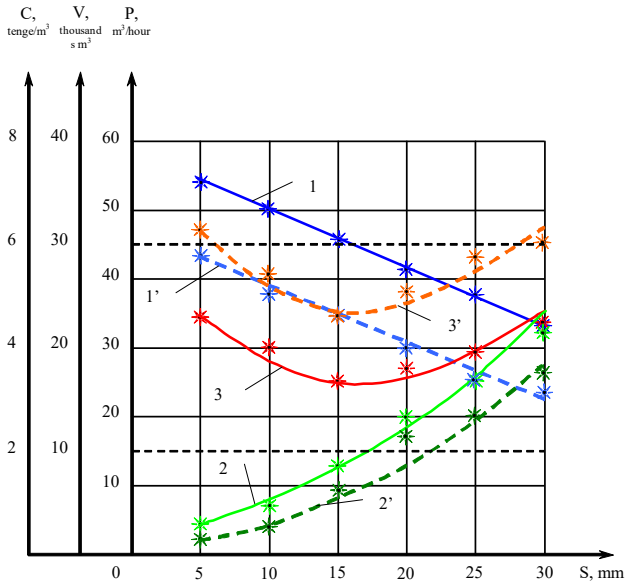

1 – productivity in the development of soils of the II category;
1' – productivity in the development of soils of the III category;
2 – operating time for category II soils;
2' – operating time for category III soils;
3 – the cost of developing category II soils;
3' – the cost of developing category III soils.

Figure 3 – Dependence of changes in productivity, operating time and cost of development in soils of categories II and III from the given size of bluntness

Figure 3 shows graphs of the above dependencies for soils of category II and III. It is seen that the cost curves have a well-defined extremum corresponding to the minimum value $S \approx 15 mm$. The obtained data show that it is advisable to take $S = 15 mm$ as the criterion for working out the blade, allowing in some cases excess of wear to $S = 18...20 mm$.

However, it was necessary to clarify the value of the maximum blunting of such a knife. Subsequent production experiments during comparative tests made it possible to establish that this value corresponds to the values previously set for standard knives: $S = 15...20 mm$.

That hexagonal knives, as well as knives of other polyhedral shapes, cannot be used as side knives of the blade, if the nature of the work requires its inclined position with an angle of inclination $\gamma > 5^0$. Here you need to use knives that have a side edge perpendicular to the working edge. Therefore, in this case, «K»-shaped knives are proposed as side knives.

On the basis of hexagonal and«K»-shaped knives, three designs of the cutting part of the grader blade were developed (figure 4):

- with hexagonal knives fixed on the blade in two rows. The design provides a continuous blade and is recommended for planning work with a horizontal blade (figure 4, a).

- with hexagonal knives fixed on the blade in two rows as medium and large «K»-shaped knives. The design provides a continuous blade and is recommended for cutting soil at any inclination of the blade (figure 4, b).

- with hexagonal, triangular and "K"-shaped knives arranged in a single row. The design provides a continuous blade and is recommended for cutting soil at any inclination of the blade (figure 4, c).

The tests were carried out according to the developed methodology based on the use of a nomo-gram of step-by-step testing of reusable knife blades, the construction of which is possible on the basis of a reduced amount of experimental data.

Three designs of the cutting part of the dumps were investigated – with standard knives, with four-sided knives, and with hexagonal knives arranged in two rows.

For these designs of the cutting part of the blade, two ways of replacing the worn blade were studied: standard (parallel)-when the entire blade is replaced, and sequential - by replacing the blade sections sequentially along the blade zones.

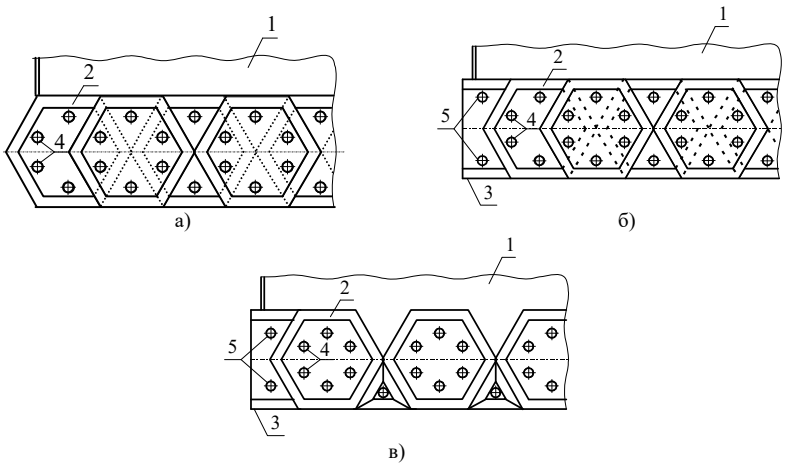

Figure 4 – Versions of the cutting part of the motor grader blade

As a result of comparative tests, data were obtained showing that hexagonal knives with sequential changes provide an increase in productivity by 10 ... 15% compared to standard knives. The resource of knives increases even more significantly. Figure 5 shows graphs of the dependence of the volume of the developed soil on the given size of wear, obtained for the tested knife designs.

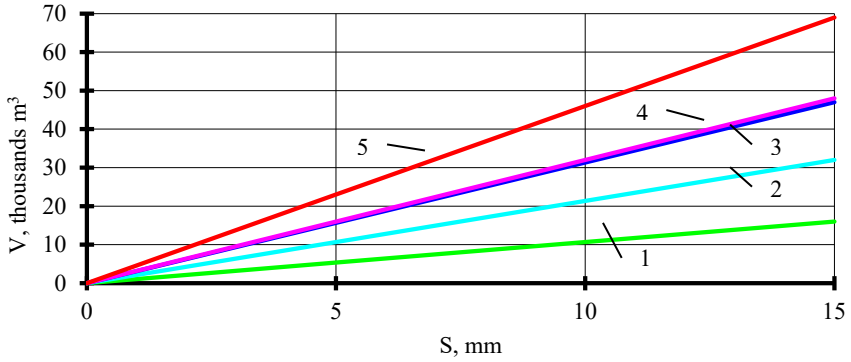

1 - standard knives; 2 - four-sided knives in a parallel change; 3 - tetrahedral knives with sequential change; 4 - hexagonal knives for parallel change; 5 - hexagonal knives with sequential chang

Figure 5 – Graph of the dependence of the volume

It is seen that compared with the standard design of the cutting blade structure with tetrahedral and hexagonal knives increase the soil production with the adopted parallel blade 2 and 3 times, and with the proposed sequential change – 3 and 4.3 times accordingly.

It is established that the main influence on the engine power from the parameters of the working body is the force of pressing the blade to the ground. The largest part of the rated power is spent on providing this power. And the fact that the force of pressing the blade depends on the ground resistance to cutting associated with the design and blunting of the re, proves the importance of studying the influence of the design of knives and their wear patterns in order to improve the design of the cutting part of the blade and develop optimal modes of their development.

Conclusion. The most significant and promising structures are identified. One of them - square knives with four cutting blades, the alternation of which increases the life of the knives - is taken as the base for improvement in the direction of increasing the number of cutting edges. Thus, it is established that the new knife must have the shape of a polygonal plate with more than four edges.

Comparative tests of dumps with the cutting part of three designs – with standard knives, with four-sided knives and with hexagonal knives arranged in two rows were carried out. The obtained results showed the advantage of the cutting part with hexagonal knives, worked out according to the proposed method of successive replacement of worn knives: its productivity is higher by 10...15%, the average resource is 4 times higher than that of the standard cutting part. And in comparison with tetrahedral knives, the resource is 1.5 times higher.

Р. А. Козбагаров[1], М. В. Таран[2], К. А. Жусупов[2],
А. Е. Канажанов[1], Н. С. Камзанов[2], А. В. Кочетков[3]

[1]Сәтбаев университеті, Алматы, Қазақстан;
[2]М. Тынышбаев атындағы Қазақ көлік және коммуникациялар академиясы, Алматы, Қазақстан;
[3]Ю. А. Гагарин атындағы Саратов мемлекеттік техникалық университеті, Саратов, Ресей

ЖҰМЫС ЭЛЕМЕНТТЕРІН ЖЕТІЛДІРУ НЕГІЗІНДЕ АВТОГРЕЙДЕРЛЕРДІҢ ЖҰМЫС ТИІМДІЛІГІН ЖОҒАРЫЛАТУ

Аннотация. Зерттеу автогрейдерлердің тиімділігін олардың жұмыс ресурсын арттыру негізінде кесу элементтері мен жұмыс органдарының конструкцияларын жетілдіру арқылы арттыру әдістерін қарастырады.

Автогрейдерлердің жұмыс органдарының параметрлерінің олардың дамуының негізгі тенденцияларын анықтау үшін статистикалық әдістермен өзара тәуелділігін зерттеуді қамтиды.

Патенттік шешімдерді талдау әдісімен автогрейдерлердің жұмыс органдарын және неғұрлым перспективалы конструкцияларды жобалаудың негізгі бағыттары анықталды. Пышақтың көлбеу бұрышы мен оның тозуын ескере отырып, бір түзу және екі көлбеу кесу жиектері бар пышақпен кесуге топырақтың қарсылығын ескеру формулалары көрсетілген. Пышақтың кесу элементтерінің тозу заңдылықтары зерттелді, оның жұмыс тиімділігі мен жұмыс органдарының құрылымдық параметрлеріне әсері анықталды. Тозудың максималды мөлшері анықталады.

Алынған нәтижелер алтықырлы пышағы бар қайырма күректің келесідей артықшылығын көрсетті: олардың өнімділігі стандартты пышағы бар қайырма күректерден 10...15% жоғары, ал ресурсы стандартты 4 есе жоғары және төртқырлы пышағы барынан 1,5 есе жоғары.

Түйін сөздер: автогрейдер, кескіш элемент, тозу, топырақ, қайырма күрек, кесу, жұмысшы орган.

Р. А. Козбагаров[1], М. В. Таран[2], К. А. Жусупов[2],
А. Е. Канажанов[1], Н. С. Камзанов[2], А. В. Кочетков[3]

[1]Сатбаев Университет, Алматы, Казахстан;
[2] Казахская академия транспорта и коммуникации им. М.Тынышпаева, Алматы, Казахстан;
[3]Саратовский государственный технический университет им. Гагарина Ю.А., Саратов, Россия

ПОВЫШЕНИЕ ЭФФЕКТИВНОСТИ РАБОТЫ АВТОГРЕЙДЕРОВ НА ОСНОВЕ СОВЕРШЕНСТВОВАНИЯ РАБОЧИХ ЭЛЕМЕНТОВ

Аннотация. В исследовании рассматриваются методы повышения эффективности автогрейдеров путем совершенствования конструкций режущих элементов и рабочих органов на основе повышения ресурса их работы.

Работа содержит исследование взаимозависимости параметров рабочих органов автогрейдеров статистическими методами с целью выявления основных тенденций их развития. Методом анализа патентных решений выявлены основные направления проектирования рабочих органов автогрейдеров и наиболее перспективных конструкций. Выведены формулы для учета сопротивления грунта резанию ножом с одной прямой и двумя наклонными режущими кромками с учетом угла наклона ножа и его износа. Исследованы закономерности износа режущих элементов лезвия, выявлено его влияние на эффективность работы и на параметры конструкции рабочих органов. Определяется максимальный размер износа.

На основе проведенных исследований определены требования к рабочему оборудованию автогрейдеров, разработаны новые конструкции ножей многократного использования и порядок их последовательной замены в соответствии с научно-исследовательской работой. Это обеспечивает повышение КПД станка на 10...15% и увеличивает ресурс ножей по сравнению с традиционной конструкцией в 3...4 раза.

Ключевые слова: автогрейдер, режущий элемент, износ, грунт, отвал, резания, рабочий орган.

Information about authors:

Kozbagarov R.A., Candidate of technical sciences, associate Professor, Department "Department of technological machines, transport and logistics", Satbayev University, Almaty, Kazakhstan; ryctem_1968@mail.ru; https://orcid.org/0000-0002-7258-0775

Taran M.V., Candidate of technical sciences, associate Professor, Department "Automobiles, road equipment and standardization", Kazakh Academy of Transport and Communications named after M. Tynyshpayev, Almaty, Kazakhstan; tmv_house@mail.ru

Zhusupov K.A., Candidate of technical sciences, associate Professor, Department "Automobiles, road equipment and standardization", Kazakh Academy of Transport and Communications named after M. Tynyshpayev, Almaty, Kazakhstan; kenes_atabai@mail.ru; https://orcid.org/0000-0002-2842-6447

Kanazhanov A.E., Master of transport, transport engineering and technology, Tutor, "Department of technological machines, transport and logistics", Satbayev University, Almaty, Kazakhstan; 280140ait@mail.ru; https://orcid.org/0000-0002-7139-1550

Kamzanov N.C., Magister of technical Sciences, Lecturer, Department "Automobiles, road equipment and standardization", Kazakh Academy of Transport and Communications named after M. Tynyshpayev, Almaty, Kazakhstan; n.kamzanov@mail.ru; https://orcid.org/0000-0002-2420-8362

Kochetkov A.V., Doctor of technical Sciences, Professor, Department "Traffic Facilities Construction", Yuri Gagarin State Technical University of Saratov, Saratov, Russia; soni.81@mail.ru; https://orcid.org/0000-0002-6523-6095

REFERENCES

[1] Taran M.V., Kabashev R.A. (1996) Vlijanie gruntovogo fona jekspluatacii na iznos nozhej avtogrejderov. Prochnost' materialov i konstrukcij na transporte. *Sbornik nauchnyh trudov*. Almaty, KazATK. P. 163-166 (in Russ.).

[2] Kozbagarov R.A., Zhussupov K.A., Kaliyev E.B., Yessengaliyev M.N., Kochetkov A.V., N.C. Kamzanov. Development of control suspension of attachment of a bulldozer // News of the National Academy of Sciences of the Republic of Kazakhstan, Series of Geology and Technical Sciences. Vol. 4, N 442 (2020), 166-174. https://doi.org/10.32014/2020.2518-170X.97 (in Eng.).

[3] Sharma D., Barakat N. Evolutionary Bi-objective Optimization for Bulldozer and Its Blade in Soil Cutting // Journal of The Institution of Engineers (India): Series C, Vol. 100, Issue 2. P. 295-310 (2019). https://doi.org/10.1007/s40032-017-0437-z (in Eng.).

[4] Taran M.V., Ahmetov M.F., Kozbagarov R.A. (2013) Sravnitel'nye ispytanija razlichnyh konstrukcij rezhushhej chasti otvala avtogrejdera. *[Sbornik materialov Mezhdunarodnoj nauchno - prakticheskoj konferencii Industrial'no-innovacionnoe razvitie transportno, transportnoj tehniki i mashinostroenija»]*. Almaty. P. 190-198 (in Russ.).

[5] Kozbagarov R.A., Kamzanov N.S. Opredelenie velichiny soprotivlenie grunta rezaniiu i shiriny rezhushchikh granei mnogougol'nymi nozhami otvala zemleroino-transportnykh mashin // Vestnik KazNTU. Almaty. 2015. N 4 (110). P. 308-315. ISSN 1680-9211 (in Russ.).

[6] Turdaliev A.T., Kozbagarov R.A., Abibullaev A.N. Vliianie iznosa lezviia nozha avtogreidera na effektivnost' rezaniia grunta // Vestnik KazNITU. Almaty. 2016. N 3 (115). P.181-184. ISSN 1680-9211 (in Russ.).

[7] Kozbagarov R.A., Kaliev E.B., Tanatarov Zh.N. Analiz bul'dozernogo otvala adaptiruemogo tipa // Vestnik KaNITU. Almaty. 2016. N 4 (116). P. l75-l77. ISSN 1680-9211 (in Russ.).

[8] Kozbagarov R.A., Kaliev E.B., Таңatarov Zh.N. Povysheniia effektivnosti primeneniia bul'dozernogo otvala adaptiruemogo tipa // Vestnik KazNITU. Almaty. 2016. N 4 (116). P. 175-177. ISSN 1680-9211 (in Russ.).

[9] Kozbagarov R.A., Bodieva A.T. Analiz vzaimodeistviia bul'dozernogo otvala adaptiruemogo tipa so sredoi // «Nauka i mir» Mezhdunarodnyi nauchnyi zhurnal. Volgograd. 2017. N 2 (42). P. 16-19. ISSN 2308-4804 (in Russ.).

N E W S
OF THE NATIONAL ACADEMY OF SCIENCES OF THE REPUBLIC OF KAZAKHSTAN
SERIES OF GEOLOGY AND TECHNICAL SCIENCES
ISSN 2224-5278
Volume 1, Number 445 (2021), 106 – 113 **https://doi.org/10.32014/2021.2518-170X.15**

UDC 577.4:628.8

A. T. Kozykeyeva[1], Zh. S. Mustafayev[1], L. V. Kireicheva [2], S. D. Dauletbay[3]

[1]Kazakh National Agrarian University, Almaty, Kazakhstan;
[2]FSBSI All-«Russian Scientific Research Institute of Hydraulic Engineering
and Melioration named after A.N. Kostyakova», Moscow, Russia;
[3]Taraz State University named after M. Kh. Dulati, Taraz, Kazakhstan.
E-mail: aliya.kt@yandex.ru

ECOLOGICAL PROFILE OF DRAINAGE IN THE SHU RIVER BASIN UNDER ANTHROPOGENIC ACTIVITY

Abstract. Based on the study, many years of information and analytical materials «Kyrgyzhydromet» and «Kazhydromet», as well as the Department of State Statistics of the Kyrgyz Republic and the Republic of Kazakhstan, characterizing the formation of water resources and their use in the economic sectors of the catchment area of the Shu River basin, were considered as a model of the "activity-natural system", which performs runoff, environment-forming, ecological and social functions and is the spatial basis of nature management for a comprehensive assessment of the state of the territory and water bodies. As a basis for assessing the main functions of the catchment area of the Shu River basin, a geosystem approach was used, which determines the scientific and practical feasibility of geomorphological schematization, within the framework of which it becomes possible to construct their ecological profile on a spatio-temporal scale, which makes it possible to establish trends in the development of cognitive and transformative activities that determine the direction and intensity of anthropogenic activity. in the region. The main natural function of the river basin of the formation of a hydrogeochemical flow, which has one object for its discharge, determines the qualitative state of the ecological profile of the catchment area of the Shu River basin, that is, depending on the zonation from the mountainous class of landscapes to the lowland class of landscapes (superaquial and subaquial facies), natural hydrological facies are gradually disrupted. rhythms, affects the hydrogeological and soil-reclamation processes and environmental conditions, especially in the lower reaches of river basins, which are zones of storage of return (collector-drainage and waste) waters of industrial and agricultural facilities.

Key words: river, catchment, basin, runoff, system, model, function, activity, transformation, cognition, ecology, profile, schematization, analysis, assessment.

Introduction. The historical development of mankind in the 15th-18th centuries, if it directly depended on the power of Mother Nature, then, starting from the 19th century, the well-being of the natural system largely depends on human activity in the system of nature management and environmental management. Over the course of two millennia, history has experienced many situations, on the successful completion of which the ecological well-being and development of mankind on planet Earth depended. However, despite the fact that society is still increasing the pace of satisfying consumer needs at the expense of the natural environment, and nature itself serves as the resource and material-spatial basis of society, until now society does not remember a natural phenomenon, which is a global threshold process, beyond which progress may turn out to be not only difficult, but generally impossible.

But society, in certain geographic regions of the planet, today faced many trials, that at the beginning of the new millennium, humanity came aggravated by the problems of survival, since the driving force in the XXI century was human needs, which were formed under the influence of the consumer spectrum of values and the apparent availability of natural resources in various areas of production.

Thus, one of the primary goals of ecology is the formation of ecological consciousness and the implementation of human ecological thinking in solving scientific and practical problems in the field of nature management, and the related arrangement of the catchment area of river basins.

The purpose of research - on the basis of the analysis of the environment-forming and economic functions of the river basins and which are the spatial basis for the use of natural resources, to construct the ecological profile of the catchment area of the Shu river basin in conditions of anthropogenic activity.

Object of study - the Shu river, which originates in the Teskey-Ala-Too glaciers and the Kyrgyz ridge. The Shu River flows through the territories of Kyrgyzstan and Kazakhstan. The length of the river is 1186 km, including 800 km within Kazakhstan. Drainage area - 67 500 km². The main tributaries: on the right – Chong-Kemin, Yrgayty, Kakpatas; on the left – Alamedin, Aksu, Kuragaty. In the lower reaches, the river flows through Kazakhstani territory, forming the northern border of the Moyynkum desert, dries up in the sands, only during floods, flowing into the closed-drainage salt lake Akzhaikyn among the vast salt marshes of the Ashchykol depression.

The geomorphological profile of the catchment area of the Shu river basin, built on the basis of the catenary approach, depending on the altitudinal zonality, is divided into zones: a mountainous class of landscapes (eluvial facies), a foothill subclass of landscapes (transeluvial facies), a foothill lowland subclass of landscapes (transaccumulative class of landscapes) and plains (superaquial and subaquial facies) (table 1) [1].

Table 1 – Geomorphological schematization of landscape catenas of the catchment area of the Shu river basin

Natural and climatic zones			Weather station	The absolute height of the earth's surface, m	Administrative regions
landscape class	facies	moisture zones			
Mountainous	Eluvial	Wet mountain	Teo-Ashuu	3090,0	Kemen, Chui-Tokmasky (KR)
Foothill	Transeluvial	Arid mountain	Baytik	1590,0	Chui-Tokmasky (KR), Issyk-Ata (KR)
Foothill plain	Transaccumulative	Dry foothill	Kordai Bishkek	1145,0 756,0	Chui-Tokmasky (KR), Alamudunsky, Sokuluk, Moskovsky, Zhayilsky, Panfilovsky (KR) Korday (RK)
Plain	Superaquial	Very dry	Tole bi Moyinkum	456,0 351,0	Moyynkum, Sarysusky (RK)
	Subaquial		Ulanbel	266,0	Sarysusky (RK)

At the same time, the catchment area of the Shu river basin, as a model of an «activity-natural system», including four categories: activity (A), natural material (NM), transformation of material (TM) and the formation of anthropogenic material (FAM), performing runoff, environment-forming, ecological and social functions, which are the spatial bases of nature management, are considered within the framework of cognitive and transformative activities [2,3].

Materials and research methods. On the basis of the study, many years of information and analytical materials «Kyrgyzhydromet» and «Kazhydromet», as well as the Department of State Statistics of the Kyrgyz Republic and the Republic of Kazakhstan, characterizing the formation of water resources and their use for economic sectors in the catchments of the river basin [1].

A quantitative assessment of the ecological situation in the catchment area of river basins can be made as follows, first, one considers the natural environment at the regional or local level, zoning by type of activity, which does not significantly change in the space-time scale $t_i \rightarrow t_O$ (where t_i - past period; t_O - modern period), Activity parameters $\overline{D_i}$ - are expressed as shares of the total volume of natural resources that were influenced by various factors (Φ_i), Within the limits of each anthropogenic activity, the reduced coefficients of negative reaction for a person are estimated - $\overline{NR} = NR_i/NR_{\max}$ and for its habitat - $\overline{nr} = nr_i/nr_{\max}$ [2-5],

The quantities $\overline{NR}$ and $\overline{nr}$ range from 0 to 1, moreover, an increase in the coefficients indicates a worsening of the situation,

Approximate dependencies for assessing the impact of anthropogenic activity have the form [2,3]:

- for human $\overline{NR} = \left(\sum_{1}^{i} \overline{D}i \cdot q_x \right) \sum_{1}^{i} \varepsilon_i(k)$;

- for its habitat $\overline{nr} = \left(\frac{\overline{D}_{вв}}{\overline{D}_{рв}} + q_x \right) \sum_{1}^{i} \beta \cdot \varepsilon_i(k)$,

where $\overline{D}_i$ - degree of contamination of drinking water with pesticides for supplying the population; $\overline{D}_{вв}$ - level of use for irrigation of river waters; $\overline{D}_{рв}$ - the level of use of return water for irrigation; ε_i - particular parameters of the deterioration of the properties of the components of the natural system (for humans, this is the dynamics of diseases associated with the consumption of polluted water and air pollution - $\varepsilon_i(r)$, for soil, plants and crops - the content of toxic salts in the soil, for groundwater - an increase in their mineralization and level - $\varepsilon_i(k)$); β - correction factor (for soil and groundwater $\beta = 1$, for crops $\beta > 1$); q_x- the intensity of the intake of pesticides and nitrates into soils and groundwater,

Intensity of input of pesticides and nitrates into groundwater ($q_x^{гв}$) and into the soil (q_x^n) are evaluated by empirical dependencies [1-3,7]:

$$q_x^{\partial в} = 1 - q_x^n ; \; q_x^n = \exp\left[-(\alpha \cdot q_w + 1 - R_ф)\right],$$

where α - constant, depending on the type of pesticide; q_w - intensity of infiltration nutrition (in shares of the norm); $R_ф$ - infiltration resistance, which is determined by the formula: $R_ф = 1/fm$, here fm - the relative area occupied by soils with low soil thickness (or fine earth),

An approximate assessment of the ecological state of the object can be carried out using the available studies [83], by dependencies:

$$\overline{Э} = 1 - q_x^n = 1 - \exp\left[-(\alpha \cdot q_w + p_i\right] ,$$

where p_i - parameter characterizing a complex of natural conditions.

Thus, the proposed methodological approach for constructing the ecological profile of the catchment area of the Shu river basin in the context of anthropogenic activity allows three main aspects in the field of nature management and environmental management: the ecological and economic function of river basins associated with the outflow and degradation of renewable natural resources; ecological and biological function of river basins, caused by the destabilization of the biological species Hono-Sapience as a result of the growth of anthropogenic impact and changes in the state of the natural environment; the social function of river basins, which is caused by the contradictions between the global (regional) manifestation of pollution and degradation of the natural environment and a private approach to their solution [6-8].

Research results. On the basis of systematization and analysis of long-term information and analytical materials «Kyrgyzhydromet» and «Kazhydromet», as well as the Department of State Statistics of the Kyrgyz Republic and the Republic of Kazakhstan, characterizing the formation of water resources and their use for economic sectors [1], an idea of the «activity-natural system» was obtained the catchment area of the Shu river basin, to build their ecological profile in the conditions of anthropogenic activity (table 2).

Table 2 – Ecological zoning of the Shu river basin

№	Indicators	Natural areas and landscape catena			
		mountain (eluvial)	Foothill (trans eluvial)	Foothill plain (trans-aqual)	plain (super aquatic)
1	2	3	4	5	6
0	Landscape area (F), mln, ha	15,00	20,80	25,78	138,78
Under natural conditions, (1920 y.)					
1	Agricultural landscape area (F_O), thousands ha.	–	2,08	2,57	13,88
2	Hydrothermal coefficient - $\bar{R}$	0,52-1,16	1,16-1,61	1,70-4,80	7,10-12,6
3	The intensity of the water cycle ($\bar{g} = \exp(-1.5 \cdot \bar{R})$	0,2837	0,2516	0,0388	0,0001

Continuation of table 2

1	2	3	4	5	6
4	The intensity of the intake of pesticides and nitrates into the soil (q_x^n)	0,5326	0,6378	0,9139	0,9512
5	Intensity of chemicals and nitrates entering groundwater ($q_x^г$)	0,4674	0,3622	0,0861	0,0488
6	The coefficient of a person's negative reaction to man-made impacts ($\overline{NR}$)	0,0000	0,0506	0,0113	0,0067
7	Coefficient of negative reaction of the environment to technogenic impact ($\overline{nr}$)	0,0000	0,1275	0,2284	0,2378
8	Assessment of the ecological state of the object – $\overline{Э} = 1 - q_x^n$	0,4674	0,3622	0,08100	0,0488
9	The volume of wastewater discharged into the river ($W_в$), км^3	0,000	0,000	0,115	0,327
10	River water volume (W_p), km^3	0,851	1,328	1,151	1,637
11	Mineralization of return waters ($C_в$),g / l	0,00	0,00	1,00	1,50
12	Degree of environmental degradation ($\overline{Э} = 1 - \exp(-q_x^n \cdot C_в \cdot V_в)$	0,00	0,00	0,01	0,02
At the beginning of anthropogenic activity (1960 y.)					
1	Agricultural landscape area (F_O), thousands. ha	-	10,0	238,0	60,00
2	Hydrothermal coefficient - $\bar{R}$	0,52-1,16	1,10-1,30	0,70-0,90	0,65-0,70
3	The intensity of the water cycle ($\bar{g} = \exp(-1.5 \cdot \bar{R})$	0,2837	0,1653	0,2725	0,3642
4	Intensity of input of pesticides and nitrates into the soil (q_x^n)	0,5326	0,6977	0,7261	0,6637
5	Intensity of chemicals and nitrates entering groundwater ($q_x^г$)	0,4674	0,3023	0,2739	0,3363
6	The coefficient of a person's negative reaction to man-made impacts ($\overline{NR}$)	0,0000	0,0560	0,0608	0,0995
7	Coefficient of negative reaction of the environment to technogenic impact ($\overline{nr}$)	0,0000	0,1744	0,2178	0,2655
8	Assessment of the ecological state of the object - $\overline{Э} = 1 - q_x^n$	0,4674	0,3023	0,2739	0,3363
9	The volume of wastewater discharged into the river ($W_в$), km^3	0,000	0,095	0,560	0,120
10	River water volume (W_p), km^3	1,148	2,264	2,923	4,378
11	Return water salinity ($C_в$), g/l	0,00	1,00	2,20	2,50
12	Degree of environmental degradation ($\overline{Э} = 1 - \exp(-q_x^n \cdot C_в \cdot V_в)$	0,000	0,030	0,260	0,050
During the period of increased intensity of anthropogenic activity (1980 y.)					
1	Agricultural landscape area (F_O), thousands. ha		20,0	343,0	80,0
2	Hydrothermal coefficient - $\bar{R}$	0,52-1,16	1,15-1,20	0,80-0,90	0,60-0,80
3	The intensity of the water cycle ($\bar{g} = \exp(-1.5 \cdot \bar{R})$	0,2837	0,1720	0,2780	0,3499
4	Intensity of input of pesticides and nitrates into the soil (q_x^n)	0,5326	0,6907	0,7189	0,6703
5	Intensity of chemicals and nitrates entering groundwater ($q_x^г$)	0,4674	0,3093	0,2811	0,3297
6	The coefficient of a person's negative reaction to man-made impacts ($\overline{NR}$)	0,0000	0,2260	0,2446	0,3155
7	Coefficient of negative reaction of the environment to technogenic impact ($\overline{nr}$)	0,0000	0,2210	0,3594	0,4357
8	Assessment of the ecological state of the object - $\overline{Э} = 1 - q_x^n$	0,4674	0,3093	0,2811	0,3297
9	The volume of wastewater discharged into the river ($W_в$), km^3	0,000	0,200	0,950	0,250
10	River water volume (W_p), km^3	0,844	1,720	2,356	3,622

Continuation of table 2

1	2	3	4	5	6
11	Return water salinity ($C_в$), g/l	0,00	1,50	2,80	3,20
12	Degree of environmental degradation ($\bar{Э} = 1 - \exp(-q_x^n \cdot C_в \cdot V_в)$	0,000	0,110	0,550	0,140
During the formation of increased anthropogenic activity (2000 y.)					
1	Agricultural landscape area (F_O), thousands. ha	-	15,0	292,0	60,0
2	Hydrothermal coefficient - $\bar{R}$	0,52-1,16	1,10-1,15	0,80-0,90	0,70-0,90
3	The intensity of the water cycle ($\bar{g} = \exp(-1.5 \cdot \bar{R})$	0,2837	0,2516	0,3570	0,4493
4	Intensity of input of pesticides and nitrates into the soil (q_x^n)	0,5326	0,6378	0,6703	0,6065
5	Intensity of chemicals and nitrates entering groundwater ($q_x^г$)	0,4674	0,3622	0,3297	0,39350
6	The coefficient of a person's negative reaction to man-made impacts ($\overline{NR}$)	0,0000	0,3151	0,3165	0,4013
7	Coefficient of negative reaction of the environment to technogenic impact ($\overline{nr}$)	0,0000	0,3827	0,53262	0,5155
8	Assessment of the ecological state of the object - $\bar{Э} = 1 - q_x^n$	0,4674	0,36220	0,32970	0,39350
9	The volume of wastewater discharged into the river ($W_в$), km^3	0,000	0,089	0,600	0,105
10	River water volume (W_p), km^3	0,747	0,448	1,536	0,703
11	Return water salinity ($C_в$), g/l	0,00	0,90	1,80	2,90
12	Degree of environmental degradation ($\bar{Э} = 1 - \exp(-q_x^n \cdot C_в \cdot V_в)$	0,160	0,110	0,370	0,230
During the formation of a very increased anthropogenic activity (2020 y.)					
1	Agricultural landscape area (F_O), thousands. ha	–	15,0	292,0	60,0
2	Hydrothermal coefficient - $\bar{R}$	0,52-1,16	1,20-1,30	1,0-1,15	1,10-1,20
3	The intensity of the water cycle ($\bar{g} = \exp(-1.5 \cdot \bar{R})$	0,2837	0,1526	0,1999	0,1791
4	Intensity of input of pesticides and nitrates into the soil (q_x^n)	0,5326	0,7047	0,7738	0,7945
5	Intensity of chemicals and nitrates entering groundwater ($q_x^г$)	0,4674	0,2853	0,2262	0,2055
6	The coefficient of a person's negative reaction to man-made impacts ($\overline{NR}$)	0,0000	0,3007	0,3257	0,3124
7	Coefficient of negative reaction of the environment to technogenic impact ($\overline{nr}$)	0,1600	0,4228	0,5417	0,6753
8	Assessment of the ecological state of the object - $\bar{Э} = 1 - q_x^n$	0,4674	0,2853	0,2262	0,2055
9	The volume of wastewater discharged into the river ($W_в$), km^3	0,000	0,150	0,700	0,200
10	River water volume (W_p), km^3	0,851	1,523	1,416	0,968
11	Return water salinity ($C_в$), g/l	0,00	1,10	2,10	3,20
12	Degree of environmental degradation ($\bar{Э} = 1 - \exp(-q_x^n \cdot C_в \cdot V_в)$	0,000	0,070	0,550	0,460

Based on the forecast calculation performed to assess the ecological situation in the catchment area of the Shu river basin on a spatial-temporal scale, it was concluded that for the period under consideration (1920-2020), the qualitative state of the ecological profile largely depends on the altitudinal zonation characterizing the class of landscapes in river basins:

- in the zone of the mountainous landscape class (eluvial facies), due to the absence of directed anthropogenic activity for the transformation and improvement of natural resources of the natural system, where changes in the components of the natural system occur under the influence of only natural processes, the preservation of their ecological stability and deterioration of the ecological situation are not

observed, which are supported by the peculiarity of the biological cycle, which are formed according to the type of accumulative balance, on the other hand, by the removal of a part of the accumulated substance during the biological active period of the year by geostocks (zone of natural regulation);

- in the zone of the foothill landscape class (transeluvial facies), insignificant anthropogenic activity for the transformation and arrangement of the natural system, where changes in the components of the natural system occur under the influence of not only natural, but also man-made processes, leads to some changes in the components of the natural system, which due to self-regulating their ability, provides natural environmental sustainability, however, some changes in the environmental situation are observed, that is, the indicator of the degree of deterioration of the environmental situation ranges from 0.00 to 0.110 (the zone of controlled and accounted for the consequences of anthropogenic activity)

- in the zone of the foothill lowland subclass of the landscape (trans-accumulative facies), which is the basis of spatial nature management, there is a high tendency of anthropogenic activity, large-scale changes occur, due to the transformation and nature management of the components of the natural system, for the economic and ecological functions of river basins, not only natural services are provided, but also technogenic services, leads not only to an increase in the intensity of biological as well as geological cycles of water and chemicals, and, therefore, the integrity of the natural system of river basins, which led to a deterioration of their ecological situation, where the indicator of the degree of deterioration of the ecological situation ranges from 0.01 to 0.550 (zone of uncontrolled, not considered consequences of anthropogenic activity);

- in the zone of the plain landscape class (superaquial and subaquial facies), which is the basis for spatial nature management and geochemical runoff, there is a growth rate of not only anthropogenic activity, but also technogenic loads, which are accompanied by negative consequences, always lead to a violation of the basic properties of the components of the natural system in the lower reaches river basins, that is, the indicator of the degree of deterioration of the ecological situation ranges from 0.02 to 0.460 (zone of controlled and accounted for the consequences of anthropogenic activity);

Conclusions. The functioning of the catchment area of the Shu River basin, as a geographic object that performs environment-forming, ecological and social functions and is the spatial basis of nature management in conditions of anthropogenic activity, was considered on the basis of systematization and analysis of long-term information and analytical materials «Kyrgyzhydromet» and «Kazhydromet», as well as statistics of the Kyrgyz Republic and the Republic of Kazakhstan, characterizing the formation of water resources and their use for economic sectors [], made it possible, within the framework of cognitive and transformative activities, to build their ecological profile on a spatial and temporal scale, which allows making a number of decisions at the state and interstate levels aimed to regulate relations in the spheres of water use, environmental, economic and social issues arising from the joint use of water resources of transboundary watercourses.

Ә. Т. Қозыкеева[1], Ж. С. Мұстафаев[1], Л. В. Кирейчева[2], С. Д. Даулетбай[3]

Қазақ ұлттық аграрлық университеті, Алматы, Қазақстан;
ФМБҒМ «А.Н. Костяков атындағы Бүкілресейлік гидротехника
және мелиорация ғылыми-зерттеу институты», Мәскеу, Ресей;
М.Х. Дулати атындағы Тараз мемлекеттік университеті, Тараз, Қазақстан

АНТОРОПЕГЕНДІК ҚЫЗМЕТ ЖАҒДАЙЫНДА ШУ ӨЗЕНІНІҢ СУ ЖИНАУ АЛАБЫНЫҢ ЭКОЛОГИЯЛЫҚ БЕЙІНІ

Аннотация. Қырғыз Республикасының «Қырғызгидромет» және Қазақстан Республикасының «Қазгидромет», сонымен қатар Мемлекеттік статистика департаменттерінің Шу өзенінің су жинау алабындағы су ресурстарының қалыптасуын және оны экономика саласына пайдалануды сипаттайтын көпжылдық ақпараттық-талдау мәліметтерінің негізінде өзен алабының су ағыны мен ортасын құрушы, экологиялық, экономикалық қызметтерді атқаратын және табиғатты пайдаланудың кеңістік базисі саналатын «қызметтік-табиғи жүйе» үлгісі ретінде қарастыру арқылы аймақ жағдайына және су нысандарына кешенді бағалау жұмыстары қарастырылған. Шу өзенінің су жинау алабының негізгі қызметтерін бағалау үшін аймақтағы

антропогендік қызмет қарқынын және бағытын анықтайтын, танымдық және түрлендіру қызметінің даму беталысын айқындауға мүмкіндік беретін геожүйелік әдісін пайдалану арқылы геоморфологиялық жүйелеудің ғылыми және тәжірбелік мақсаттының негізінде, экологиялық бейнесін кеңістік-уақыт масштабында тұрғызу жолы негізделген. Өзен алабының негізгі қызметі – бір ғана жеңілдеу нысаны бар гидрогеохимиялық ағынды қалыптастыру, Шу өзенінің су жинау алабының экологиялық бейнесінің сапалық жағдайын анықтай отырып, яғни белдеулік заңдылықтарға байланысты Ландшафттың таулы тобынан ландшафтардың жазықтық тобына (супераквиальдық және субаквиальдық фацияға) дейін, әсіресе, ауылшаруашылық және өндірістік нысандардың қайтарма (коллектор-кәріз) суын жинайтын аймақ болып саналатын өзен алабының төменгі саласында табиғи гидрологиялық тербеліс бұзылатындықтан, аймақтың гидрогеологиялық және топырақ-мелиоративтік үдерісіне және экологиялық жағдайына үлкен әсер тигізеді.

Түйін сөздер: өзен, су жинау алабы, ағын, жүйе, үлгі, функция, қызмет, түрлендіру, таным, экология, бейне, желілеу, талдау, бағалау.

А. Т. Козыкеева[1], Ж. С. Мустафаев[1], Л. В. Кирейчева[2], С. Д. Даулетбай[3]

[1]Казахский национальный аграрный университет, Алматы, Казахстан;
[2]ФГБНУ «Всероссийский научно-исследовательский институт гидротехники и мелиорации им. А.Н. Костякова», Москва, Россия;
[3]Таразский государственный университет им. М. Х. Дулати, Тараз, Казахстан

ЭКОЛОГИЧЕСКИЙ ПРОФИЛЬ ВОДОСБОРА БАССЕЙНА РЕКИ ШУ В УСЛОВИЯХ АНТРОПОГЕННОЙ ДЕЯТЕЛЬНОСТИ

Аннотация. На основе проведенного исследования многолетние информационно-аналитические материалы «Кыргызгидромета» и «Казгидромета», а также Департамента государственной статистики Кыргызской Республики и Республики Казахстан, характеризующие формирование водных ресурсов и их использование в хозяйственных секторах водосборного бассейна реки Шу, были рассмотрены в качестве модели "деятельность-природная система", осуществляющей сток, природообразующую деятельность., эколого-социальные функции и является пространственной основой природопользования для комплексной оценки состояния территории и водных объектов. В качестве основы оценки основных функций водосбора бассейна реки Шу был использован геосистемный подход, определяющий научно-практическую целесообразность геоморфологической схематизации, в рамках которой становится возможным построение их экологического профиля в пространственно-временном масштабе, что позволяет установить тенденции развития познавательной и преобразующей деятельности, определяющие направленность и интенсивность антропогенной деятельности в регионе. Основная природная функция речного бассейна – формирование гидрогеохимического потока, имеющих один объект для своей разгрузки, определяет качественное состояние экологического профиля водосбора бассейна реки Шу, то есть в зависимости от поясности от горного класса ландшафтов до равнинного класса ландшафтов (супераквиальная и субаквиальная фация) постепенно нарушаются природные гидрологические ритмы, оказывает влияние на гидрогеологические и почвенно-мелиоративные процессы и экологические обстановки, особенно в низовьях речных бассейнов, являющихся зонами магазинирования возвратных (коллекторно-дренажных и сточных) вод промышленных и сельскохозяйственных объектов.

Ключевые слова: река, водосбор, бассейн, сток, система, модель, функция, деятельность, преобразования, познание, экология, профиль, схематизация, анализ, оценка.

Information about authors:

Kozykeyeva Aliya Tobazhanovna, Doctor of Technical Sciences, Associate Professor, Professor of the Department «Water Resources and Melioration», Kazakh National Agrarian University; aliya.kt@yandex.ru; https://orcid.org/0000-0003-0581-0881

Mustafayev Zhumakhan Suleimenovich, Doctor of Technical Sciences, Professor, Professor of the Department «Water Resources and Melioration», Kazakh National Agrarian University; z-mustafa@rambler.ru; https://orcid.org/0000-0003-2425-8148

Kireicheva Lyudmila Vladimirovna, Scientific adviser on land reclamation, FGBICU «All-Russian Scientific Research Institute of Hydraulic Engineering and Land Reclamation named after A.N. Kostyakov», Doctor of Technical Sciences, Professor; kireychevalw@mail.ru; https://orcid.org/0000-0002-7114-2706

Dauletbay Saltanat Dauletbaykyzy, Taraz State University named after M.Kh. Dulati, Master, dauletbai-sal@mail.ru; https://orcid.org/0000-0002-5376-9468

REFERENCES

[1] Mustafayev Zh.S. Methodological and ecological principles of agricultural land reclamation. Taraz, 2004. 306 p.

[2] Mustafayev Zh.S., Kozykeyeva A.T. The Aral Sea Basin: Past, Present and Future. Taraz, 2012. 318 p.

[3] Kireicheva L.V., Kozykeyeva A.T., Dauletbai S.D. Complex development of the Shu river - Saarbrucken: Lambert Academy Publishing, 2016. 149 p.

[4] Khachaturyan V.Kh. Assessment of the ecological situation in the justification of reconstruction projects // Melioration and water management, 1990. N 3. P. 17-21.

[5] Khachaturyan V.Kh. Justification of agricultural land reclamation from an ecological point of view // Bulletin of agricultural science, 1990. N 5. P. 43-48.

[6] Adilbektegi G.A., Mustafayev J.S., Uvatayeva T.K., Dulatbekova Z.N., Jozef Mosiej. A new approach to the evaluation of bioclimatic potential of landscapes on the example of northern Kazakhstan // N e w s of the National Academy of sciences of the republic of Kazakhstan series of geology and technical sciences. ISSN 2224-5278. Vol. 5, N 437 (2019). P. 16-25 (in Eng.).

[7] Adilbektegi G. A., Mustafayev J. S., Uvatayeva T. K., Dulatbekova Z. N., JozefMosiej. Quantitative and qualitative assessment of biological and ecological potential of tne landscapes of southern Kazakhstan // N e w s of the National Academy of sciences of the republic of Kazakhstan series of geology and technical sciences. ISSN 2224-5278. Vol. 6, N 438 (2019). P. 96-103 (in Eng.).

[8] Mustafayev Zh. S., Kozykeyeva A. T., Kalmashova A. N., Aldiyarova A. E., Arvydas Povilaitis.Ecological and water economic assessment of the Yesil river basin catchment area // N e w s of the National Academy of sciences of the republic of Kazakhstan series of geology and technical sciences. ISSN 2224-5278. Vol. 2, N 440 (2020). P. 123-131.

N E W S
OF THE NATIONAL ACADEMY OF SCIENCES OF THE REPUBLIC OF KAZAKHSTAN
SERIES OF GEOLOGY AND TECHNICAL SCIENCES
ISSN 2224-5278
Volume 1, Number 445 (2021), 114 – 120 **https://doi.org/10.32014/2021.2518-170X.16**

UDC 556.543.32

I. Sh. Normatov[1], V.V. Goncharuk[2], N.A. Amirgaliev[3], A.S. Madibekov[3], A.I. Normatov[4]

[1]Tajik National University, Dushanbe, Tajikistan;
[2]A.V. Dumansky Institute of Colloid and Water Chemistry, Kiev, Ukraine;
[3]Geography and Water safety Institute of the Ministry of Education and science of the Republic of Kazakhstan, Almaty, Kazakhstan;
[4]Technological University of the Tajikistan,Dushanbe, Tajikistan.
E-mail: inomnor@gmail.com, honch@iccwc.kiev.ua, namirgaliev@mail.ru, madibekov@mail.ru, normatov.2012@mail.ru

HYDROCHEMISTRY OF THE PYANJ TRANSBOUNDARY RIVER UPSTREAM, MIDDLE AND DOWNSTREAM AND THE CRITERION ITS USE FOR IRRIGATION

Abstract. The water quality of the transboundary Pyanj River in the formation zone and along the riverbed before merging with another tributary of the transboundary Amu Darya River-the Vakhsh River was studied. The water quality on the upstream river corresponds to the very soft class (> 1.5 mmol/dm^3) and in the middle and the downstream to the soft class (1.5-3.0 mmol/dm^3). At the upper, middle and lower reaches of the Pyanj river the concentration of alkaline earth exceeds alkali metals ($Ca^{2+} + Mg^{2+} > Na^+ + K^+$) at $HCO_3^- > SO_4^{2-} + Cl^-$ and according to the Handa classification they are characterized by temporary rigidity. To assess the criterion of applicability of the Pyanj river water for irrigation the coefficient of sodium adsorption (SAC) was calculated for water samples from the upstream (Khorog), middle (Darvaz) and the downstream (Lower Pyanj) of the Pyanj river that were equal to 0.88; 1.07; 1.71, respectively. The SAC values for all water samples (from the upper, middle and lower reaches) of the Pyanj river indicate their good qualities for irrigation of agricultural land. The concentration of heavy metals in the Pyanj river is significantly lower than the maximum permissible concentration (MPC).

Key words: agriculture, underground water, solubility of cations, adsorbtion, irrigation.

Introduction. The problem of water quality of river systems and providing the population with safe drinking water, preventing the transfer of water pollutants through crops are one of the Millennium Priority Goals. Solving these problems requires an integrated approach to monitoring water quality from the formation zone to downstream. River systems are polluted mainly in the middle reaches and in the downstream dispersion zone. To determine the sources of river pollution and establish a balance of polluting chemicals, it is necessary to determine the quantitative values coming from the upstream river pollutants.

The formation of the quality of natural waters depends on their physical, chemical, biological and radiological characteristics that are greatly influenced by the geological structures, climate and topography of the zone of formation of water resources [1-5]. However, anthropogenic pressure is a major factor in the pollution of water bodies and arteries [1,2,8,9,10]. A wide and comprehensive review of the literature on the selection of optimal indicators for a comprehensive assessment of surface water quality was done in [6,7,11,12]. The importance of systematic monitoring of water quality is determined by the fact that pollutants in the aquatic environment, due to the occurrence of appropriate physicochemical processes, can transform into more toxic components or generate the appearance of other compounds that are dangerous to the environment and living organisms [13,14].

It is worth mentioning, the problem of water quality is especially relevant for Transboundary Rivers when the formation and dispersal zone of river is located in two or more countries.

For example, the water quality problem of the Zeravshan River the Transboundary River between Tajikistan and Uzbekistan has long been the subject of heated debate and mutual claims arising from the operation of the Anzob mining and processing plant in the middle reaches of the Zeravshan River on the territory of Tajikistan [15,16].

The database on transboundary freshwater disputes (DBTFW) at Oregon State University (OSU) has identified 263 water basins that cross national borders and cover more than 40% of the world's population. Now, humanity is faced with the cataclysms of global climate change manifested in the reduction of water resources and areas of glaciation, water scarcity and significant changes in the water cycle and increases of emergencies [17-20].

A reliable and effective way to solve water quality problems of Transboundary rivers and prevent conflicts and disagreements between neighboring countries is to create a database of real data on water quality indicators in the formation and dispersion zone of river and their quantitative value in the border-crossing zone.

The Pyanj river is one of the tributaries of the Transboundary Amu Darya river with the basin areas 113.6 thousand km^2 that about 73% (82.9 thousand km^2) is located in Tajikistan, 27% (30.6 thousand km^2) in Afghanistan.

The average long-term runoff of the Pyanj River is 7.0 km^3 at the upstream and increase up to 39.8 km^3 in downstream. The norm of the average annual maximum discharge of the Pyanj River is 3670 m^3/s and minimum water discharge (193 m^3/s) is observed in December-February.

Water resources formed in the Aral Sea basin are 148.5 km^3/year (116.5 km^3/year – natural river flow and about 32.0-33.0 km^3/year-return water) and their distribution between the countries of the basin is as follows: Uzbekistan – about 53%, Turkmenistan – 20%, Tajikistan and Kazakhstan – 10%, Kyrgyzstan – less than 5% and Afghanistan – about 2% [21]. According to the World Bank, from 400 thousand ha irrigated in northern Afghanistan of land about 100 thousand ha irrigated directly from the Pyanj and Amu Darya Transboundary Rivers. The growth potential of irrigated lands in the Afghan territory in the basin of these rivers is huge and the irrigation area of fertile lands can reach, according to various estimates, about 500 thousand ha.

Consequently, after the stabilization of the political situation, Afghanistan will claim additional water from the water resources of the Amudarya river basin, and Afghanistan's water withdrawal will reach 9.0 km^3/year by the middle of the XXIst century that will lead to a runoff decrease in the downstream of the Amu Darya.

This means that when the full potential of agricultural land in the north of Afghanistan is developed, it is likely that the anthropogenic pressure on the water resources of the Pyanj River will increase with the influx of municipal sewage and return water from agricultural land. The issue of water quality will appear on the agenda – which country of the basin, in what quantities pollutes the waters of the Pyanj River. The statement that in the mountainous territories of the river catchment in Tajikistan anthropogenic pollution is minimized will not be sufficient to solve the problem. This will require evidence of river water quality in the relevant sections of the river.

The aim of this work is to monitor the water quality of the Pyanj Transboundary River – the main tributary of the Amu Darya.

Objects and Methodology. Water sampling in the Pyanj river upstream, middle and downstream was performed at the Khorog (37º30'N 71º30'E) Darvaz (38º28'N 70º53'E) and Nijniy Pyanj (37º11'N 68º35'E) hydrological stations, respectively (figure 1). The physical and chemical analyses of the waters samples were carry out by use of the «TaLab» spectrophotometer according corresponding state standards.

At chemical analyses and interpretation of results was guided by the normative document «Sanitary and epidemiological requirements to water sources, water intake sites for drinking purposes, drinking water supply and places of cultural and domestic water use and security of water facilities» (Order of the Minister of national economy of the Republic of Kazakhstan, March 16, 2015 No. 209). In addition, state standards were relevant: Na^+ (State standart 26449.1-85, п.17.1), K^+ (State standart 26449.1-85, п. 18.1), Ca^{2+} (State standart 26449.1-85, п. 11.1), Mg^{2+} (State standart 26449.1-85, п.12), NO_3^- (State standart 33045-2014).

Figure 1 – Sampling points of water from the Pyanj river (Khorog Darvaz, Nizhniy Pyanj)

Results and discussion. The World Health Organization (WHO) has developed international water quality standards in the form of guidelines that are used as basic rules and standards in developing and developed countries. According to these standards, the maximum permissible concentration of the total hardness of drinking water is 15 mmol/dm^3 and the most favorable is 3.0 mmol/dm^3.

The results of chemical analyses of water samples from the formation zone (Gunt), the middle (Darvaz) and the downstream (Nijniy Pyanj) of the Pyanj river are presented on the Table.

From the Table it follows that the water in all three section (upstream, middle and downstream) of the Pyanj river meet the requirements for drinking water. In addition, the water of the Pyanj river in the upstream corresponds to the very soft class (>1.5 mmol/dm^3), in the middle reaches and downstream to the soft class (> 1.5-3.0 mmol/dm^3).

At the upper, middle and lower reaches of the Pyanj river the concentration of alkaline earth exceeds alkali metals (Ca^{2+} + Mg^{2+}> Na^+ + K^+) (figure 2) at $HCO3^-$ > SO_4^{2-} + Cl^- (figure 3) and according to the Handa classification they are characterized by temporary hardness.

The chemical indicators of water in the upstream (Khorog), middle (Darvaz) and the downstream (Nijniy Pyanj) of the Pyanj river

Indicators	Unit	Value		
		Khorog	Darvaz	Nijniy Pyanj
Hydrogen index	pH	6.4	7.86	7.88
Total mineralization	mg/dm^3	86	257	286
Dry residue	mg/dm3	22	190	224
Total hardness	mmol/dm^3	1.34	2.35	2.65
Permanganate oxidability	mgO$_2$/dm^3	0.32	1.04	0.98

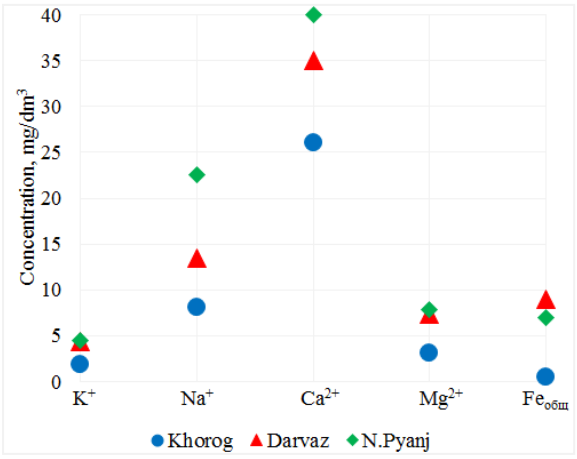

Figure 2 – Concentration of water composition cations on the upstream (Khorog), middle (Darvaz) and downstream (Nijniy Pyanj) of the Pyanj river

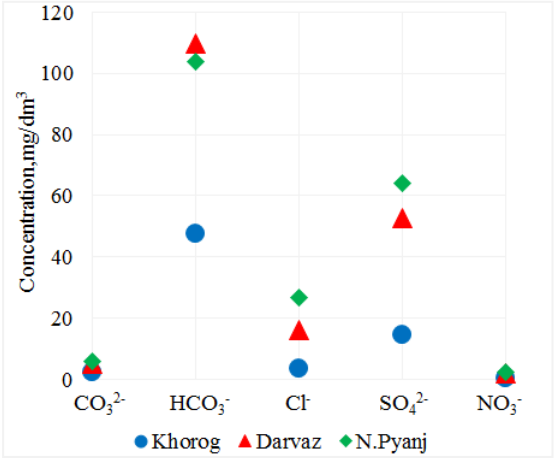

Figure 3 – Concentration of water composition anions on the upstream (Khorog), middle (Darvaz) and downstream (Nijniy Pyanj) of the Pyanj river

To assess water quality for irrigation purposes Na^+ or alkaline hazard expressed by the coefficient of sodium adsorption (SAC), is widely used. If the water used for irrigation has a high Na^+ and low Ca^{2+} contents the ion-exchange sites can be saturated by Na^+ that destroys the soil structure due to the dispersion of clay particles. Such soils reduce plant growth

The sodium adsorption coefficient for the test waters is expressed as follows [22]:

$$SAC = Na^+ / ((Ca^{2+} + Mg^{2+}) / 2)^{1/2}$$

The concentration of cations at the Pyanj river upstream is insignificant and increases downstream. A particularly noticeable increase of the Na^+ and Ca^{2+} cations is observed (figure 2). According to Table at the Darvaz and the Nijniy Pyanj hydrological stations, the water of the Pyanj river is slightly alkaline. Therefore, it can be assumed that leaching of coastal ground sediments occurs downstream of the river and water is enriched by Na^+ and Ca^{2+} cations.

Thus, the calculated SAC values for water samples at the three water sampling points of Khorog, Darvaz, and Nijniy Pyanj correspond to 0.88; 1.07; 1.71 respectively. The obtained SAC values for all water samples from the Pyanj River indicate their good qualities for irrigation of agricultural land.

The NO_3^- content in upstream water samples corresponds to 0.3 mg/dm^3 and increases to 2.2 mg/dm^3 in the Pyanj river downstream. Relatively low concentration of the NO_3^- anion along the Pyanj riverbed indicate that there are no stationary sources of anthropogenic pollution from agricultural and municipal wastewater.

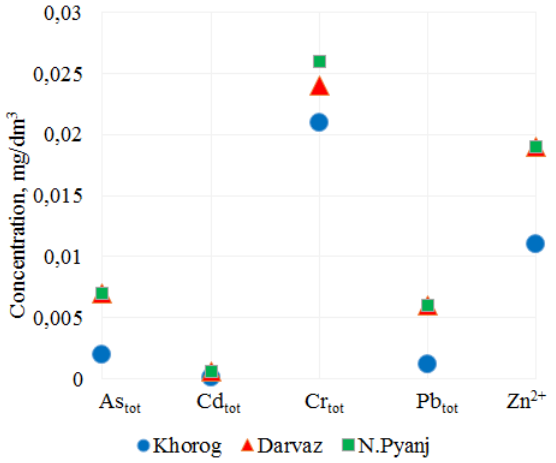

Figure 4 – Concentration of heavy metals on the water composition at the upstream (Khorog), middle reaches (Darvaz) and downstream (Nijniy Pyanj) of the Pyanj river

The content of heavy metals in the composition of the Pyanj river water in the formation zone, the middle course and the Nijniy Pyanj river show that the concentration of heavy metals along the entire channel of the Pyanj River is significantly lower the MPC (figure 4).

Conclusion. Summary of the results of chemical analyzes established that the transboundary Pyanj river is not affected by stationary sources of anthropogenic pollution. The nature of the formation of the chemical composition of water is due to the geological properties of the formation zone and the processes of leaching of rocks. In terms of quality, the Pyanj river water throughout the river channel meets all the requirements for drinking water. According to the values of the sodium adsorption coefficient (SAC), the water flow of the Pyanj river is quite suitable for irrigation of agricultural land. The content of heavy metals in the composition of water is significantly lower than the MPC.

И. Ш. Норматов[1], В. В. Гончарук[2], Н. А. Амиргалиев[3], А. С. Мадибеков[3], А. И. Норматов[4]

[1]Тәжік ұлттық университеті, Душанбе, Тәжікстан;
[2]А. В. Думанский атындағы коллоидты және су химиясы институты;
Украина Ұлттық ғылым академиясы, Киев, Украина;
[3] «География және су қауіпсіздігі институты» АҚ, ҚР БҒМ, Алматы, Қазақстан;
[4]Тәжікстан технологиялық университеті, Душанбе, Тәжікстан

ПЯНДЖ ТРАНСШЕКАРАЛЫҚ ӨЗЕНІНІҢ ЖОҒАРҒЫ, ОРТА ЖӘНЕ ТӨМЕНГІ АҒЫСЫНЫҢ ГИДРОХИМИЯСЫ ЖӘНЕ СУАРУ ҮШІН ПАЙДАЛАНУ КРИТЕРИЙЛЕРІ

Аннотация. Жұмыс Пяндж трансшекаралық өзенінің қалыптасу аймағынан бастап, өзен арнасы бойымен Амудария трансшекаралық өзенінің басқа саласы – Вахш өзеніне қосылғанға дейінгі суының сапасын кешенді зерттеуге арналған. Пяндж өзенінің суы қалыптасу аймағында өте жұмсақ класқа (шекті мәні 1.5 ммоль/дм^3), ал орташа және төменгі ағысындағы суы – жұмсақ класқа (шекті мәні 1.5-3.0 ммоль/дм^3) сәйкес келеді. Пяндж өзенінің жоғарғы, орта ағысы мен төменгі ағысынан алынған су сынамаларында сілтілік жер металдары сілтіліктен асып түседі ($Ca^{2+} + Mg^{2+} > Na^+ + K^+$) және әлсіз гидрокарбонат қышқылы күшті қышқылдардан асып түседі ($HCO_3^- > SO_4^{2-} + Cl^-$), жалпы қабылданған Handa жіктемесіне сәйкес оларға уақытша кермек тән. Суару үшін Пяндж өзенінің суын қолдану критерийлерін бағалау үшін сәйкесінше 0,88; 1,07; 1,71 болатын Пяндж өзенінің жоғарғы (Хорог), орта (Дарваз) және төменгі (төменгі Пяндж) су сынамалары үшін натрийдің адсорбция коэффициенті (САС) есептелді. Пяндж өзенінің барлық су үлгілері үшін SAC мәні (жоғарғы, орта және төменгі ағыстардан) ауылшаруашылық жерлерін суару үшін олардың жақсы қасиеттерін көрсетеді. Пяндж өзеніндегі ауыр металдардың концентрациясы шекті рұқсат етілген концентрациядан (ШРК) әлдеқайда төмен.

Түйін сөздер: ауылшаруашылығы, жерасты суы, катион ерігіштігі, адсорбциялық, ирригация

И. Ш. Норматов[1], В. В. Гончарук[2], Н. А. Амиргалиев[3], А. С. Мадибеков[3], А. И. Норматов[4]

[1]Таджикский национальный университет, Душанбе, Таджикистан;
[2]Институт коллоидной химии и химии воды им. А.В. Думанского,
Национальная Академия наук Украины, Киев, Украина;
[3]АО «Институт географии и водной безопасности» Министерства образования
и науки Республики Казахстан, Алматы, Казахстан;
[4]Технологический университет Таджикистана, Душанбе, Таджикистан

ГИДРОХИМИЯ ТРАНСГРАНИЧНОЙ РЕКИ ПЯНДЖ В ВЕРХНЕМ, СРЕДНЕМ И НИЖНЕМ ТЕЧЕНИИ И КРИТЕРИЙ ЕЕ ИСПОЛЬЗОВАНИЯ ДЛЯ ОРОШЕНИЯ

Аннотация. Изучено качество воды трансграничной реки Пяндж в зоне формирования и вдоль русла до слияния с другим притоком трансграничной реки Амударьи – рекой Вахш. Качество воды в верхнем течении реки соответствует очень мягкому классу (> 1,5 ммоль/дм3), а в среднем и нижнем течении – мягкому классу (1,5-3,0 ммоль/дм3). В верхнем, среднем и нижнем течении реки Пяндж концентрация щелочноземельных

металлов превышает концентрацию щелочных металлов (Ca2+ + Mg2+> Na+ + K+) при HCO3- > SO42- + Cl – и по классификации Ханда они характеризуются временной жесткостью. Для оценки критерия применимости воды реки Пяндж для орошения был рассчитан коэффициент адсорбции натрия (CAC) для проб воды верхнего (Хорог), среднего (Дарваз) и нижнего (Нижний Пяндж) течения реки Пяндж, которые были равны 0,88; 1,07; 1,71 соответственно. Значения SAC для всех проб воды (из верхнего, среднего и нижнего течения) реки Пяндж указывают на их хорошие качества для орошения сельскохозяйственных угодий. Концентрация тяжелых металлов в реке Пяндж значительно ниже предельно допустимой концентрации (ПДК).

Ключевые слова: сельское хозяйство, подземные воды, растворимость катионов, адсорбция, ирригация.

Information about authors:

Normatov Inom, Head of the Department of Meteorology and Climatology of the Tajik National University, Dushanbe, Tajikistan; inomnor@gmail.com; https://orcid.org/0000-0001-5474-584X

Goncharuk Vladislav Vladimirovich, Director of the Institute of colloid chemistry and water chemistry named after A.V. Dumansky of the National Academy of Sciences of Ukraine, Kiev, Ukraine; honch@iccwc.kiev.ua; https://orcid.org/0000-0003-4594-2440

Amirgaliev Nariman, Chief researcher of the Laboratory of Hydrochemistry and environmental toxicology of the Institute of geography and water safety of the Ministry of Education and Science of the Republic of Kazakhstan, Almaty, Kazakhstan; namirgaliev@mail.ru; http://orcid.org/0000-0002-2664-7473

Madibekov Azamat, Chief researcher of the Laboratory of Hydrochemistry and environmental toxicology of the Institute of geography and water safety of the Ministry of Education and Science of the Republic of Kazakhstan, Almaty, Kazakhstan; madibekov@mail.ru; http://orcid.org/0000-0001-9303-6640

Normatov Ayubjon Ismoilovich, postgraduate student of the Technological University of Tajikistan, Dushanbe, Tajikistan; normatov.2012@mail.ru; https://orcid.org/0000-0001-9624-092X

REFERENCES

[1] Tomas D., Curlin M., Maric A. (2017). Assessing the surface water status in Pannonian ecoregion by the water quality index model. Ecological Indicators 79, 182-190.

[2] Erickson J.J., Smith C.D, Goodridge A., et al. (2017). Water quality effects of intermittent water supply in Arraij an, Panama. Water Research 114, 338-350.

[3] Helena B., Pardo R., Vega M., et al. (2000). Temporal evolution of groundwater composition in an alluvial aquifer (Pisuerga River, Spain) by principal component analysis. Water Research 34 (3) (2000), 807-816.

[4] Subramani T., Elango L., Damodarasamy S.R. (2005). Groundwater quality and its suitability for drinking and agricultural use in Chithar River Basin, Tamil Nadu, India. Environmental Geology 47 (8) (2005), 1099-1110.

[5] Zhu B., Wang Y. (2016). Statistical study to identify the key factors governing ground water recharge in the watersheds of the arid Central Asia. Environmental Monitoring and Assessment 188 (1) (2016), 66-74.

[6] Normatov I. Sh., Markaev B.A., et al. (2018). Hydrochemistry and isotopic composition of the Vakhsh river and its tributaries. Proc. Rus. St. Hydromet Univ. N 50. (2018). P. 81-87.

[7] Groll M., Opp Ch., Normatov I. Sh., et al. (2015). Water quality, potential conflicts and solutions – an upstream-downstream analysis of the transnational Zarafshan River (Tajikistan, Uzbekistan) // J. Environmental Earth Sciences. Vol. 73. N 2. (2015). P. 743-764.

[8] Dinelli E., Lima A., De Vivo B., et al. (2010). Hydrogeochemical analysis on Italian bottled mineral waters: effects of geology. J. Geochemical Exploration 107 (3), 317-335.

[9] Singh A., Mondal G.C, Singh, T.B., et al. (2012). Hydrogeochemical processes and quality assessment of groundwater in Dumka and Jamtara districts, Jharkhand, India. Environmental Earth Sciences 67 (8), 2175-2191.

[10] Oyarzun R., Jofre E., Morales P., et al. (2015). A hydrogeochemistry and isotopic approach for the assessment of surface water-groundwater dynamics in an arid basin: the Limarı´ watershed, North-Central Chile. Environmental Earth Sciences 73 (1), 39-55.

[11] Amirgaliev N., Askarova M., Normatov I., et al. (2019). On the choice of optimal parameters for the integrated assessment of surface water quality. News of the National Academy of sciences of the Republic of Kazakhstan. Series Geology & Tech. Science. Vol. 3, N 435 (219). P. 150-158. https://doi.org/10.32014/2019.2518-170X.81 ISSN 2224-5278 (in Eng)

[12] Amirgaliev N., Madibekov A., Normatov I. (2019) About the criteria of estimation of surface water quality of Kazakhstan on the basis of accounting of its natural features. News of the National Academy of Sciences of the Republic of

Kazakhstan. Series of geology and technical sciences. Vol. 4, N 436 (2019). P. 188-198. https://doi.org/10.32014/2019.2518-170X.114 ISSN 2224-5278 (in Eng.).

[13] Absametov M.K., Adenova D.K., Nusupova A.B. (2019) Assessment of the impact of anthropogenic factors water resources of Kazakhstan // News of the National Academy of sciences of the Republic of Kazakhstan. Series Geology & Tech. Science. Vol. 1, N 433 (2019). P. 248-254. ISSN 2224-5278. https://doi.org/10.32014/2019.2518-170X.30

[14] Madibekov A., Nysanbaeva M., Kurmanova M. (2018) Role of chemical composition of an atmosphere precipitation in pollution of a surface water // News of the National Academy of sciences of the Republic of Kazakhstan. Series Geology & Tech. Science. Vol. 5, N 431 (2018). P. 120-127. https://doi.org/10.32014/2018.2518-170X.17 ISSN 2224-5278 (in Eng.).

[15] Normatov P., Normatov I. (2019) Contamination risk assessment of the Transboundary Zeravshan River using chemical and isotopic studies. E3S Web Conf. Vol. 98, 2019: 16th International Symposium on Water-Rock Interaction (WRI-16) and 13th International Symposium on Applied Isotope Geochemistry (1st IAGC International Conference), July 21-26, 2019 Tomsk, Russia. https://doi.org/10.1051/e3sconf/20199807021.

[16] Normatov P., Armstrong R., Normatov I. (2016) Variations in hydrological parameters of the Zeravshan river and its tributaries depending on meteorological conditions // J. Meteorology and Hydrology 9, 91-96.

[17] Menzel L., Burger G. (2002) Climate change scenarios and runoff response in the Mulde catchment (Southern Elbe, Germany) // J. Hydrology 267, 53-64.

[18] Roudier P., Ducharne A., Feyen L. (2014) Climate change impacts on runoff in West Africa: a review // Hydrology & Earth System Sciences 18 (7), 2789-2801.

[19] Wangerlandsson L., Van Der J., Gordon L.J, et al. (2014) Contrasting roles of interception and transpiration in the hydrological cycle - Part 1: Simple Terrestrial Evaporation to Atmosphere Model // Earth System Dynamics 5 (1), 441-469.

[20] Oisson T., Jakkila J., Veijalainen N., et al. (2015) Impacts of climate change on temperature, precipitation and hydrology in Finland - studies using bias corrected Regional Climate Model data // Hydrology & Earth System Sciences Discussions 12 (3), 2657-2706.

[21] Medvedev A. (2017) The history of the problem of using the transboundary water resources of Central Asia and the role of non-regional partners in resolving them. Online. Available at: http://www.jeen.com/news_view/702/ [Date of access 03.03.2019].

[22] Kalra Y.P., Maynard D.G. (1991) Methods manual for forest soil and plant analysis. Information report NOR-X-319, Northwest Region, Northern Forestry Centre, Forestry Canada.

N E W S
OF THE NATIONAL ACADEMY OF SCIENCES OF THE REPUBLIC OF KAZAKHSTAN
SERIES OF GEOLOGY AND TECHNICAL SCIENCES
ISSN 2224-5278
Volume 1, Number 445 (2021), 121 – 126 **https://doi.org/10.32014/2021.2518-170X.17**

UDC 002.6:004.89
IRSTI 20.23.27

D. B. Nurseitov[1], N. A. Toiganbayeva[2], M. O. Kenzhebayeva[2]

[1]Satbayev University, National Scientific Laboratory for the Collective Use
of Information and Space Technologies, Almaty, Kazakhstan;
[2]al-Farabi Kazakh National University, Almaty, Kazakhstan.
E-mail: ndb80@mail.ru, bodinaz@mail.ru, merey-mex-2017@mail.ru

IMAGES CONVERTER OF GEOLOGIC- LITHOLOGICAL PROFILES

Abstract. The article is devoted to the program "Converter", which allows you to translate the geologic-lithological profile of a mineral field into a digital format in the form of a two-dimensional array.

The object-oriented programming language Python was used to write the program. The NumPy, OpenCV, and MatPlotlib libraries are actively used. The implementation of this program is based on image segmentation and finding the prevailing colors in the OpenCV library. Image segmentation is a preliminary step in image processing. The obtained values allow you to find out the density distribution in the area under consideration. The program "Converter" has a good graphical representation of the results obtained using the MatPlotlib library. The program writes the final converted result as a two-dimensional array to a text file along the desired path. Thus, the matrix is easy to read for further use in conjunction with other programs.

The purpose of this work was to create a program that converts the geologic-lithological profile of the field into a digital format in the form of a two-dimensional array, for further use of this matrix as the distribution density of the oil field. The "Converter" program converts any geologic-lithological profile into a two-dimensional array in a matter of minutes.

Key words: geologic-lithographic profiles, Converter, density distributions, colors, pixel, matrix, invers problem.

Introduction. Long-term development of oil and gas fields can lead to negative consequences. For timely detection of various negative phenomena, gravimetric monitoring of deposits is regularly carried out with subsequent identification of experimental data. Gravimetric monitoring is a method in the complex of control tools for the development of oil and gas fields. The use of gravimetric monitoring complements and refines the results of standard methods. Gravimetric monitoring is based on gravimetric surveys. Gravimetric survey is a set of measurements of quantities that characterize the gravitational field of a given area. This survey allows you to solve geological problems. The final product of gravimetric survey is gravimetric maps. Based on changes in the gravimetric survey readings and other factors, conclusions are drawn about changes in the internal geological structure of the profile. You can do this by solving the inverse problem of gravimetry. But in the process of solving it, you will have to solve a direct problem. This requires a density distribution. Where can we get it? In particular, there are data of geologic-lithographic profiles (obtained during the initial exploration of the field). They are maps (drawings) in graphic form, which depict the location of certain materials in this area. This information allows you to find out the density distribution in the area at the initial stage. Knowing the density distribution, we can find the distribution of the gravitational field by solving the direct gravimetry problem [1-4]. To solve a direct problem, you need to have a density distribution in digital form rather than graphical. The purpose of this work is to create a program that automatically implements this procedure [5].

Problem statement. Figure 1 shows the geologic-lithological profile of the oil field. The drawing shows oil deposits in brown, gas deposits in yellow, and water deposits in blue. Around the minerals-the ground is white. The composition of the soil depends on the depth of the Deposit. The left side of figure 1 shows the depth scale in meters. Vertical lines in the form of arrows are drilled wells. Well numbers are written on the tops of the heads. Geologic-lithological profiles have different scales horizontally and vertically, which should be taken into account when implementing the program. The main object of research is to obtain a density distribution matrix in a given area by converting geological and lithological profiles. The drawing sets the distribution of materials by section.

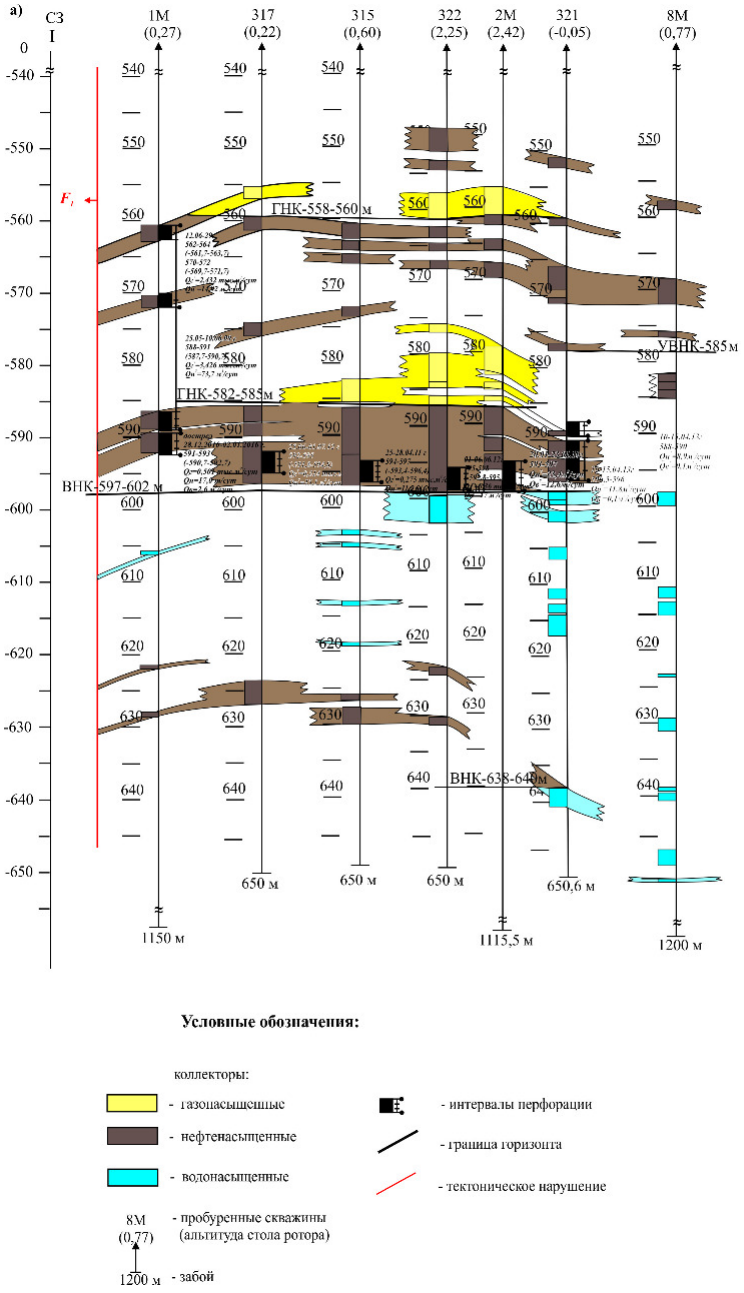

Figure 1 – Geological and lithological profile of the oil field.

We need to have geologic-lithological profiles in the form of initial information about the density of materials, to obtain a density distribution matrix. To do this, you must have a program that implements this transformation. We called this program "Converter". The program should be easily integrated with other parts of the global program and of course meet the latest requirements of the scientific community.

Research methods. Since Python is a modern and good choice for system integration in scientific computing. All calculations were performed in Python, an object-oriented language. The big advantage of an interpreted language is that programs can be tested and debugged quickly, which allows the user to focus more on the program principles and less on the programming itself. Since there is no need to compile, link, and execute after each fix, Python programs can be developed in a shorter time than equivalent programs in Fortran or C. On the negative side, interpreted programs do not create standalone applications. Thus, a Python program can only run on computers that have the Python interpreter installed [6]. Python has a rich standard library and a large number of extension modules for almost all the needs of the information technology industry. The program "Converter" used the libraries cv2 (library for working with graphic data and pixels), numpy (library for working with matrices), pyplot (library for plotting), and others. One of the fundamental aspects of NumPy is providing a powerful N-dimensional array object, ndarray, to represent a collection of items (all of the same type) [7].Thanks to the clear syntax, learning the language is not a big problem. Programs written in it are structured in form, and it is easy to follow the logic of their operation.

Algorithm of the program «Converter». The program **«Converter»** works according to the following algorithm:

1) To process images of geologic-lithographic profiles of deposits in digital format, an image is fed to the input. The program takes a drawing of a geologic-lithological profile, reads its width and height in pixels.

2) Divides the number of pixels into N parts, thus splitting the original pixel area into small rectangles.

3) In each small rectangle, we calculate the color distance of each pixel from the colors in the density table based on the Euclidean distance formula (in this case, we only have 4 colors – blue, brown, yellow, and white).

4) Having determined which of the four colors this pixel is closest to, it counts the number of each of the four colors in this rectangle. This is how the program determines how many pixels of a particular color (one of four colors) are contained in a small rectangle.

5) The Program determines the color that is most in this small rectangle. In addition, assigns this rectangle the color that is most there.

6) The Program goes through all the small rectangles, assigning each a certain color-the key number from the dictionary (brown, blue, yellow or white).

7) Using the color key, a density value corresponding to this color is requested, and the rectangle cell assigns this density value.

8) Running through all the rectangles, we get the density matrix, which is a digital format of the geological and lithological profile.

Note that the partition into N parts can be arbitrarily large. This allows you to get accurate interpretations down to pixels.

Dictionaries are useful for storing tables of information with a unique identify or for each record. Dictionaries provide a mapping from a set of keys to a set of values. In other words, given a key, a dictionary can look up the value associated with it [8]. In the Python programming language, dictionaries (the dict type) are another type of data structure, along with lists and tuples. This schema describes the syntax of a Python dictionary:

{key: value, key: value, key: value, …}

Therefore, each dictionary element consists of two objects: a key and a value. In our example, the key is the name 0,1,2,3 and color, name, density, the value is [255, 255, 255], [153, 204, 255], [204,150, 102], [255, 255, 0]; Earth, Water, Oil, Gas; [2.1], [1.55], [0.9], [0.00085]. Key identify dictionary item, the value is the data, which correspond to the given key. Key values is a unique, two identical keys in the dictionary cannot be.

OpenCV provides the *imread* function to load an image from a file and the *imwrite* function to write an image to a file. These functions support various file formats for still images. The supported formats vary – as formats can be added or removed in a custom build of OpenCV – but normally BMP, PNG, JPEG, and TIFF are among the supported formats [9]. An important feature of OpenCV is the

representation of images as multidimensional NumPy arrays and the saving of images in BGR colors. To return to standard RGB, use the cv2.COLOR_BGR2RGB function, which converts the BGR format to RGB format. This was necessary because the pixel colors were in RGB format.

As a result, *def converter_pix_to_massiv* function returns a matrix of densities of geological and geographical profiles of the field (figure 2).

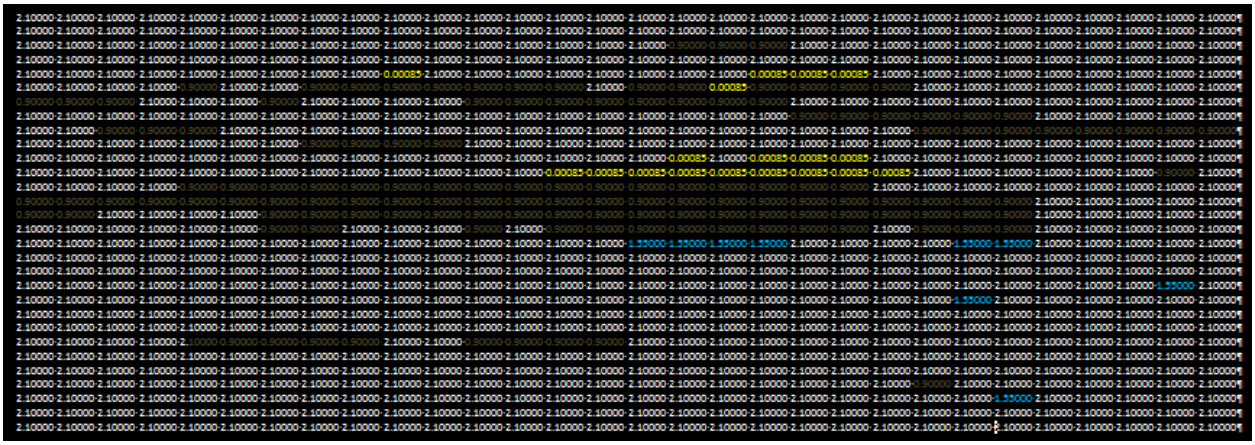

Figure 2 – Matrix of densities of geological and lithographic profiles of the Deposit.

Effective scientific and technical visualization of data requires a wide variety of graphing techniques. Matplotlib implements many types of plotting techniques as methods of the Axes object. For example, in the previous examples, we have already used the plot method, which draws curves in the coordinate system provided by the Axes object. As a consequence of the multilanguage model, scientific and technical computing with Python involves much more than just the Python language itself. In fact, the Python language is only a piece of an entire ecosystem of software and solutions that provide a complete environment for scientific and technical computing [10].

Conclusion. The developed program "Converter" actually converts the geological and lithographic profile of an oil field into a digital format in the form of an array in the Python environment. The results obtained will be used in the future to solve the main direct problem, which allows us to find out the distribution of the gravitational field, as if the structure of the field would be the same as indicated in those sections. And by monitoring deposits and identifying this information, it is supposed to solve the inverse problem in order to find out what changes have occurred in the reservoir compared to the distribution that is obtained in the process of solving a direct problem based on information from sections. Thus, the developed program becomes one of the key elements of the developed GIS project AP05135158 ”Development of geographic information system for solving the problem of gravimetric monitoring of the state of the subsoil of oil and gas regions of Kazakhstan based on high performance computing in conditions of limited experimental data”.

Д. Б. Нурсеитов[1], Н. А. Тойганбаева[2], М. О. Кенжебаева[2]

[1] Satbayev University, Ақпараттық және космостық технологияларды ұжымдық қолданудың Ұлттық ғылыми зертханасы, Алматы, Қазақстан;
[2]Әл-Фараби атындағы Қазақ Ұлттық университеті, Алматы, Қазақстан

КЕН ОРНЫНЫҢ ГЕОЛОГИЯЛЫҚ-ЛИТОЛОГИЯЛЫҚ КЕСКІНДЕРІНІҢ ГРАФИКАЛЫҚ БЕЙНЕЛЕРІН ТҮРЛЕНДІРУ

Аннотация. Мақала кен орындарының геологиялық-литографиялық кескіндерінің графикалық бейнесін екіөлшемді массив түрінде сандық форматқа түрлендіретін «Конвертер» бағдарламасына арналған.

Бағдарлама жазу үшін нысанға бағытталған Python бағдарламалау тілі қолданылды. NumPy, OpenCV, matplotlib кітапханалары белсенді түрде пайдаланылды. Пиксельдермен жұмыс істеу үшін OpenCV кітапханасының мүмкіндігін зерттеу мен қолдану жұмыстары іске асты, BGR және RGB форматтары, графикалық бейнелерімен жұмыс атқаруда қажетті форматты ұтымды қолдану жолдары қарастырылды. Бұл бағдарламаның іске асуы Python ортасында OpenCV кітапханасын пайдалану арқылы бейнені сегменттеуге және басым түсті табуға негізделген. Бейнені сегменттеу – бейнені өңдеудің бастапқы қадамы болып саналады. Жуық өлшемі ретінде Евклид қашықтығы қолданылады. Алынған мәндер қарастырылатын аймақта тығыздықтың таралуын анықтауға мүмкіндік береді. «Converter» бағдарламасы matplotlib кітапханасы арқылы алынған нәтижелерді көрнекті графикалық түрде бейнелеп береді. Бағдарлама екіөлшемді массив түрінде түрленген соңғы нәтижені таңдалған жол арқылы мәтіндік файлға жазып береді. Сөйтіп, алынған матрицаны болашақта басқа бағдарламаларда кешенді түрде қолдануға болады.

Түйін сөздер: геологиялық-литографиялық кескіні, Converter, тығыздықтың таралуы, түстер, пиксель, матрица.

Д. Б. Нурсеитов[1], Н. А. Тойганбаева[2], М. О. Кенжебаева[2]

[1]Satbayev University, Национальная научная лаборатория коллективного пользования информационных и космических технологий, Алматы, Казахстан;
[2]Казахский Национальный университет им. аль-Фараби, Алматы, Казахстан

КОНВЕРТЕР ИЗОБРАЖЕНИЙ ГЕОЛОГО-ЛИТОЛОГИЧЕСКИХ ПРОФИЛЕЙ

Аннотация. Статья посвящена программе "Конвертер", позволяющей перевести геолого-литологический профиль месторождения полезных ископаемых в цифровой формат в виде двумерного массива.

Для написания программы был использован объектно-ориентированный язык программирования Python. Активно использованы библиотеки NumPy, OpenCV, matplotlib. Была проведена работа по изучению и применению возможности библиотеки OpenCV при работе с пикселями, изучен формат BGR и RGB и корректное использование нужного формата при работе с геолого-литологическими профилями месторождения. Реализация данной программы основана на сегментации изображении и нахождении преобладающих цветов в среде Python с использованием библиотеки OpenCV. Сегментация изображения является предварительным этапом обработки изображений. В качестве меры близости используется Евклидово расстояние. Полученные значения позволяет узнать распределение плотности в рассматриваемой области. Программа «Converter» имеет хорошее графическое представление полученных результатов при помощи библиотеки matplotlib. Конечный преобразованный результат в виде двумерного массива программа записывает в текстовый файл по желаемому пути. Таким образом, матрицу легко считывать для дальнейшего использования в комплексе с другими программами.

Ключевые слова: геолого-литографические профили, Converter, распределения плотности, цвета, пиксель, матрица, обратная задача, гравиметрия, прямая задача.

Information about authors:

Nurseitov D.B., Head of the National Scientific Laboratory for collective use of information and space technologies, Candidate of Physical and Mathematical Sciences, associate professor, Almaty, Kazakhstan; ndb80@mail.ru; https://orcid.org/0000-0003-1073-4254

Toiganba*y*eva N.A., Al-Farabi Kazakh National University, PhD doctoral student, Almaty, Kazakhstan; bodinaz@mail.ru; https://orcid.org/0000-0003-2661-8661

Kenzhebayeva M.O., Al-Farabi Kazakh National University, PhD doctoral student, Almaty, Kazakhstan; merey-mex-2017@mail.ru; https://orcid.org/0000-0001-7982-9804

REFERENCES

[1] Serovajsky S.Ya., Kenzhebayeva M.O. (2018) Modeling of the potential of the gravitational field at the upper boundary of the region with the existence of a subterranean anomaly // International Journal of Mathematics and Physics. Vol. 1. P. 20-26. (in Eng.).

[2] Serovajsky S.Ya., Azimov A.A., Kenzhebayeva M.O., Nurseitov D.B., Nurseitova A.T., Sigalovskiy M.A. (2019) Mathematical problems of gravimetry and its applications // International Journal of Mathematics and Physics. Vol. 1 (29). P. 29-35. ISSN 2409-5508 (Online), ISSN 2218-7987 (Print) (in Eng.).

[3] Marchenko M.A., Serovajsky S.Ya, Smirnov D.D., Kenzhebayeva M.O. (2019) Solving the inverse problem of gravimetry by the Monte Carlo method on a supercomputer using distributed computing [Reshenie obratnoi zadachi gravimetrii metodom Monte-Karlo na supercomputer s ispolzovaniem raspredelennih vichislenii] // Parallel computing technologies - XIII international conference, Pavt'2019. [Parallelnie vichislitelnie tehnologii – XIII mejdunarodnaya konferenciya, Pavt'2019], Kaliningrad, April 2-4 (2019). P. 327-338 (in Russ.).

[4] Serovajsky S.Ya., Kenzhebayeva M.O. (2018) Modeling of the potential of the gravitational field at the upper boundary of the region with the existence of a subterranean anomaly // International Journal of Mathematics and Physics. Vol. 1 (20). P. 20-26. ISSN 2409-5508 (Online), ISSN 2218-7987 (Print) (in Eng.).

[5] Toyganbaeva N., Kenzhebayeva M. (2020) Development of a program for converting graphic information of geological and lithographic profiles into digital information. Traditional international April mathematical conference in honor of the day of science workers of the Republic of Kazakhstan, dedicated to the 1150th anniversary of Abu Nasir al-Farabi and the 75th anniversary of the Institute of mathematics and mathematical modeling. Almaty. 143 p. (in Eng.).

[6] Jaan Kiusalaas (2005) Numerical methods in Engineering with Python, Cambridge University Press, ISBN –I3 978-0-511-12810-3. (in Eng.).

[7] Sandro Tosi (2009) Matplotlib for Python Developers, Published by Packt Publishing Ltd. UK. ISBN 978-1-847197-90-0 (in Eng.).

[8] Laura Tateosian (2015) Python For ArcGIS, Springer Cham Heidelberg New York Dordrecht London, ISBN 978-3-319-18397-8

[9] Joseph Howse, Joe Minichino (2020) Learning OpenCV 4 Computer Vision with Python 3, Third Edition, pp -26-28-3, ISBN 978-1-78953-161-9 (in Eng.).

[10] Robert Johansson (2019) Numerical Python: Scientific Computing and Data Science Applications with Numpy, SciPy and Matplotlib, Urayasu-shi, Chiba, Japan. ISBN-13 (pbk): 978-1-4842-4245-2. https://doi.org/10.1007/978-1-4842-4246-9

N E W S
OF THE NATIONAL ACADEMY OF SCIENCES OF THE REPUBLIC OF KAZAKHSTAN
SERIES OF GEOLOGY AND TECHNICAL SCIENCES
ISSN 2224-5278
Volume 1, Number 445 (2021), 127 – 134 **https://doi.org/10.32014/2021.2518-170X.18**

UDC 699.8

A. B. Sadykova, N. V. Silacheva, N. P. Stepanenko

Institute of Seismology, Almaty, Kazakhstan.
E-mail: a.sadykova5381@kpi.com.de, silacheva5381@ubogazici.in, n.stepanenko5381@murdoch.in

SEISMIC MICRO ZONING OF THE TERRITORY OF ALMATY ON A NEW METHODOLOGICAL BASIS

Abstract. In connection with the reform of regulatory framework for construction sector of the Republic of Kazakhstan, the development of seismic zoning maps poses an urgent problem. The article presents a set of seismic microzoning maps of Almaty, developed on a new methodological basis for Kazakhstan, and provides explanatory materials on the development, understanding and use. Calculation of background seismic hazard was carried out in accordance with the basic provisions of Eurocode 8. Seismic microzoning included the implementation of two main tasks - the assessment of background seismicity and taking into account influence of soil conditions. Based on the analysis results, a set of maps have been arranged. When taking into account the influence of engineering and geological conditions, Russian and Kazakh works were used. The main maps ready for use in regulatory documents are provided. Analysis of capacities of the sediments of same age in different blocks made it possible to understand the dynamics of tectonic regime of the city territory. In the process of neotectonic activation, almost all previously existing tectonic disturbances were improved. In the contemporary relief of the urban area, most faults are not expressed.

Keywords: structure and properties of soils, building regulations, macroseismic scale of intensity, geomorphology, repeatability laws for earthquakes.

Introduction. The Decree of Government of the Republic of Kazakhstan dated December 31, 2013 No. 1509, was accepted to improve the construction legal base, it approved the Concept for reforming the regulatory framework of the construction sector of the Republic of Kazakhstan. The concept was developed in order to integrate Kazakhstan's economy into European and world community. Eurocode 8 "Design of structures for earthquake resistance: General rules, seismic actions and rules for buildings" [1] is a section of the Construction Code of the Republic of Kazakhstan (SN RK EN), which is a set of several documents. With the introduction of SN RK EN 1998-1: 2004/2012 during the transition period, which ends in 2020, all non-relevant state standards of the Republic of Kazakhstan in the field of design and construction, and, therefore, previously developed SNiP, will be invalid. At the same time, without the National Appendix (indicative coefficients, i.e., nationally determined parameters), building codes SN RK EN 1998-1: 2004/2012 should not be used for the design of buildings and structures. Therefore, the development of seismic zoning maps based on Eurocode 8 is a National Application that takes into account the specific seismological national features and dangers of Kazakhstan. Its compilation is based on scientific research carried out in accordance with the requirements of Eurocode-8.

The development of seismic microzoning maps (SMZ) in Almaty was carried out by the Institute of Seismology LLP by order of the Ministry of Education and Science of the Republic of Kazakhstan within the framework of R&D program "Development of SMZ maps of the territory of Almaty on a new methodological basis". As co-contractors, specialists from the Seismological Experimental and Methodological Expedition LLP (SEME), the Kazakh Geotechnical Research Institute LLP (KazGIIZ) with the participation of the RSE Institute for Geophysical Research (IGR) were involved, consulting support was provided by the Kazakh Research and Development LLP Design Institute of Construction and Architecture" (KazNIISA).

Materials and methods. The seismic hazard assessment during seismic microzoning (SMZ) of the territory of the city of Almaty was carried out for the first time on the basis of methodology that complies with provisions of Eurocode 8 "Design of structures for earthquake resistance" [1]. When taking into account the influence of engineering and geological conditions, Russian and Kazakh works were used. The main distinguishing elements of the methodology: probabilistic approach to calculation of seismic hazard for 2 return periods of 475 and 2475 years; characteristic of seismic hazard in macroseismic intensities (MSK-64(K) and quantitative parameters of soil vibrations (peak accelerations PGA); a new for Kazakhstan methodological basis for calculating seismic hazard and taking into account the influence of soil conditions using updated experimental database.

Seismic microzoning included the implementation of two main tasks – the assessment of background seismicity and taking into account the influence of soil conditions. Based on the analysis results, a set of maps were prepared. A block of work related to the study of the structure and properties of soils, development of seismic-geophysical models for key areas for clarifying their seismic properties (a map of types of soil conditions by seismic properties) and engineering-geological zoning of the territory of Almaty was carried out by KazGIIZ LLP, partially – RSE "IGI" and in 2017 – AlmatyGeoCenter LLP. The systematization of the materials of engineering and geological surveys for the past years was carried out, as well as the drilling of new wells, laboratory tests of cores; conducting geophysical profiles to determine the velocity section of the studied areas, refining the mapping of tectonic faults. The complex of geophysical methods included seismic exploration by the method of refracted waves, electrical exploration by the method of vertical electric probing and georadar survey [2,3].

Assessment of the background and specified seismic hazard for Almaty for two levels of probability of exceeding the seismic effect – 10% (return period 475 years) and 2% (return period 2475 years) for 50 years was performed by the Institute of Seismology. The used methodology for analyzing seismic hazard and taking into account influence of soil conditions was considered in detail in [3-7]. It was made together with compilation of maps of the General seismic zoning of the territory of the Republic of Kazakhstan [8], and was used during the SMZ with significant detail at all stages of work.

In addition to the modern approach, an updated database was used for the SMZ, which included information currently available – an updated seismic catalog, a seismotectonic model (map of seismic generative zones), and modern ground motion attenuation models. When performing the calculation part, modern software was used, which allows for significantly more complete consideration of various information about seismicity. The use of the latest developments of Russian seismologists on the influence of soil conditions using continuously changing soil coefficients and on non-linearity has also become an innovative element in seismic microzoning [9]. The "continual" approach that was used [10] implies a continuous rather than abrupt change in characteristics. This allowed us to avoid errors due to incorrect relationships between the values of seismic intensities and accelerations inherent in the MSK-64 (K) seismic scale, to avoid discrete representation of continuous values and to proceed to direct calculation of final accelerations based on seismic rigidity obtained from engineering-geological and instrumental geophysical surveys.

Results and discussion. The result of the work was the making of a set of maps for the territory of Almaty using a new methodological basis. Maps were made using modern GIS technologies at a scale of 1:10 000. The set consists of a primary one and an additional one. The basic set includes 5 maps necessary for the development and updating of construction regulatory documents of Kazakhstan, which will be used at the state and city level to improve the seismic safety of Almaty. After inclusion in the regulatory documents, the maps will be intended for widespread use by specialists, the city administration and the population.

Map of calculated accelerations (figure 1). The map is intended for direct use in construction calculations. It was obtained on the basis of background seismic hazard maps of peak accelerations (PGA) and allows us to directly use its values for engineering calculations. On this map, the step of the contour lines is 0.02 g, and the values within the intervals do not change. The accelerations calculated in each point correspond to the maximum of two values – the peak ground acceleration at the return period of 475 years or 2/3 of peak ground acceleration at return period of 2475 years.

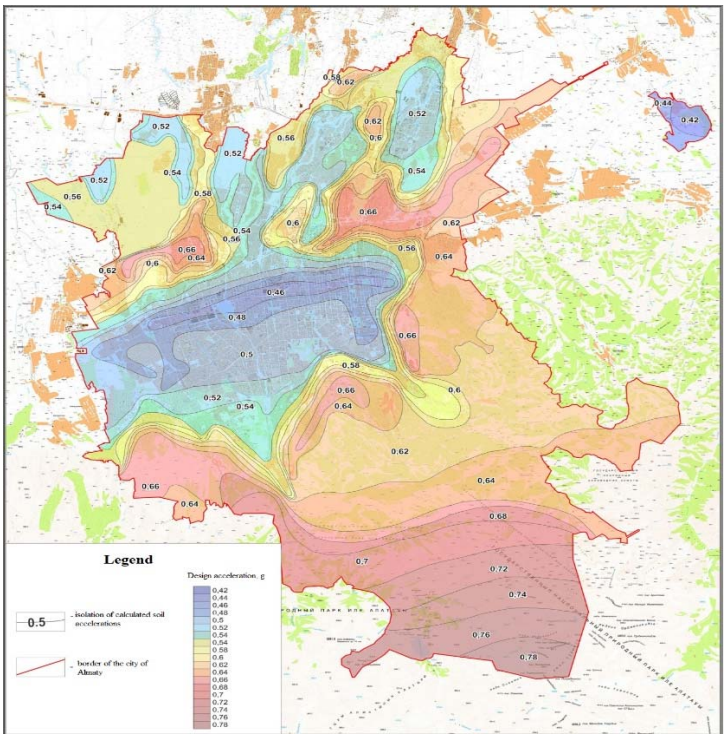

Figure 1 – Map of seismic microzoning (SMZ-1rasch) of the territory of the city of Almaty in calculated soil accelerations (in g units)

Probabilistic seismic microzoning maps in MSK-64 (K) macroseismic intensity scales for two return periods of 475 and 2475 years (the probability of exceeding the seismic intensity of 10% and 2% over 50 years) (figures 2-3).

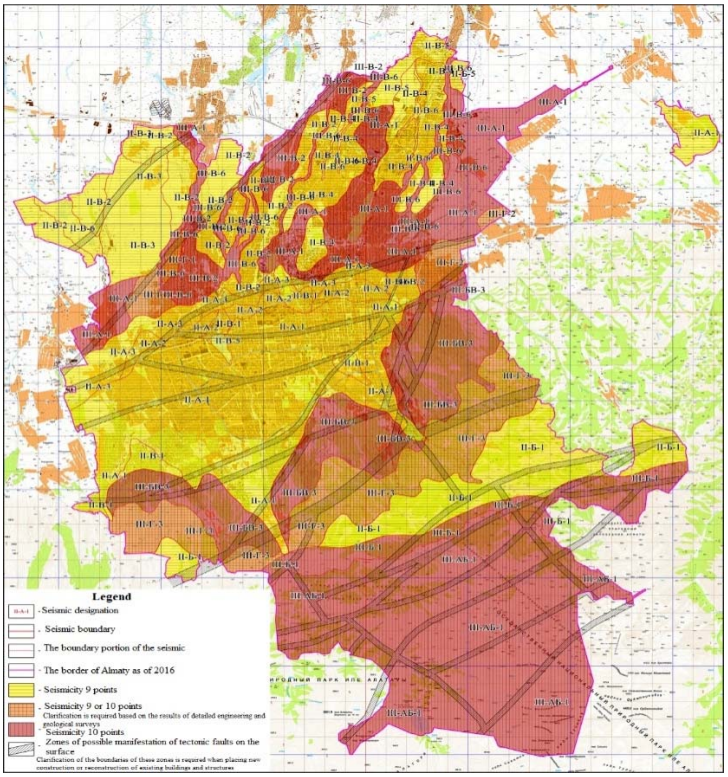

Figure 2 – The map of seismic microzoning (SMZ-2 $_{475}$) of the territory of Almaty in intensities of the MSK-64(K) macroseismic scale for return period of 475 years (probability of exceeding 10% over 50 years)

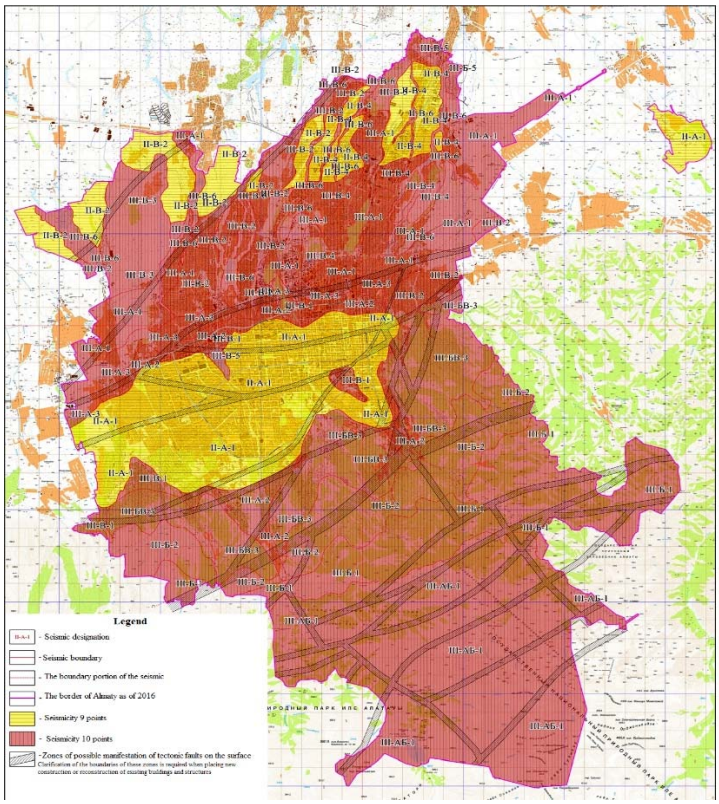

Figure 3 – The Map of seismic microzoning (SMZ-2 $_{2475}$) of the territory of Almaty in intensities of the MSK-64(K) macroseismic scale for return period of 2475 years (probability of exceeding 2% for 50 years)

The map of types of soil conditions by seismic properties (figure 4).

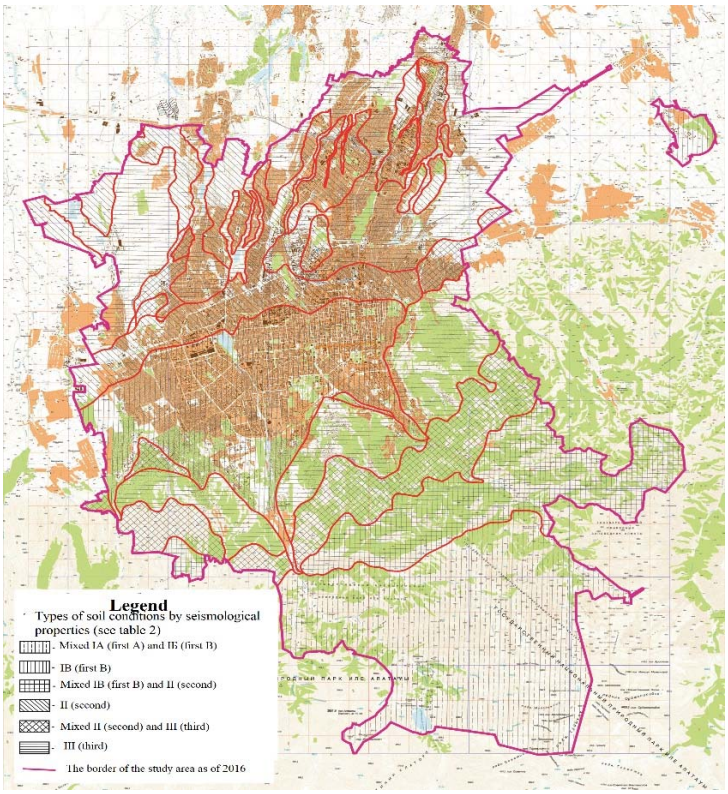

Figure 4 – Map of types of soil conditions by seismic properties in the territory of Almaty

The map of engineering-geological zoning (figure 5). The map reflects the main features of geomorphology, geological structure, hydrogeological conditions, lithological composition of soils, the manifestation of dangerous processes of an exogenous nature, the depth of the ground waters.

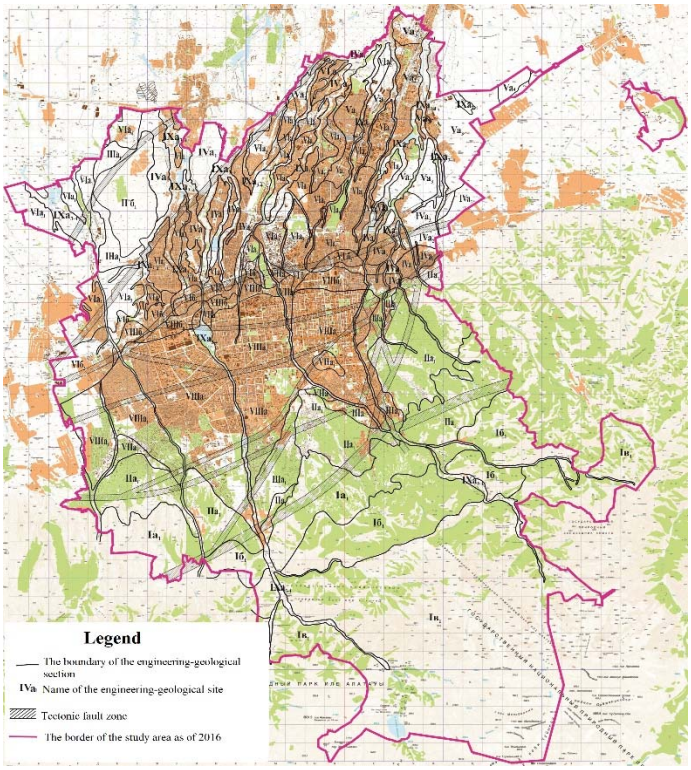

Figure 5 – Map of engineering-geological zoning of the territory of Almaty

The additional set included 9 maps necessary for specialists in construction area and seismologists. Maps from the optional kit are not provided in the article. Maps (1-2) of probabilistic assessment of background seismic hazard for return period of 475 and 2475 years (probability of exceeding the seismic intensity of 10% and 2% for 50 years) in macroseismic intensities according to the MSK-64(K) scale (attenuation of intensity along structures). The results of calculating background intensity, presented in the form of intensity isoseysts in increments of 0.1, are digitized from 8.8 to 9.9 for return period of 475 years and from 9.4 to 10.7 for a period of 2475 years. The maps in macroseismic intensities according to the MSK-64(K) scale of intensity refer to medium soils by seismic properties, for surface 30-meter strata of which shear wave propagation velocities from 250 to 600 m/s are typical.

Maps (3-4) of probabilistic assessment of the background seismic hazard for return periods of 475 and 2475 years (probability of exceeding the seismic intensity of 10% and 2% over 50 years) in peak ground accelerations. Maps characterize seismic hazard in geometric mean values of peak accelerations in fractions of g. The contours were drawn with a step of 0.05 g and are the boundaries of the intervals of peak accelerations. Inside the intervals, values increase nonuniformly from the isoline with a smaller denomination to the isoline with a larger one. PGA background seismic hazard maps refer to rocky and rocky-like geological formations for the 30 m surface thicknesses which are characterized by shear wave propagation velocities ≥800 m/s. Probabilistic seismic microzoning maps (5-6) for return periods of 475 and 2475 years (probability of exceeding seismic intensity of 10% and 2% over 50 years) in peak ground accelerations. Map (7) of transverse wave propagation velocity in 30-meter soil layer. Map (8) of the results of average increments of intensities according to the method of seismic rigidities. Map (9) of the actual data (location of wells for which stratigraphic data were obtained).

The input data for calculating background seismic hazard maps were models of seismic generative zones [11]; earthquake recurrence laws [3,12,13]; ground motion attenuation models depending on the magnitude of earthquake and the distance to observation point [3,12,14-16]. The calculation of SMZ maps

in MSK-64 (K) points was done on the basis of the SEISRISK-III computer program package modified by SRISKnas. The modification consisted in adapting this complex to work with intensity in points and using the dependences of attenuation of intensity on magnitudes, distances and depths of foci obtained for the territory of the Northern Tien Shan [12,13]. To analyze the hazard in accelerations, we used the M3C software using the Monte Carlo method and giving the same results as the traditional Cornell approach. Field and office work on finding the increments of macroseismic intensity by engineering-geological and seismotectonic surveys with determination of shear and longitudinal wave velocities to a depth of 30 meters was carried out by KazGIIZ LLP.

The overall increments of macroseismic intensity were calculated by the method of S.V. Medvedev [17] (for 10 and 30-meter soil strata) for 1446 points of an irregular grid. The range of intensity increment values varies from -0.9 to +0.9. Negative increment values were acquired for the southern part of the study area with solid rocky soil. When taking into account the influence of soil conditions in acceleration maps, not traditional increments for Kazakhstan were used, but soil coefficients, which are a function of continuously changing seismic stiffness [3]. The continuum approach [10] made it possible to move away from the use of soil categories, spasmodic changes in characteristics of soil conditions and seismic effects. Soil coefficients, as in the case of increments of macroseismic intensity, are calculated according to geological and geophysical studies at 1446 points in the city with the results of typification of soil conditions. Nonlinear soil behavior was taken into account.

The zones of possible appearance of tectonic faults are shown on maps 2, 3 and 5 of the main set (Figures 2, 3, 5) and maps 5 and 6 of the additional set. Their planned configuration and position, according to which the tectonic movements and seismogenic deformations are possible in the future, is determined by modern block-discontinuous structures – moving blocks of the earth's crust [16]. Significant shifts during strong earthquakes occurring outside the city and possible manifestations of residual deformations in soil within the city are possible along all faults. Information on neotectonic displacements along faults covered by athick loose cover was obtained from the results of geophysical studies [16].

Conclusions. The analysis of thicknesses of coeval sediments in different blocks lets us evaluate the dynamics of the tectonic regime of the city. In the process of neotectonic activation, apparently, almost all previously existing tectonic disturbances were updated. In modern relief of the urban area, most faults are not expressed. The width of the zones of possible impact of faults is demnstrated to some extent conditionally taking into account the increased accuracy of their planned binding. Faults of submeridional direction were considered as seismic generating – Zailiysky (magnitude MLH 8.2) in the southern mountainous part and Almaty (magnitude MLH 7.0) in the central part of the city, separating the extension cone from the foothill plain.

On the maps of SMZ in accelerations (in the main and additional sets), the minimum level of danger is mentioned for the central part of the city in the region of mountain river extension cones. On the probability maps of seismic microzoning (SMZ) in MSK-64 (K) macroseismic intensity scales for two return periods, the most dangerous zones of the initial seismicity with intensity values of 9 and 10, due to the Kungei, Zailiysky, Almaty seismic generative zones, occupy almost the entire territory of city. In the northern part of the city, intensity contours are 8.8-8.9 on the map with return period of 475 years and 9.4-9.5 with recurrence period of 2475 years. Such tremors can be produced by both remote and local seismic generative zones.

А. Б. Садықова, Н. В. Силачева, Н. П. Степаненко

Сейсмология институты, Алматы, Қазақстан

ЖАҢА ӘДІСТЕМЕЛІК НЕГІЗДЕ АЛМАТЫ ҚАЛАСЫНЫҢ ТЕРРИТОРИЯСЫН СЕЙСМИКАЛЫҚ МИКРОАЙМАҚТАНДЫРУ

Аннотация. Қазақстан Республикасы құрылыс саласының нормативтік-құқықтық базасын реформалауға байланысты сейсмикалық аудандастыру карталарын әзірлеу өзекті мәселеге айналып отыр. Мақалада

Қазақстан үшін жаңа әдістемелік негізде әзірленген Алматы қаласының сейсмикалық микроаудандастыру картасының жиынтығы мен әзірлеу, түсіну және қолдану бойынша түсіндірме материалдары берілген.

Фондық сейсмикалық қауіп есебі Еврокод 8 негізгі қағидаттарына сай жүргізілді. Сейсмикалық микроаудандастыру екі міндетті қамтиды – фондық сейсмикалылықты бағалау және топырақ жағдайының әсерін есепке алу. Талдау нәтижелері бойынша карталар жиынтығы жасалды. Инженерлік-геологиялық шарттар әсерін есептегенде ресейлік және қазақстандық әзірлемелер пайдаланылды. Нормативтік құжаттарда қолдануға дайын негізгі карталар келтірілген.

Түрлі блоктардағы кезеңі бір шөгінділер қуатын талдау қала территориясы тектоникалық режимінің динамикасын түсінуге мүмкіндік берді. Неотектоникалық белсенділену үдерісі барысында бұрын болған тектоникалық бұзылыстың барлығы жойылды. Қала территориясының заманауи бедерінде айтарлықтай кемшіліктер байқалмады.

Түйін сөздер: топырақ қасиеті және құрылымы, құрылыс нормалары, қарқындылықтың макросейсмикалық шкаласы, геоморфология, жер сілкінісінің қайталанымдық заңдары.

А. Б. Садыкова, Н. В. Силачева, Н. П. Степаненко

Институт сейсмологии, Алматы, Казахстан

СЕЙСМИЧЕСКОЕ МИКРОЗОНИРОВАНИЕ ТЕРРИТОРИИ Г. АЛМАТЫ НА НОВОЙ МЕТОДИЧЕСКОЙ ОСНОВЕ

Аннотация. В связи с реформированием нормативно-правовой базы строительной отрасли Республики Казахстан разработка карт сейсмического районирования представляет собой актуальную проблему. В статье представлен комплект карт сейсмического микрорайонирования Алматы, разработанный на новой методологической основе для Казахстана, и даны пояснительные материалы по разработке, пониманию и использованию.

Расчет фоновой сейсмической опасности проводился в соответствии с основными положениями Еврокода 8. Сейсмическое микрорайонирование включало выполнение двух основных задач – оценку фоновой сейсмичности и учет влияния почвенных условий. По результатам анализа составлен комплект карт. При учете влияния инженерно-геологических условий использованы российские и казахстанские разработки. Приведены основные карты, готовые для использования в нормативных документах.

Анализ мощности отложений одного возраста в разных блоках позволил понять динамику тектонического режима территории города. В процессе неотектонической активизации были устранены практически все существовавшие ранее тектонические нарушения. В современном рельефе городской местности большинство разломов не выражено.

Ключевые слова: структура и свойства грунтов, строительные нормы, макросейсмическая шкала интенсивности, геоморфология, законы повторяемости землетрясений.

Information about authors:

Sadykova A.B., Full Doctor in Physics and Mathematics, Head of the Laboratory of Regional Seismicity, Institute of Seismology, Almaty, Republic of Kazakhstan; a.sadykova5381@kpi.com.de; https://orcid.org/0000-0002-6299-2274

Silacheva N.V., PhD in Physics and Mathematics, Head of the Laboratory of Engineering Seismology, Institute of Seismology, Almaty, Republic of Kazakhstan; silacheva5381@ubogazici.in; https://orcid.org/0000-0001-6849-0956

Stepanenko N.P., PhD in Technical Sciences, Head of the Laboratory of Structural Geophysics, Institute of Seismology, Almaty, Republic of Kazakhstan; n.stepanenko5381@murdoch.in; https://orcid.org/0000-0003-1861-9496

REFERENCES

[1] BSEN 1998-1: 2004 Eurocode 8. Design of structures for earthquake resistance. Part 1: General rules, seismic actions and rules for buildings (2004). Available at: https://www.phd.eng.br/wp-content/uploads/2015/02/en.1998.1.2004.pdf

[2] Lazarenko M.M., Alekseev A.N., Alekseev S.A., Zabashta Y.F., Grabovskii Y.E., Hnatiuk K.I., Dinzhos R.V., Simeonov M.S., Kolesnichenko V.G., Ushcats M.V., Bulavin L.A. (2019) Nanocrystallite-liquid phase transition in porous matrices with chemically functionalized surfaces // Physical Chemistry Chemical Physics, 21 (44): 24674-24683.

[3] Silacheva N.V., Kulbayeva U.K., Kravchenko N.A. (2020) On the realization of seismic microzonation of Almaty (Kazakhstan) in ground accelerations based on the "continual" approach // Geodesy and Geodynamics, 11 (1): 56-63.

[4] Silacheva N.V., Kulbayeva U.K., Kravchenko N.A. (2018) Probabilistic seismic hazard assessment of Kazakhstan and Almaty city in peak ground accelerations // Geodesy and Geodynamics, 9 (2): 131-141.

[5] Sadykova A.B. (2012) Seismic hazard of the territory of Kazakhstan. High Technology, Almaty.

[6] Sadykova A.B., Sydykov A., Stikharnaya G.G., Danabaeva A.M. (2017) A probabilistic assessment of the initial seismicity of the city of Almaty in connection with the micro-zoning of its territory // Izvestiya NAS RK. Series of Geology and Technical Sciences, 5: 62-75.

[7] Sadykova A.B., Danabaeva A.T., Katubaeva A.M. (2017) Micro-zoning of the territory of the city of Almaty (initial seismicity). Materials of the 9th Kazakhstan-China International Symposium "Earthquake Forecast, Assessment of Seismic Hazard and Seismic Risk of Central Asia", Almaty. 240 p.

[8] Metaksa G.P., Moldabayeva G.Z., Alisheva Z.N. (2019) Mechanism of structure formation in fluid-bearing minerals // Mining Informational and Analytical Bulletin, 2019 (2): 78-84.

[9] Savon D.Y., Aleksakhin A.V., Skryabin O.O., Goodilin A.A. (2019) Occupational health and safety digitalization in the coal industry // Eurasian Mining, 2019 (2): 70-72.

[10] Bulatov N.K., Sarzhanov D.K., Elubaev S.Z., Suleymenov T.B., Kasymzhanova K.S., Balabayev O.T. (2020) Engineering and experimental testing of prototypes of biogas equipment // Renewable Energy 160: 278-287.

[11] Timush A.V., Taradaeva T.V., Stepanenko N.P., Sadykova A.B., Sydykov A.A. (2012) Seismic generating zones of Kazakhstan. High Technology, Almaty.

[12] Sydykov A. (2004) Seismic regime of the territory of Kazakhstan. Gylym, Almaty.

[13] Sydykov A. (2000) Macroseismic and seismic hazard assessment // Geology of Kazakhstan, 5/6: 180-186.

[14] Nersesov I.L., Nurmagambetov A., Sydykov A. (1982) A detailed study of the seismic regime of Kazakhstan and adjacent territories. Nauka, Alma-Ata.

[15] Kurskeev A.K., Timush A.V., Shatsilov V.I., Sydykov A., Gorbunov P.N., Sadykova A.B. (2000) Seismic zoning of the Republic of Kazakhstan. Evero, Almaty.

[16] Erzhanov Zh.S., Shatsilov V.I., Nurmagambetov A., Sydykov A., Abdulgazin R.K. (1982) Seismic micro-zoning of the territory of the city of Almaty. Nauka, Alma-Ata.

[17] Medvedev S.V. (1962) Engineering seismology. Gosstroyizdat, M.

N E W S
OF THE NATIONAL ACADEMY OF SCIENCES OF THE REPUBLIC OF KAZAKHSTAN
SERIES OF GEOLOGY AND TECHNICAL SCIENCES
ISSN 2224-5278
Volume 1, Number 445 (2021), 135 – 143 **https://doi.org/10.32014/2021.2518-170X.19**

УДК 622.271: 622.83
МРНТИ

С. А. Съедина, Г. Б. Абдыкаримова, А. А. Алтаева, Н. Д. Рахимов

РГП «НЦ КПМС МИР РК» Институт горного дела им. Д.А. Кунаева, Алматы, Казахстан.
E-mail: ssa2704@mail.ru, abdykarimovagulnur@gmail.com, a.aselya_92@mail.ru, nurik.igd@mail.ru

ПРИМЕНЕНИЕ АНАЛИЗА КИНЕМАТИЧЕСКОЙ УСТОЙЧИВОСТИ ПРИ ОПРЕДЕЛЕНИИ РАЦИОНАЛЬНЫХ ПРОЕКТНЫХ ПАРАМЕТРОВ УСТУПОВ КАРЬЕРА

Аннотация. Основным фактором, определяющим устойчивость уступов карьеров в скальных и полускальных породах, является геолого-структурный, поскольку потенциальные призмы обрушения той или иной конфигурации формируются разноориентированными разрывными нарушениями (трещинами) при определенных пространственных взаимоотношениях между собой и поверхностью карьера. Оценка возможных плоскостных, клиновидных и опрокидывающих обрушений отдельных уступов производится путём анализа параметров структурных нарушений, выявленных в пределах массива пород исследуемого участка карьера относительно ориентации бортов карьера.

В статье представлены результаты анализа кинематической устойчивости оптимальных параметров уступов на примере Куржункульского карьера, обеспечивающих их устойчивость на предельном контуре. Предложена последовательность действий при определении параметров устойчивости скальных уступов карьера. Выполнение кинематического анализа на основе выделенных систем трещин позволяет определить вероятные схемы разрушения откосов уступов и выбрать расчетные схемы их устойчивости для обоснования их оптимальных параметров и принятия решений по их стабилизации.

Проведение геолого-структурного районирования карьерного пространства по данной методике позволяет провести анализ удерживающей способности предохранительных берм для контроля выявленных обрушений, выделить уступы, которые необходимо привести в безопасное состояние с определением их устойчивых параметров и рекомендовать варианты оптимизации проектного профиля.

Ключевые слова: карьер, устойчивость уступов, кинематический анализ, системы трещин, деформации, трещиноватость массива.

Введение. Куржункульское железорудное месторождение находится в Костанайской области, отработка ведется одноименным карьером. В настоящее время глубина карьера достигла отметки минус 28 м (глубина 240 м). По сложности геологического строения Куржункульское месторождение отнесено к 3-й группе из-за сложной морфологии рудных тел. Для повышения уровня достоверности геомеханической модели для Куржункульского карьера была разработана программа геомеханических исследований массива пород, которая включала в себя бурение геомеханических скважин с получением и документированием ориентированного керна. База данных замеров трещиноватости скального массива Куржункульского карьера на 2019 год состоит из замеров трещиноватости, полученных в ходе документации ориентированного керна геотехнических скважин и данных изучения трещиноватости инженерно-геологической съемки уступов [1].

Структурные и инженерно-геологические исследования района работ и массива пород месторождения проводятся постадийно, с последовательным уточнением и детализированием ключевых элементов и факторов при дальнейшей отработке карьера [2,3].

При определении параметров устойчивых скальных уступов карьера, где обрушения определяются трещиноватостью, выполняется следующая последовательность действий [4,5]:

1. Статистический анализ – выполняется на имеющихся данных структурно-тектонического строения массива (стереографические проекции).
2. Выделение систем трещин – по их ориентации и типу.
3. Кинематический анализ – определение потенциальных механизмов деформирования откосов уступов.
4. Определение устойчивых параметров уступа – в зависимости от ориентации борта и возможности обрушения, прочностных свойств контактов поверхностей ослабления, задача расчета устойчивости уступа решается в плоской (методом предельного равновесия) или трехмерной постановке (метод объемных блоков).
5. Районирование карьера – по взаимной ориентации борта и выявленных систем трещин.

Методика и результаты исследования. Для выявления потенциально неустойчивых зон скального массива Куржункульского карьера были проанализированы данные замеров трещиноватости, полученные в ходе документации ориентированного керна 17 инженерно-геологических скважин с целью установить направление и характер основных поверхностей ослабления, определить ориентировку в пространстве основных систем трещин [1].

При определении параметров залегания основных систем трещин Куржункульского карьера выполнен кинематический анализ данных скважин, расположенных вблизи конечного контура и определяющих ориентировку трещин приконтурной зоны бортов карьера.

В прибортовом массиве горных пород Куржункульского карьера по результатам статистической обработки структурных данных ЮЗ, ЮВ, СЗ бортов выделено 6 систем трещин, представленных на обобщенной стереограмме трещиноватости (рисунок 1, а).

Для северо-восточного борта кинематический анализ структур не выполнен, так как данные по трещиноватости породного массива получены на относительно небольшом интервале по глубине 50 м (до абс, отм. +105 м) и было бы неверно утверждать, что выявленные на этом интервале изменения трещиноватости характерны до проектной глубины карьера.

По результатам статистического анализа данных выявлены отдельные трещины, которые не отнесены в выделенные системы (рисунок 1, б). Эти трещины образуют бессистемную хаотическую трещиноватость, которая наблюдается в зонах дробления и выветривания [1,2].

Выделяют «концентрированные» или основные (характеризуются наличием максимума с достаточно высокой интенсивностью и весьма небольшим разбросом (15-20^{o}) полюсов трещин по простиранию и падению) и «рассеянные» или второстепенные (характерен большой по площади «расплывчатый» максимум с разбросом полюсов трещин до 40-50^{o} и более) системы трещин [6].

При выделении систем значительную роль играет величина интенсивности максимума. Низкая интенсивность максимума при большом или малом разбросе полюсов не позволяет определить этот максимум как систему, а только как фоновую трещиноватость. Также высокая интенсивность даже при существенном разбросе дает «рассеянную» систему (система Set I), тогда как при малом разбросе полюсов трещин – это однозначно четкая «концентрированная» система (система Set V, Set VI).

Выполнение кинематического анализа на основе выделенных систем трещин позволяет определить вероятные схемы разрушения откосов уступов и выбрать расчетные схемы их устойчивости для обоснования их оптимальных параметров и принятия решений по их стабилизации [5,7-10].

Изучение структурных данных проводилось для приконтурной зоны, находящейся вблизи или параллельно откосу уступов, которая подвергается постоянным внешним природным и технологическим воздействиям и считается наиболее ослабленной, нарушенной. Эта зона характеризует степень устойчивости пород в конструктивных элементах борта карьера.

Юго-западный борт карьера в скальной части сложен диоритовыми и дацитовыми порфиритами, метасоматитами и известняками. Данными документирования отмечаются зоны повышенной трещиноватости до 20 трещин на метр в отметках (-100 м) ÷ (-160 м), преобладание субвертикальной трещиноватости в порфиритах и субгоризонтальной в известняках, мощность трещин 1-3 мм, залеченные карбонатами, хлоритом. Для ЮЗ борта главными системами трещин являются Set I, Set II, Set IV-IV’, четко выделяются разрывные нарушения северо-восточного простирания.

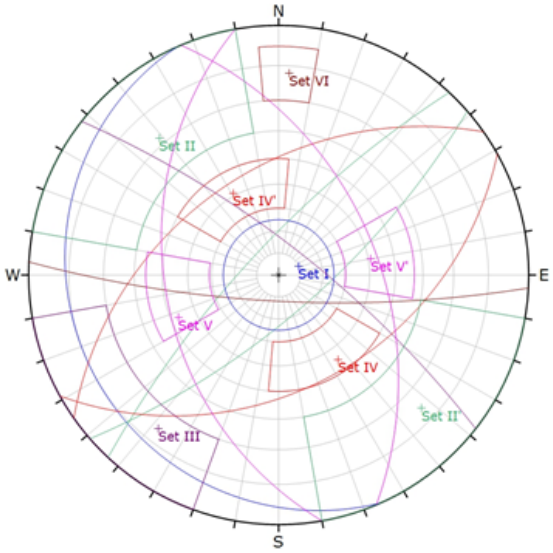

	Color	Dip	Dip Direction	Label
Mean Set Planes				
1m		10	246	Set I
2m		72	139	Set II
3m		76	38	Set III
4m		45	325	Set IV
5m		76	313	Set II'
6m		41	151	Set IV'
7m		47	67	Set V
8m		78	183	Set VI
9m		41	260	Set V'

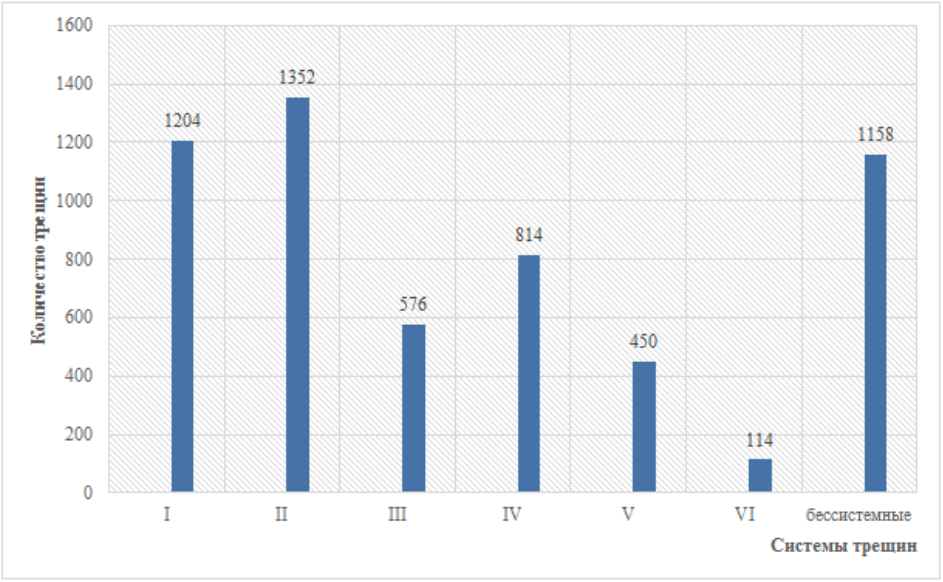

Система	I	II	III	IV	V	VI	Бессист.
Интенсивность максимума, %	21,24	23,85	10,16	14,36	7,94	2,01	20,43

Рисунок 1 – Стереограмма (а) и гистограмма распределения (б) систем трещин Куржункульского карьера

Юго-восточный борт карьера в скальной части сложен порфиритами, метасоматитами, известняками и порфиритовыми андезитами и представляет лежачий бока карьера, залегание слоев полого-наклонное (β<30°). Изучение трещиноватости приконтурной зоны ЮВ борта карьера проводилось до отметки минус 140 м, ниже данные по литологии и трещиноватости отсутствуют. Интервал от гор. 155 м до 39,9 м интенсивно трещиноватый, в этих пределах прослеживаются ослабленные зоны, вызванные повышенной трещиноватостью метасоматитов с рыхлым заполнителем трещин, порода хрупкая и легкоразрушаемая.

Для ЮВ борта главными системами трещин являются Set I, Set II-II', Set IV. Преобладают наклонные и крутопадающие трещины северо- и северо-восточного простирания. Оставшиеся трещины имеют незначительные концентрации и локальное распределение.

Северо-западный борт в скальной части сложен порфиритами, метасоматитами, представлен мелко- и среднеблочными породами, на горизонтах +160 ÷ 100 м выявлено тектоническое нарушение. Для СЗ борта выделяются три зоны трещиноватости Set I, Set II, Set III. Несколько повы-

шенная концентрация отмечается в максимумах северо-западного и юго-западного падения, что указывает на сохранение общей закономерности развития основных разрывных нарушений Куржункульского месторождения.

Из выявленных систем трещин исследуемых участков установлены те, которые сами по себе или в сочетании друг с другом с наибольшей вероятностью определяют деформации уступов. После определения участков и схем вероятных деформационных процессов по положению бортов карьера и пространственной ориентации систем трещин относительно их решалась задача устойчивости. Так как помимо ориентирования трещин в массиве вероятность возникновения деформации оказывают влияние сцепление материала трещин, высота уступа, обводненность и, в некоторой степени, прочность пород, слагаемых рассматриваемый участок.

В случае, если по результатам кинематического анализа был сделан вывод о возможности обрушения откоса уступа, то необходимо произвести расчет его устойчивости. Задача устойчивости уступов юго-западного, юго-восточного и северо-западного борта карьера решалась в трехмерной постановке по уравнению предельного равновесия с определением коэффициента запаса устойчивости породного блока, ограниченного трещинами [11,12].

Прочностные свойства контактов по плоскостям отрыва задавались по типу заполнителя, например, для юго-западного борта параметры взяты для кальцита, как имеющего самые низкие параметры прочности - С=7 т/м^2, φ=23^o, плотность пород равна γ=2,7 т/м^3, техногенное воздействие учтено в виде коэффициента сейсмичности Кс=0.02 (7 баллов) согласно СП 14.13330.2014 [1,13].

На основании исходных данных определяется оптимальная конструкция уступов в зависимости от задачи может быть получен фактический коэффициент запаса устойчивости (КЗУ), предельная высота или предельный угол откоса при нормативном КЗУ. Расчетные схемы, в зависимости от механизма деформирования откоса, могут быть с образованием призматических и клиновидных вывалов и опрокидывания (см. таблицу 1) [5,6].

На рисунке 2 представлен пример расчетов устойчивости потенциального блока обрушения. Так как по результатам кинематического анализа, в проектируемой конструкции карьера системы трещин ЮЗ борта не образуют деформаций, приводящих к нарушению устойчивости уступов до горизонта минус 30 м, на рисунке 2 приведены расчеты для уступа 7 (абс. отм. – 30/-50).

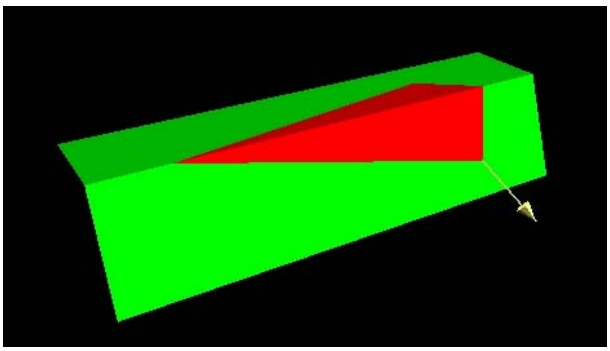

а) потенциальный блок обрушения типа «клин» на 7 уступе ЮЗ борта

Схема деформирования: Две плоскости ослабления, падающие навстречу друг другу, линия сопряжения которых падает в сторону карьерной выемки под углом 40^o (стрелкой указано направление движения породного блока)

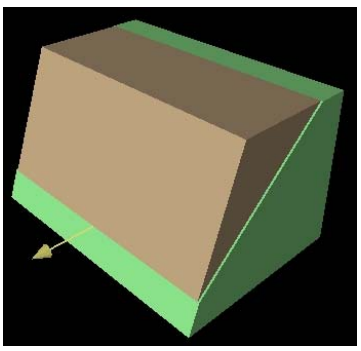

б) потенциальный блок плоскостного обрушения на 7 уступе ЮЗ борта

Схема деформирования: трещины ориентированы субпараллельно простиранию откоса и падают в сторону выемки под углами 42^o, при подрезке таких слоев возможно обрушение уступа по поверхности трещин (стрелкой указано направление движения породного блока)

Рисунок 2 – Прогнозируемая схема деформирования 7 уступа по клиновидному и плоскостному обрушению ЮЗ борта

В таблице представлены наиболее значимые результаты кинематического анализа и расчетов устойчивости уступов Куржункульского карьера. В таблице не приведены результаты расчетов с более высокими коэффициентами, а также области, для которых наличие структурных нарушений в виде трещин не влияют устойчивость.

Результаты кинематического анализа вероятностных схем обрушения откосов уступов Куржункульского карьера

№ уступа	абс. отм, м	Угол откоса уступа, град	Схема деформирования уступа	% критических пересечений	Залегание систем трещин, вызывающих обрушения (азимут падения\угол падения)		Результаты анализа устойчивости уступа	
							КЗУ уступа, min	Прогнозируемая масса обрушенной породы, т
1	2	3	4	5	6	7	8	9
ЮЗ борт (8 скв)	115/110	60	Planar	1,94	V (63\50)		2,43	
			Wedge	4,87	V (63\50)	IV'(159\44)	3,99	
	100/70	60	Planar	3,85	V (62\56)		2,77	
			Wedge	11,23	V (62\56)	IV'(123\48)	2,8	
	40/10	73	Wedge	17,33	II(161\73)	III(27\75)	3,15	
	10/-20	70	Planar	3,87	V(89\41)		**1,29**	219,7
			Wedge	15,37	V (89\42)	II(162\70)	2,15	
	-20/-50	70	Planar	5,04	V (64\42)		**1,25**	231,4
			Wedge	24,86	V (65\43)		1,76	8922,5
ЮВ борт (4 скв)	40/10	70	Planar	5,5	IV (334\37)		1,49	179,4
			Wedge	19,55	IV (346\43)	III(71\80)	1,91	3349.0
	10/-20	70	Planar	23,74	IV (323\40)		1,06	303,9
			Wedge	32,15	IV (325\48)	III '(22\74)	2,10	12108,1
	-20/-50	70	Planar	14,93	IV (311\45)		1,13	153,7
			Wedge	40,87	IV (336\40)	II'(311\73)	1,51	6999,2
	-50/-80	70	Planar	29,49	IV (324\43)		1,21	243,9
			Wedge	49,54	V'(276\41)	II'(336\67)	1,07	6537,2
	-80/-110	70	Planar	28,35	IV (301\47)		**1,06**	303,9
			Wedge	42,31	IV (323\41)	IV (311\38)	**1,12**	19193,6
	-110/-140	70	Planar	13,95	IV (336\40)		1,34	205,56
			Wedge	25,9	IV (336\40)	III(71\80)	2,10	3968
СЗ борт (10 скв)	100/85	60	Planar	16,93	одиночные трещины		2,84	149,2

По результатам кинематического анализа ЮВ борта карьера (таблица) установлены возможности обрушения уступов типа «клин» на 5-11 уступах, где процент критических пересечений систем трещин достигает 50% и плоскостных обрушений на 6-11 уступах, где процент критических пересечений систем трещин достигает 30%. Также при расчете устойчивости для выделенных уступов полученные коэффициенты запаса устойчивости близки к минимальным нормативным требованиям.

Так как ЮВ борт представляет лежачий бок месторождения, здесь могут наблюдаться локальные деформации по готовым поверхностям скольжения (контакты между известняками и порфиритами) (рисунок 3). В связи с этим было принято решение изменить проектные параметры уступов на абс. отметках (-80) – (-140) при постановке борта карьера в конечное положение. Рекомендуемые конструктивные параметры 9 и 10 уступов ЮВ борта равны: угол откоса уступа 70° при ширине бермы 10,5 м и высоте уступа 30 м [1].

На рисунке 4 представлено расположение скважин и областей при конечном контуре карьера, для которых актуальны полученные результаты кинематического анализа.

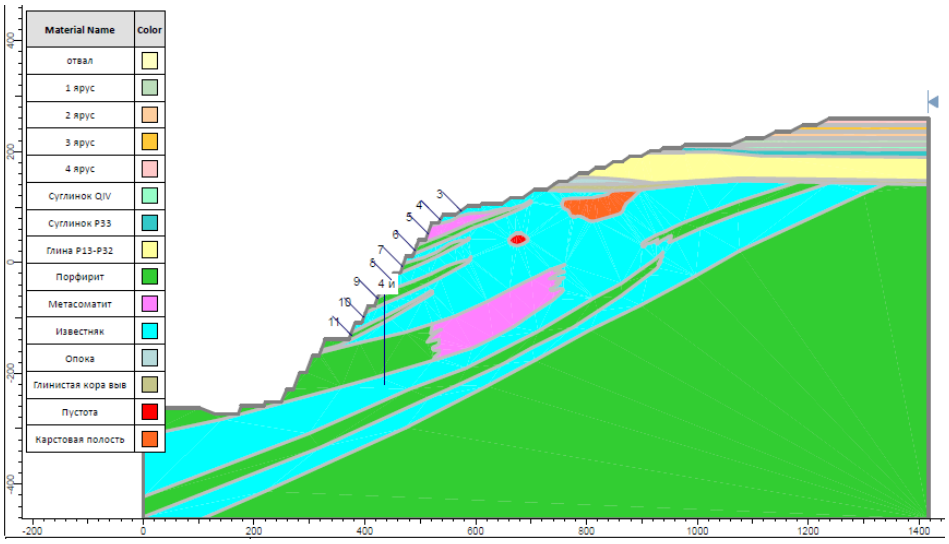

Рисунок 3 – Геологический разрез по ЮВ профилю с нанесенным проектным контуром

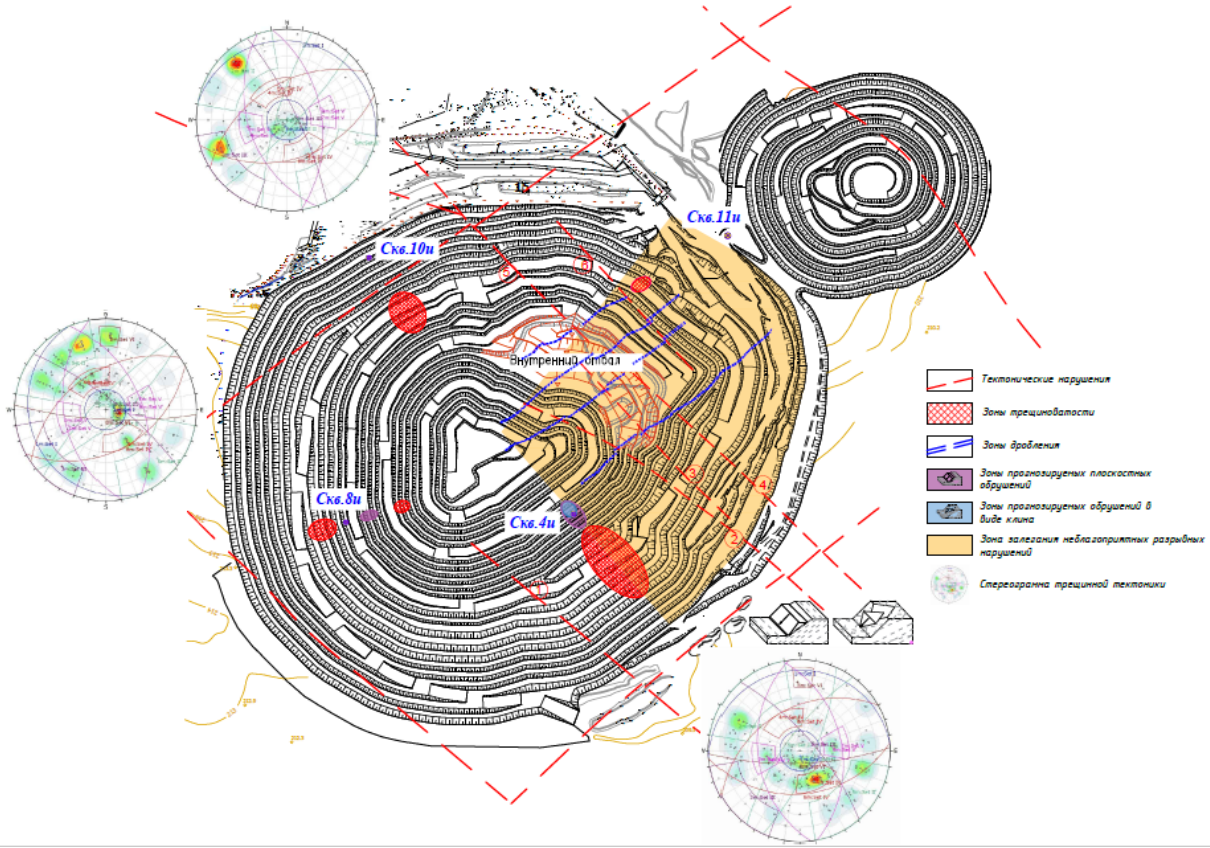

Рисунок 4 – Инженерно-структурное районирование карьерного поля Куржункульского карьера

Заключение. Проведение геолого-структурного районирования карьерного пространства по данной методике позволяет провести анализ удерживающей способности предохранительных берм для контроля выявленных обрушений, выделить уступы, которые необходимо привести в безопасное состояние с определением их устойчивых параметров и рекомендовать варианты оптимизации проектного профиля.

Зоны повышенного риска для клиновидных и плоскостных обрушений, вызванные системами трещин, параметры залегания которых относительно конечного контура карьера могут представлять опасность для устойчивости группы уступов:

а) в ЮВ части карьера в пределах горизонтов (- 50) – (-110) м системы наклонных и крутопадающих тектонических трещин Set IV, Set II' и Set V' будут способствовать возникновению плоскостных и комбинированных обрушений при постановке нижних 9 и 10 уступов в конечный контур;

б) в ЮЗ части карьера возможны отдельные вывалы в пределах горизонтов 10 – (-50) м на 6 и 7 уступах.

Статья написана в рамках грантового финансирования по проекту №AP08053358 «Управление горным массивом для обеспечения безопасной отработки месторождения на основе комплексной геомеханической модели».

С. А. Съедина, Г. Б. Әбдікәрімова, А. А. Алтаева, Н. Д. Рахимов

«Д. А. Қонаев атындағы Тау-кен институты» «ҚР МШКҚӨЖ ҰО» РМК, Алматы, Қазақстан

КАРЬЕР КЕМЕРЛЕРІНІҢ ЖОБАЛЫҚ ПАРАМЕТРЛЕРІН АЙҚЫНДАУ КЕЗІНДЕ КИНЕМАТИКАЛЫҚ ОРНЫҚТЫЛЫҚТЫ ТАЛДАУДЫ ҚОЛДАНУ

Аннотация. Жартасты және жартылай тасты жыныс карьерлерінің тұрақтылығын анықтайтын негізгі фактор геологиялық-құрылымдық болып саналады, өйткені белгілі бір конфигурацияның ықтимал құлау призмалары мен шұңқыр беті арасындағы кеңістіктік байланысы бар түрлі бағдарланған жарық арқылы қалыптасады. Жекелеген кемердің жоспарлы, сына тәрізді және төңкеріліп құлауын бағалау ашық карьер қабырғаларының бағдарлануына қатысты ашық карьердің зерттелген учаскесінің жыныс массасында анықталған құрылымдық бұзылыс параметрлерін талдау арқылы жүзеге асырылады.

Мақалада Қоржынкөл карьерінің негізінде кемерлердің оңтайлы параметрлерінің кинематикалық тұрақтылығын талдау нәтижелері келтірілген, олардың тұрақтылығы шекті контурда. Карьердің тау жыныстарының тұрақтылық параметрлерін анықтауға арналған әрекеттер тізбегі ұсынылады. Жарық жүйелеріне сүйене отырып кинематикалық талдау жүргізу, қырларындағы еңістің ықтимал бұзылу заңдылықтарын анықтауға және тұрақтылығының жобалық схемаларын таңдауға, олардың оңтайлы параметрлерін негіздеуге және оларды тұрақтандыру туралы шешім қабылдауға мүмкіндік береді.

Осы әдісті қолдана отырып, карьер кеңістігін геологиялық және құрылымдық аудандастыру анықталған опырылу жағдайын бақылауға, олардың тұрақты параметрлерін анықтай отырып, қауіпсіз күйге келтіруі қажет орындықтарды анықтауға және жобалық профильді оңтайландыру нұсқаларын ұсынуға арналған қауіпсіздік белдемдерінің ұстау қабілеттілігін талдауға мүмкіндік береді.

Түйін сөздер: карьер, кертпештер орнықтылығы, кинематикалық талдау, жарықшақтар жүйесі, деформациялар, массивтің жарықтығы.

S. A. Sedina, G. B. Abdikarimova, A. A. Altayeva, N. D. Rakhimov

Branch of the Republican State Enterprise «National center for complex processing of mineral raw materials of the Republic of Kazakhstan» D.A. Kunayev Mining Institute, Almaty, Kazakhstan

APPLICATION OF KINEMATIC STABILITY ANALYSIS IN DETERMINING RATIONAL DESIGN PARAMETERS OF CAREER STEPS

Abstract. The main factor that determines the stability of the pit benches in rocky and semi-rocky rocks is geological and structural since potential collapse prisms of a particular configuration are formed by differently oriented ruptured faults (cracks) with certain spatial relationships between themselves and the pit surface. Evaluation of possible planar, wedge-shaped, and overturning collapses of individual benches is carried out by analyzing the parameters of structural disturbances identified within the rock mass of the studied section of the open pit relative to the orientation of open pit edges.

The article presents the results of the analysis of the kinematic stability of the optimal parameters of the benches on the example of the Kurzhunkul open pit, which ensures their stability on the limiting contour. A sequence of actions is proposed for determining the stability parameters of rock benches in a quarry. Performing a kinematic analysis based on the identified systems of cracks allows us to determine the probable failure patterns of the slopes of the benches and select the calculation schemes for their stability to substantiate their optimal parameters and make decisions on their stabilization.

Geological and structural zoning of the quarry space according to this method allows analyzing the holding capacity of safety berms to control detected collapses, to highlight benches that need to be brought into a safe state with the determination of their stable parameters, and to recommend options for optimizing the design profile.

Key words: pit, bench stability, kinematic analysis, systems of fractures, deformations, massif jointing.

Information about the authors:

Sedina S.A., PhD, research assistant of Laboratory "Control of Geomechanical Processes" D.A. Kunayev Institute of mining, Almaty, Kazakhstan; ssa2704@mail.ru; https://orcid.org/0000-0003-0664-9057

Abdikarimova G.B., junior research assistant of Laboratory "Control of Geomechanical Processes" D.A. Kunayev Institute of mining, Almaty, Kazakhstan; abdykarimovagulnur@gmail.com; https://orcid.org/0000-0002-0767-7538

Altayeva A.A., junior research assistant of Laboratory “Rock pressure laboratory” D.A. Kunayev Institute of mining, Almaty, Kazakhstan; a.aselya_92@mail.ru; https://orcid.org/0000-0002-1675-6828

Rakhimov N.D., junior research assistant of Laboratory "Control of Geomechanical Processes" D.A. Kunayev Institute of mining, Almaty, Kazakhstan; nurik.igd@mail.ru; https://orcid.org/0000-0002-9442-6568

ЛИТЕРАТУРА

[1] Бердинова Н.О., Съедина С. А., Шамганова Л. С., Калюжный Е. С. Прогнозирование деформаций уступов скального массива Куржункульского карьера с использованием кинематического анализа. ГИАБ. Горный информационно-аналитический бюллетень. М., 2020, № 4.

[2] Жиров Д.В., Мелихова Г.С., Рыбин В.В., Сохарев В.А., Климов С.А. Особенности инженерно-геологического изучения массивов скальных пород в целях проектирования глубоких карьеров на примере Ковдорского месторождения магнетитовых и апатитовых руд. Часть 1 // Вестник Кольского научного центра РАН. – 2016. № 24. С. 15-25.

[3] Жиров Д.В., Мелихова Г.С., Рыбин В.В., Сохарев В.А., Климов С.А. Особенности инженерно-геологического изучения массивов скальных пород в целях проектирования глубоких карьеров на примере Ковдорского месторождения магнетитовых и апатитовых руд. Часть 2 // Вестник Кольского научного центра РАН. – 2016. № 25. С. 19-29.

[4] Бушков В. К. Применительная практика кинематического анализа устойчивости при обосновании параметров основных конструктивных элементов борта карьера // Горный информационно-аналитический бюллетень. - 2018. - № 10. - С. 30–42. DOI: 10.25018/0236-1493-2018-10-0-30-42.

[5] Read J., Stacey P. Guidelines for open pit slope design. Australia : CSIRO, 2009. 496 p.

[6] Чернышев С.Н. Трещины горных пород / С.Н. Чернышев. - М.: Наука, 1983. - 240 с.

[7] Obregon C., Mitri H. Probabilistic approach for open pit bench slope stability analysis – A mine case study // International Journal of Mining Science and Technology Volume 29, Issue 4. – 2019. - P. 629-640.

[8] Xiao S., Gao Y. T., Wu S. C., Liu B., Tian Q. M. Kinematic analysis of slope failure modes based on stereographic projection // Progress in Civil, Architectural and Hydraulic Engineering IV. – 2016. – Pp. 313 – 317. ISBN 978-1-138-02916-3.

[9] Bawa H. E., Yendaw J. A., Kansake B. A., Bansah K. J. Rockmass characterization for open pit slope design using kinematic analysis // 51st U.S. Rock Mechanics/Geomechanics Symposium, 25-28 June, San Francisco, California, USA. – 2017. – P. 6.

[10] Lephatsoe M. N., Hingston E. D. C., Ferentinou M., Ltfu N. Kinematic analysis of the western pitwall of the main pit at the Letseng Daimond mine, Lesotho // Rock Engineering and Rock Mechanics: Structures in and on Rock Masses. – 2014. – P. 613 – 618.

[11] Немова Н.А., Бельш Т.А. Геомеханическая оценка параметров устойчивости откосов бортов и уступов при отработке месторождения апатит-нефелиновых руд "Олений ручей" // Известия Томского политехнического университета. Инжиниринг георесурсов. – 2019. Т.330. – №11. – С. 109 - 120.

[12] Soren K., Budi G., Sen P. Stability analysis of open pit slope by finite difference method // International Journal of Research in Engineering and Technology. 2014. Vol. 3. Iss. 5. P. 326–334.

[13] СП 14.13330.2014 «Строительство в сейсмических районах. Нормы проектирования». Москва, 2014

REFERENCES

[1] Berdinova N.O., Sedina S.A., Shamganova L.S., Kalyuzhny E.S. Prediction of strains in strong rock mass of the Kurzhunkul open pit mine by the kinematic analysis. MIAB // Mining Informational and Analytical Bulletin, 2020; (4): 58-68.

[2] Zhirov D.V., Melikhova G.S., Rybin V.V., Sokharev V.A., Klimov S.A. Peculiarities of geotechnical study of rock massifs for the purpose of designing deep quarries on the example of the Kovdor deposit of magnetite and apatite ores. Part 1 // Bulletin of the Kolsky Scientific Center of the Russian Academy of Sciences. 2016. N 24. P. 15-25.

[3] Zhirov D.V., Melikhova G.S., Rybin V.V., Sokharev V.A., Klimov S.A. Peculiarities of geotechnical study of rock massifs for the purpose of designing deep quarries on the example of the Kovdor deposit of magnetite and apatite ores. Part 2 // Bulletin of the Kolsky Science Center RAS. 2016. N 25. P. 19-29.

[4] Bushkov V.K. Applied practice of kinematic analysis of stability in the substantiation of the parameters of the main structural elements of the pit side // Mining informational and analytical bulletin. 2018. N 10. P. 30-42. DOI: 10.25018 / 0236-1493-2018-10-0-30-42.

[5] Read J., Stacey P. Guidelines for open pit slope design. Australia: CSIRO, 2009. 496 p.

[6] Chernyshev S.N. Joints of rocks / Chernyshev S.N. M.: Science, 1983. 240 p.

[7] Obregon C., Mitri H. Probabilistic approach for open pit bench slope stability analysis – A mine case study // International Journal of Mining Science and Technology. Vol. 29, Issue 4. 2019. P. 629-640.

[8] Xiao S., Gao Y. T., Wu S. C., Liu B., Tian Q. M. Kinematic analysis of slope failure modes based on stereographic projection // Progress in Civil, Architectural and Hydraulic Engineering IV. 2016. P. 313-317. ISBN 978-1-138-02916-3.

[9] Bawa H.E., Yendaw J.A., Kansake B.A., Bansah K.J. Rockmass characterization for open pit slope design using kinematic analysis // 51st U.S. Rock Mechanics / Geomechanics Symposium, 25-28 June, San Francisco, California, USA. 2017. 6 p.

[10] Lephatsoe M. N., Hingston E. D. C., Ferentinou M., Ltfu N. Kinematic analysis of the western pitwall of the main pit at the Letseng Daimond mine, Lesotho // Rock Engineering and Rock Mechanics: Structures in and on Rock Masses. 2014. P. 613-618.

[11] Nemova N.A., Belsh T.A. Geomechanical assessment of the stability parameters of the slopes of the sides and benches during the development of the "Oleniy Ruchey" apatite-nepheline ore deposit // Bulletin of the Tomsk Polytechnic University. Engineering of georesources. 2019. Vol. 330, N 11. P. 109 - 120.

[12] Soren K., Budi G., Sen P. Stability analysis of open pit slope by finite difference method // International Journal of Research in Engineering and Technology. 2014. Vol. 3, Iss. 5. P. 326-334.

[13] SP 14.13330.2014 “Construction in seismic regions. Design standards ". M., 2014

N E W S
OF THE NATIONAL ACADEMY OF SCIENCES OF THE REPUBLIC OF KAZAKHSTAN
SERIES OF GEOLOGY AND TECHNICAL SCIENCES
ISSN 2224-5278
Volume 1, Number 445 (2021), 144 – 150 **https://doi.org/10.32014/2021.2518-170X.20**

UDC 621. 658

K. T. Sherov[1], D. E. Alikulov[2], M. R. Sikhimbayev[3], A. K. Sherov[4], B. N. Absadykov[5], E. B. Imanbaev[1], R. Gabdysalyk[6]

[1]Karaganda Technical University, Karaganda, Kazakhstan;
[2]Tashkent State Technical University, Tashkent, Uzbekistan;
[3]Karaganda Economic University of Kazpotrebsoyuz, Karaganda, Kazakhstan;
[4]LLP «Kazakhstan Aviation Industry», Nur-Sultan, Kazakhstan;
[5]A. B. Bekturov Institute of Chemical Sciences, Almaty, Kazakhstan;
[6]D. Serikbayev East Kazakhstan State Technical University, Ust-Kamenogorsk, Kazakhstan.
E-mail: shkt1965@mail.ru, lofazu@yandex.com, smurat@yandex.ru, knyazluni@mail.ru, b_absadykov@mail.ru, y.imanbayev@gmail.com, riza.gabdyssalyk@mail.ru

THE METHOD OF SELECTING THE OPTIMAL LAYOUTS OF THE SIZE LIMIT DEVIATIONS DURING ASSEMBLY

Abstract. The development of mechanical engineering in recent years has led to a special focus on the processing of functionally connected surfaces. In world practice, more attention is paid to the creation of methods, techniques, technological processes, tools, measures, etc., which would reduce the complexity of processing and assembling functionally connected surfaces (FCS) of details and connections.

Currently, the connection between the dimensions and positions of surfaces is not standardized for all details. These details include body parts and frames that have V-shaped surfaces and associated planes. Apparently, this is due to the large variety of functionally connected surfaces and the complexity of controlling the technological support of dimensions.

When coupling details of metal-cutting machines FCS, it is necessary to ensure simultaneous contact of two combined surfaces of the guides.

This article provides a method for selecting the optimal layouts of the size limit deviations when assembling details with FCS. The influence of the location of the size limit deviations on the complexity of the fitting operation when assembling two combined surfaces of details is considered. Possible layouts of the size limit deviations are shown, as well as a diagram of the relative position of the two combined surfaces before the fit operation, depending on the values of the size limit deviations.

Some recommendations are given for choosing the optimal layouts of the limit deviations of the dimensions of the adjacent planes:

- the position of the adjacent planes depends on the size values and their deviations;
- the position of the adjacent planes is significantly affected by the position of the size deviations of the connected planes;
- depending on the location of the limit deviations of the size of the joints, the amount of removed allowance varies considerably and leads to a significant change in the labor intensity of the scraping process.

Key words: Functionally connected surfaces, scraping, limit deviations, adjacent plane, fitting, allowance.

Introduction. The creation of numerical control machines, measuring machines of various foreign companies, created prerequisites for reducing the complexity of manufacturing and monitoring details and connections with functionally connected surfaces (FCS) [1,2]. However, not all problems of ensuring accuracy and reducing the complexity of processing and assembling such surfaces are solved. The FCS includes the surfaces of mobile and fixed joints, when the coupling is performed simultaneously on several surfaces, and the accuracy of their coupling is determined by the contact norms [3,4].

Table 1 shows classes of details with functionally connected surfaces [5]. For some details, such as gears, spline shafts, threaded surfaces, and others, there are standards that normalize the connection of the FCS [6,7].

Table 1 – Classification of details with surfaces that have functionally related dimensions

№	Name of details	Surfaces with functionally related dimensions	Note
1	Cogwheels	Ring gear	GOST standard 1643-81 and etc.
2	Splined parts	Slotted surfaces	GOST standard 1139-80 and etc.
3	Chain wheels	Ring gear	_____
4	Threads and screws	Helical surface	GOST standard 16093-81 and etc.
5	Case details	Flat and V–shaped flat surfaces	_____
6	Case details	The surface of the “dovetail” type	_____
7	Frames	Flat and V–shaped flat surfaces	_____
8	Other details	Rack, key and other surfaces	_____

Table 1 shows that there is a wide variety of details with functionally connected surfaces. Moreover, the surfaces may have a certain regular profile, for example, in gear wheels: involute, Novikov’s, arch, etc. In other cases, it may be flat surfaces, for example, in spline shafts with a straight-line profile, or screw surfaces in threads, running screws, etc. [8-10].

Such surfaces for metal-cutting machines are guide frames and calipers. Phenomena that occur in the joints of V-shaped and flat guide machines significantly affect the accuracy of machining, vibration resistance of machine components and the quality of the machined surfaces of parts [11,12].

The accuracy of the position of the parts when moving along the guides is due to errors in the guide from the theoretical given shape. The reasons for deviations in the shape of the guides depend on the process. Deviations of the guides from the theoretically specified shape are formed by errors in the processing of the guides and their assembly. Machine guides lose their shape during operation under the influence of forces and external factors (humidity, dust, etc.) and temperature fields in the machine during processing of details [13,14].

In machines, in the nodes of machines, devices, technological equipment and other structures, it is very common to have problems of ensuring the fit of the FCS simultaneously on several planes located relative to each other in parallel or at certain angles. Several known methods are used to ensure that the planes fit in production conditions [15-17]. In cases where it is necessary to ensure high accuracy of fitting, a locksmith operation is used – manual scraping [18,19]. Manual scraping is a very time-consuming process that takes from several hours to several shifts of work [20,21]. Figure 1 shows a diagram for checking the surface to be treated when scraping.

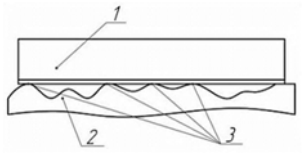

Figure 1 – Scheme for checking the surface to be processed when scraping. 1 - ruler; 2 - guide surface; 3 - paint

The scraping begins with a thin layer being applied to the surface of the ruler or plate (1 ... 2 microns) easily removed paint (for example, typographic or blueing). After that, the ruler 1 is moved along the surface of the guides 2, while the paint 3 is transferred to the protrusions (figure 1), and the hollows remain unpainted. Painted protrusions are treated with a scraper. For one movement of the scraper, a hole up to 5 microns deep should be formed during preliminary scraping and up to 1.5 microns during final scraping. After processing all the protrusions, a second check is made "for paint" and, if it is necessary, repeat the scraping. The pre-scraping is carried out "pushing away from oneself", and final is made on the direction of "pulling towards oneself".

Scraping is an extremely unproductive method of processing. The use of a mechanized tool with pneumatic or electric drive is possible only with preliminary scraping. The performance of scraping depends to a large extent on the size of the allowance. The allowance must be minimal, but sufficient to obtain the required technical accuracy and surface roughness. The allowance for scraping guides up to 1000 mm in length should not exceed 0.05-0.1 mm [22].

The working surfaces of high-precision machines are scraped with a shallow penetration of the scraper into the metal (0.5-1.5 microns), providing large areas of contact with large intervals, which allows you to bring to the minimum values of the moving parts movement force. The working surfaces of heavily loaded guides are scraped when the scraper penetrates into the metal to a fairly significant depth (4-5 microns) [22,23]. The complexity of scraping operations depends mainly on the amount of allowance to be removed. In the literature, information on allowances for approval is almost not described. Each company, based on its experience and some data on the processing technology of such compounds in related enterprises, independently sets the allowances, and at the same time the size and limit deviations between the planes of fit. In this regard, the development of a method for choosing the optimal layout of the size limit deviations is an **actual problem**.

The methodology of optimal choice of layouts extreme deviations of dimensions and discussion of the results. Due to the lack of detailed data in the literature on the features of the technology for ensuring the accuracy of the planes of fit, we have considered and given some recommendations for choosing the optimal layout of the limit deviations of dimensions. Figure 2 shows a diagram of the relative position of the two planes of fit and the two parts to be assembled. For simplicity of the image and description of these details, they are shown in a simplified form.

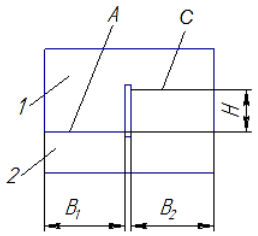

Figure 2 – Diagram of the relative position of two combined surfaces of details after fitting. 1 – the first part; 2 – the second part; A - one of the adjacent plane; C – the other adjacent plane; B_1 – width of the adjacent plane of A; B_2 – the width of the adjacent plane of C; H – the dimension between the adjacent planes

Figure 2 does not show the length of the adjacent planes. The designations for the length of the adjacent planes will be used later in the text. If the width of the adjacent planes is equal, the designation B is used. If the length of the adjacent planes differs, the following notations are used: $B_{1\text{-}1}$ and $B_{1\text{-}2}$ for the first part, $B_{2\text{-}1}$ and $B_{2\text{-}2}$ for the second part. Figure 3 shows the layout of the dimensions and the designation of the adjacent planes of 1 and 2 parts.

Figure 3 – Layouts of the dimensions of the combined surfaces of parts. *a - part 1; b- part 2*

Figures 3a, 3b, A_1 and C_1 show the adjacent planes of the part 1, and A_2 and C_2 of the part 2. Dimensions H_1 and H_2 are the dimensions between the adjacent planes of the 1 and 2 parts.

When connecting 1 and 2 parts, we can consider a simple dimensional chain consisting of two constituent links H_1 and H_2 and a closing link, which we mark as H_Σ.

If the nominal values of the dimensions H_1 and H_2 are equal, then the nominal value of the closing link H_Σ will be zero, and its limit deviations will depend on the value of the limit deviations of the dimensions H_1 and H_2.

Figure 4 shows the layouts of the size limit deviations H_1 and H_2, as well as four possible layouts of the size limit deviations.

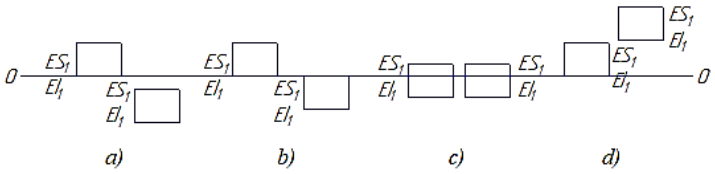

Figure 4 – Diagram of possible locations of size deviations before the fit operation.
a - mobile landing with guaranteed clearance; *b* - mobile landing with zero clearance;
c - transitional landing; d - tight landing

These schemes differ in the relative location of the limit deviations. There can be an infinite number of location schemes. The chosen schemes meet the requirements of three types of landings – mobile, transitional and tight landing.

The choice is conditional and is made only for a more visual presentation of the proposed method for selecting the layouts of the limit deviations of dimensions. The schemes for mobile landing are shown in two positions. Figure 4*a* shows the "guaranteed clearance". Figure 4*б* shows a possible "zero" clearance. Figure 5 shows four diagrams of the relative position of two pairs of combined surfaces of details which dimensions between the adjacent planes have deviations according to the four diagrams shown in figure 4.

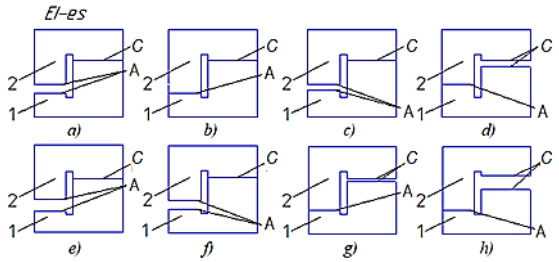

Figure 5 – Diagram of the relative position of two combined surfaces before the fitting operation, depending on the values of the size limit deviations

If the accuracy of the adjacent planes is provided by the locksmith operation of one of the connected parts – as scraping, then for the four connection schemes shown in figure 5, you can come to the following conclusions. When ensuring accuracy by scraping the planes of part 1, there are the following options. According to figure 5*a* and e, the accuracy must be ensured by scraping along the $Б_1$ plane for all parts 1, since $H_1 > H_2$. According to figure 5b and f, the accuracy must be ensured by scraping along the $Б_1$ plane for parts 1 while size is $H_1 > H_2$. According to figure 5c and g, the accuracy must be ensured by scraping along the planes either A_1 or C_1, depending on the values of the dimensions H_1 and H_2. According to figure 5d and h, the accuracy must be ensured by scraping along the A_1 plane for all parts 1, since $H_2 > H_1$. It should be noted that if, after mechanical treatment, the requirements for the accuracy of the contact surfaces do not meet the number of contact spots, then it is necessary to provide a minimum allowance for scraping, after removal, which ensures the requirements for the accuracy of the adjacency. This allowance value can be designated as Z_{min}, and its value can be defined as a value that depends on the amount of roughness and macro-roughness. Then for each of the processed surfaces it can be written

$$Z_{\min} = R_z + \Delta, \quad (1)$$

where R_z - is the height of the profile irregularities; Δ - deviation of the surface shape.

For the scraping surfaces of two parts, the total value of the minimum allowance can be determined using the formula:

$$Z_{\sum \min} = (R_{z1} + R_{z2}) + (\Delta_1 + \Delta_2), \quad (2)$$

In formula (2), the indexes 1 and 2 refer to the two adjacent surfaces of each part.

For the two scraping surfaces of one detail on the size of the H, the greatest value out of two Z_{min} needs to be provided. Ensuring the accuracy of the adjacency, as a rule, is carried out either by scraping

both planes, or one of the planes. Depending on this, the amount of removed allowance varies. In the case of ensuring the accuracy of the adjacency by scraping the plane of one of the two parts, the maximum allowance is determined by the formula:

$$Z_{\max} = \left(ES_1 - EI_2\right) + Z_{\min}, \quad (3)$$

In the case of ensuring the accuracy of the adjacency by scraping the planes of both of the parts, the maximum allowance is determined by the formula:

$$Z_{\max} = \left(ES_1 - EI_2\right) + Z_{\sum \min}, \quad (4)$$

Formulas (3) and (4) are valid for the positions of the limit deviations shown in Figures 3*a* and 3*b* and are possible for the positions shown in figure 3c when $(ES_1 - EI_2) > (ES_2 - EI_1)$. In the case where the position of the limit deviations will correspond to the figure 3*d*, in the formulas (3) and (4) of the Z_{max} calculation, instead of $(ES_1 - EI_2)$ it is necessary to write $(ES_2 - EI_1)$.

Figure 5 shows that at the same tolerance values, but at different locations of the size limit deviations, the allowance value changes. However, the labor intensity of the scraping operation is affected by the amount of allowance, as well as the volume of the removed metal. To determine the volume of the removed metal, it is necessary to consider the size of the allowance, the length and width of the processed surface. So, it can be written as:

$$V_{\max} = Z_{\max} \times L \times B, \quad (5)$$

where V_{max} is the maximum amount of removed metal during scraping.

Conclusions:

- the position of the adjacent planes depends on the size values and their deviations;
- the position of the adjacent planes is significantly affected by the position of the size deviations of the connected planes;
- depending on the location of the limit deviations of the size of the joints, the amount of allowance removed varies significantly and leads to a significant change in the labor intensity of the scraping process.
- depending on the location of the limit deviations of the size of the joints, the amount of removed allowance varies considerably and leads to a significant change in the labor intensity of the scraping process.

К. Т. Шеров[1], Д. Е. Аликулов[2], М. Р. Сихимбаев[3], А. К. Шеров[4], Б. Н. Абсадыков[5], Е. Б. Иманбаев[1], Р. Ғабдысалық[6]

[1]Қарағанды техникалық университеті, Қарағанды, Қазақстан;
[2]Ташкент мемлекеттік техникалық университеті, Ташкент, Өзбекстан;
[3]Қазтұтынуодағы Қарағанды экономикалық университеті, Қарағанды, Қазақстан;
[4]«Қазақстандық авиациялық индустрия» ЖШС, Нұр-Сұлтан, Қазақстан;
[5]Ә. Б. Бектұров атындағы химия ғылымдары институты, Алматы, Қазақстан;
[6]Д. Серікбаев атындағы Шығыс Қазақстан мемлекеттік техникалық университеті, Өскемен, Қазақстан

ҚҰРАСТЫРУ КЕЗІНДЕ ӨЛШЕМДЕРДІҢ ШЕКТІ АУЫТҚУЫ ОРНАЛАСУЫНЫҢ ОҢТАЙЛЫ СҰЛБАСЫН ТАҢДАУ ӘДІСТЕМЕСІ

Аннотация. Машина жасауды дамыту жағдайы соңғы жылдары функционалдық байланысты қабаттарды өңдеуге ерекше назар аударта бастады. Әлемдік тәжірибеде әдістеме, технологиялық үдеріс, құрал, өлшеуіш және т.б. жасауға айрықша назар аударылды, олар бөлшектер мен қосылыстардың функционалды байланысқан қабаттарын (ФБҚ) өңдеу мен құрастырудың еңбек сыйымдылығын азайтуы мүмкін.

Қазіргі уақытта қабаттардың өзара байланысты көлемі мен жағдайы бөлшектердің бәрінде бірдей нормаланған жоқ. Мұндай бөлшектерге корпустық бөлшектер мен V-үлгілі қабаттарды және соған байланысты жазықтықты жатқызуға болады. Бұл функциональды байланысты қабаттардың көптеген жағдайда түрлі болуымен және көлемін технологиялық қамтамасыз етуді бақылаудың күрделі болып келуімен түсіндірілуі тиіс.

Метал кескіш станок бөлшектерінің жанасуы кезінде ФБҚ бағыттаушылардың қосарланып араласқан қабатының бір мезгілде байланысқа түсуін қамтамасыз етеді. Бұл мақалада FKS-тен бөлшектерді жинау

кезінде өлшемдердің шекті ауытқуларының оңтайлы орналасуын таңдау әдісі келтірілген. Өлшемдердің шекті ауытқуларының орналасуының бөлшектердің екі біріктірілген бетін жинау кезінде сәйкестендіру жұмысының күрделілігіне әсері қарастырылады. Өлшемдердің шекті ауытқуларының ықтимал орналасуы, сондай-ақ өлшемдердің шекті ауытқуларының мәндеріне байланысты сәйкестендіру операциясынан бұрын екі біріктірілген беттің өзара орналасу схемасы көрсетілген.

Іргелес жазықтықтар өлшемдерінің шекті ауытқуларының оңтайлы орналасу схемасын таңдау бойынша кейбір ұсыныстар берілген:

- жазықтықтардың орналасуы Өлшем мәндеріне және олардың ауытқуларына байланысты;
- іргелес жазықтықтардың орналасуына жанасатын жазықтықтардың өлшемдерінің ауытқу позициясы айтарлықтай әсер етеді;
- қосылыстар мөлшерінің шекті ауытқуларының орналасуына байланысты алынатын жәрдемақының мөлшері айтарлықтай өзгереді және кесу процесінің күрделілігінің айтарлықтай өзгеруіне әкеледі.

Түйін сөздер: функционалды байланыстағы қабаттар, тегістеу, шекті ауытқу, жанасу жазықтығы, қиюластыру, өңдеу әдібі.

К. Т. Шеров[1], Д. Е. Аликулов[2], М. Р. Сихимбаев[3], А. К. Шеров[4], Б. Н. Абсадыков[5], Е. Б. Иманбаев[1], Р. Габдысалык[6]

[1]Карагандинский технический университет, Караганда, Казахстан;
[2]Ташкентский государственный технический университет, Ташкент, Узбекистан;
[3]Карагандинский экономический университет Казпотребсоюза, Караганда, Казахстан;
[4]ТОО «Казахстанская авиационная индустрия», Нур-Султан, Казахстан;
[5]Институт химических наук им. А. Б. Бектурова, Алматы, Казахстан;
[6]Восточно-Казахстанский государственный технический университет им. Д. Серикбаева, Усть-Каменогорск, Казахстан

МЕТОДИКА ВЫБОРА ОПТИМАЛЬНЫХ СХЕМ РАСПОЛОЖЕНИЯ ПРЕДЕЛЬНЫХ ОТКЛОНЕНИЙ РАЗМЕРОВ ПРИ СБОРКЕ

Аннотация. Развитие машиностроения в последние годы привело к уделению особого внимания к обработке функционально связанных поверхностей. В мировой практике всё большее внимание уделяется созданию методик, технологических процессов, инструментов, мерителей и др., которые бы привели к снижению трудоёмкости обработки и сборки функционально связанных поверхностей (ФСП) деталей и соединений.

В настоящее время связь между размерами и положением поверхностей не стандартизирована для всех деталей. Эти детали включают в себя детали кузова и рамы, имеющие V-образные поверхности и связанные с ними плоскости. По-видимому, это связано с большим разнообразием функционально связанных поверхностей и сложностью управления технологическим обеспечением размеров.

При соединении деталей металлорежущих станков ФТС необходимо обеспечить одновременный контакт двух совмещенных поверхностей направляющих.

В данной статье приводится методика выбора оптимальных компоновок предельных отклонений размеров при сборке деталей с ФКС. Рассмотрено влияние расположения предельных отклонений размеров на трудоемкость операции подгонки при сборке двух совмещенных поверхностей деталей. Показаны возмож-ные схемы расположения предельных отклонений размеров, а также схема взаимного расположения двух совмещенных поверхностей перед операцией подгонки в зависимости от значений предельных отклонений размеров.

Даны некоторые рекомендации по выбору оптимальной схемы расположения предельных отклонений размеров плоскостей прилегания:

- положение плоскостей прилегания зависят от значений размеров и их отклонений;
- на положение плоскостей прилегания существенное влияние оказывают положение отклонений размеров контактируемых плоскостей;
- в зависимости от расположения предельных отклонений размеров соединений величина снимаемого припуска существенно меняется и приводит к значительному изменению трудоёмкости процесса шабрения.

Ключевые слова: функционально связанные поверхности, шабрение, предельные отклонения, плоскость прилегания, пригонка, припуск.

Information about authors:

Sherov Karibek Tagayevich, Doctor of Engineering Sciences, Professor, Karaganda state technical university, Karaganda, Kazakhstan; shkt1965@mail.ru; https://orcid.org/0000-0003-0209-180X

Alikulov Dzhavlan Ergeshovich, Doctor of Engineering Sciences, Professor, Tashkent State Technical University, Tashkent, Uzbekistan; lofazu@yandex.com; https://orcid.org/0000-0002-7787-0245

Sikhimbayev Muratbay Ryzdikbayevich, Doctor of Economic Sciences, Professor, Karaganda economic university of Kazpotrebsoyuz, Karaganda, Kazakhstan; smurat@yandex.ru; https://orcid.org/0000-0002-8763-6145

Sherov Aibek Karibekovich, PhD, Lead Designer, Kazakhstan Aviation Industry LLP, Nur-Sultan, Kazakhstan; knyazluni@mail.ru; https://orcid.org/0000-0002-1433-957X

Absadykov Bakhyt Narikbayevich, Doctor of Technical Sciences, Professor, the Corresponding member of National Academy of Sciences of the Republic of Kazakhstan, A. B. Bekturov Institute of Chemical Sciences, Almaty, Kazakhstan; b_absadykov@mail.ru; https://orcid.org/0000-0001-7829-0958

Imanbaev Yernat Bakytovich, doctoral student, Karaganda State Technical University, Karaganda, Kazakhstan; y.imanbayev@gmail.com; https://orcid.org/0000-0002-8490-6672

Gabdyssalyk Riza, PhD, Senior Lecturer, D. Serikbayev East Kazakhstan State Technical University, Ust-Kamenogorsk, Kazakhstan; riza.gabdyssalyk@mail.ru; https://orcid.org/0000-0001-9184-0897

REFERENCES

[1] Murashkin S.L. Technology of mechanical engineering. Book 1. Fundamentals of mechanical engineering technology. M.: Higher school. 2003. 278 p.

[2] Koganov I.A., Kiselev V.N., Yamnikov A.S. Precision machining on metal-cutting machines: Textbook / TulSU. Tula, 1996. 132 p.

[3] Sherov K.T., Alikulov D.E. System of measurement and control of functionally connected surfaces (monograph). Karaganda: Publishing house KarSTU, 2011. 173p.

[4] Sherov K.T., Alikulov D.E. Control ruler for angles between planes of V-shaped guides / Measurement Techniques. July 2012, Vol. 55, Issue 4. P. 397-399. https://doi.org/10.1007/s11018-012-9971-5. (in English.).

[5] Sherov K.T. System of measurement and control of functionally connected surfaces (monograph). 2-A, B. Karaganda: Publishing house KarSTU, 2011. 178p.

[6] Pavlov L.E. Modern designs of the tooth-processing tool / L.E. Pavlov, Yu.V. Tsvis. M.: Engineering, 1972. 40 p.

[7] Production of gears: a reference Book / S.N. Kalashnikov, A.S. Kalashnikov, G.I. Kogan, and others. Under the General editorship of B.A. Taits. 3rd ed., Rev. and extra. M. engineering, 1990. 440 p.

[8] Taits B.A., Markov N.N. Accuracy and control of gears. L.: Engineering,1978. 137 p.

[9] Novikov V.Yu., Skhirtladze A.G. Technology of machine-tool construction. M.: Engineering, 1990. 256 p.

[10] Matalin A.A. Technology of mechanical processing. L.: Engineering, 1977. 464 p.

[11] Sherov K.T., Sikhimbayev M.R., Absadykov B.N., Sikhimbayeva D.R., Buzauova T.M., Karsakova N.G., Gabdysalyk R. Control's accuracy improvement and reduction of labor content in adapting of ways of metalcutting tools // News of the National Academy of Sciences of the Republic of Kazakhstan. Series of geology and technical sciences. 2018. Vol. 6, N 432. P. 170-179. https://doi.org/10.32014/2018.2518-170x.47, ISSN 2518-170X. (Online), ISSN 2224-5278 (Print).

[12] Alikulov D.E., Sherov K.T., Sherov A.K. Ways to reduce the limit values of allowances removed from the surfaces of the guide calipers of the lathe NT-250I // Vestnik TashSTU. Tashkent: 2008. N 1. P. 47-49.

[13] Reshetov D.N., Portman V.T. Precision of metal-cutting machines. M.: Engineering, 1986. 336 p

[14] Mukhin A.V., Spiridonov O. V., Skhirtladze A. G., Kharlamov G. A. Production of metal-cutting machine parts: A textbook for engineering specialties of universities. M.: Engineering, 2001. 560 p.

[15] Dalsky A.M., Kuleshova Z. G. Assembly of high-precision joints in mechanical engineering. M.: Engineering, 1984. 304 p.

[16] Yakobson M.O. "Engineering Technology". M.: Engineering, 1966, 475 p.

[17] Balakshin B.S. Theory and practice of mechanical engineering technology: In 2 books. M.: Engineering, 1982. Book 1. Machine tool technology, 1982. 239 p.

[18] Technological bases of machine quality management / A.S. Vasiliev, A.M. Dalsky, S.A. Klimenko, L.G. Polonsky, M.L. Heifets, P.I. Yashcheretsyn. M.: Engineering, 2003. 256 p.

[19] Mamet O.P. Brief reference of the machine-tool Builder designer. Moscow: Engineering, 1968. 215p.

[20] Pokrovsky B.S. Fundamentals of Assembly technology [Text]: studies. manual / B.S. Pokrovsky. M.: Publishing center "Academy", 2004. 157 p. ISBN 5-7695-1673-9

[21] Yashcheritsyn P.I. Fundamentals of mechanical processing and Assembly technology in mechanical engineering. Minsk: Higher school, 1974. 328 p.

[22] Pokrovsky B.S. Handbook of mechanic Assembly works / Textbook for primary professional education. M.: Academy, 2013. 224 p. ISBN 978-5-7695-4966-3.

[23] Novikov M.P. Fundamentals of Assembly technology for machines and mechanisms. M.: Engineering, 1980. 592 p.

N E W S
OF THE NATIONAL ACADEMY OF SCIENCES OF THE REPUBLIC OF KAZAKHSTAN
SERIES OF GEOLOGY AND TECHNICAL SCIENCES
ISSN 2224-5278
Volume 1, Number 445 (2021), 151 – 157 **https://doi.org/10.32014/2021.2518-170X.21**

UDC 546.824-31
IRSTI 61.31.51

M. Zh. Zhurinov[1], A. Z. Abilmagzhanov[1], N. S. Ivanov[1], B. B. Teltayev[2], A. E. Nurtazina[1]

[1]JSC "D. V. Sokolskiy Institute of Fuel, Catalysis and Electrochemistry", Almaty, Kazakhstan;
[2]JSC "Kazakhstan Highway Research Institute", Almaty, Kazakhstan.
E-mail: m.zhurinov@ifce.kz, a.abilmagzhanov@ifce.kz, xumuk777@mail.ru,
ao_kazdornii@mail.ru, nurtazina.aizhan@bk.ru

TITANIUM OXIDE-OXIFLUORIDE SYNTHESIS AND STUDY OF ITS PHOTOCATALYTIC PROPERTIES

Abstract. The research article discusses a new method for the photocatalyst synthesis based on a mixture of titanium oxide - titanium oxyfluoride. The synthesis was performed by dissolving titanium metal in an acidified solution of ammonium bifluoride, followed by oxidation to the highest oxidation state and hydrolysis with ammonia to obtain metatitanic acid. The decomposition of metatitanic acid was carried out in a muffle furnace at a temperature of 380°C. It was found that during the precipitation of metatitanic acid, the titanium compound with the fluoride ion also passes into the precipitate, which, after calcination, transforms into titanium oxyfluoride. Photocatalytic activity was determined by the oxidation reaction of the methyl orange dye upon irradiation with ultraviolet radiation. The source of ultraviolet radiation was a DRT-125 lamp with a wavelength in the range of 200-400 nm. Suspensions containing 60 mg/L of the dye and various contents of the photocatalyst in the concentration range of 1-7 g/L were subjected to oxidation. The construction of the calibration graph and the determination of the concentrations were carried out on an SF-2000 spectrophotometer at a wavelength of 466.4 nm. The operating wavelength was determined by scanning the solution in the wavelength range of 200-800 nm. It was found that as a result of oxidation, the solution pH shifts to the acidic side to 3.5, which leads to a shift in the wavelength of the maximum absorption; in this regard, the solutions pH was adjusted to the same values.

Key words: Titanium oxide, titanium oxyfluoride, photocatalyst, ultraviolet radiation, oxidation.

Introduction. Highly dispersed titanium oxide in its pure form, as well as doped with various elements in the processes of heterogeneous oxidation of various organic compounds, exhibits high photocatalytic activity, and oxidation proceeds to carbon dioxide and water [1-4]. This phenomenon formed the basis of numerous developments aimed at cleaning air and water environments from various organic compounds [5]. Nanocrystalline titanium oxide also has bactericidal activity, which makes it possible to use it not only for photocatalytic purification, but also for simultaneous disinfection [6-8].

The mechanism of photocatalytic reactions proceeding on titanium oxide was proposed. Light absorption in TiO_2 occurs at wavelengths less than 387 nm (for anatase with a band gap of 3.2 eV), which leads to electron advancement from the valence band to the conduction band of the semiconductor. This excitation process creates an electron in the conduction band and an electron hole in the valence band. The electron-hole pairs formed in this way migrate to the surface, where they can initiate oxidation-reduction reactions with adsorbed organic molecules [9].

The most common method for titanium dioxide synthesis today is the hydrolysis of its compounds both in an aqueous medium, where its inorganic salts are precursors, and in an organic medium using titanium tetrabutoxide or tetraisopropoxide [10-13]. When precipitating in an aqueous medium with ammonia, alkalis and alkali metal carbonates, the minimum size of primary particles does not depend on precipitant nature, but varies by the synthesis conditions, while aggregates of various sizes are formed [14]. The sol-gel method makes it possible to synthesize titanium dioxide with various geometric shapes

of primary particles - spherical, needlelike, filamentous and others [15-17]. Electrochemical anodizing of titanium foil in fluorine-containing ethylene glycol resulted in a self-assembled membrane of titanium dioxide nanotubes with a high ratio of length to diameter (about 1500) [18].

Materials and methods of research. In this research work, the precursor was synthesized by dissolving a titanium plate in an ammonium hydrogen fluoride solution with a concentration of 100 g/L. In the first hour, dissolution proceeds very intensively, then the rate decreases by half for each hour, while the plate surface was covered with a layer of insoluble violet-red precipitate. When the solution is acidified with hydrochloric acid, there was an intensification of the process. After complete dissolution, a green solution with a precipitate was obtained. By air flush and heating to 90°C, the precipitate was completely dissolved. Then the solution was electrochemically oxidized in the anode half-space until discoloration. Hydrolysis was carried out with an aqueous solution of ammonia with vigorous stirring for 4 hours. The precipitate that formed was washed and calcined at a temperature of 380°C.

Photocatalytic activity was determined by the oxidation reaction of the methyl orange dye upon irradiation with ultraviolet radiation. The source of ultraviolet radiation was a DRT-125 lamp with a wavelength in the range of 200-400 nm. Suspensions containing 60 mg/L of the dye and various contents of the photocatalyst in the concentration range of 1-7 g/L were subjected to oxidation. The construction of the calibration graph and the determination of the concentrations were carried out on an SF-2000 spectrophotometer at a wavelength of 466.4 nm. Operating wavelength was evaluated by scanning the solution in the wavelength range of 200-800 nm. It was found that as a result of oxidation, the pH of the solution shifts to the acidic side to 3.5, which leads to a shift in the wavelength of the maximum absorption; therefore, the pH of the solutions was adjusted to the same values. To compensate for the thermal energy released by the lamp, the oxidation process was carried out in a thermostatically controlled cell.

Result and discussion. According to figure 1, subsequent to the results of X-ray phase analysis, the obtained sample is a mixture of titanium dioxide in the anatase form and titanium oxyfluoride ($TiOF_2$). Such a composite material is a promising anode material in lithium-ion batteries [19].

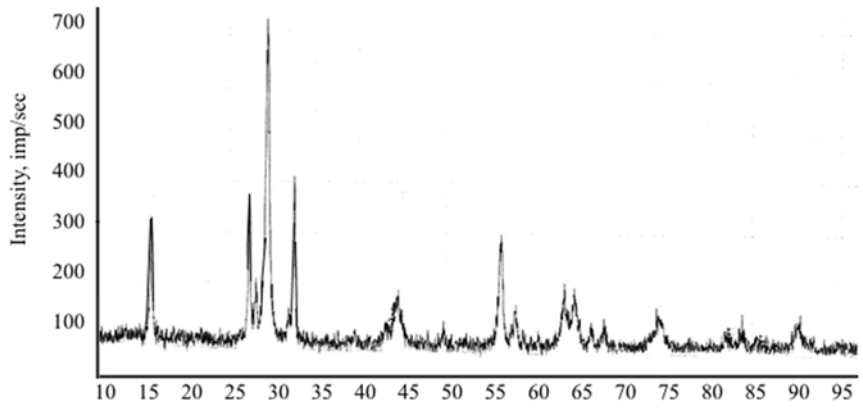

Figure 1 – X-ray diffraction pattern of a photocatalyst sample

In accordance with figure 2, electron microscopic studies have shown that powder aggregates consist of smaller particles; the average particle size calculated from the X-ray diffraction patterns using the Scherrer formula is 30-35 nm.

A spectrophotometric study of the prepared suspensions made it possible to estimate the adsorption degree of methyl orange on photocatalyst surface. The study was carried out with vigorous stirring without light access. In conformity with curve 1 in Figure 3a, in the first half hour the adsorption was 4.67%, followed by attenuation. Function selection for a given curve gives an equation of the form y = -5.506ln (x) + 99.722. As follows from equation, after 10 hours the maximum adsorption will be about 18%. It ought to be noted that there is no visual change in the photocatalyst color. Conforming to curve 2 in figure 3a, intense oxidation of the dye is observed under ultraviolet irradiation. In addition, according to figure 3b, an oxidation intensity increases with an increase in the content of the catalyst in the suspension.

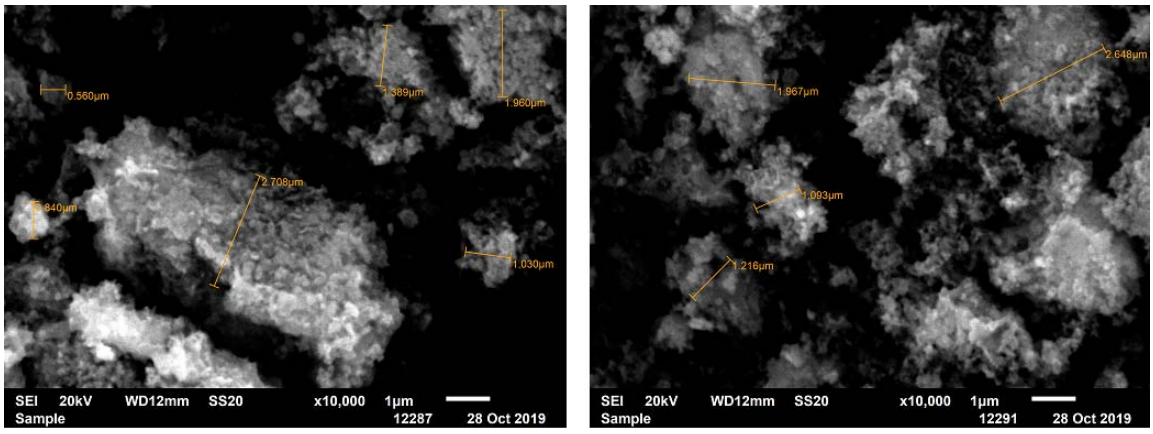

Figure 2 – Microphotography of a photocatalyst sample

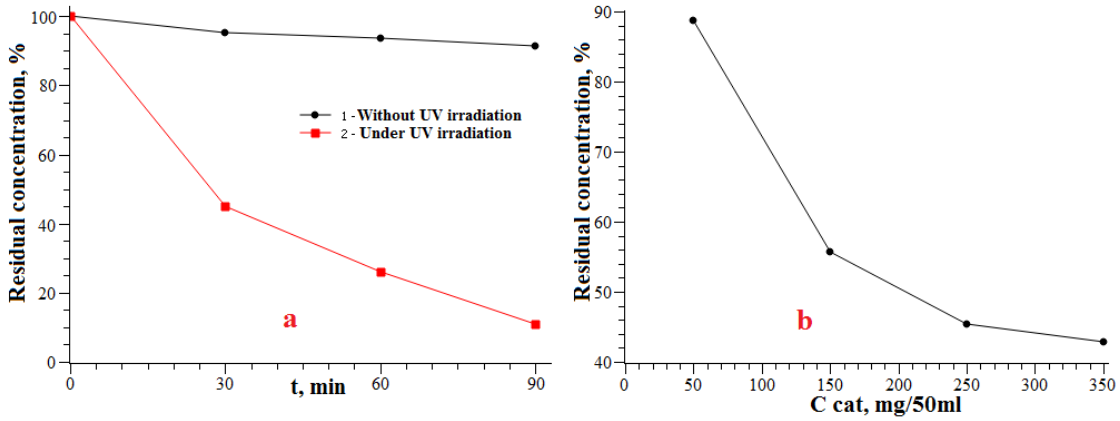

Figure 3 – Dye adsorption and oxidation dynamics

In the kinetics of homogeneous, fermentative and heterogeneous catalytic reactions, the Michaelis - Menten equation is often used [20]:

$$W_0 = \frac{kcat*[E]t*[A]}{A+Km}$$

where K_m and product of $k_{cat}[E]_t$ – parameters of the Michaelis - Menten equation: Michaelis constant and limiting speed; W_0 – initial reaction rate; [A] – initial reagent concentration (substrate). The Michaelis-Menten model assumes that substrate A initially forms a complex with catalyst E, which converts to product B much faster than in catalyst absence. The rate constant k_{cat} is much higher than the non-catalytic reaction constant k. The constant k_{cat} is also called the "number of rotations" because it corresponds to the number of substrate molecules converted into a product by one catalyst molecule in 1 s. The equation contains two parameters that do not depend on substrate [A] concentration, but characterize the properties of the catalyst: this is the product k_{cat} [E] t, which corresponds to the maximum reaction rate W_{max} at a high substrate concentration, and K_m, which characterizes the affinity of the catalyst to the substrate. The Michaelis constant is numerically equal to the substrate [A] concentration at which W_0 reaches half the maximum value W_{max}. The high affinity of the enzyme for the substrate is characterized by a low K_m value and vice versa.

To calculate W_{max} and K_m, it is necessary to find the values of W_0 at different initial concentrations of the dye and at a constant concentration of the catalyst. Figure 4a shows the kinetic curves. W_0 conforms to the slope of the corresponding curve. Water was taken as the resulting reaction product, as a final product in the oxidation of organic compounds. In obedience to figure 4b, plotting in coordinates $W_0 = f(W_0/[A])$ (Eadie-Hofstee coordinates) gives a straight line, the tangent of inclination angle is equal to "minus" K_m, and the segment cut off on the ordinate corresponds to W_{max}. When processing the results, W_{max} is 0.026 mmol/min, and K_m = 0.12 mmol.

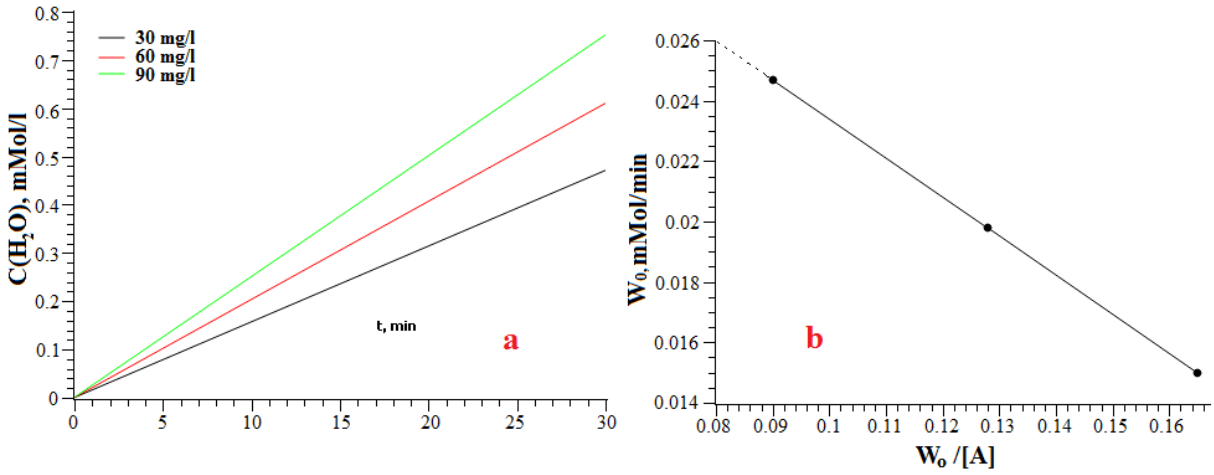

Figure 4 – Kinetic curves of methyl orange oxidation process

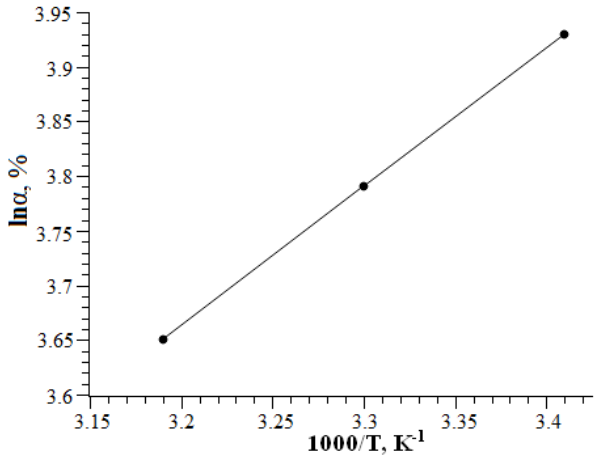

Figure 5 – The action of temperature on the oxidation state of methyl orange

The influence of temperature on the process under study was investigated. Plotting lnα/1000*T coordinates in accordance with figure 5 gives the slope tangent of 1.27. With these data, we can calculate the value of the effective activation energy: $E_{eff} = R*10^3a$, which will be 10.5 kJ/mol.

М. Ж. Журинов[1], А. З. Абильмагжанов[1], Н. С. Иванов[1], Б. Б. Тельтаев[2], А. Е. Нуртазина[1]

[1]АҚ "Д. В. Сокольский атындағы жанармай, катализ және электрохимия институты", Алматы, Қазақстан;
[2]АҚ "Қазақстан жол ғылыми-зерттеу институты", Алматы, Қазақстан

ТИТАН ОКСИДІ-ОКСИФОРИДІНІҢ СИНТЕЗІ ЖӘНЕ ОНЫҢ ФОТОКАТАЛИТИКАЛЫҚ ҚАСИЕТТЕРІН ЗЕРТТЕУ

Аннотация. Мақалада титан оксиді – титан оксифторидінің қоспасы негізінде фотокатализаторды синтездеудің жаңа әдісі қарастырылған. Синтез металл титанды аммоний бифторидінің қышқылданған ерітіндісінде еріту арқылы, одан кейін мететитан қышқылын алу үшін жоғары тотығу күйіне дейін және аммиак гидролизімен тотығу арқылы жүзеге асырылды. Мететитан қышқылының ыдырауы муфельді пеште 380°С температурада жүргізілді. Мететитан қышқылын тұндыру кезінде титан қосылысы фтор ионымен бірге тұнбаға өтетіндігі анықталды, ол кальциленгеннен кейін титан оксифторидіне айналады. Электронды микроскопиялық зерттеулер нәтиежесінде, алынған ұнтақтың агрегаттары ұсақ бөлшектерден тұрады, олардың орташа мөлшері Шеррер формуласын қолданып рентгендік дифракция үлгілері бойынша есептелген, 30-35 нм құрайды.

Фотокаталитикалық белсенділік ультракүлгін сәулесімен сәулелену кезінде метил қызғылт сары бояғышының тотығу реакциясы арқылы анықталды. Ультракүлгін сәулелену көзі ДРТ-125 шамы болды, оның толқын ұзындығы 200-400 нм аралығында болды. Концентрациясы 1-7 г/л аралығында 60 мг/л бояғыш пен фотокатализатордың әр түрлі мазмұны бар суспензиялар тотығуға ұшырады. Концентрациясы 466,4 нм толқын ұзындығында анықталды, ол 200-800 нм толқын ұзындығындағы ерітіндіні сканерлеу арқылы анықталды. Тотығу нәтижесінде ерітіндінің pH-ы қышқыл жағына қарай 3,5-ке ауысады, бұл максималды сіңірудің толқын ұзындығының ығысуына әкелетіндігі анықталды, осыған байланысты ерітінділердің pH мәні бірдей мәндерге келтірілді.

Түйін сөздер: Титан оксиді, титан оксифториді, фотокатализатор, ультрафиолет сәулеленуі, тотығу.

М. Ж. Журинов[1], А. З. Абильмагжанов[1], Н. С. Иванов[1], Б. Б. Тельтаев[2], А. Е. Нуртазина[1]

[1]АО "Институт топлива, катализа и электрохимии им. Д. В. Сокольского", Алматы, Казахстан;
[2]АО "Казахстанский дорожный научно-исследовательский институт", Алматы, Казахстан

СИНТЕЗ ОКСИДА-ОКСИФТОРИДА ТИТАНА И ИССЛЕДОВАНИЕ ЕГО ФОТОКАТАЛИТИЧЕСКИХ СВОЙСТВ

Аннотация. В статье рассматривается новый метод синтеза фотокатализатора на основе смеси оксид титана – оксифторид титана. Синтез осуществлялся путем растворения металлического титана в подкисленном растворе бифторида аммония с последующим окислением до высшей степени окисления и гидролизом аммиаком с получением метатитановой кислоты. Разложение метатитановой кислоты производилось в муфельной печи при температуре 380°С. Установлено, что при осаждении метатитановой кислоты в осадок переходит также соединение титана со фторид-ионом, которое после прокаливания переходит в оксифторид титана. Электронно-микроскопические исследования показали, что агрегаты полученного порошка состоят из более мелких частиц, средний размер которых рассчитан из рентгенограмм по формуле Шеррера 30-35 нм.

Фотокаталитическую активность определяли по реакции окисления красителя метилового оранжевого при облучении ультрафиолетовым излучением. Источником ультрафиолетового излучения служила лампа ДРТ -125 с длиной волны в диапазоне 200-400 нм. Окислению подвергались суспензии, содержащие 60 мг/л красителя и различные содержания фотокатализатора в диапазоне концентраций 1-7 г/л. Определение концентраций производилось при длине волны 466,4 нм, которая определялась путем сканирования раствора в диапазоне длин волн 200-800 нм. Установлено, что в результате окисления pH раствора смещается в кислую сторону до 3,5, что приводит к смещению длины волны максимального поглощения, в связи с этим производилась корректировка pH растворов до одинаковых значений.

Ключевые слова: оксид титана, оксифторид титана, фотокатализатор, ультрафиолетовое излучение, окисление.

Information about authors:

Zhurinov Murat Zhurinovich, Doctor of Chemical Sciences, Professor, Academician, President of NAS RK, Almaty, Kazakhstan; m.zhurinov@ifce.kz, https://orcid.org/0000-0001-5314-1219

Abilmagzhanov Arlan Zainutallaevich, Candidate of Chemical Sciences, head of Applied Research laboratory of JSC “D.V. Sokolskiy Institute of Fuel, Catalysis and Electrochemistry”, Almaty, Kazakhstan; a.abilmagzhanov@ifce.kz, https://orcid.org/0000-0001-8355-8031

Ivanov Nikolai Sergeevich, Candidate of Chemical Sciences, Leading Researcher in Laboratory of Applied Research, JSC “D.V. Sokolskiy Institute of Fuel, Catalysis and Electrochemistry”, Almaty, Kazakhstan; n.ivanov@ifce.kz; https://orcid.org/0000-0002-2153-2802

Teltayev Bagdat Burkhanbaiuly, Doctor of Technical Sciences, Professor, President of JSC “KazdorNII”, Almaty, Kazakhstan; ao_kazdornii@mail.ru; https://orcid.org/0000-0002-8463-9965

Nurtazina Aizhan Erkinbekkyzy, PhD student, master’s degree, junior researcher of Applied Research laboratory of JSC “D.V. Sokolskiy Institute of Fuel, Catalysis and Electrochemistry”, Almaty, Kazakhstan; nurtazina.aizhan@bk.ru; https://orcid.org/0000-0001-7202-5344

REFERENCES

[1] Wang Y., Saitow K. (2020) Mechanochemical synthesis of red-light-active green TiO_2 photocatalysts with disorder: defect-rich, with polymorphs, and no metal loading // Chem. of Materials, 32: 9190-9200. https://doi.org/10.1021/acs.chemmater.0c02676 (in Eng.).

[2] Min C., Changbin Z., Hong H. (2020) Insights into designing photocatalysts for gaseous ammonia oxidation under visible light // Environm. Sci. & Techn., 54: 10544-10550. https://doi.org/10.1021/acs.est.0c02589 (in Eng.).

[3] Pellegrino F., Morra E., Mino L., Martra G., Chiesa M., Maurino V. (2020) Surface and bulk distribution of fluorides and Ti^{3+} species in TiO_2 nanosheets: Implications on charge carrier dynamics and photocatalysis // J. of Phys. Chem., 124: 3141-3149. https://doi.org/10.1021/acs.jpcc.9b10912 (in Eng.).

[4] Fujishima A., Rao T.N., Tryk D.A. (2000) Titanium dioxide photocatalysis // J. of Photochem. and Photobiol. 1: 1: 1-21. https://doi.org/10.1016/S1389-5567(00)00002-2 (in Eng.).

[5] Magalhães F, Lago RM (2009) Floating photocatalysts based on TiO_2 grafted on expanded polystyrene beads for the solar degradation of dyes, Solar Energy, 83:9: 1521-1526 https://doi.org/10.1016/j.solener.2009.04.005 (in Eng.).

[6] Guillard C., Bui T.H., Felix C., Moules V., Lina B., Lejeune P. (2008) Microbiological disinfection of water and air by photocatalysis // C R Chim, 11: 1: 107-113. doi: 10.1016/j.crci.2007.06.007 (in Eng.).

[7] Lu Z., Zhang K., Liu X., Shi Y. (2019) High efficiency inactivation of microalgae in ballast water by a new proposed dual-wave UV-photocatalysis system (UVA/UVC-TiO_2) // Environ. Sci. Pollut. Res Int., 26: 8: 7785-7792. doi: 10.1007/s11356-019-04268-1 (in Eng.).

[8] Kim B., Kim D., Cho D., Cho S. (2003) Bactericidal effect of TiO_2 photocatalyst on selected food-borne pathogenic bacteria // Chemosphere., 52: 1: 277-81. doi: doi.org/10.1016/s0045-6535(03)00051-1 (in Eng.).

[9] Asahi R., Morikawa T., Irie H., Ohwaki T. (2014) Nitrogen-doped titanium dioxide as visible-light-sensitive photocatalyst: designs, developments, and prospects // Chem. Reviews, 114: 19: 9824-9852. DOI: 10.1021/cr5000738 (in Eng.).

[10] Pusit P., Sukon P. (2009) Titanium dioxide powder prepared by a sol-gel method // J. of Ceramic Process. Research, 10: 2: 167-170 (in Eng.).

[11] Devi R.S., Venckatesh D.R., Sivaraj D.R. (2014) Synthesis of titanium dioxide nanoparticles by sol-gel technique, Internat // J. Innovative Research in Sci., 03: 15206-15211. 10.15680/IJIRSET.2014.0308020 (in Eng.).

[12] Shailendra S. (2016). Synthesis of TiO_2 nanoparticle using sol-gel route and testing its photovoltaic performance in dye-sensitized solar cell // Applied Solar Energy, 52: 309-314. 10.3103/S0003701X16040149 (in Eng.).

[13] Liang Y., Sun S., Deng T., Ding H., Chen W., Chen Y. (2018) The preparation of TiO_2 film by the sol-gel method and evaluation of its self-cleaning property // Materials (Basel), 11: 3: 450. doi:10.3390/ma11030450 (in Eng.).

[14] Ismagilov Z.R., Tsikoza L.T., Shikina N.V., Zarytova V.F., Zinoviev V.V., Zagrebelny S.N. (2009) Synthesis and stabilization of nano-sized titanium dioxide // Russ. Chem. Reviews, 78: 9: 873-885 (in Eng.).

[15] Ahn J.Y., Cheon H.K., Kim W.D., Kang Y.J., Kim J.M., Lee D.W., Cho C.Y., Hwang Y.H., Park H.S., Kang J.W., Kim S.H. (2012) Aero-sol-gel synthesis and photovoltaic properties of mesoporous TiO_2 nanoparticles, Chem. Eng. J., 188: 216-221 (in Eng.).

[16] Suciu R., Marian I., Bratu I. (2014) Metal propionate synthesis of TiO_2 nanomaterials, J. Alloys and Comp., 584: 159-166. DOI 10.1016/j.jallcom.2013.09.027 (in Eng.).

[17] Khomane R.B. (2011) Microemulsion-mediated sol-gel synthesis of mesoporous rutile TiO_2 nanoneedles and its performance as anode material for Li-ion batteries, J. Colloid and Interface Sci., 356:1: 369-372. DOI: 10.1016/j.jcis.2010.12.048 (in Eng.).

[18] Jun W., Zhiqun L. (2008) Freestanding TiO_2 nanotube arrays with ultrahigh aspect ratio via electrochemical anodization // Chem. Materials, *20*: 4: 1257-1261. DOI: 10.1021/cm7028917 (in Eng.).

[19] Gnedenkov S.V., Oprah D.P., Kuryavyi V.G., Sinebryukhov S.L., Ustinov A.Y., Sergienko V.I. (2014) TiO_2-$TiOF_2$ nanostructured composite anode material for Li-ion battery [Nanostrukturirovannyj kompozitnyj anodnyj material TiO2-TiOF2 dlya Li-ionnogo akkumulyatora] // Electrochem. Power Engin, 14: 2: 68-77 (in Russ.).

[20] Gabrielsson J., Peletier L. (2018) Michaelis-Menten from an in vivo perspective: open versus closed systems, The AAPS J., 20: 102. DOI: 10.1208/s12248-018-0256-z (in Eng.).

N E W S
OF THE NATIONAL ACADEMY OF SCIENCES OF THE REPUBLIC OF KAZAKHSTAN
SERIES OF GEOLOGY AND TECHNICAL SCIENCES
ISSN 2224-5278
Volume 1, Number 445 (2021), 157 – 163 **https://doi.org/10.32014/2021.2518-170X.22**

U. Shokirov[1], S. Turabdjanov[1], H. Kadirov[2], F. Badriddinova[2], B. Kedelbaev[3]

[1]Tashkent State Technical University named after Islam Karimov, Tashkent, Uzbekistan;
[2]Tashkent Institute of Chemical Engineering, Tashkent, Uzbekistan;
[3]South-Kazakhstan State University named after M. Auezov, Shymkent, Kazakhstan.
E-mail: umid52@mail.ru, tur_sad@mail.ru, tkti.kodirov@mail.ru,
badritdinova_f@mail.ru, kedelbaev@yandex.kz

CALCULATION AND DESIGN OF AN INDUSTRIAL REACTOR FOR PYRROLES SYNTHESIS

Abstract. Industry of pyrroles synthesis on the basis of acetylene, ammonia and amines over polyfunctional catalyst can be organised only when for its recovery the rational industrial technology allowing to synthesize this product in necessary quantity and demanded quality cheap enough from accessible raw materials is developed. Considering the issues related to the development of a new reactor with high productivity and economic efficiency, the processes running in the reactor were studied.

Phase characteristics have been investigated in response to changes in acetylene conversion rate due to the height of the catalyst layer. As a result, high productivity of acetylene production with zinc-chromaluminum catalyst at the temperature range of 340-440^{o}C is achieved for 92% when the layer height is 1200 mm from the reactor top point. Based on the mass balance as well as the experimental result, a reactor for the industrial synthesis of pyrroles has been proposed.

Key words: pyrrol, acetylene, ammonia, amines, catalyst, dehydration, heterocyclization.

Introduction. The present-day level of development of innovative technologies promotes research in the field of chemistry of heterocyclic compounds [1-3]. Condensation of acetylene with ammonia and amines is of great theoretical and practical interest, which opens a perspective for the synthesis of complex organic nitrogen-containing compounds of pyrrole and its derivatives, which are currently of practical importance [4,5].

The pyrrole ring is contained in the molecules of blood - hemoglobin and green substances of plants - chlorophyll, a number of antibiotics, and in many compounds [6,7]. The pyrrole fragments contained are potentially important as optical electron-active materials [7]. Plasma copolymers of polypyrrole and polyethylene glycol are used to produce an implant that promotes neuroprotection and the restoration of a compound in the spinal cord after damage [8]. If the pyrrole structure contains two bound rings, then a high degree of planarity is observed and as a result leads to improvement of optical and electronic properties [9].

For the synthesis of pyrrole and its homologs there is a large number of methods [10-16], which we will conditionally divide into three main groups:

- Synthesis of pyrroles from ketoximes and acetylene.
- Synthesis of pyrroles from ketoamines.
- Synthesis of pyrroles from acetylene and amines.

However, the known diverse methods of synthesis of the pyrrole cycle are multistage. The lifetime of the catalysts used is limited and there are difficulties in separating the resulting complex mixture.

We have studied the reaction of synthesis of pyrrol and N-vinylpyrrol together with catalytic heterocyclization of acetylene, ammonia and amines in the presence of zinc-chrome-aluminum (ZCA) and cadmium-fluorine-zinc-chrome-aluminum (CFZCA) catalysts [17-19].

Methods. In laboratory environment, heterocyclization reactions were performed at the temperature range of 340 - 440 °C, the volumetric flow rate of gases 140-150 hour^{-1}. Processes running in the reactor are determined by the phase state of the initial reagents and reaction products (phase characteristic), type of catalyst (solid or liquid), reaction heat, respectively, thermal regime (energy and thermodynamic characteristics), process dynamics, the nature of movement of reagents and reaction products, as well as system hydrodynamics.

In order to select optimal process and reactor parameters, we have conducted a series of experiments with different reactor designs. The reactor design must ensure that the following basic process parameters are maintained [20-22]:

[1] reaction period;
[2] temperature: at various points of the reaction zone;
[3] reactor pressure;
[4] mass transfer rate to the active surface of the catalyst and between phases;
[5] catalyst activity.

Heterocyclization reaction was carried out in tubular reactors of size $\boldsymbol{d \cdot \ell = (\mathscr{b}.mm)}$

21×500;	21×1000;	21×1500
30×500;	30×1000;	45×1000

Results and discussion. Reactors with fixed granular catalyst bed are the most common type of devices for carrying out catalytic processes. Granular bed is a set of randomly stacked catalyst particles at intervals in which the acetylene flows, i.e. a kind of coarse-grained medium, which must be strongly exposed to various random factors related to the heterogeneity of particle-particle packing and distribution of the reaction mixture flow.

The relationship of acetylene conversion rate change to catalyst layer height has been studied. It has been established that the acetylene conversion rate changes in direct proportion to the catalyst layer height (table).

Relationship of acetylene conversion rate change to catalyst layer height ZCA at 340 - 440 °C
Reactor d×l = 21x1500 mm; V = 140 - 150 hour^{-1}

No.	Layer height from the top point of the reactor, mm	Acetylene conversion rate, %
1	400	41.0
2	600	57.0
3	800	76.0
4	1000	86.0
5	1200	92.0
6	On reactor outlet	96,0 - 99,0

The table shows that the reaction takes place in the inner diffused area. We considered the kinetics of catalytic reactions, in which the speed was determined by chemical processes inside of reactor: adsorption, surface reaction, desorption. The ZCA catalysts used by us are porous bodies. Heterogeneous reactions of acetylene and ammonia are rather fast, the speed of the total catalytic action is the diffusion of reagents in the pores of the ZCA catalyst grain, i.e. inside of the diffusion region.

The internal surface of porous catalyst grains can exceed 99 % of the total catalyst surface. Catalyst grain is described as a medium in which the substance is transferred with an effective diffusion coefficient, and the catalytic reaction of acetylene and ammonia proceeds with an effective speed constant, referred to grain volume unit, and these constants are constant throughout the volume of grain. Thus, the reaction in the reactor proceeds somewhat homogeneously in the mass of the catalyst, and the reagents come from another phase [23,24].

High efficiency of heterogeneous processes is achieved by the right choice of the reactor device, due to the required selectivity of chemical transformations of the initial substances, as well as the productivity of the target product.

The reactor design must ensure the maintenance of the following basic process parameters:

[1] reaction time;
[2] temperatures at various points of the reaction zone;
[3] reactor pressure;
[4] mass transfer rate to the active surface of the catalyst and between phases;
[5] catalyst activity.

For acetylene and ammonia catalytic reactions we proposed a catalyst layer.

The mass balance of the main parameters of flow-type reactor for pyrrole synthesis was calculated [25,26].

For plug-flow reactor, the mass balance equation for the reacting substance is as follows:

$$-\frac{\omega}{S_{ov}} \cdot \frac{d(UA)}{dx} = W + \frac{\omega}{S_{ov}} \cdot \frac{dA}{dt} \quad (1)$$

where $\omega = \frac{S_1}{S_2}$, S_1 is reactor cross-sectional area free of catalytic material; S_2 is reactor cross-sectional area; S_{ov} is catalyst volume unit area, m^2/m^3; A is current acetylene concentration, $mole/m^3$; U is reactor gas mixture rate, m/sec.; W is acetylene flow rate, $mole/m^2 \cdot sec.$; X is the coordinate of the volume element for which the process is described.

When the reactor reaches a steady-state condition

$$\frac{dA}{dt} = 0$$

and the equation is as follows:

$$W = \frac{\omega}{S_{ov}} \cdot \frac{d(UA)}{dx} \quad (2)$$

The rate of acetylene consumption reaction is described by the equation:

$$W = K \cdot e^{-\frac{E}{RT}} \cdot A$$

where, E is activation energy, J; $\hat{E}$ is catalyst activity parameter, m/sec.

In the process of the catalyst activity it is deactivated due to deposition of high-molecular carbon products on its surface.

We assume that the deactivation speed is proportional to the acetylene conversion rate.

Based on these assumptions, the equation reflecting the catalyst deactivation process becomes as follows:

$$\frac{dK}{dt} = -K^1 \cdot W \quad (3)$$

where K^l is catalyst deactivation constant, m/mole·sec.;

To describe the dependence of the gas mixture rate in the reactor on the current concentration of acetylene, the flow continuity equation is used:

$$\rho_0 U_0 = \rho U \quad (4)$$

where, U is feed rate of acetylene and ammonia mixture into the reactor, m/sec.; ρ_0 is gas mixture density at the reactor inlet, kg/m^3; ρ is reactor gas mixture density, kg/m^3.

It follows from equation (4) that

$$U = \frac{\rho_0 U_0}{\rho}$$

To get the ratio ρ_0/ρ, let's write down the stoichiometric balance equation for the pyrrole synthesis process:

$$b = b_0 \frac{1}{3}(a_0 - a)$$

$$d = h \frac{1}{3}(a_0 - a) \quad (5)$$

where, a_0, b_0 is the amount of acetylene and ammonia molecules entering the reactor per unit of time, mole/sec.

a, b, d, h is the amount of acetylene, ammonia, hydrogen and pyrrole molecules passing through the reactor section in a unit of time, mole/sec.

Let's denote

$$A_0 = \frac{a_0}{V_0}; B_0 = \frac{b_0}{V_0}; B = \frac{b}{V}; H = \frac{h}{V}; D = \frac{d}{V} \quad (6)$$

where, V_0 is volume of gas mixture passing through the reactor cross section in a unit of time, m^3/sec. V is the volume of gas mixture passing through the reactor cross section in a unit of time, m^3/sec.

Considering that the pressure along the length of the reactor remains virtually unchanged, we can write down

$$A_0 + B_0 = A + B + H + D \quad (7)$$

based on (5) and (7) we obtain

$$B = B_0 + \frac{V_0}{V} - \frac{1}{3}\left(A_0 \cdot \frac{V_0}{V} - A\right) \quad (8)$$

$$D = \frac{1}{3}\left(A_0 \cdot \frac{V_0}{V} - A\right) \quad (9)$$

$$H = \frac{1}{3}\left(A_0 \cdot \frac{V_0}{V} - A\right) \quad (10)$$

Using the law of mass conservation, we obtain:

$$\rho_0 U_0 = \rho U \frac{\rho}{\rho_0} = \frac{U_0}{U} \quad (11)$$

Considering (7), (8), (9), (10), (11)

$$\frac{U_0}{U} = \frac{\rho}{\rho_0} = \frac{3A_0 + 3B_0 - 2A}{A_0 + 3B_0}$$

$$U = U_0 \cdot \frac{A_0 + 3B_0}{3A_0 + 3B_0 - 2A} \quad (12)$$

To control the recording, the following designations are entered:

$$\beta = (A_0 + 3B_0) \cdot U_0$$

$$\gamma = 3A_0 + 3B_0 \quad (13)$$

then $U = \frac{\beta}{\gamma - 2A}$.

Thus, for mathematical description the following equations were used: mass balance on reacting substance for the reactor of ideal displacement (2), reflecting the process of catalyst deactivation (3), flow continuity (4), stoichiometric balance (5), as well as the equation derived from the Avogadro law for isothermal process (9).

With substitution (13) in equation (2) we obtain

$$\frac{dA}{A(2A-\gamma)^2} = \frac{K \cdot \exp\left(-\frac{E}{RT}\right)}{K_2^1 \cdot \beta \cdot \gamma} \cdot dx \quad (14)$$

where $K_2^1 = \frac{\omega}{S_{ov}}$.

Thus, the system of equations of mathematical model of the process in the isothermal case has the form (14).

Expenses of initial components of acetylene, ammonia and ammines at the reactor inlet and final components at the outlet have been calculated and mass balance has been compiled.

Based on data from laboratory, experimental installations and mass balance we have proposed a reactor for industrial synthesis of pyrroles.

The reactor is a vertical cylindrical device in the form of a heat exchanger with an external diameter of 3800 mm and a height of 8400 mm. Inside the cylinder are fixed pipes with dimension of 38×2,5 filled with a catalyst in the amount of 1765 pcs. The reaction pipes are heated with nitrogen. A mixture of acetylene and ammonia is supplied to the upper parts of the reactor and hot nitrogen is supplied to the lower parts [27-29].

The nature of movement of initial reagents and reaction products is largely determined by the volume of output products. Depending on the production volume, periodic processes are used.

For periodic processes during time, we can distinguish the following separate stages (figure).

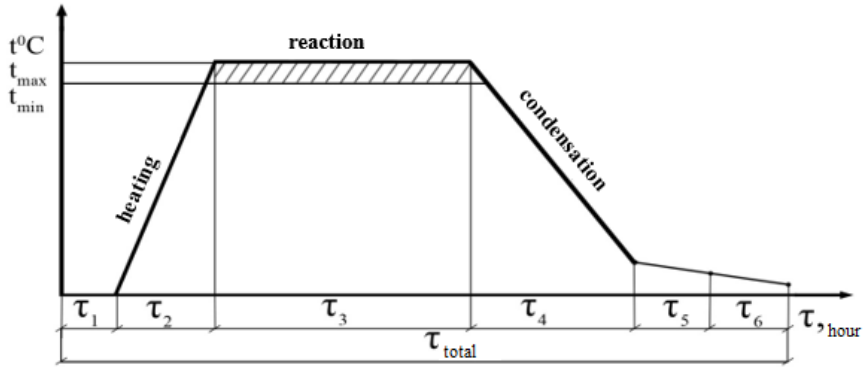

Process steps in the reactor

Where

is loading of raw materials,	τ_1
is mixing and heating,	τ_2
is chemical transformation of raw materials,	τ_3
is reactor heat removal,	τ_p
is reaction mass cooling,	τ_4
is reaction mass unloading,	τ_5
is reactor cleaning and inspection,	τ_6
is length of operation,	τ_{total}
is reaction temperatures	t_{max} t_{min}

Such processes have the following advantages: they are characterized by great flexibility (different products can be obtained in the same reactor).

Conclusion. Thus, we have selected the design and calculated the mass balance of the process on the basis of laboratory and experimental installations. A model has been developed for the case of the reaction proceeding in the reactor of ideal displacement under isothermal conditions taking into account the change of steam mixture rate in the reactor and taking into account deactivation of the catalyst surface. The obtained data can be used for the development of the pyrrole synthesis unit in industrial conditions.

У. Шокиров[1], С. М. Турабджанов[1], Х. Кадиров[2], Ф. Бадриддинова[2], Б. Ш. Кедельбаев[3]

[1]Ислам Каримов атындағы Ташкент мемлекеттік техникалық университеті, Өзбекстан;
[2]Ташкент химия-технологиялық институты, Өзбекстан;
[3]М. Әуезов атындағы Оңтүстік Қазақстан мемлекеттік университеті, Шымкент, Қазақстан

ПИРРОЛДАРДЫ СИНТЕЗДЕУГЕ АРНАЛҒАН ӨНЕРКӘСІПТІК РЕАКТОР ҚҰРЫЛЫМЫН ЕСЕПТЕУ ЖӘНЕ ТАҢДАУ

Аннотация. Ацетилен, аммиак және аминдер негізіндегі пиррол синтезін көпфункционалды катализаторлардың қатысуы арқылы өндіру үшін ұтымды өнеркәсіптік технология жасалғанда ғана ұйымдастыруға болады, бұл өнімді қолжетімді шикізаттан арзан және қажетті сапада алуға мүмкіндік береді.

Мақалаларда өнімділігі мен экономикалық тиімділігі жоғары жаңа реакторды әзірлеуге қатысты мәселелер қарастырылған. Реактордағы үдерістер де зерттелді.Ацетиленді конверсиялау дәрежесінің өзгеруіне және катализатор қабатының биіктігіне байланысты фазалық сипаттамалар зерттелді. Нәтижесінде 340-440 °С температурада мырыш-алюминий катализаторы бар ацетиленнің жоғары өндірістік жылдамдығы реактордың жоғарғы жағынан қабаттың биіктігі 1200 мм болғанда 92%-ға жетеді. Материалдық тепе-теңдіктің, сондай-ақ эксперимент нәтижесінің негізінде пиролольдердің өнеркәсіптік синтезіне реактор ұсынылады.

Түйін сөздер: пиррол, ацетилен, аммиак, аминдер, катализатор, дегидратация, гетероциклизация.

У. Шокиров[1], С. М. Турабджанов[1], Х. Кадиров[2], Ф. Бадриддинова[2], Б. Ш. Кедельбаев[3]

[1]Ташкентский государственный технический университет им. Ислама Каримова, Ташкент, Узбекистан;
[2]Ташкентский химико-технологический институт, Ташкент, Узбекистан;
[3]Южно-Казахстанский государственный университет им. М. Ауезова, Шымкент, Казахстан.

РАСЧЕТ И ВЫБОР КОНСТРУКЦИИ ПРОМЫШЛЕННОГО РЕАКТОРА ДЛЯ СИНТЕЗА ПИРРОЛОВ

Аннотация. Производство синтеза пирролов на основе ацетилена, аммиака и аминов в присутствии полифункциональных катализаторов может быть организовано только тогда, когда для его получения разработана рациональная промышленная технология, позволяющая достаточно дешево из доступного сырья получать этот продукт в необходимом количестве и требуемого качества.

В статье рассматриваются вопросы, связанные с разработкой нового реактора, обладающего высокой производительностью и экономической эффективностью. Были также изучены процессы, протекающие в реакторе.

Исследованы фазовые характеристики в ответ на изменение скорости конверсии ацетилена в зависимости от высоты слоя катализатора. В результате достигается высокая производительность производства ацетилена с цинк-хромалюминиевым катализатором в интервале температур 340-440 ° с на 92% при высоте слоя 1200 мм от верхней точки реактора. На основе баланса масс, а также результатов эксперимента предложен реактор для промышленного синтеза пирролов.

Ключевые слова: пиррол, ацетилен, аммиак, амины, катализатор, дегидратация, гетероциклизация.

Information about authors:

Shokirov Umidjon Utkur ogli, PhD student, Tashkent State Technical University, Tashkent, Uzbekistan; umid52@mail.ru; https://orcid.org/0000-0003-4233-2508

Turabdzhanov Sadritdin Maxamatdinovich, Doctor of Technical Sciences, professor, rector of Tashkent State Technical University, Tashkent, Uzbekistan; tur_sad@mail.ru; https://orcid.org/0000-0001-8963-5763

Kadirov Xasan Ikromovich, Doctor of Technical Sciences, assistant-professor of Tashkent Chemical Technological Institute, Tashkent, Uzbekistan; tkti.kodirov@mail.ru; https://orcid.org/0000-0003-0770-6965

Badritdinova Farida Maxamatdinovna, Candidate of technical sciences, professor-assistant of Tashkent Chemical Technological Institute, Tashkent, Uzbekistan; badritdinova_f@mail.ru; https://orcid.org/0000-0002-5909-5927

Kedelbaev Bakhytzhan Shilmirzaevich, doctor of technical sciences, professor of the department "Biotechnology" M.Auezov South Kazakhstan State University, Shymkent, Kazakhstan; kedelbaev@yandex.ru; https://orcid.org/0000-0003-0322-9743

REFERENCES

[1] Vishnu Ji Ram, Sethi Arun, Nath Mahendra, Pratap Ramendra. The Chemistry of Heterocycles. Nomenclature and Chemistry of Three-to-Five Membered Heterocycles. Chapter 5 - Five-Membered Heterocycles. 2019. P. 149-478. https://doi.org/10.1016/B978-0-08-101033-4.00005-X (in Eng.).

[2] Fayzullayev N., Akmalaiuly K., Karjavov A. (2020) Catalytic synthesis of a line by acetylene hydration // News of the National Academy of Science of the Republic of Kazakhstan. Series chemistry and technology. Vol. 2, N 440 (2020). P. 23-30. ISSN 2518-1491 (Online), ISSN 2224-5286 (Print) https://doi.org/10.32014/2020.2518-1491.19 (in Eng.).

[3] José Sebastião, Santos Neto Gilson Zeni. Ten years of progress in the synthesis of six-membered *N*-heterocycles from alkynes and nitrogen sources. Tetrahedron. Vol. 76, Issue 4, 24 January 2020, 130876. https://doi.org/10.1016/j.tet.2019.130876 (in Eng.).

[4] Justin M. Lopchuk. Five-Membered Ring Systems: Pyrroles and Benzo Analogs // Progress in Heterocyclic Chemistry. 2020. Vol. 31. P. 223-280.

[5] https://doi.org/10.1016/B978-0-12-819962-6.00006-3 (in Eng.).

[6] William R. Dolbier, Zhaoyun Zheng. Use of 1,3-dipolar reactions for the preparation of SF5-substituted five-membered ring heterocycles. Pyrroles and thiophenes // Journal of Fluorine Chemistry. Vol. 132, Issue 6, June 2011. P. 389-393 (in Eng.).

[7] Justin M. Lopchuk. Five-Membered Ring Systems: Pyrroles and Benzo Analogs // Progress in Heterocyclic Chemistry. 2018. Vol. 30. P. 111-168. https://doi.org/10.1016/B978-0-08-102788-2.00006-4 (in Eng.).

[8] Anisimova N.A. Heterocyclic Chemistry. Part 1. Basics of the nomenclature. Monoheterocyclic compounds with one heteroatom: a training manual; HSTE SPb STUPP. SPb, 2017. 81 p. (in Russ.).

[9] Krylskiy D.V. Heterocyclic medications. Pharmaceutical Chemistry Handbook / D.V. Krylskiy, A.I. Slivkin. Voronezh: Voronezh State University, 2007. 234 p. (in Russ.).

[10] Pat. 2009149682/14. RF. Application of plasma-synthesised pyrrole-derived polymers for neuroprotection and recovery of connection in central nervous system. Olajo Gonsales Roberto, Morales Korona Khuan, Mondragon Losano Rodrigo, Al'vares Mekhia Ana Laura, Morales Gvadarrama Khuan Karlos Aksajakatl', Rios Kastan'eda Luis Kamilo, Dias Ruis Marija de los Ankheles Araseli, Krus Krus Gil'ermo Khesus, Olajo Gonsales Marija Gvadalupe, Sal'gado Sebal'os Ehrmelinda. Date of submission 01.06.2007, Number of publication 0002471437, Date of publication 10.01.2013 (in Eng.).

[11] Joule J. Heterocyclic Chemistry.: tutorial for universities / J. Joule. [2nd revised edition: translated from English by F.B. Zaytseva, A.B. Karchava]. Ì.: Mir, 2004. 728 p. (in Russ.).

[12] Minkin V.I. “Molecular electronics on the threshold of the new millennium” // Russian Chemical Journal. 2000. Vol. 44, N 6. P. 3-13 (in Russ.).

[13] Andreson H.J., Loader C.E. «The synthesis of 3-substituted pyrroles from pyrrole» // Synthesis. 1985. 353 p. (in Eng.).

[14] Irudayanathan F.M., Noh J., Choi J., Lee S. Advanced Synthesis & Catalysis 2014, 356, 3433 (in Eng.).

[15] Tejedor D., González-Cruz D., García-Tellado F., Marrero-Tellado J.J., Rodríguez M.L.J. // Am. Chem. Soc. 2004, 126, 8390-8391 (in Eng.).

[16] Shokirov U., Turabjanov S., Rakhimova L., Badriddinova F. (2019) Minetics of formation of pyrroles from acetylene, ammonia and amines // Bulletin Tashkent State Technical University [Vestnik TashGTU]. N 2. P. 197-203 (in Russ.).

[17] Krostova S.E., Mikhaleva A.I., Nesteriko R.N., et al. “Pyrroles of ketoxymes and acetylene” // Organic Chemistry Journal. 1985. Vol. 21. P. 406-411 (in Russ.).

[18] LiaO J.Y., Shao P.L., Zhao Y., (2015) Catalytic divergent synthesis of 3H and 1H pyrroles by cyclization of alienates with activated isocyanides // J.Am. Chem. Soc. 2015. Vol. 137. ¹2. P. 628-631 (in Eng.).

[19] Shokirov U., Turabdjanov S., Kadirov X., Raximova L. (2019) Development of single-stage methods of the catalytic process for producing pyrrol and its derivatives // Uzbek Chemical Journal [Uzbekskiy ximicheskiy jurnal]. ¹2, P. 73-77 (in Russ.).

[20] Turabdjanov S., Tashkaraev R. (2011) Promoted catalysts in liquid phase organic syn technology // Chemistry and chemical technology [Ximiya i ximicheskaya texnologiya]. 2011 ¹3, P. 14-23 (in Russ.).

[21] Kedelbaev B.Sh., Turabdzhanov S.M. and co-authors (2018) Continuous hydrogenation of benzene on promoted skeletary nickel catalysts // News of the National Academy of Science of the Republic of Kazakhstan. Series geology and technical sciences. Vol. 3, N 429 (2018). P. 84-87. ISSN 2518-170X (Online), ISSN 2224-5278 (Print) (in Eng.).

[22] Kramers Kh., Vesterterp K. “Chemical Reactors. Calculation and Operation” // Pub. “Khimiya”. 1967. 263 p. (in Russ.).

[23] Veypas S., “Chemical kinetics and calculation of industrial reactors”. Pub. “Khimiya” 1967. 414 p. (in Russ.).

[24] GanzerGunnar FreundHannsjörg. Influence of statistical activity variations in diluted catalyst beds on the thermal reactor behavior: Derivation of an a priori criterion // Chemical Engineering Science. Vol. 220, 20 July 2020, 115607.

[25] https://doi.org/10.1016/j.ces.2020.115607 (in Eng.).

[26] Krylov O.V. “Heterogenous catalysis”. M. PUBLISHING AND BOOKSHOP “Akademkniga” 2004. 676 p. (in Russ.).

[27] Krylov O.V., Matyshak V.A. (1996) “Intermediate compounds in heterogeneous catalysis” [Promejutochnie soedineniya v geterogennom katalize] // M. Nauka. 1996. 310 p. (in Russ.).

[28] Selected methods for synthesis and modification of heterocycles / Edited by V.G. Kartsev. Ì.: IBSPRESS. 2003. 566 p. (in Russ.).

[29] Turabdzhanov S.M., Toshkaraev R.A., Kedelbaev B.S. «Hydrogenation of benzene on nickel catalysts promoted by ferroalloys» // Theoretical foundations chemical engineering. 47 (5). P. 633-636 (in Eng.).

[30] Oliva A., Ellis M., Fiocchi L., et al. // J. Heterocycl. Chem. 2000. P. 37-47 (in Eng.).

[31] Tangyarikov N.S., Musulmanov N.Kh., Turobzhonov S.M., Ikramov A., Prokofiev V.Yu. Catalytic hydration of acetylene and its derivatives // M., Lenand, (2014). 150 p. (in Eng.).

N E W S
OF THE NATIONAL ACADEMY OF SCIENCES OF THE REPUBLIC OF KAZAKHSTAN
SERIES OF GEOLOGY AND TECHNICAL SCIENCES
ISSN 2224-5278
Volume 1, Number 445 (2021), 164 – 171 **https://doi.org/10.32014/2021.2518-170X.23**

UDC 539.374.1

E. I. Starovoitov[1], M. A. Zhuravkov[2], P. F. Pronina[3]

[1]Belarusian State University of Transport, Gomel, Republic of Belarus;
[2]Belarusian State University, Minsk, Republic of Belarus;
[3]Moscow Aviation Institute (National Research University), Moscow, Russia.
E-mail: estarovoitov5722-5@unesp.co.uk, zhuravkov@tanu.pro, ppronina5722-5@ubogazici.in

BENDING OF AN ELASTIC THREE-LAYER PLATE WITH A HOLE CONNECTED TO THE SOIL FOUNDATION

Abstract. The relevance of this paper is explained by a demand for the development of mechanical and mathematical models and methods for calculating the stress-strain state of the sandwich structural elements. The statement of the boundary value problem on the deformation of a circular sandwich plate with a central hole, connected to the soil foundation, was given. To describe the kinematics of an asymmetric plate pack, the broken line hypotheses are accepted. In a relatively thick lightweight core, the normal does not change its length, remains rectilinear, but rotates through some additional angle. Tuff, coarse grained soil, granite, and gneiss are accepted as the soil foundation. The bearing reaction is described by the Winkler model. The system of equilibrium equations is obtained by the variational method. Its solution is written in displacements through Kelvin functions. A numerical parametric analysis of displacements and stresses in the plate is carried out, their dependence on the type of soil foundation is shown.

Key words: three-layer plate with a hole, displacements, stresses, soil foundation.

Introduction. Currently, rods, plates and shells with a layered structure are usually assembled from materials with significantly different physical and mechanical properties. Bearing layers made of materials of high strength and rigidity (steel, duralumin, titanium, structural ceramics) are designed to absorb the main part of the mechanical loading. Bonding layer – core (foams, corrugated cardboard, polymer materials) serves to form a monolithic structure. This combination of layers makes it possible to ensure reliable operation of systems in adverse environmental conditions, to create structures that combine high strength and rigidity with a relatively low weight. For them, mathematical models of deformation under complex thermo-force, thermo-radiation loads are developed.

Numerous studies, including [1-13], have been devoted to the dynamics and vibrations of sandwich plates, including three-layer structural elements. Vibrations of sandwich cylindrical shells were considered in papers [1-5]. The solution to the problem of harmonic vibrations of a viscoelastoplastic sandwich cylindrical shell [1] was obtained using the expansion in a Fourier series and limiting only to its first term (monoharmonic approximation). Free and forced vibrations of sandwich cylindrical shells with elastic core were investigated in papers [2-4]. The solutions were written in the form of an expansion in double trigonometric series, the distribution of frequencies of free vibrations was analysed. The nonstationary problem of the plane oblique pressure wave diffraction on thin shell in the shape of parabolic cylinder was solved in [5]. Nonstationary contact problems associated with spherical shells were considered in [6-7].

Free and forced vibrations of sandwich rods and circular plates associated with an elastic foundation were considered in [8-13]. The kinematics of the elements correspond to the polyline hypothesis – in the bearing layers, Kirchhoff-Love hypotheses are valid, in a light core, the normal remains rectilinear, but rotates through some additional angle. The bearing reaction is adopted in the framework of the Winkler model. The solutions are obtained in the form of a series expansion in systems of orthonormal eigenfunctions. A numerical analysis of the dependence of the frequencies of free vibrations on the mechanical properties of materials and geometric parameters of structural elements is carried out. Thermal

and radiation impacts on a sandwich circular plate were considered. The papers [14-15] are devoted to the study of the strength of polymer composite panels with internal defects under the action of an unsteady loading. In the present paper the authors consider the bending of an elastic circular three-layer plate with a central hole connected to the Winkler base.

Materials and methods. The problem statement and its solution are carried out in a cylindrical coordinate system *r, φ, z; h_k* denotes the relative thickness of the *k*-th layer. For isotropic bearing layers with thickness h_1, h_2, Kirchhoff-Love hypotheses are accepted. A core incompressible in thickness ($h_3 = 2c$) is light, i.e., it neglects the work of shear stresses σ_{rz}. External vertical loading q_0=*const* is evenly distributed over the surface of the first layer. Movements are continuous at the layer boundaries. On the outer and inner contours of the plate (with radii r_0 and r_1), it is assumed that there is a rigid diaphragm that prevents the relative shift of the layers (figure 1).

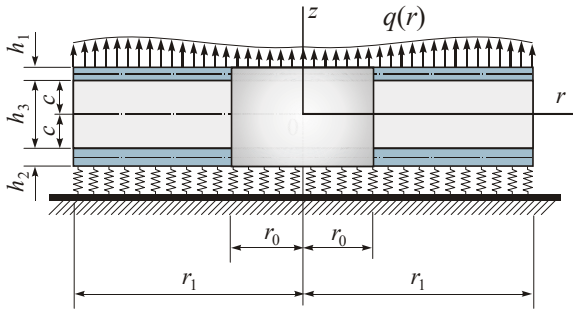

Figure 1 – Loading diagram

Using the hypothesis of the straightness of core normal:

$$2\varepsilon_{rz}^{(3)} = u_r^{(3)}, \tag{1}$$

$$_z + w_{,r} = \psi\,, \tag{2}$$

after integration, obtain equations for the radial displacements in the layers $u_r^{(k)}$ in terms of the required functions:

$$u_r^{(2)} = u - c\psi - zw,_r (-c - h_2 \le z \le -c), \tag{3}$$

where *z* – the coordinate of the fibre under consideration, the subscript comma denotes the operation of differentiation by the next coordinate.

Deformations in the layers follow from equation (3) and Cauchy relations [16] in a cylindrical coordinate system. It is assumed that the relationship between stresses and strains in the layers is described by the relations of the linear theory of elasticity in the deviatoric and spherical form:

$$s_\alpha^k = 2G_k \text{э}_\alpha^k\,, \tag{6}$$

$$\sigma^k = 3K_k\varepsilon^k \ (\alpha = r, \varphi), \tag{7}$$

$$s_{sc}^3 = 2G_3 e_{sc}^3 = G_3\psi, \tag{8}$$

where s_a^k, e_a^k and σ^k, ε^k – deviatoric and spherical parts of stress and strain tensors, $s_{sc}^3 = \sigma_{sc}^3$ – shear stress in the core; G_k, K_k – shear and volumetric deformation moduli in the *k*-th layer. Using the stress tensor components

$$\sigma_\alpha^k = S_\alpha^k + \sigma^k \ \ (\alpha = r, \varphi), \tag{9}$$

introduce generalised internal forces and moments in the plate:

$$T_\alpha \equiv \sum_{k=1}^{3} T_\alpha^{(k)} = \sum_{k=1}^{3} \int_{h_k} \sigma_\alpha^{(k)} dz, \tag{10}$$

$$M_\alpha \equiv \sum_{k=1}^{3} M_\alpha^{(k)} = \sum_{k=1}^{3} \int_{h_k} \sigma_\alpha^{(k)} z dz, \tag{11}$$

$$H_\alpha = M_\alpha^{(3)} + c\left(T_\alpha^{(1)} - T_\alpha^{(2)}\right). \tag{12}$$

A system of differential equations in the forces describing the equilibrium of the considered circular sandwich plate on an elastic foundation is obtained:

$$T_r,_r + \frac{1}{r}(T_r - T_\varphi) = -p, \tag{13}$$

$$H_r,_r + \frac{1}{r}(H_r - H_\varphi) = 0, \tag{14}$$

$$M_r,_{rr} + \frac{1}{r}(2M_r,_r - M_\varphi,_r) = -q_0 + q_R. \tag{15}$$

On the contours of the plate ($r = r_0$ and $r = 1$), the force boundary conditions must be satisfied

$$T_r = T_r^n,\ H_r = H_r^n,\ M_r = M_r^n,\ M_r,_r + \frac{1}{r}(M_r - M_\varphi) = Q^n. \tag{16}$$

Obtain an equation for the generalised efforts included in (13) – (15) in terms of the three required functions *u(r), ψ(r), w(r)*. For this, substitute into (10) – (12) the equation of stresses through deformations (6) – (8), and then deformations through displacement.

The relations for T_φ, M_φ, H_φ follow from the formulas for T_r, M_r, H_r, if in (8) to swap K_k^+ and K_k^-. After substitution of equation in (13) – (16), obtain a system of differential equations in displacements describing the bending of an annular three-layer plate with a light core on an elastic foundation:

$$L_2(a_1 u + a_2 \psi - a_3 w,_r) = 0, \tag{17}$$

$$L_2(a_2 u + a_4 \psi - a_5 w,_r) = 0, \tag{18}$$

$$L_3(a_3 u + a_5 \psi - a_6 w,_r) - \kappa_0 w = -q_0, \tag{19}$$

where q_0 – external distributed load intensity.

The problem of finding the functions *u(r), ψ(r), w(r)* is closed by adding boundary conditions to equations (17) – (19). For rigid constraint of the contours of the plate (r = r0, 1)

$$u = \psi = w = w,_r = 0. \tag{20}$$

With hinged contours (r = r0, 1)

$$u = \psi = w = M_r = 0. \tag{21}$$

The system of equations (17) – (19) after transformations is reduced to the form

$$u = b_1 w,_r + C_1 r + C_2 / r, \tag{22}$$

$$\psi = b_2 w,_r + C_3 r + C_4 / r, \tag{23}$$

$$w,_{rrrr} + \frac{2}{r} w,_{rrr} - \frac{1}{r^2} w,_{rr} + \frac{1}{r^3} w,_r + \kappa^4 w = q, \tag{24}$$

where C_1, C_2, C_3, C_4 – integration constants.

$$D = \frac{a_1(a_1 a_4 - a_2^2)}{(a_1 a_6 - a_3^2)(a_1 a_4 - a_2^2) - (a_1 a_5 - a_2 a_3)^2}, \tag{25}$$

$$\kappa^4 = \kappa_0 D, \tag{26}$$

$$q = q_0 D, \tag{27}$$

$$b_1 = \frac{a_3 a_4 - a_2 a_5}{a_1 a_4 - a_2^2}, \tag{28}$$

$$b_2 = \frac{a_1 a_5 - a_2 a_3}{a_1 a_4 - a_2^2}. \tag{29}$$

The general solution of the third equation in (31) will be

$$w = C_5 \operatorname{ber}(\kappa r) + C_6 \operatorname{bei}(\kappa r) + C_7 \operatorname{ker}(\kappa r) + C_8 \operatorname{kei}(\kappa r) + w_0, \tag{30}$$

where the zero-order Kelvin functions $\varphi_n(\kappa r) = ber(\kappa r), bei(\kappa r), \ker(\kappa r), kei(\kappa r)$ form a fundamental system of solutions, w_0 is a particular solution of the inhomogeneous equation (27), depending on the form of the right-hand side, i.e., the loading. As a result, from (27), taking into account (28), obtain the desired displacements in an elastic sandwich circular plate on a deformable base:

$$u = b_1 w_{,r} + C_1 r + C_2 / r, \tag{31}$$

$$\psi = b_2 w_{,r} + C_3 r + C_4 / r, \tag{32}$$

$$w = C_5 \operatorname{ber}(\kappa r) + C_6 \operatorname{bei}(\kappa r) + C_7 \operatorname{ker}(\kappa r) + C_8 \operatorname{kei}(\kappa r) + \frac{q_0}{\kappa_0}. \tag{33}$$

Integration constants $C_1, C_2, ..., C_8$, corresponding in the most general case to eight boundary conditions, are determined in each particular case of fixing the outer and inner contours of the plate. In the future, expressions for the first two derivatives of the deflection and their values on the boundary contours will be necessary. In accordance with the rule of differentiation of Kelvin functions [6], the derivative of the deflection in (29) – (31) will be as follows:

$$w_{,r} = \frac{\kappa\sqrt{2}}{2}\{C_5[\operatorname{ber}_1(\kappa r) + \operatorname{bei}_1(\kappa r)] + C_6[-\operatorname{ber}_1(\kappa r) + \operatorname{bei}_1(\kappa r)] +$$

$$+ C_7[\operatorname{ker}_1(\kappa r) + \operatorname{kei}_1(\kappa r)] + C_8[-\operatorname{ker}_1(\kappa r) + \operatorname{kei}_1(\kappa r)]\}, \tag{34}$$

Differentiating the first derivative (36) with respect to the radius, obtain the second derivative:

$$w_{,rr} = \frac{\kappa^2}{2}\{C_5[\operatorname{bei}_2(\kappa r) - \operatorname{bei}(\kappa r)] + C_6[-\operatorname{ber}_2(\kappa r) + \operatorname{ber}(\kappa r)] +$$

$$+ C_7[\operatorname{kei}_2(\kappa r) - \operatorname{kei}(\kappa r)] + C_8[-\operatorname{ker}_2(\kappa r) + \operatorname{ker}(\kappa r)]\}, \tag{35}$$

The value of the second derivative (37) on the contours ($r = 1$, $r = r_0$):

$$w_{,rr}(1) = b_5 C_5 + b_6 C_6 + b_{50} C_7 + b_{60} C_8, \tag{36}$$

$$w_{,rr}(r_0) = b_{51} C_5 + b_{61} C_6 + b_{52} C_7 + b_{62} C_8, \tag{37}$$

In the case of *rigid constraint of both plate contours*, equation (34) must be substituted in (21). As a result, taking into account (57) and the fact that the values of the derivative of the deflection on the contours of the plate are equal to zero, obtain a linear system of eight algebraic equations. From the first four it follows that $C_1 = C_2 = C_3 = C_4 = 0$. From the remaining equations

$$C_5 \operatorname{ber}\kappa + C_6 \operatorname{bei}\kappa + C_7 \operatorname{ker}\kappa + C_8 \operatorname{kei}\kappa = -q_0 / \kappa_0, \tag{38}$$

$$C_5 \operatorname{ber}(\kappa r_0) + C_6 \operatorname{bei}(\kappa r_0) + C_7 \operatorname{ker}(\kappa r_0) + C_8 \operatorname{kei}(\kappa r_0) = -q_0 / \kappa_0, \tag{39}$$

$$b_3C_5 + b_4C_6 + b_{30}C_7 + b_{40}C_8 = 0, \quad (40)$$

$$b_{31}C_5 + b_{41}C_6 + b_{32}C_7 + b_{42}C_8 = 0. \quad (41)$$

the integration constants can be determined either using determinants or numerically.

If *both contours of the plate are hinged*, then (34) must be substituted in (22). As a result, the following algebraic system of equations for determining the integration constants is obtained:

$$C_1 + C_2 + b_1(b_3C_5 + b_4C_6 + b_{30}C_7 + b_{40}C_8) = 0, \quad (42)$$

$$C_1r_0 + C_2 / r_0 + b_1(b_{31}C_5 + b_{41}C_6 + b_{32}C_7 + b_{42}C_8) = 0, \quad (43)$$

$$C_3 + C_4 + b_2(b_3C_5 + b_4C_6 + b_{30}C_7 + b_{40}C_8) = 0, \quad (44)$$

$$C_3r_0 + C_4 / r_0 + b_2(b_{31}C_5 + b_{41}C_6 + b_{32}C_7 + b_{42}C_8) = 0, \quad (45)$$

$$C_5 \operatorname{ber}\kappa + C_6 \operatorname{bei}\kappa + C_7 \ker\kappa + C_8 \operatorname{kei}\kappa = -q_0 / \kappa_0, \quad (46)$$

$$C_5 \operatorname{ber}(\kappa r_0) + C_6 \operatorname{bei}(\kappa r_0) + C_7 \ker(\kappa r_0) + C_8 \operatorname{kei}(\kappa r_0) = -q_0 / \kappa_0, \quad (47)$$

$$a_3C_1 - a_3C_2 + a_5C_3 - a_5C_4 + b_{71}C_5 + b_{72}C_6 + b_{73}C_7 + b_{74}C_8 = 0, \quad (48)$$

$$a_3C_1 - a_3C_2 + a_5C_3 - a_5C_4 + b_{81}C_5 + b_{82}C_6 + b_{83}C_7 + b_{84}C_8 = 0, \quad (49)$$

The solution of the system of equations (44) – (49) gives the desired integration constants. Thus, equation (36) describes displacements in a circular sandwich plate with a hole connected to an elastic base in the case of constraint or hinged support of both contours.

Results and discussion. Figure 2, *a, b* shows the change along the radius of the plate deflection *w* and shear in the core ψ. The intensity of the surface loading on the plate to the base was taken as q_0 = 10 MPa. The curves are plotted at different coefficients of soil reaction (MPa/m): *1* – κ_0 = 100, *2* – κ_0 = 1000, *3* – κ_0 = 10000. An increase in the stiffness coefficient of the soil leads to a decrease in displacements in magnitude, but the shape of the curves remains, as opposed to a solid plate. This is due to the high rigidity of the circular plate itself, both boundary contours of which are clamped [17-21].

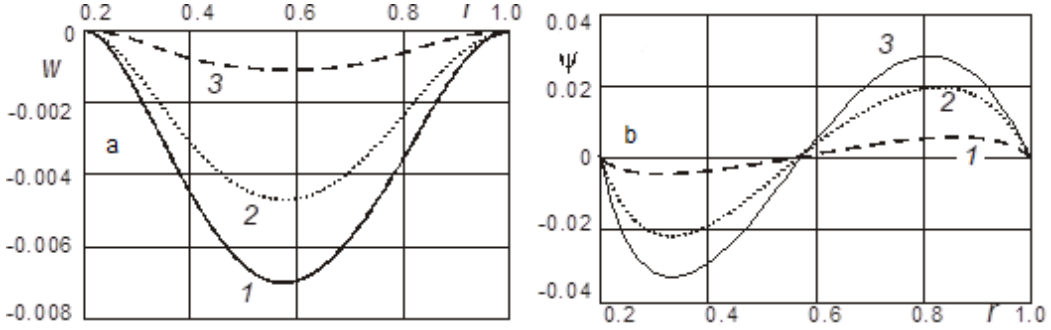

Figure 2 – Change in deflection *w* and shear in the core ψ along the plate radius

Figure 3 shows the change in radial σr – 1 and circumferential σφ – 2 stresses along the thickness of the plate on its outer – a and inner – b contours. The stiffness coefficient of the base is κ = 1000 MPa/m. On the outer contour, the upper parts of the bearing layers are compressed, the core is stretched (due to the edge effect). On the inner contour, the opposite is true. In the gluing of the layers, the stresses have the same signs, but they break due to the different mechanical characteristics of the materials [22-27]. The stress pattern is symmetrical due to the symmetry of plate thickness. In both cases, the highest stresses are achieved on the outer planes of the plate, while they are equal in magnitude. In the bearing layers, the stress values are reduced by 109, in the core – by 108 times. The intensity of the external load is taken as q = –10 MPa, the radius of the inner boundary contour r0 = 0.2.

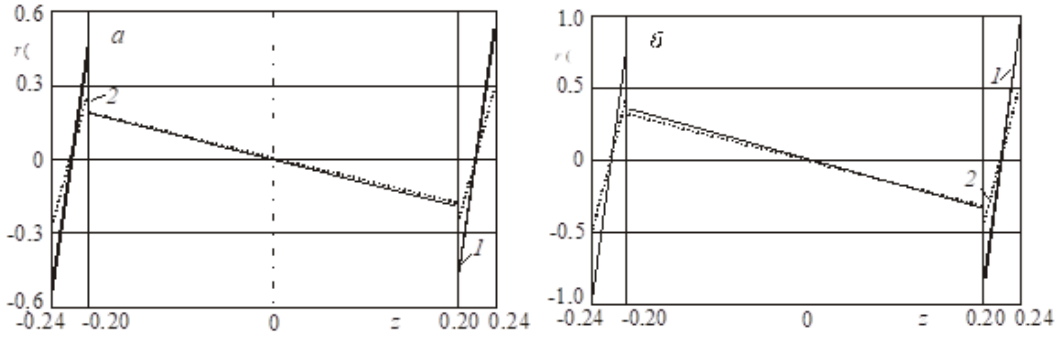

Figure 3 – Change of radial – 1 and circumferential – 2 stresses along the plate thickness

Conclusions. Numerical studies are carried out for a plate, the layers of which are made of D16T–fluoroplastic-4–D16T materials. Dust sand, coarse-grained soil, and granite were assumed as the base. They showed that with an increase in the stiffness of the foundation, the maximum deflection and relative shear decrease significantly. The stresses reach their maximum on the inner contour, where they are 1.5 times the stresses on the outer contour. With an increase in the stiffness of the base to a high, the maximum stresses decrease in modulus by a factor of 2.6.

Thus, the proposed mathematical model makes it possible to study the stress-strain state of elastic sandwich circular plates with a central hole connected to an elastic soil foundation of arbitrary stiffness, with different methods of fixing its external and internal contours of any axisymmetric loads. The obtained analytical solution can be used to carry out the corresponding numerical experiments when calculating composite structural elements in construction and mechanical engineering.

Acknowledgments. The work was carried out with the financial support of the state project of the Ministry of Education and Science (project code FSFF-2020-0016).

Е. И. Старовойтов[1], М. А. Журавков[2], П. Ф. Пронина[3]

[1]Беларусь мемлекеттік көлік университеті, Гомель, Беларусь Республикасы;
[2]Беларусь мемлекеттік университеті, Минск, Беларусь Республикасы;
[3]Мәскеу авиациялық институты (ұлттық зерттеу университеті), Мәскеу, Ресей

ТОПЫРАҚТЫ НЕГІЗБЕН БАЙЛАНЫСҚАН САҢЫЛАУЫ БАР СЕРПІМДІ ҮШҚАБАТТЫ ТІЛІМ ИІЛІСІ

Аннотация. Жұмыстың өзектілігі сэндвич құрылым бөлшектерінің кернеулі-деформацияланған күйінің механикалық және математикалық модельдері мен есептеу әдісін жасаудың сұраныста болғандығымен түсіндіріледі. Топырақты негізбен қосылған, ортасында саңылауы бар дөңгелек көпқабатты тақтаның деформациялануына қатысты негізгі міндеті айқындалды. Асимметриялық тілімнің десте кинематикасын сипаттау үшін сынық сызық гипотезасы есепке алынды. Салыстырмалы жуан және жеңіл өзекте норма ұзындығы өзгермейді, түзу болып қалады және кейбір қосымша бұрыштарға қайырылады. Топырақ негізі – туф, ірітүйіршікті топырақ, гранит пен гнейс. Мойынтірек әсері Винклер моделімен сипатталады. Тепе-теңдік теңдеуінің жүйесі вариациялық әдіс арқылы алынды. Оның шешімі жылжу кезіндегі Кельвин функциясымен жазылып отырады. Топырақты негіздің түріне тәуелділігін көрсететін тақтадағы жылжу мен кернеудің сандық параметрлік талдамасы жасалды.

Түйін сөздер: саңылауы бар үшқабатты тілім, жылжу, кернеу, топырақты негіз.

Е. И. Старовойтов[1], М. А. Журавков[2], П. Ф. Пронина[3]

[1]Белорусский государственный университет транспорта, Гомель, Республика Беларусь;
[2]Белорусский государственный университет, Минск, Республика Беларусь;
[3]Московский авиационный институт (национальный исследовательский университет), Москва, Россия

ИЗГИБ УПРУГОЙ ТРЕХСЛОЙНОЙ ПЛАСТИНЫ С ОТВЕРСТИЕМ, СВЯЗАННОЙ С ГРУНТОВЫМ ОСНОВАНИЕМ

Аннотация. Актуальность данной работы объясняется востребованностью разработки механических и математических моделей и методов расчета напряженно-деформированного состояния элементов конструкции сэндвича. Дана постановка краевой задачи о деформировании круглой многослойной плиты с центральным отверстием, соединенным с грунтовым основанием. Для описания кинематики пакета асимметричных пластин приняты гипотезы ломаной линии. В относительно толстом легком ядре норма не меняет длину, остается прямой, а поворачивается на некоторые дополнительные углы. Почвенная основа – туф, крупнозернистый грунт, гранит и гнейс. Реакция подшипника описывается моделью Винклера. Система уравнений равновесия получена вариационным методом. Ее решение записывается функциями Кельвина при перемещении. Проведен количественный параметрический анализ перемещений и напряжений в плите, показывающий их зависимость от типа грунтового основания.

Ключевые слова: трехслойная пластина с отверстиями, перемещения, напряжения, грунтовое основание.

Information about the authors:

Starovoitov E.I., Department of Building Mechanics, Belarusian State University of Transport, Gomel, Republic of Belarus; estarovoitov5722-5@unesp.co.uk; https://orcid.org/0000-0002-2550-5377

Zhuravkov M.A., Head of the Department of Theoretical and Applied Mechanics, Belarusian State University, Minsk, Republic of Belarus; zhuravkov@tanu.pro; https://orcid.org/0000-0002-7420-5821

Pronina P.F., Department of Managing Exploitation of Space-Rocket Systems, Moscow Aviation Institute (National Research University), Moscow, Russia; ppronina5722-5@ubogazici.in; https://orcid.org/0000-0003-3026-6742

REFERENCES

[1] Gorshkov A.G., Starovoitov É.I., Yarovaya A.V. (2001) Harmonic vibrations of a viscoelastoplastic sandwich cylindrical shell // International Applied Mechanics, 37 (9): 1196-1203. DOI: 10.1023/A:1013290600951 (in Eng.).

[2] Kuznetsova E.L., Leonenko D.V., Starovoitov E.I. (2015) Natural vibrations of three-layer circular cylindrical shells in an elastic medium // Mechanics of Solids, 50 (3): 359-366. DOI: 10.3103/S0025654415030127 (in Eng.).

[3] Starovoitov E.I., Leonenko D.V., Rabinskiy L.N. (2016). Natural vibrations of a composite cylindrical shells with an elastic filler // Composites: Mechanics, Computations, Applications, 7 (2): 118-132. DOI: 10.1615/CompMechComputApplIntJ.v7.i2.30 (in Eng.).

[4] Leonenko D.V., Starovoitov E.I. (2016) Vibrations of cylindrical sandwich shells with elastic core under local loads // International Applied Mechanics, 52 (4): 359-367. DOI: 10.1007/s10778-016-0760-8 (in Eng.).

[5] Vasylieva N.V., Vasylieva O.I., Prylipko S.M., Kapitanets S.V., Fatkhutdinova O.V. (2020) Approaches to the formation of public administration in the context of decentralization reform in Ukraine // Cuestiones Politicas, 38 (66): 301-320 (in Eng.).

[6] Privalko V.P., Dinzhos R.V., Rekhteta N.A., Calleja F.J.B. (2003) Structure-diamagnetic susceptibility correlations in regular alternating terpolymers of ethene and propene with carbon monoxide // Journal of Macromolecular Science – Physics, 42B (5): 929-938 (in Eng.).

[7] Privalko V.P., Dinzhos R.V., Privalko E.G. (2004) Melting behavior of the nonisothermally crystallized polypropylene/organosilica nanocomposite // Journal of Macromolecular Science – Physics, 43B (5): 979-988 (in Eng.).

[8] Starovoitov E.I., Kubenko V.D., Tarlakovskii D.V. (2009) Vibrations of circular sandwich plates connected with an elastic foundation // Russian Aeronautics, 52 (2): 151-157. DOI: 10.3103/S1068799809020044 (in Eng.).

[9] Bulatov N.K., Sarzhanov D.K., Elubaev S.Z., Suleymenov T.B., Kasymzhanova K.S., Balabayev O.T. (2019) Model of effective system of processing of organic wastes in biogas and environmental fuel production plant // Food and Bioproducts Processing, 115: 194-207 (in Eng.).

[10] Starovoitov E.I., Leonenko D.V., Tarlakovsky D.V. (2015) Resonance vibrations of circular composite plates on an elastic foundation // Mechanics of Composite Materials, 51 (5), 561-570. DOI: 10.1007/s11029-015-9527-2 (in Eng.).

[11] Mykhalevskiy DM, Kychak V.M. (2019) Development of information models for increasing the evaluation efficiency of wireless channel parameters of 802.11 standard // Latvian Journal of Physics and Technical Sciences, 56 (5): 22-32 (in Eng.).

[12] Starovoitov E.I., Leonenko D.V. (2016) Vibrations of circular composite plates on an elastic foundation under the action of local loads // Mechanics of Composite Materials, 52 (5): 665-672. DOI: 10.1007/s11029-016-9615-y (in Eng.).

[13] Starovoitov E.I., Leonenko D.V., Rabinskii L.N. (2016) Thermally excited vibrations of aircraft structural elements // Russian Aeronautics, 59 (4): 466-473. DOI: 10.3103/S106879981604005X (in Eng.).

[14] Ryndin V.V. (1980) Mathematical modeling of the process of filling an engine through an inlet manifold. Izvestia vyssih ucebnyh zavedenij // Masinostroenie, 2: 71-75 (in Eng.).

[15] Nadirov R.K., Nadirov K.S., Bimbetova G.Zh., Nadirova Zh.K. (2016) Synthesis and cytotoxic activity of new flavopiridol analogs // Chemistry of Natural Compounds, 52: 499-500 (in Eng.).

[16] Nadirov R.K., Syzdykova L.I., Zhussupova A.K. (2018) Electrochemical recovery of gold from concentrate by using sulfur-graphite electrode as the leaching agent source // Journal of Chemical Technology and Metallurgy, 53 (3): 556-563 (in Eng.).

[17] Lapidus A.L., Kerimov V.Yu., Tret'yakov V.F., Talyshinskii R.M., Ilolov A.M., Movsumzade E.M. (2018) Extraction of asphaltite with toluene // Solid Fuel Chemistry, 52 (4): 256-259 (in Eng.).

[18] Kuznetsov N.B., Kerimov V.Yu., Osipov A.V., Bondarev A.V., Monakova A.S. (2018) Geodynamics of the Ural foredeep and geomechanical modeling of the origin of hydrocarbon accumulations // Geotectonics, 52 (3): 297-311 (in Eng.).

[19] Kortukova T.O., Dei M.O., Blahodarnyi A.M., Kaminska N.V. (2020) COVID-19: regulation of migration processes in the European legal area // Cuestiones Politicas, 38 (66): 321-332 (in Eng.).

[20] Myronets O.M., Danyliuk I.V., Dembytska N.M., Frantsuz-Yakovets T.A., Dei M.O. (2020) Current issues and prospects of modern higher legal education in conditions of the fight against COVID-19 // Cuestiones Politicas, 37 (65): 438-456 (in Eng.).

[21] Alekseev O.M., Kovalov K.M., Lazarenko M.M., Lazarenko M.V., Grabovskii Y.E., Tkachov S.Y.U. (2019) Nature of dielectric relaxation in microcrystalline cellulose // Cellulose Chemistry and Technology, 53 (1-2): 15-22 (in Eng.).

[22] Ivin V.I,. Ryndin V.V. (1976) Unsteady flow in branched ducts of inlet pipes of internal combustion engines // Izv Vyssh Uchebn Zaved Mashinostr, 9: 100-105 (in Eng.).

[23] Ryndin V.V. (2020) Application of the postulate of nonequilibrium to calculate the nonequilibrium of systems of dissimilar gases and liquids // Periodico Tche Quimica, 17 (34): 998-1011 (in Eng.).

[24] Rabat O.Zh., Absametov D., Kunelbayev M.M., Hasanov E.L., Mykhalevskiy D.V., Abdrashitova R.N., Salnikova Y.I. (2018) Performance calculation of solar water heating unit at a petrol filling station // Periodico Tche Quimica, 15 (30): 589-598 (in Eng.).

[25] Bulatov N.K., Sarzhanov D.K., Elubaev S.Z., Suleymenov T.B., Kasymzhanova K.S., Balabayev O.T. (2020) Engineering and experimental testing of prototypes of biogas equipment // Renewable Energy, 160: 278-287 (in Eng.).

[26] Buktukov N.S., Buktukov B.Z., Moldabayeva G.Z. (2020) Sail-aerodynamic wind power station with automatically changing blade-swept area // International Journal of Mechanical and Production Engineering Research and Development, 10 (3): 911-920 (in Eng.).

[27] Moldabayeva G.Zh., Suleimenova R.T., Turdiyev M.F., Shayakhmetova Zh.B., Karimova A.S. (2020) Scientific and technical substantiation of reducing oil viscosity // International Journal of Engineering Research and Technology, 13 (5): 967-972 (in Eng.).

N E W S
OF THE NATIONAL ACADEMY OF SCIENCES OF THE REPUBLIC OF KAZAKHSTAN
SERIES OF GEOLOGY AND TECHNICAL SCIENCES
ISSN 2224-5278
Volume 1, Number 445 (2021), 172 – 176 **https://doi.org/10.32014/2021.2518-170X.24**

UDC 625.7/.8:691.163

M. Zh. Zhurinov[1], B. B. Teltayev[2]

[1]JSC "D. V. Sokolskiy Institute of Fuel, Catalysis and Electrochemistry", Almaty, Kazakhstan;
[2]JSC "Kazakhstan Highway Research Institute", Almaty, Kazakhstan.
E-mail: nanrk.mzh@mail.ru, ao_kazdornii@mail.ru

BITUMENS AND POLYMER BITUMENS - NANODISPERSE SYSTEMS

Abstract. This work shows the data regarding the elemental and chemical group compositions of the road bitumens. The short characteristic has been shown for the components of the bitumens - the asphaltenes, the resins and the oils. The properties have been described for the bitumens on which they have the direct impact. The description is given for the micellar model of the bitumens from the point of view of the colloid chemistry.

The analysis has been performed for the results of the study by other authors for the asphaltenes of a bitumen and an oil. The group chemical compositions are given for the bitumen of the grades BND 50/70, BND 70/100 and BND 100/130 produced by the plants of Kazakhstan. It has been shown that the content of the asphaltenes in them is from 15.8% to 24.3%; in most cases, the content of the asphaltenes is within the range of 20-25%, i.e. the asphaltenes nanoclusters are almost a fourth of the bitumen by weight.

The brief description is given for the best known polymers used for the modification of the road bitumen: 1) the reactive polymers Elvaloy 4170 and Elvaloy AM; 2) the polymers of the group SBS - Kraton D 1192A, Calprene 501, SBS L 30-01 A, KUMHO KTR and Butonal NS 198.

It is proposed to consider the bitumen and the polymer bitumen as the peculiar nanodisperse systems. The structures are described for the polymer bitumen nanodisperse systems occurring during the modification of the road bitumen with the polymers of the above two groups.

Key words: Bitumens, polymers, polymer bitumens, asphaltenes, oils, resins, nanodisperse systems.

Introduction. The bitumen is one of the main road materials. The need for it is growing due to the increase in the volume of the road construction and the repair works. For example, over 1 million tons of the road bitumen were used in Kazakhstan in 2020.

Despite the fact that the bitumen content in an asphalt concrete is only 5-6% (by weight), many physical and mechanical, almost all the rheological properties of the asphalt concrete depend on the bitumen.

Currently, there are both practical methods for assessing quality and calculation models for predicting the properties of the road bitumen. But many of them are based on the ideas about the bitumen as viscous liquids and colloidal systems with dispersed particles of macro dimensions.

This paper proposes to consider the bitumen and the polymer bitumen as the peculiar nanodisperse systems.

Bitumen nanodisperse systems. The bitumen is a complex mixture of the residual high molecular weight hydrocarbon compounds also comprising different chemical structures in a relatively small amount. An estimated elemental composition of the bitumen (by weight): carbon is 80-85%; hydrogen is 8-11.5%; oxygen is 0.2-4%; sulfur is 0.5-7%; nitrogen is 0.2-0.5%. The metals - iron, nickel and vanadium - are in a small amount in the composition of the bitumen [1-3].

At present, it is common to characterize the bitumen by the group of chemical compounds included in their composition. Meanwhile, all chemical compounds in the bitumen are divided into the following 3 groups:

1) Asphaltenes are the highest molecular weight part of the bitumen which is dissolved in carbon disulfide and chloroform and it is not dissolved in light alkanes (n-pentane, n-hexane, n-heptane, petroleum ether, etc.);

2) Resins are red-brown solids consisting of cyclic and heterocyclic structures interconnected by aliphatic chains;

3) Oils are the mixture of cyclic hydrocarbons of light yellow color.

The synthesis of the results for the numerous studies [4] made it possible to determine that the asphaltenes are a structural framework of the bitumen, they give hardness and heat resistance to the bitumen; resins characterize plasticity, ductility and cementing properties of the bitumen; oils cause plasticization of the bitumen, they reduce viscosity and heat resistance, increase fluidity and frost resistance.

Many properties of the bitumen, including rheological ones, can be explained using the so-called micellar model. It considers the bitumen as a colloidal system. Colloidal systems are known to be the dispersion of one body (disperse phase) in another body (disperse medium). The dispersed particles are not individual molecules, but aggregates of molecules in colloidal systems.

Back in 1940, it was proposed to consider the bitumen as a colloidal system [5]. In such a colloidal system, the micelles are formed that play the role of a dispersed phase. Micelles consist of asphaltenes. The disperse medium is maltenes (mixture of oils and resins).

The results for the analysis of the known works [4, 6-15] show that at present the following ideas are the most common among the specialists about the structure of the asphaltenes and their structural parameters: asphaltenes are the ordered polycyclic condensed aromatic structures (with the inclusion of heterocycles and lateral substituents) in the form of a packet of flat sheets with the radius of 0.85-1.5 nm and the thickness of 1.6-2.0 nm; the distance between the layers in the packet is 0.355-0.370 nm; the number of layers in the packet is 5-6; the distance between the elements in the saturated structures is 0.55-0.60 nm.

The more detailed studies have shown that the size of the asphaltene molecule is varied between 1.2-2.4 nm [7-9,14]. The sizes of nanoaggregates are increased to 10 nm with the increase in the concentration of the asphaltenes (up to 200 mg/l) in petroleum media [16]. Separate nanoaggregates, combining, create nanoclusters consisting of 8-10 nanoaggregates. The sizes of the nanoclusters reach 100 nm. The average size of the nanoaggregates is about 40-50 nm [17].

Thus, according to the concepts of the colloidal chemistry, the bitumen is a nanodispersed system where the maltenes (a mixture of oils and resins) are dispersed medium, and the asphaltene nanoclusters are dispersed phase.

Table shows group chemical compositions of bitumens of grades of BND 50/70, BND 70/100 and BND 100/130 produced by Kazakhstan plants. As it is seen from this Table, the content of the asphaltenes in them is within the range of 15.8% and 24.3%. In most cases, the content of the asphaltenes is within the range of 20-25%, i.e. the asphaltenes nanoclusters are almost a fourth of the bitumen by weight.

Group chemical composition of the bitumens produced by the plants of Kazakhstan

Group of chemical compounds	Plant-producer, bitumen grade				
	Pavlodar petrochemical plant		Caspiy Bitum		Gazpromneft
	BND 70/100	BND 100/130	BND 50/70	BND 70/100	BND 70/100
Paraffin-naphtenes	19.6	20.3	21.3	15.2	21.6
Light aromatics	6.2	5.5	4.2	5.0	5.4
Medium aromatics	2.1	4.3	4.6	3.9	3.6
Heavy aromatics	10.8	21.6	17.5	20.6	19.6
Petroleum-benzene	6.7	7.1	8.0	9.9	10.7
Alcohol-benzene	30.3	20.4	23.5	22.4	23.3
Asphaltenes	24.3	20.8	20.9	23.0	15.8
Group chemical composition					
Oils	38.7	51.7	47.6	44.7	50.2
Resins	37.0	27.5	31.5	32.3	34.0
Asphaltenes	24.3	20.8	20.9	23.0	15.8

Polymers. The best known polymers used for the modification of the road bitumen are Elvaloy 4170, Elvaloy AM, Kraton D 1192A, Calprene 501, SBS L 30-01 A, KUMHO KTR and Butonal NS 198.

Elvaloy 4170 and Elvaloy AM are chemically active elastomeric copolymers of ethylene with butyl acrylate and glycidyl methacrylate.

The modifiers Kraton D 1192A, Calprene 501, SBS L 30-01 A, KUMHO KTR and Butonal NS 198 belong to the same group of the polymer compositions; they are linear block copolymers of styrene and butadiene. The ratio of styrene and butadiene blocks is almost the same in them. For example, the content of styrene (% by weight): in Kraton - 30; Calprene - 31; SBS - 30±1,5; KUMHO - 30. However, Butonal NS 198 is a cationic aqueous dispersion of a styrene-butadiene copolymer. It contains 64% by weight of the solids.

Bitumen polymer nanodisperse systems. After mixing with the bitumen, the polymers of the SBS group (styrene-butadiene-styrene) swell in the maltene part (mixture of resins and oils) of the bitumen; their volume becomes 5-10 times higher compared to the initial one. Meanwhile, the polystyrene blocks are assembled into rigid domains, which are connected by rubbery (rubber-like) chains of the polybutadiene. Polystyrene domains have dimensions of the order of 10-40 nm [3]. Thus, when the bitumen is modified by the SBS group polymers, an additional spatial amorphous nanostructured mesh is created in bitumen in the initial nanodomain system, at the nodes of which there are rigid polystyrene nanodomains connected to each other by elastic chains of the polybutadiene. Rigid polystyrene nanodomains increase the viscosity of bitumen, thereby improving its high temperature characteristics, and polybutadiene chains give elastic properties to the bitumen, which increases their low temperature stability.

The butyl acrylate ethylene base of the polymers Elvaloy 4170 and ElvaloyAM imparts elasticity to the bitumen polymer system. The presence of an epoxy group in glycidyl methacrylate creates the possibility for its chemical effect with functional groups (-OH, -COOH, -NH_2, -SH, etc.) contained in the asphaltenes of the bitumen. Thus, rather than the polymers of SBS group, the asphaltene bitumen nanoclusters when modified with Elvaloy polymers will be rigidly (chemically) interconnected by a spatial elastic polymer network. In other words, a peculiar nanodisperse system is created where the dispersed phase - the nanoclusters of asphaltenes are located in the nodes of the spatial amorphous elastic nanostructured mesh. It is expected that the obtained nanodisperse system should have the improved high and low temperature characteristics.

Conclusion. 1. The asphaltenes of bitumens are the ordered polycyclic condensed aromatic structures (with the inclusion of heterocycles and lateral substituents) in the form of a packet of flat sheets with the radius of 0.85-1.5 nm and the thickness of 1.6-2.0 nm; the distance between the layers in the packet is 0.355-0.370 nm; the number of layers in the packet is 5-6; the distance between the elements in the saturated structures is 0.55-0.60 nm.

2. The sizes of the asphaltene molecule are varied between 1.2-2.4 nm. The sizes of nanoaggregates of the asphaltenes are increased to 10 nm with the increase in the concentration of the asphaltenes (up to 200 mg/l). Separate asphaltene nanoaggregates, combining, create nanoclusters consisting of 8-10 nanoaggregates. The sizes of the asphaltene nanoclusters reach 100 nm. The average sizes of the nanoaggregates are about 40-50 nm

3. The content of the asphaltene nanoclusters in the road bitumens produced by the plants of Kazakhstan is within the range of 15.8% and 24.3% by weight; in most cases, their content is within the range of 20-25%, i.e. the asphaltene nanoclusters are almost a fourth of the road bitumens by weight.

4. It is proposed to consider the road bitumens and the polymer bitumens as the peculiar nanodisperse systems.

М. Ж. Жұрынов[1], Б. Б. Телтаев[2]

[1]«Д. В. Сокольский атындағы жанармай, катализ және электрохимия институты» АҚ, Алматы, Қазақстан;
[2]«Қазақстан жол ғылыми-зерттеу институты» АҚ, Алматы, Қазақстан,

БИТУМДАР МЕН ПОЛИМЕРБИТУМДАР - НАНОДИСПЕРСТІК ЖҮЙЕЛЕР

Аннотация. Осы жұмыста жол битумдарының элементтік және химиялық топтық құрамы туралы деректер келтіріледі. Битумдардың құрамдас бөліктеріне, асфальтендерге, шайырлар мен майларға қысқаша сипаттама берілген. Олар тікелей әсер ететін битумдардың қасиеттері көрсетілген. Коллоидты химия тұрғысынан битумдардың мицеллярлық моделінің сипаттамасы келтірілген.

Битум және мұнай асфальтендері бойынша басқа авторлардың зерттеу нәтижелеріне талдау жасалды. Қазақстан зауыттары шығарған МЖБ 50/70, МЖБ 70/100 және МЖБ 100/130 маркалы битумдардың топтық химиялық құрамдары келтірілген. Олардағы асфальтендердің мөлшері 15,8 %-дан 24,3%-ға дейін; көп жағдайда асфальтендердің мөлшері 20-25 % аралығында болады, яғни битумның массасы бойынша төрттен бір бөлігі асфальтты нанокластерлер болып табылады.

Жол битумдарын модификациялау үшін қолданылатын ең танымал полимерлердің қысқаша сипаттамасы берілген: 1) Elvaloy 4170 және Elvaloy AM рективтік полимерлер; 2) СБС тобының полимерлері - Kraton D 1192A, Calprene 501, SBS L 30-01 A, KUMHO KTR және Butonal NS 198.

Битумдар мен полимербитумдарды нанодисперсті жүйелер ретінде қарастыру ұсынылады. Жол битумдарын аталған екі топтың полимерлерімен модификациялау кезінде пайда болатын полимербитумды нанодисперстік жүйелердің құрылымы сипатталған

Түйін сөздер: Битумдар, полимерлер, полимербитумдар, асфальтендер, майлар, шайырлар, нанодисперстік жүйелер.

М. Ж. Журинов[1], Б. Б. Телтаев[2]

[1]“Институт топлива, катализа и электрохимии им. Д. В. Сокольского”, Алматы, Казахстан;
[2]“Казахстанский дорожный научно-исследовательский институт”, Алматы, Казахстан

БИТУМЫ И ПОЛИМЕРБИТУМЫ - НАНОДИСПЕРСНЫЕ СИСТЕМЫ

Аннотация. В настоящей работе приводятся данные об элементном и химическом групповом составах дорожных битумов. Приведена краткая характеристика составляющих битумов-асфальтенов, смол и масел. Указаны свойства битумов, на которые они оказывают прямое влияние. Дано описание мицеллярной модели битумов с позиции коллоидной химии.

Выполнен анализ результатов изучения другими авторами асфальтенов битумов и нефтей. Приведены групповые химические составы битумов марок БНД 50/70, БНД 70/100 и БНД 100/130, произведенных заводами Казахстана. Показано, что содержание асфальтенов в них составляет от 15,8 % до 24,3 %; в большинстве случаев содержание асфальтенов находится в пределах 20-25 %, т.е. почти четвертая часть битума по массе – это асфальтеновые нанокластеры.

Дано краткое описание наиболее известных полимеров, применяемых для модификации дорожных битумов: 1) рективные полимеры Elvaloy 4170 и Elvaloy AM; 2) полимеры группы СБС - Kraton D 1192A, Calprene 501, SBS L 30-01 A, KUMHO KTR и Butonal NS 198.

Предложено рассматривать битумы и полимербитумы как своеобразные нанодисперсные системы. Описаны структуры полимербитумных нанодисперсных систем, возникающих при модификации дорожных битумов полимерами указанных двух групп.

Ключевые слова: битумы, полимеры, полимербитумы, асфальтены, масла, смолы, нанодисперсные системы.

Information about authors:

Zhurinov M.Zh., Doctor of Chemical Sciences, Professor, Academician, President of NAS RK; nanrk.mzh@mail.ru, https://orcid.org/0000-0001-5314-1219

Teltayev B.B., Doctor of Technical Sciences, Corresponding Member of NAS RK, Professor, President of JSC “Kazakhstan Highway Research Institute”; bagdatbt@yahoo.com, https://orcid.org/0000-0002-8463-9965

REFERENCES

[1] Gun R.B. Oil bitumens. M. Khimiya. 1973. P. 1-429.

[2] Aminov Sh. Kh., Kutiyn Yu.A., Strugovetz I.B., Telyashev E.G. Modern bituminous binders for road construction. St. Petersburg. Nedra. 2007. P. 1-336.

[3] Kutiyn Yu.A., Telyashev E.G. Bitumens and bitumen materials. Standard norms, quality, technologies. Ufa. Publisher SUE PCPI RB. 2018. P. 1-272.

[4] Kolbanovskaya A.S., Mikhailov V.V. Road bitumens. M. Transport. 1973. P. 1-264.

[5] Pfeiffer J.Ph, Saal R.N. Asphaltic bitumen as colloid system // Journal of Physical Chemistry. 1940. 44 (2). P. 139-149.

[6] Yen T.F., Erdman J.A., Pollak S.S. Investigation of the structure of petroleum asphaltenes by X-ray diffraction // Analitical Chemistry. 1961. 33(1). P. 1587-1594.

[7] Dickie J.P., Yen T.F. Microstructures of the asphaltic fractions by various instrumental methods. Anatical Chemistry. 1967. 39 (14). P. 1847-1852.

[8] Mullins O.C. The modified Yen model // Energy Fuels. 2010. 24. P. 2179-2207.

[9] Mullins O.C. The asphaltenes // Annual Review of Analitical Chemistry. 2011. 4. P. 393-418.

[10] Sergienko S.R. High molecular oil compounds. M. Khimiya. 1964. P. 1-539.

[11] Posadov i.A., Pokonova Yu.V. Structure of oil asphaltenes. Leningrad. 1977. P. 1-76.

[12] Rozental D.A., Posadov I.A., Popov O.G., Paukku A.N. Methods for determination and calculation of structural parameters for fractions of heavy oil residue. Leningrad. 1981. P. 1-84.

[13] Gokhman L.M. Complex organic binders based on block-copolymers of SBS type. M. ZAO “ECON-INFORM”. 2004. P. 1-510.

[14] Ganeyeva Yu.M., Yusupova T.N., Romanov G.V. Asphaltene nanoaggregates: structure, phase transformations, impact on properties of oil systems // Advances of chemistry. 2011. 80 (10). P. 1034-1050.

[15] Zolotarev V.A. Road bituminous binders and asphalt concretes. Part 1. Road bituminous binders. Kharkov. Kharkov Automobile Road University. 2014. P. 1-180.

[16] Evdokimov I.N., Losev A.P. Oil nanotechnologies – coping with stereotypes // Neftyanoye khozyaistvo. 2008. 8. P. 78-81.

[17] Imanbayev Ye., Tileuberdi Ye., Ongarbayev Ye. et al. Changing the structure of resin-asphaltenes molecules in cracking // Eurasian Chemico-Technological Journal. 2017. 19. P. 147-154.

N E W S
OF THE NATIONAL ACADEMY OF SCIENCES OF THE REPUBLIC OF KAZAKHSTAN
SERIES OF GEOLOGY AND TECHNICAL SCIENCES
ISSN 2224-5278
Volume 1, Number 445 (2021), 177 – 185 **https://doi.org/10.32014/2021.2518-170X.25**

UDC 550.8:553.98; 553.98.048

K. M. Taskinbayev[1], S. M. Akhmetov[1], D. K. Azhgaliyev[1], M. D. Diarov[1], D. T. Bizhanov[2]

[1]Atyrau University of Oil and Gas named after S. Utebaev, Atyrau, Kazakhstan;
[2] JSC "Financial Academy", Nur-Sultan, Kazakhstan.
E-mail: taskin53@mail.ru, axmetov_aing@mail.ru, dulat.azhgaliev@gmail.com,
muftah.diarov@mail.ru, rector@aogu.edu.kz

CLARIFICATION OF DIRECTIONS OF GEOLOGICAL EXPLORATION WORKS IN KAZAKHSTAN BASED ON FEATURES OF THE OIL AND GAS CONTENT OF SEDIMENTARY BASINS

Abstract. This article presents an assessment of the regional position and clarification of various characteristics of the oil and gas content of the basins of Western Kazakhstan and the Torgai-Syrdarya tectonic belt, which together represent the most active and mobile part of the territory of Kazakhstan. The necessity of further improvement of the existing ideas about the model of the structure and the prospects of oil and gas content of these basins is justified from the standpoint of clarifying the specific features of their oil and gas content and the geochemical environment of the formation of oil and gas deposits in them.

Based on this and considering temporary crisis phenomena in the economy and the oil and gas industry, there is a proposal for rational approaches and the organization of geological exploration works in the most promising areas of the South Torgai, North Torgai and Shu-Sarysu basins. A joint analysis of the available theoretical concepts and new data will allow to clarify the history of the geological development of the regions, the possibilities and routes of hydrocarbon migration, the provisions of the modern theory of the origin of the so-called "deep oil", and based on that justify the forecast of oil and gas content in the bowels of Kazakhstan as a whole.

Considering this, it is proposed to conduct prospecting work in certain areas of this territory, with an emphasis on clarifying the differences in the nature and characteristics of the oil and gas content of individual basins. The formulation of comprehensive scientific research will contribute to further improvement of ideas about the structure and prospects of oil and gas content of this territory, to the choice of the most rational approach to the development of the estimated substantial forecast potential, and to a deeper scientific study of issues related to the nature of specific features of oil and gas content and the geochemical environment of the formation of oil and gas deposits.

Key words: oil and gas content, sedimentary basins, complex researches, geology, geophysics, analysis, geochemistry, forecast, hydrocarbon trap.

Relevance. The systematic sale of raw materials and the reproduction of the mineral resource complex are at all times relevant tasks, regardless of the objective factors that restrain the activity of production facilities. In this process, the key link is the rational study of promising areas and the conduction of exploration works, since the specifics of the geological exploration process assumes the achievement of commercially significant results, providing an advance (10-15 years) preparation of local structures in compliance with its all necessary stages. Of no small importance in this is the state of geological and geophysical study of the regions (basins), as well as taking into account some factors that allow, according to one or another indicator, to differentiate a promising territory of significant area. Significance of the state of geological and geophysical knowledge of the regions (basins) is of no small importance, as well as considering some factors that allow differentiating a promising territory with significant area according to some indicators.

As known, the regional position of the main oil and gas regions is determined, first of all, by the sedimentary basins of Western Kazakhstan that concentrate the bulk of the hydrocarbon potential (the Caspian depression, Ustyurt-Bozashi and Mangyshlak), as well as the South Torgai and Shu-Sarysu basins located to the east (figure 1).

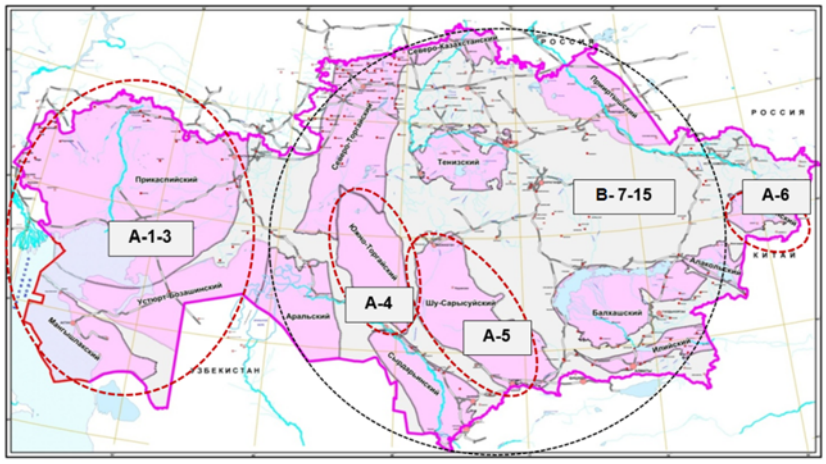

Figure 1 – Oil and gas containing and prospective sedimentary basins of Kazakhstan (Akchulakov U.A. et al.; 2009-2013): A. Oil and gas basins (6): A-1-3 - Caspian, Ustyurt-Bozashi, Mangyshlak, A-4 – South Torgay, A-5 - Shu-Sarysu, A-6 - Zaysan. B. Prospective basins (9): B-7-15 - Aral, Syrdarya, Balkhash, Teniz, Irtysh, Alakol, Ili, North Kazakhstani, North Torgai

These two basins, due to their paleotectonic belonging to the Kazakhstan folded system and the generality of sedimentation environments, along with the North Torgai, Aral and Syrdarya basins, determine the Torgai-Syrdarya tectonic belt (hereinafter referred to as TSTB) stretched in the submeridional orientation [1-3].

The main features of the structure of sedimentary basins. Globally, the territory under consideration is the most tectonically active area of the Earth's crust within Kazakhstan, is a wide zone of interaction between large ancient megastructures of the East European Platform (hereinafter - EEP) and the Kazakhstani lithospheric plate (hereinafter - KLP) [4,5]. In this area, the EEP (Caspian depression) contacts in the east with the western (frontal) edge of the KLP. Taking into account the historically formed appearance and macro-drawing of this area in the plan, clarification of the nature of the phenomena occurring in this entire active tectonic strip (from the point of view of the depth and stratigraphic interval of their manifestation) acquires great practical importance.

The interaction of the eastern margin of the EEP and the active “leading” edge of the KLP at the end of the Paleozoic stage of formation was accompanied by the formation of diverse basins of the back-arc (Torgai, Syrdarya), inter-arc (North Kyzylkum, Aral) and intracontinental (Teniz) types [6,7]. Later, in the Mesozoic (Triassic - Jurassic), a single East European-Kazakhstan plate was formed. From the south, after the closure of the Paleotethis, the ancient Ustyurt block (now the territory of Ustyurt-Bozashi and Mangyshlak) joined it. Presumably, it is the difference in the conditions and time of formation of sedimentary basins that predetermines one or another (individual) specificity of oil and gas content in the section of the Caspian basin, basins of the western Turan plate and TSTB.

As can be seen, the level of interaction of internal processes occurring in the basins determines their global nature and significance in terms of clarifying the genesis of oil, the conditions for the formation of oil and gas accumulation zones (hereinafter referred to as OGAZ), oil and gas generation and etc. In practical terms, relatively more complex mining and geological conditions and, often, the characteristics of the chemical composition of oil and gas in the reservoir state, in comparison with the fields of other oil and gas basins, are characteristic and fair for the OGAZ of the Caspian basin. This means the complex chemical composition of hydrocarbons, the presence of a salt-bearing stratum in the section, the presence of aggressive components (sulfur, hydrogen sulfide, mercaptan) in the oil of the deposits of the subsalt and partially post-salt complex. Accordingly, these features of the Caspian basin deposits and factors determine more difficult conditions for the development of hydrocarbon deposits and a high production cost in comparison with deposits in other sedimentary basins.

In comparison with the Caspian Basin, the nature of oil and gas content and mining and geological conditions of occurrence of deposits in the section of the TSTB basins are more favorable from a practical point of view. The hydrocarbon deposits are characterized by shallow depths, the absence of aggressive

components in the section and deposits. In some cases, oil and gas deposits contain valuable associated components, as exemplified by the unique gas-helium-bearing province of the Shu-Sarysu basin. Also, the well-known factor of an unusually high density of distribution of hydrocarbon volumes over the territory can be noted (in the section and in the area) and in general the uniqueness of oil and gas systems in the Paleozoic and Mesozoic parts in the section of the South Torgai basin.

In Mangyshlak, there is a sharp unevenness in the distribution of HC volumes, ie: about 90% of hydrocarbon reserves in Mangyshlak are concentrated only in 3 nearby Mesozoic fields that are Uzen, Zhetybai and Tenge (out of a total of 55 known deposits of Mangyshlak) [8,9]. In addition, the zoning of deposits with different phase composition is noted, depending on the gypsometry and stepped immersion of blocks (links), which is clearly expressed within the northern side of the South Mangyshlak deflection when it is immersed in the south direction [10].

Research methodology. As you know, the proven volume of recoverable oil reserves in the Republic of Kazakhstan is about 4.525 billion tons [9]. Among the currently active fields, most of which lie in the post-salt deposits of the Caspian depression, have already exhausted their active resource and are at a late stage of development [9,11,12]. At the same time, studies within the framework of the large regional Project "Complex Study of Sedimentary Basins of the Republic of Kazakhstan" (hereinafter - CSSB RK), carried out by the Consortium of leading scientific and research companies in 2009-2013, justified the significant predictive potential of all 15 sedimentary basins of the Republic of Kazakhstan, which is many times higher than the estimate made earlier in previous years and is now 76 billion tons [9].

These results indicate a high oil and gas potential of Kazakhstan's bowels, the implementation of which implies more complex geological conditions for the occurrence of new oil and gas fields, associated both with an increase in the depth of prospecting studies, and with objects occurring at shallow depths, but associated with an unconventional environment and the environment of sedimentation.

Along with the traditional directions of exploration works in the basins of Western Kazakhstan (the post-salt complex of the Caspian basin, etc.), it seems important to carry out prospecting works in the basins of the TSTB, taking into account the currently unfavorable situation on the oil market.

First of all, this concerns the conduct of geochemical studies of oil and gas, which make it possible to identify and clarify potential sources of generation, migration routes and accumulation of hydrocarbons and accordingly study the patterns of formation of traps (natural reservoirs and reservoirs for hydrocarbon).

Thus, in relation to the TSTB in terms of solving the problems of geological prospecting for the discovery of new deposits occurring in relatively favorable geological conditions, certain areas of exploration geology and the zones currently estimated as high prospects in certain areas of the South Torgay, North Torgay and Shu-Sarysu sedimentary basins are of great interest. *An important factor in this regard is that on the territory of these basins, the recently approved State Program for Geological Exploration for the period up to 2025 provides for large-scale exploration work, including research on new and cost-effective technologies (direct methods of exploration) and geochemical research.*

New directions of work and promising areas. Below, in connection with the proposed accents, certain promising areas and directions will be considered according to which it is rational to organize exploration works at present in the opinion of authors.

The Paleozoic complex of deposits in the South Torgai basin is substantiated as one of the prioritized areas of research. In the recent past, significant deposits were discovered in it (Kenlik, Kyzylkiya North-West, Kenlik North, Karabulak, Kokbulak, Doschan, Karavanchi, etc.). Oil and gas reservoirs in the Paleozoic are confined to zones of elevated occurrence / protrusions, they are often characterized by a predominantly carbonate composition (Kenlik, Kyzylkiya North-West, etc.). The results of the work and new data indicate a contrasting severity and a large amplitude of traps, which makes it possible to predict their probable non-anticlinal character [13,14]. According to the data from the Kenlik and Kyzylkiya areas, traps in thick carbonates have the character of structures and buildings on seismic materials (the central part of the Aksai horst-anticline) (figure 2). At the same time, very high flow characteristics of Paleozoic deposits, obtained from reservoirs of predominantly carbonate and carbonate-terrigenous composition, "strengthen" the idea of the presence of non-anticlinal traps in these zones (Kenlik North, Kyzylkiya North-West, Karabulak).

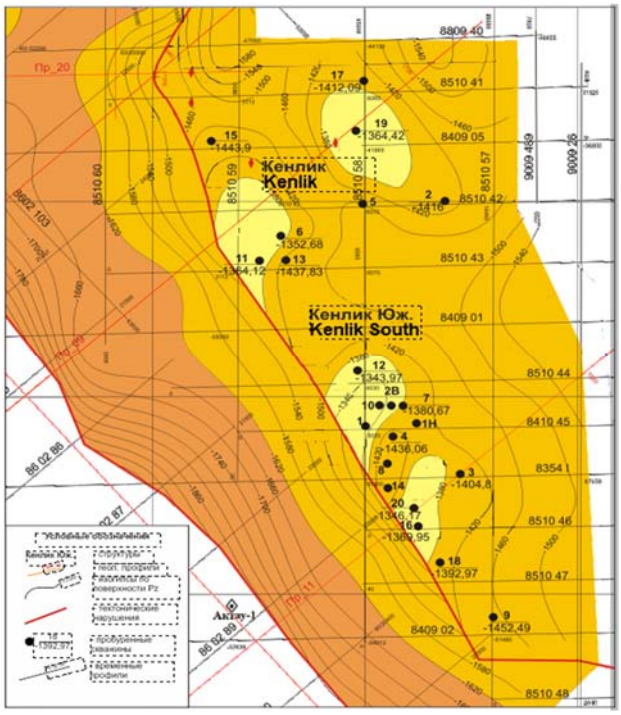

Figure 2 – South Torgai Basin. Structural diagram of the surface of the PZ exhaust gas and non-anticlinal traps of the Kenlik - Kyzylkiya uplift zone: 1 - structures (uplifts), 2 - regional geological profiles, 3 - isohypses along the surface of the PZ OG, 4 - tectonic faults, 5 - drilled wells, 6 - seismic profiles

The range of favorable objects is unusually wide, and along with horst-anticlines, areas of significant subsidence are highly estimated for forecasting promising objects of presumably non-structural type. In this regard the prospects of graben-synclines are highly appreciated, on which the slopes and bands of regional pinching out of pre-Jurassic and Jurassic-Cretaceous deposits, representing areas of distribution of non-structural traps capable of accumulating new hydrocarbon deposits, remain poorly studied.

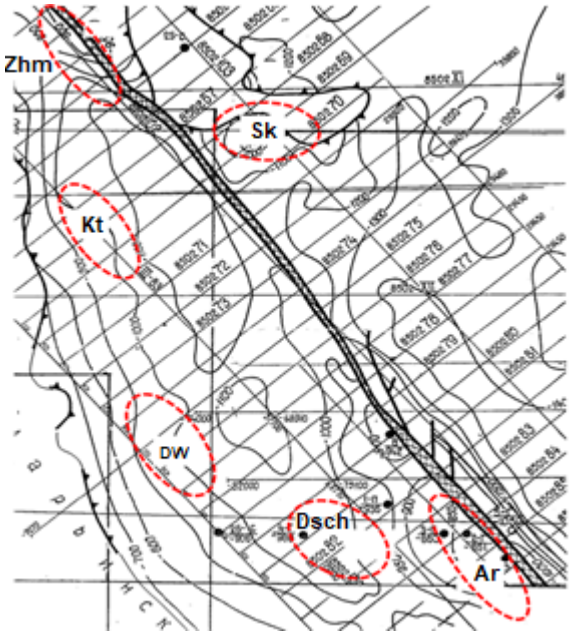

Figure 3 – Forecast NAL in the Doschan zone of uplifts. Block diagram for reflecting horizon No. III (upper Jurassic roof). According to Geotex JSC, 1993-1995: NAT contours: Kt - Kitpay, Sk - Sakpay, DW - Doschan Western, Dsch - Doschan, Ar – Aryskum

It is believed that a more detailed level of study of objects in graben synclines is far from complete. In another case, in the southwestern part of the Aryskum graben-syncline, structures associated with possible "paleo-incisions" of river channels and deltaic sediments (Nuraly, Doschan, etc.) are substantiated as priority objects in non-anticlinal traps (hereinafter - NAT) (figure 3 and 4). In this regard, the zones of depressions in deep troughs (Aryskum, Akshabulak, Sarylan, Bozingen troughs) are promising for discovering new deposits in traps associated with faults [15]. In the side parts of the troughs, the pre-Mesozoic strata is complicated by the active manifestation of faults of various orientations. Historically, large faults contributed to greater expansion of space and the formation of deep depressions.

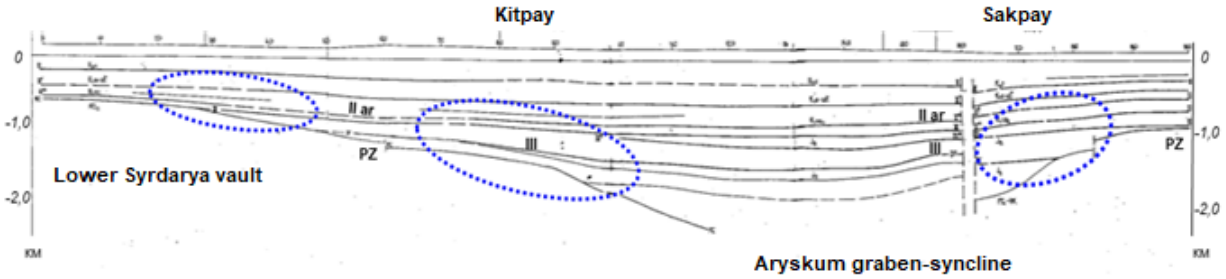

Figure 4 – Areas of paleo-incisions in the section of the Doschanskaya uplift zone:
Geological and seismic profile 850269 (Filipyev G.P., Alpayev A.A. et al., 1990)

The Amangeldy group is in the Moyinkum trough of the Shu-Sarysu basin, includes the Amangeldy, Zharkum, Kumyrly, Maldybai, Airakty, Anabai deposits, which is the object of close attention of researchers in search terms. The potential for identifying shallow objects with favorable commercial characteristics of fluid components is far from being exhausted here and, in the authors' opinion, the study of objects of this category is at a beginning stage. It is believed that a full-fledged concept and the development on its basis of a promising exploration program in the Shu-Sarysu basin (after the discovery of the Amangeldy gas accumulation zone) at one time were left without due attention.

According to new data for 2019-2020 in the Paleozoic part of the basin section various genetic types of deposits are distinguished. An analysis of the sedimentation conditions allows us to preliminarily make a river / lacustrine-boggy genesis of sediments, indicating a rather diverse and probably very complex pattern of sedimentation (PGS-Kazakhstan, 2020). Considering the new ideas in 2020 (figure 5) in the section, it is possible to predict the distribution of objects of non-structural type. Objects associated with NAT, considering the specifics and features of sedimentation of the basin and the probable genesis of structures, can have different sizes and scales of manifestation over the area.

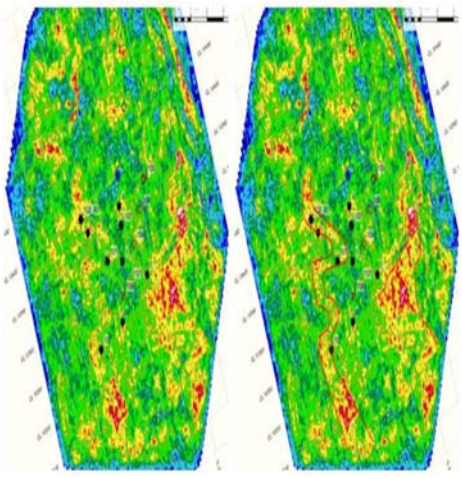

Figure 5 – Forecast of the productive complex associated with NAT in terrigenous sediments
of the Lower Visean age. Slice of the Vp / Vs attribute (according to PGS - Kazakhstan; 2020)

Many researchers rightly note the need to consider the South Torgai and North Torgai basins in a unified manner, as large geostructures formed at the leading edge of the TSTB (KLP) [1,3,16].

Further to the north, within the North Torgai basin, according to the results of geological exploration works in the early years many oil and gas shows were encountered during drilling of structural and exploratory wells (Karasor, Novonezhinskaya, etc.). Direct signs of hydrocarbons are noted in the deposits of the Upper Paleozoic (D_3-C_1). The Jurassic-Cretaceous deposits covering the Paleozoic complex are not of interest in terms of oil and gas due to insufficient development and strong tectonic disturbance. When assessing the prospects, the Triassic period of the formation of this territory is of interest, with which the activity of rifting in the Torgai megabasin is associated. The sharp difference in the hydrocarbon saturation of sedimentary strata along the strike of the TSTB is associated with the sliding and weakening of the amplitude and thickness of rifting in the direction from south to north [17, 18, 19]. In the South Torgai section, Triassic sediments have not been exposed and their development at the most submerged points of the graben-synclines seems to be ambiguous, and the Upper Triassic Turin Group developed in the North Torgai section.

The Ubagano-Kushmurun zone, together with the Priishimsky district in the south, borders on the Zhilanshik trough of the South Torgai basin. The extended grabens that developed in the North Torgai basin are a source of initial material that could participate in the formation of hydrocarbon deposits. Deposits in their location, in turn, may not coincide in plan with grabens. Despite the fact that until now hydrocarbon deposits with commercial conditions have not yet been identified, this region is of significant prospecting interest due to the favorable conditions for the occurrence of Paleozoic deposits within the Kushmurun trough and in the west of the Valeryanov zone (central part of the North Torgai basin).

One of the directions of work in this complex are thrust and underthrust sections, the probability of which is high, considering the peculiarities of geodynamic development and paleotectonic reconstructions. Along with the objects of thrust-nappe nature, the likelihood of forecasting objects associated with NAT is also not excluded. According to Zholtayev G.Zh. et al. (2015) in the carbonate strata of carbon it is assumed the formation of objects of sedimentation origin [20]. It is supposed that the main generation potential of the North Torgai basin is associated with the OGSS in the Upper Devonian-Lower Carboniferous strata. The distribution of reservoir rocks in the Upper Devonian and Lower Carboniferous carbonate-terrigenous strata may have a regional character. At the areal level, the development and distribution of reservoir rocks is associated with zones of disintegration of Proterozoic-Lower Paleozoic folded-metamorphic complexes of rocks and basement protrusions.

Conclusion. Clarification of the structural features and nature of oil and gas content in connection with the regional geotectonic position of the sedimentary basins of Western Kazakhstan and TSTB allows to outline and clarify promising areas of exploration works. Based on the following conclusions and provisions, for this and considering the specific features of sedimentary basins, favorable and economically optimal options are proposed:

- Emphasis is made on the choice of promising and priority areas of prospecting, considering the specifics of oil and gas content of sedimentary basins and the state of individual components in the composition of fluid hydrocarbon systems;
- It is rational to strengthen initiatives in the direction of improving the quality of geochemical research of oil in order to clarify the genesis of oil and the features of the formation of hydrocarbon systems, to predict probable oil and gas accumulation zone and oil and gas generation;
- The basis for the widespread implementation of the recommendations should be the methodological "approaches" proposed by the authors in the integration of data of various directions for forecasting and clarifying the genesis of oil and gas deposits, characterized by shallow depths of occurrence and not containing aggressive components in the composition of formation fluids.
- The results of prospecting works in the recommended version and available generalizations on geochemical studies, as well as methodological recommendations for forecasting promising objects in the South Torgai, North Torgai and Shu-Sarysu basins will help to clarify the guidelines in exploration geology and expand the possibilities of geological exploration in general.
- Implementation of the practical recommendations proposed by the authors, which are based on new objects of unconventional type, will make it possible to concretize the directions of prospecting research in Kazakhstan for the coming years and contribute to improving the quality of forecasting potentially oil and gas objects.

Қ. М. Тасқынбаев[1], С. М. Ахметов[1], Д. К. Ажғалиев[1],
М. Д. Диаров[1], Д. Т. Бижанов[2]

[1]С. Өтебаев атындағы Атырау мұнай және газ университеті, Атырау, Қазақстан;
[2]«Қаржы академиясы» АҚ, Нұр-Сұлтан, Қазақстан

ШӨГІНДІ БАССЕЙНДЕРДІҢ МҰНАЙГАЗДЫЛЫҚ ЕРЕКШЕЛІКТЕРІ НЕГІЗІНДЕ ҚАЗАҚСТАНДАҒЫ ГЕОЛОГИЯЛЫҚ БАРЛАУ ЖҰМЫСТАРЫНЫҢ БАҒЫТТАРЫН НАҚТЫЛАУ

Аннотация. Мақалада жиынтығында Қазақстан аумағының неғұрлым белсенді және жылжымалы бөлігін білдіретін Батыс Қазақстан бассейндері мен Торғай-Сырдария тектоникалық белдеуінің мұнайгаздылығының өңірлік жағдайына баға беріліп, олардың түрлі сипаттамаларын нақтылау ұсынылды. Осы бассейндердің мұнайгаздылығының құрылымын көрсететін модельдер мен перспективалары туралы белгілі түсініктерді олардың мұнайгаздылығы мен мұнай және газ кен орындары қалыптасуының геохомиялық жағдайының өзіндік ерекшеліктерін нақтылау тұрғысынан одан әрі жетілдіру қажеттілігі негізделеді.

Осының негізінде және экономика мен мұнай-газ саласындағы уақытша дағдарыс құбылыстарын ескере отырып, Оңтүстік Торғай, Солтүстік Торғай және Шу-Сарысу бассейнінің перспективалы учаскелерінде геологиялық барлау жұмыстарын ұтымды жүргізу тәсілдері ұсынылды. Теориялық түсініктер мен жаңа деректерді бірлесіп талдау өңірлердің геологиялық даму тарихын, көмірсутек көші-қонының мүмкіндіктері мен жолдарын, сондай ақ «терең мұнайдың» пайда болуының қазіргі заманғы теориялық ережелерін нақтылауға және осының негізінде тұтастай алғанда Қазақстан жер қойнауының мұнайгаздылық болжамын негіздеуге мүмкіндік береді.

Аталған аумақтың кейбір учаскелерінде жекелеген бассейндердің мұнайгаздылығының сипаты мен ерекшеліктеріндегі айырмашылықтарды анықтауға назар аудара отырып, іздеу жұмыстарын жүргізу ұсынылады.

Кешенді ғылыми зерттеу жүргізу аталған аумақтың мұнайгаздылығының құрылымы мен перспективалары туралы түсініктерді одан әрі жетілдіруге, бағаланатын болжамды әлеуетті игеруге неғұрлым ұтымды тәсілді таңдауға, сондай-ақ, мұнай мен газ кен шоғырларын қалыптастырудың геохимиялық жағдайы мен мұнайгаздылығының өзіндік ерекшеліктерінің табиғатына байланысты мәселелерді неғұрлым терең ғылыми түрде пысықтауға ықпал ететін болады.

Мақала ҚР Білім және ғылым министрлігі Ғылым комитетінің 2018-2020 жылдарға арналған мақсатты қаржыландыру бағдарламасы (МҚБ) бойынша «Қазақстан Республикасындағы мұнай мен газдың антиклинальды емес тұзақтарын кешенді зерттеу» тақырыбындағы жобаны орындау аясында жүргізілген зерттеу нәтижелері бойынша дайындалды (18.03.2018 ж., №231 келісімшарт).

Түйін сөздер: мұнайгаздылық, шөгінді бассейндер, кешенді зерттеулер, геология, геофизика, талдау, геохимия, болжам, көмірсутектер тұзағы

К. М. Таскинбаев[1], С. М. Ахметов[1], Д. К. Ажгалиев[1],
М. Д. Диаров[1], Д. Т. Бижанов[2]

[1]Atyrau University of Oil and Gas named after S. Utebaev, Atyrau, Kazakhstan;
[2]АО «Финансовая Академия», Нур-Султан, Республика Казахстан

УТОЧНЕНИЕ НАПРАВЛЕНИЙ ГЕОЛОГОРАЗВЕДОЧНЫХ РАБОТ В КАЗАХСТАНЕ НА ОСНОВЕ ОСОБЕННОСТЕЙ НЕФТЕГАЗОНОСНОСТИ ОСАДОЧНЫХ БАССЕЙНОВ

Аннотация. В статье дана оценка региональному положению и уточнение различных характеристик нефтегазоносности бассейнов Западного Казахстана и Торгайско-Сырдарьинского тектонического пояса, представляющих в совокупности наиболее активную и подвижную часть территории Казахстана. Обосновывается необходимость дальнейшего совершенствования имеющихся представлений о модели строении и перспективах нефтегазоносности данных бассейнов с позиции уточнения специфических особенностей их нефтегазоносности и геохимической обстановки формирования в них залежей нефти и газа.

На основе этого и с учетом временных кризисных явлений в экономике и нефтегазовой отрасли предложены рациональные подходы и постановка геологоразведочных работ на наиболее перспективных участках Южно-Торгайского, Северо-Торгайского и Шу-Сарысуского бассейна. Совместный анализ имеющихся теоретических представлений и новых данных позволит уточнить историю геологического развития регионов, возможности и пути миграции углеводородов (УВ), положения современной теории происхождения «глубинной нефти», и на основании этого обосновать прогноз нефтегазоносности недр Казахстана в целом.

С учетом этого предлагается проведение на некоторых участках данной территории поисковых работ, с акцентом на выяснение различий в характере и особенностях нефтегазоносности отдельных бассейнов. Постановка комплексных научных исследований будет способствовать дальнейшему совершенствованию представлений о строении и перспективах нефтегазоносности данной территории, выбору наиболее рационального подхода к освоению оцениваемого значительного прогнозного потенциала, а также более глубокой научной проработке вопросов, связанных с природой специфических особенностей нефтегазоносности и геохимической обстановки формирования залежей нефти и газа.

Статья подготовлена по результатам исследований, проведенных в рамках выполнения проекта на тему «Комплексные исследования неантиклинальных ловушек нефти и газа в Республике Казахстан» по программе целевого финансирования (ПЦФ) Комитета науки Министерства образования и науки РК на 2018-2020 гг. (договор №231 от 18.03.2018г.).

Ключевые слова: нефтегазоносность, осадочные бассейны, комплексные исследования, геология, геофизика, анализ, геохимия, прогноз, ловушка углеводородов.

Information about authors:

Taskinbayev K.M., Candidate of Geological and Mineralogical Sciences, Professor, Director of the Scientific Center for Geology, Geophysics and Geochemistry of Atyrau University of oil and gas named after S. Utebayev; Atyrau, Kazakhstan; taskin53@mail.ru; https://orcid.org/0000-0002-6475-6486

Akhmetov S.M., Doctor of Technical Sciences, Professor, Vice-rector for science and innovation of Atyrau University of oil and gas named after S. Utebayev, Academician of the National Engineering Academy of the Republic of Kazakhstan, Academician of the Russian Academy of Natural Sciences; Atyrau, Kazakhstan; axmetov_aing@mail.ru; https://orcid.org/0000-0002-1983-457X

Azhgaliyev D.K. Candidate of Geological and Mineralogical Sciences, Associate Professor, Leading Researcher at the Center for Geology, Geophysics and Geochemistry of Atyrau University of oil and gas named after S. Utebayev; Atyrau, Kazakhstan; dulat.azhgaliev@gmail.com; https://orcid.org/0000-0001-9770-0473

Diarov M., Doctor of Geological and Mineralogical Sciences, Professor, Chief researcher Of the scientific laboratory "Geoecology" of Atyrau University of oil and gas named after S. Utebayev, Academician of the National Academy of Sciences of the Republic of Kazakhstan; Atyrau, Kazakhstan; muftah.diarov@mail.ru; https://orcid.org/0000-0002-4799-5821

Bizhanov D.T., master of science, PhD student of JSC "Financial Academy", Nur-Sultan, Kazakhstan; rector@aogu.edu.kz; https://orcid.org/0000-0003-3205-8744

REFERENCES

[1] Volozh Y.A., Bykadorov V.A., Sapozhnikov R.B. Features of the structure of Paleozoic deposits of the Torgai-Syrdarya and Ustyurt regions (in connection with the prospects for oil and gas content of deep horizons of the sedimentary cover) // Neftegazovaya Geologiya. Theory and practice. 2016. Vol. 11, N 4. P. 1-46.

[2] Mailibayev M.M. Directions of prospecting and exploration for oil and gas within South and South-East Kazakhstan based on investments // Mineral resources of Kazakhstan. Almaty. 1995. N 2. P. 3-7.

[3] Ozdoyev S.M., Madisheva R.K., Seilkhanov T.M. et al. On the oil and gas content of the weathering crust of the folded basement of the Aryskum trough of the South Torgai basin // Oil and gas. 2020. N 1 (115). P.17-32.

[4] Akishev T.A., Ashimov R.U., Kunin N.Ya. and others. Seismostratigraphic research in the search for oil and gas / Materials of the All-Union School-Seminar in Chimkent. M. 1988. 2 volumes (242 p., 150 p.).

[5] Zholtayev G.Zh. Geodynamic model and oil and gas potential of the Aral region / seminar "Geological structure and oil and gas potential of the Aral Sea" (JSC "Kazakhstancaspian shelf"). Almaty. 1997.

[6] Zholtayev G.Zh. Paleozoic sedimentary basins of the junction zone of the Urals and the Tien Shan // Geology and exploration of mineral resources of Kazakhstan. 1997. N 5-6. P. 2-7.

[7] Zholtayev G.Zh., Kuandykov B.M. Geodynamic model of the structure of the south of Eurasia // Oil and gas. 1999. N 2. P. 62-74.

[8] Abdullin A.A. et al. Tectonics of the junction area of the structures of the Urals, Tien Shan and Central Kazakhstan. Almaty. 1976. 238 p.

[9] Akchulakov U.A. New resource base of hydrocarbons in the Republic of Kazakhstan and ways of their possible implementation / "Oil and gas basins of Kazakhstan and prospects for their development." PO KONG. Almaty. 2015. 476 p.

[10] Azhgaliyev D.K., Markabayev K.Zh. Geological and geophysical prerequisites for oil and gas exploration in the northern part of the South Mangistau trough // Oil and Gas. Almaty. 2008. N 6. P. 15-20.

[11] Taskinbaev K.M. Non-anticlinal traps - a significant reserve for increasing the hydrocarbon resources of Kazakhstan // Oil and Gas. Almaty. 2018. N 2. P. 52-58.

[12] Taskinbaev K.M., Azhgaliev D.K., Kurmetov B.K. and others. Paleozoic complex of sedimentary basins in the west of the Turan plate and the territory east of the Ural fold system // Geophysics. RSCI. M. 2020. N 1. P. 60-69.

[13] Azhgaliyev D.K., Karimov S.G. Prospects for oil and gas content in the northern part of the Aryskum trough of the South Torgai depression // PETROLEUM. Analytical journal. Almaty. 2005. N 3. P. 52-59.

[14] Karimov S.G. Prospects for oil and gas potential of the South Torgai depression // Karotazhnik. RSCI. M. 2005.

[15] Akchulakov U.A., Bigarayev A.B. On the prospects of the South Torgai basin // Oil and gas. 2014. N 1.

[16] Ozdoyev S.M., Rabkin F.S. Riftogenic structures - a new promising direction of oil and gas exploration (Aral-Caspian and South-Torgai regions of Kazakhstan) // Geology of Kazakhstan. 1996. N 2. P. 47-52.

[17] Ozdoyev S.M. A new direction in predicting oil and gas content by structural zones of possible decompaction of rocks // Geology of Kazakhstan. 1999. N 5-6. P. 28-35.

[18] Pilifosov V.M., Volozh Y.A., Pevzner L.A. Seismogeological analysis in the study of sedimentary basins // Izvestiya SA RK. Geological series. 1983. N 2.

[19] Rabkin F.S. Theoretical preconditions and directions of prospecting for unconventional hydrocarbon deposits in oil and gas basins of Kazakhstan // Izvestiya SA RK. Geological series. 1992. N 1.

[20] Zholtayev G.Zh., Nalibayev M.I. Devonian reefs of North Torgay - highly promising objects for prospecting new oil and gas fields // News of the Academy of Sciences of the Republic of Kazakhstan. Series of Geology and Technical Sciences. 2017. Vol. 2. P. 5-11 (in Russ.).

N E W S
OF THE NATIONAL ACADEMY OF SCIENCES OF THE REPUBLIC OF KAZAKHSTAN
SERIES OF GEOLOGY AND TECHNICAL SCIENCES
ISSN 2224-5278
Volume 1, Number 445 (2021), 186 – 193 **https://doi.org/10.32014/2021.2518-170X.26**

UDC 624:628.8:613.646:691.328 (574)

S. S. Uderbayev[1], K. A. Bissenov[1], N. A. Saktaganova[1], N. A. Mashkin[2], I.S.Dunaev[1]

[1]Korkyt Ata Kyzylorda University, Kyzylorda, Kazakhstan;
[2]Novosibirsk State Technical University, Novosibirsk, Russia.
E-mail: saken_uderbayev@mail.ru, bisenov_ka@mail.ru, amanovna.75@mail.ru, mashkin@corp.nstu.ru, stig_58_96_ab@mail.ru

MICROCLIMATE IN THE BUILDINGS FROM VOLUME BLOCKS

Abstract. Providing the necessary parameters of the microclimate is one of the necessary conditions in the modern construction. For these purposes, there is a set of measures and microclimate support systems applicable in all types of the structural design of buildings. But the features of houses form the modular blocks allow us to move away from standard solutions and use energy-efficient construction technologies, namely, walls with a ventilated interlayer. This design allows us to provide the necessary air exchange in the premises while providing the necessary inlet air temperature. Walls with a ventilated interlayer complement the central ventilation systems or even make it possible to abandon their use. In this article the issue of using walls with ventilated interlayers in the modular blocks, with the use of additional heating of the incoming air in the cold season by using film infrared heaters was considered. The question of the integration of this design with the system of "smart home" was also considered, which will lead to the possibility of creating an energy-efficient building by ensuring cellular regulation of the microclimate parameters. The result of the research is the data required for an approximate calculation of walls with ventilated interlayers and infrared film heating systems, and the possibilities of creating active buildings were also considered. To ensure the energy efficiency of the building, it is proposed to control air exchange and temperature. The control will be carried out directly as follows: in the ventilated walls, at the holes, sensors are installed that will control the speed and temperature of the supply air; a radiant heating film and a recuperator plate that heats the supply air are mounted in the inner heating layer of the wall panel. If the plate temperature is insufficient, the heating film is switched on, which increases the temperature of the supply air masses to the desired temperature.

Key words: volume block, building automation, ventilated wall, infrared heating film, heat engineering.

Introduction. Industrialization is one of the important events in construction. After all, construction, like other industrial processes, has a high energy and material intensity, i.e. it requires a large number of raw materials and energy to create the final product. They are spent on: the extraction of this raw material and its processing, production processes. At the same time in construction, there are several types of these processes.

Production of building materials, i.e. the creation of raw materials necessary for the construction of buildings and structures, and their engineering systems. As you know, the method of activation of binding systems [1-4] increases the strength properties of concrete. The composition of aerated concrete [5-9] affects the mechanical properties of aerated concrete products. In this case, there is a high level of industrialization, because modern materials are manufactured at specialized factories.

Construction. This point implies processes for the construction of buildings and structures, and the level of industrialization of these processes ranges from low, in which most processes are carried out on the construction site, to the high, i.e. installation of sections (parts) of the building that are manufactured at the factory.

Building operation - the processes associated with the creation of the necessary microclimate in a building or a structure.

The high level of industrialization in construction is ensured by transferring most of the processes to factory conditions by introducing a block type of construction, consisting in dividing a building into modular blocks and sections, manufactured in factories and house-building factories. The only processes carried out outside the workshop: transportation of blocks to the construction site and their installation.

When a building is divided into volumetric blocks, they are unified, i.e. blocks have standard sizes. This unification allows us to create experimental samples that use lightweight materials or non-standard types of joints, the production of which directly on the construction site is impossible.

But, bearing in mind the above, the engineering systems in block buildings do not differ from the usual ones: the same ventilation systems are used (natural, by means of windows and doors, or intake and exhaust systems) and heating. Although the block type of a building itself, using the systems that used in energy-efficient buildings, makes it possible to apply new schemes to ensure the necessary parameters of the indoor microclimate.

One type of efficient heating is a radiant heating system. The radiant heating is a system used in modern houses, consisting of panels or pipes laid in the floor or walls, creating infrared radiation that heats internal objects and air, and this system also increases the concentration of negative ions by 4 times. More than 90% of the radiation belongs to the far infrared range (5-20 microns). The water, gas or electricity is used as a heat-transfer material. The heating elements of this system can be installed in the walls, while the heat irradiation is from 160 to 200 W/m2.

Also, there are heating elements in the form of a film. These films are low-temperature heaters, up to 1 mm thick, with a surface heating temperature of 40-65.

Radiant heating systems provide electrical energy savings (about 40%) [10-12] provided by thermostatically controlled elements.

The ventilation is one of the systems that create normative parameters of the indoor microclimate, namely, providing the necessary quantity and quality of indoor air. The natural ventilation is carried out through doorways and window openings, vents in bathrooms and kitchens. The forced ventilation is a system consisting of a pump and pipes and can be inlet, exhaust or inlet and exhaust. But the greater the volume of the incoming air, the greater the load on the room heating system, in this case, the rate of heat loss due to ventilation is 45% of the total heat consumption.

Therefore, in energy-efficient buildings, mechanical ventilation systems with heat recovery systems are used, ensuring the inflow of the required air volume with the required temperature. These systems consist of a pump, a piping system, and a recuperator. In this case, in a block building, it becomes possible to abandon the piping system by using a system like a wall with ventilated devices. This system also works as mechanical ventilation with a heat exchanger, but there are no bulky pipelines. In this system, the outside air enters the room through the outer enclosing structures.

Research methodology. In order to study the possibility of using the above systems, let us consider the design of modern modular blocks.

The blocks are made of various materials and have different structural schemes. The most common scheme consists of ceiling, floor slabs and walls panels. Also, blocks of steel bearing frame, with hung external enclosing structures, are produced. Thus, the wall panels are not bearing. Therefore, it is possible to use walls with ventilated devices. The design consists of a ventilated layer, the inner and outer layers and insulation. In the outer and inner layers are inlet openings with control valves.

The meaning of the construction is to allow air to pass through the walls. The external air penetrates into the internal space through the holes in the inner and outer layers of the walls. To heat the supply air, the heat of the heated wall is used. There are also designs with multiple air movement. For example, to make a double movement of air masses, the walls of two ventilated interlayers are used, separated by a partition, which has high heat irradiation ability. The heating of this partition is carried out by the warm air of the interior space entering the interlayer. Thus, the incoming air is heated to the desired temperature before entering the room γs. The walls with multiple air movement have several air spaces. During the production of wall panels with windows, holes are located under the window opening.

In the warm season, when the air temperature is more than 21 ℃, the heat of the incoming air can be used in the internal systems as an additional source of heat. But in the winter season, when the air temperature is below -25 ℃, it is necessary to apply additional heating of the incoming air.

This construction can be considered a kind of modification of the inlet and exhaust system with a heat exc hanger, which differs from the latter in that the air flow is carried out naturally due to the difference in temperature between the internal and external air. To improve the performance of the system, the system of supply and exhaust ventilation can be used, which increases the flow of air into the room.

This system can be used in panel and block construction: the production of such panels requires precision and tightness, which can only be ensured through the factory conditions.

According to [11], the thickness of the insulation for the inner layer will be 40-55 mm, at the outside air temperature $t_н = -25 \ldots -33$℃, the outer layer - 60-65 mm, and the thickness of the channels should be more than 20 mm.

The channels in the thickness of the panel are formed with the help of pipes, void formers or embedded parts.

The precise calculation of this system is made on a computer. During the calculation, the temperatures of the inner and outer layers, the change in the air temperature along the height of the channels, the amount of heat passing through 1 m^2 of the inner layer per 1 hour are determined.

For the manual calculation of the wall with one layer, the following method is used.

The temperature on the surface of the inner wall of the air gap τ_1, the temperature on the outer surface of the air gap τ_3 and the temperature change in the layer along the height $\Delta\tau_2$ is calculated by the formulas:

$$\tau_1 = \frac{B_3^2+25{,}5B_1+\left(200+50\frac{\lambda_в}{\delta_{щ}}-2B_3\right)\tau_3+4B_3\tau_2+2\tau_3^2}{2B_3+200+50\frac{\lambda_в}{\delta_{щ}}+2\tau_3} \quad (1)$$

where, B_1, B_3 – the coefficients, determined by the formulas:

$$B_3 = B_1\delta_{щ}/2\lambda_в \quad (2)$$

$$B_1 = \alpha_в(t_в - \tau_в) + \alpha_н(t_н - \tau_н) \quad (3)$$

$$\tau_3 = B_3 + \tau_1 - 2\sqrt{B_3(\tau_1 - \tau_2)} \quad (4)$$

$$\alpha_в = 1{,}66\sqrt{t_в - \tau_в} + 3{,}97 + 0{,}0245(t_в + \tau_в) \quad (5)$$

$$\alpha_н = 11{,}6\sqrt{\upsilon} + 3{,}97 + 0{,}0245(t_н + \tau_н) \quad (6)$$

where, $\delta_{щ}$ – the air interlayer thickness, m; $\lambda_в$ – the coefficient of the air thermal conductivity, W/(m · ℃); $\alpha_в$ – the heat transfer coefficient of the inner surface of the interlayer, W/(m · ℃); $t_н$ – the outside temperature, ℃; $\tau_н$ – the outer surface temperature, ℃; $t_в$ – the indoor air temperature, ℃; $\tau_в$ – the inner surface temperature, ℃; υ – the movement speed of air flows, m/s.

The amount of heat penetrating through 1 m^2 per 1 h through the inner layer of the enclosure Q_1 is determined by the formula:

$$Q_1 = \frac{\tau_в - \tau_1}{R_{mв}} \quad (7)$$

$$\tau_в = \frac{\tau_1 + t_в\alpha_в R_{mв}}{1+\alpha_в R_{mв}} \quad (8)$$

$$R_{mв} = \frac{\delta_1}{\lambda_1} + \frac{\delta_2}{\lambda_2} \quad (9)$$

where, $R_{mв}$ – heat transfer resistance of the inner layer, (m^2·℃)/W; δ_1, δ_2 – the thickness of the layers of materials of the inner layer, m; λ_1, λ_2 - the thermal conductivity of the layers of materials of the inner layer, W/(m·℃).

The amount of heat penetrating through 1 m^2 per 1 h through the outer layer of the enclosure Q_2 is determined by the formula:

$$Q_2 = \frac{\tau_3 - \tau_н}{R_{mн}} \quad (10)$$

$$\tau_н = \frac{\tau_3 + t_н \alpha_н R_{mн}}{1 + \alpha_н R_{mв}} \quad (11)$$

$$R_{mH} = \frac{\delta_4}{\lambda_4} + \frac{\delta_5}{\lambda_5} \quad (12)$$

where, δ_4, δ_5 – the thickness of the layers of materials of the outer layer, m; λ_4, λ_5 – the thermal conductivity of the layers of materials of the outer layer, W/(m·°C).

The amount of heat passing through 1 m2 of the outer surface per 1 h, $Q_н$is calculated by the formula:

$$Q_н = \alpha_н(\tau_н - t_н) \quad (13)$$

where, $\alpha_н$ – the heat transfer coefficient of the outer surface of the interlayer, W/(m^2·°C)

The change in the air temperature by the height of the layer is determined by the formula:

$$\Delta\tau_2 = \frac{H}{WCn}\left(\frac{\alpha_в(t_в - \tau_1)}{1 + \alpha_в\left(\frac{\delta_1}{\lambda_1} + \frac{\delta_2}{\lambda_2}\right)} - \frac{\alpha_н(\tau_3 - t_н)}{1 + \alpha_н\left(\frac{\delta_4}{\lambda_4} + \frac{\delta_5}{\lambda_5}\right)}\right) \quad (14)$$

where, H – the section height, m; W – the airflow, kg/(m^2·h); C – the specific heat capacity of air , 1010 J/(kg·K); n – the number of the discrete sections, pcs.

The airflow is determined by the formulas [2]. The amount of air W is calculated by the formula:

$$W = 3600 \upsilon \delta h \gamma \quad (15)$$

where, υ – the air velocity in the interlayer, m/s; δ, h - accordingly, the thickness and height of the air interlayer, m; γ – air volume weight, kg/m^3.

During the designing a block building we have several possible positions of the walls with ventilated interlayers. In the first case, such walls are external, in the second case, such walls are internal (by which the contact of two blocks occurs).

Let us define the characteristics of the walls in the second case in the cold season. Let us accept climatic parameters for the city of Kyzylorda: $t_н = -24$°C, $t_н = 20$°C, airspeed 0,2 m/s. The construction of the wall panel looks like: $\delta_1 = 0{,}1$ м, $\delta_2 = 0{,}8$ м, $\delta_4 = 0{,}8$, $\delta_5 = 0{,}1$. The mineral wool plates with the thermal conductivity of 0,04 W/(m·°C) is taken as insulation.

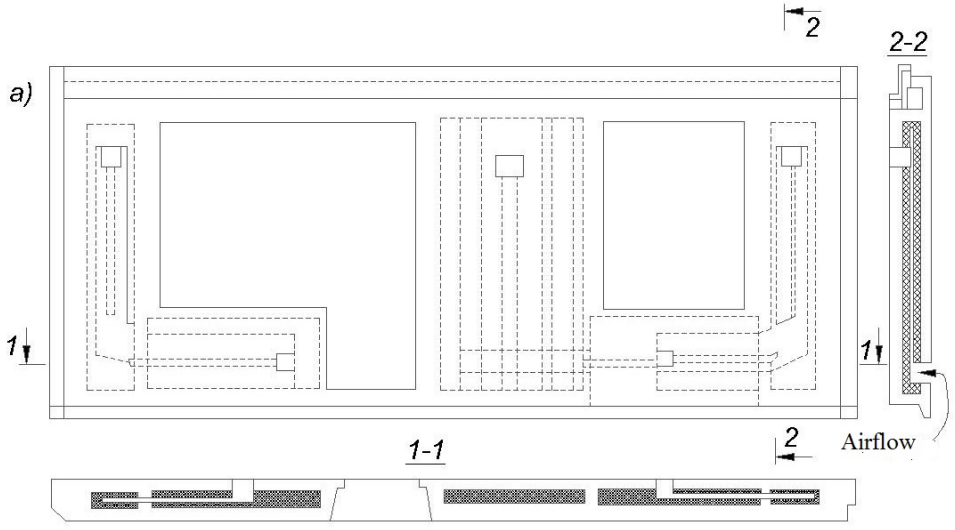

By using the iteration method, let us define the following values for the panels of external walls: $\tau_1 = -23{,}4$°C, $\tau_3 = -23{,}8$°C, $\tau_н = -24$°C, $\tau_в = -19{,}6$°C. The amount of heat penetrating into the interlayer through the inner layer of the panel is $Q_1 = 2{,}14$ J/m^2 · h.

When using panels with two air interlayers with parallel air movement, the inlet mass is heated by 9.6.

In order to determine the required inlet air temperature, let us use [12]:

$$t_x^{'} = t_n - \Delta t_2 \quad (16)$$

where, $t_x^{'}$ - the minimum premises temperature during assimilation of the premises heat, ℃; t_n – the normalized air temperature, 20 ℃;

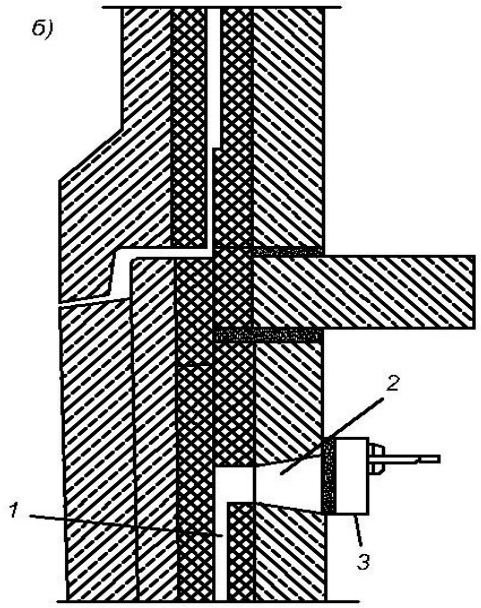

Three-layer ventilated panel: а – with ribs; б – on connections; 1 – ventilation duct; 2 – air vents; 3 – valve

Δt_2 – the permissible variation of the air temperature,1 ℃. $t_x^{'} = 20 + 1 = 21$℃

Results and discussion. According to [13-20], this system will require additional heating, separately from the main heating system. To compensate for the losses, we can use radiant heating.

The scheme is as follows: the heating element is laid in the inner layer of the wall panel in the form of the heating film, which raises the temperature of the inner surface of the interlayer and inlet air. Since the duct area is rather small, the film costs are insignificant. For example, according to [19,20], the power per 1 m2 will be 110 watts.

This system is effective in the modular block housing. By production of blocks, especially with the frame scheme, it is possible to apply this system in wall panels. The efficiency is that during designing blocks, they are considered as autonomous cells, and, depending on the type of block (residential or technical premises), each cell requires its own microclimate parameters. By combining ventilated walls with a radiant heating system and a smart home system, it is possible to create a comfort regulation system in each cell of the building.

The smart home system (automation of microclimate control) is a complex of devices that make up the overall control system that controls the following parameters: heating, ventilation, fire alarms, lighting control, pumping stations (if heat pumps are used), emergency situations, power consumption, and others.

The system works as follows. Special sensors (temperature, speed of a movement of air masses) connected to the automatic control system are installed in the wall panels and in the room itself, with which the microclimate parameters are adjusted and controlled in all cells of the building. The interrelation of various systems is carried out according to standard, general protocols, and according to certain scenarios. The scenarios are the algorithms for the operation of these systems, i.e., they support the necessary parameters of the internal microclimate under the varying environmental conditions.

During designing the ventilated walls, we are faced with a dynamic system, the parameters of which periodically change. And in order to ensure energy conservation and increase the energy efficiency of the system, automation systems should be used.

The “Smart Home” implements a cellular climate control system, the purpose of which is to create the necessary temperature, airflow, air`s quality through special programs, and this system will ensure the building’s energy efficiency.

Thus, the control of air exchange and temperature will be carried out as follows: in ventilated walls, sensors that control the speed and temperature of the inlet air are installed in the ventilated walls; in the inner, heating layer, the radiant heating film and recuperator plate are installed, that raises the temperature of the inlet air masses to the required temperature.

Conclusion. The districts with such "smart" block buildings are combined into "smart" districts. The system of this districts works the same way as in a “smart” house, while its area of influence is much greater: control of traffic, waste, power supply systems and other public services. The optimization of the district`s work affects the operation of buildings. Such a system increases the efficiency of using the city’s infrastructure through the mutual influence of every citizen and the city’s electronic system and the ability of the system to continuously learn.

Thus, the "smart home" is one of the main factors of energy-efficient construction, giving the building flexibility - the necessary quality of effective systems.

С. С. Удербаев[1], К. А. Бисенов[1], Н. А. Сактаганова[1], Н. А. Машкин[2], И. С. Дунаев[1]

[1]Қорқыт Ата атындағы Қызылорда университеті, Қызылорда, Қазақстан;
[2]Новосібір мемлекеттік техникалық университеті, Новосібір, Ресей

КӨЛЕМДІ БЛОКТАРДАН ЖАСАЛҒАН ҒИМАРАТ МИКРОКЛИМАТЫ

Аннотация. Микроклимат параметрлерін қамтамасыз ету – заманауи құрылысқа қажетті шарттың бірі. Ғимараттардың құрылымдық схемаларының барлық түрінде қолданылатын шаралар жиынтығы және микроклиматты қолдау жүйелері бар. Бірақ көлемді блоктардан жасалған үй ерекшеліктері стандартты шешімдерді қолданбауға және энергия үнемдейтін құрылыс технологияларын, атап айтқанда, желдетілетін қабаты бар қабырғалар қолдануға мүмкіндік береді. Бұл дизайн ауа ағынының қажетті температурасын қамтамасыз ете отырып, бөлмелерде қажетті ауа алмасуды қамтамасыз етуге мүмкіндік береді. Желдетілетін қабаты бар қабырғалар орталық желдету жүйелерін толықтырады немесе тіпті оларды пайдаланудан бас тартуға мүмкіндік береді.

Мақалада желдеткіш қабаттары бар қабырғаларды үлкен көлемдегі блоктарда пайдалану әрі жыл мезгілінде кіретін ауаны инфрақызыл жылытқыштармен қосымша жылытуды қолдану мәселесі қарастырылды. Бұл конструкцияны микроклимат параметрлерін жасушалық реттеуді қамтамасыз ету арқылы энергия үнемдейтін ғимарат құруға мүмкіндік беретін «ақылды үй» жүйесімен біріктіру мәселесі де қарастырылды. Зерттеу нәтижесі желдеткіш қабырғалармен және инфрақызыл пленкамен жылыту жүйелері бар қабырғаларды шамамен есептеу үшін қажетті деректер анықталды, сондай-ақ белсенді ғимараттарды құру мүмкіндіктері қарастырылды.

Ғимараттың энергия тиімділігін қамтамасыз ету үшін ауа ауыстыру және температураны бақылау ұсынылады. Бақылау тікелей келесі жолмен жүзеге асырылады: желдетілетін қабырғаларда, тесік орындарында, берілетін ауаның жылдамдығы мен температурасын басқаратын датчиктер анықталады; қабырға панелінің ішкі жылыту қабатында сәулелі қыздыру пленкасы және қоректендіретін ауа қыздыратын рекуператор табақшасы орнатылады. Егер пластина температурасы жеткіліксіз болса, қыздыру пленкасы қосылып, ауа массасының температурасын қажетті температураға дейін арттырады.

Түйін сөздер: көлемді блок, «ақылды үй», желдетілетін қабырғалар, инфрақызыл таспалы қыздырғыш, жылу техникасы.

С. С. Удербаев[1], К. А. Бисенов[1], Н. А. Сактаганова[1], Н. А. Машкин[2], И. С. Дунаев[1]

[1]Кызылординский университет им. Коркыт Ата, Кызылорда, Казахстан;
[2]Новосибирский государственный технический университет, Новосибирск, Россия

МИКРОКЛИМАТ В ЗДАНИЯХ ИЗ ОБЪЕМНЫХ БЛОКОВ

Аннотация. Обеспечение необходимых параметров микроклимата – одно из необходимых условий в современном строительстве. Для этих целей существует комплекс мер и систем обеспечения микроклимата,

применяемый во всех видах конструктивных схем зданий. Но особенности блочных домов позволяют нам отойти от стандартных решений и использовать технологии энергоэффективного строительства, а именно стены с вентилируемой прослойкой. Такая конструкция позволяет обеспечить необходимый воздухообмен в помещениях при обеспечении необходимой температуры приточного воздуха. Стены с вентилируемой прослойкой дополняют центральные системы вентиляции или даже дают возможность отказаться от их использования.

В данной статье был рассмотрен вопрос применения стен с вентилируемыми прослойками в объемных блоках с применением дополнительного обогрева приточного воздуха в холодное время года путем использования пленочных инфракрасных нагревателей. Также был рассмотрен вопрос интеграции данной конструкции с системой «умного дома», что приведет к возможности создания энергоэффективного здания, путем обеспечения поячеистого регулирования параметров микроклимата. Результатом исследования являются данные, необходимые для приблизительного расчета стен с вентилируемыми прослойками и системы инфракрасного пленочного нагрева, а также были рассмотрены возможности создания активных зданий.

Для обеспечения энергоэффективности здания предлагается контролировать воздухообмен и температуру. Контроль будет осуществляться следующим образом: в вентилируемых стенах в местах отверстий уславливаются датчики, которые будут контролировать скорость и температуру приточного воздуха, во внутренний, нагревающий слой панели стены монтируется пленка лучистого отопления и пластина рекуператора, осуществляющего нагрев приточного воздуха. При недостаточной температуре пластины в работу включается пленка отопления, повышающая температуру приточных воздушных масс до нужной температуры.

Ключевые слова: объемный блок, «умный дом», вентилируемые стены, инфракрасный пленочный нагреватель, теплотехника.

Information about authors:

Uderbaev Saken Seytkanovich, Doctor of Technical Sciences, Professor of the Department of Architecture and Construction Production of the Kyzylorda University named after Korkyt ata, Kyzylorda, Kazakhstan; saken_uderbayev@mail.ru; https://orcid.org/0000-0003-4492-8364

Bissenov Kylyshbai Aldabergenovich, Doctor of Technical Sciences, Professor of the Department of Architecture and Construction Production of the Kyzylorda University named after Korkyt ata, Kyzylorda, Kazakhstan; bisenov_ka@mail.ru; https://orcid.org/0000-0002-0167-3560

Saktaganova Nargul Amanovna, Doctor of Philosophy (PhD), Head of the Department of Postgraduate Education of Kyzylorda University named after Korkyt ata, Kyzylorda, Kazakhstan; amanovna.75@mail.ru; http://orcid.org/0000-0003-1218-4946

Mashkin Nikolai Alekseevich, Doctor of Technical Sciences, Professor of the Department of Engineering Problems of Ecology, Novosibirsk State Technical University; mashkin@corp.nstu.ru; https://orcid.org/0000-0001-5116-2016

Dunaev I.S., master - carried out the writing of the first version of the article, carried out a literature search, defined the research objectives; stig_58_96_ab@mail.ru; https://orcid.org/0000-0003-2049-8654

REFERENCES

[1] Bisenov K.A., Uderbayev S.S. (2014) Development of a new method of aggregate treatment in the technology of lightweight concrete–wood concrete // Mediterranean Journal of Social Sciences MCSER Publishing, Rome-Italy, 5 (20): 2682-2686. ISSN:2039-9340E-ISSN:2039-2117

[2] Shalbolova U., Narmanova R., Elpanova M. (2012) Methodical peculiarities of tariff setting at oil transportation via main pipelines // Actual problems of economics, 138: 540-555. ISSN: 1993-6788.

[3] Bisenov K.A., Uderbayev S.S., Shalbolova U.Z. (2014) Environmental and economic efficiency of application of constructional insulating arbol from agricultural and industrial wastes // Actual problem of economics, 151 (1): 304-311. ISSN:1993-6788

[4] Abdibattayeva M., Bisenov K., Rysmagambetova A., Itzhanova K. (2016) Sgem in Integrated oil waste processing with using solar energy. 16th International Multidisciplinary Scientific Geoconference (SGEM 2016). Albena, Bulgaria. P. 443-450.

[5] Bisenov K.A., Uderbayev S.S., Saktaganova N.A. (2016) Optimization of the structure and process parameters of aerated concrete production with the use of oil sludge. // International Journal of Pharmasy and Technology, 8 (3): 17733-17744. E-ISSN: 0975-766X.

[6] Bisenov K.A., Uderbayev S.S., Saktaganova N.A. (2016) Physicochemical Analysis of Structure of Foamed Concrete with Addition of Oil Sludges // Research Journal of Pharmaceutical Biological and Chemical Sciences, 7 (4): 1701-1708. E-ISSN: 2249-8958.

[7] Montayev S.A., Zharylgapov S.M., Bisenov K.A., Shakeshev B.T., Almagambetova M.Z. (2016) Investigating Oil Sludges and Their Application as Energy Efficient and Modifying Component in Ceramic Pastes // Research Journal of Pharmaceutical Biological and Chemical Sciences, 7 (3): 2407-2415. ISSN: 0975-8585.

[8] Narmanova R.A., Bishimbayev V.K., Tapalova A.S., Appazov N.O. (2020). Polymer additive effect on the structural and mechanical properties of the organic part of oil bituminous rock // News of NAS RK. Series of chemistry and technology, 5 (443): 141-150. https://doi.org/10.32014/2020.2518-1491.91

[9] Isembergenov N., Taissariyeva K., Seidalieva U., Danilchenko V. (2019) Microprocessor control system for solar power station // News of the National Academy of Sciences of the Republic of Kazakhstan. Series of Geology and Technical Sciences, 1 (431): 107-111. https://doi.org/10.32014/2019.2518-170X.13 (in Eng.).

[10] Bisenov K.A., Narmanova R.A., Appazov N.O. (2020). Physical and chemical studies of the oil sludge hydrocarbon composition and the prospects for their use in the technology of expanded clay production // News of NAS RK. Series of chemistry and technology, 5 (443): 28-37. https://doi.org/10.32014/2020.2518-1491.77. (in Eng.).

[11] Appazov N.O., Seitzhanov S.S., Zhunissov A.T., Narmanova, R.A. (2017) Synthesis of Cyclohexyl Isovalerate by Carbonylation of Isobutylene with Carbon Monoxide and Cyclohexanol in the Presence of Pd(PPh3) (4)-PPh3-TsOH and Its Antimicrobial Activity // Russian Journal of Organic Chemistry, 53 (10): 1596-1597. ISSN: 1608-3393 (Online), ISSN: 1070-4280. doi: 10.1134/S1070428017100189.

[12] Proektirovanie energoekonomichnyih i energoeffektivnyih grazhdanskih zdaniy: Ucheb. posobie dlya stud. vuzov po spets. «Promyishlennoe i grazhdanskoe stroitelstvo» / Belyaev V. S., Hohlova L. P. M.: Vyissh. shk., 1991. 255 p.: il. ISBN: 5-06-001816-4 (in Russ.).

[13] SP RK 3.02-138-2013. Energy saving buildings.

[14] SP RK 4.02-101-2012. Heating, ventilation and air conditioning.

[15] SP RK 5.03-107-2013. Bearing and enclosing structures.

[16] GOST 34.XXX-XX. Information technology. A set of standards and guidance documents for automated systems.

[17] ABOK STANDART-5-2004. Building automation and control systems.

[18] EN ISO 16484-X. Building Automation and Control Systems - BACS:

[19] https://www.tmelekt.ru/blog/plen-plenochnyy-elektronagrevatel.html

[20] https://teplospec.com/elektricheskoe-otoplenie/chto-takoe-plen-otoplenie-kharakteristiki-preimushchestva-pravila-montazha.html

N E W S
OF THE NATIONAL ACADEMY OF SCIENCES OF THE REPUBLIC OF KAZAKHSTAN
SERIES OF GEOLOGY AND TECHNICAL SCIENCES
ISSN 2224-5278
Volume 1, Number 445 (2021), 194 – 202 **https://doi.org/10.32014/2021.2518-170X.27**

UDC 625.7/.8:691.16

M. Zh. Zhurinov[1], B. B. Teltayev[2], E. D. Amirbayev[2]

[1]JSC "D. V. Sokolskiy Institute of Fuel, Catalysis and Electrochemistry", Almaty, Kazakhstan,
[2]JSC "Kazakhstan Highway Research Institute", Almaty, Kazakhstan.
E-mail: nanrk.mzh@mail.ru, ao_kazdornii@mail.ru

MAIN STANDARD INDICATORS OF POLYMER ASPHALT CONCRETES

Abstract. The main indicators of 29 types of asphalt and polymer asphalt concretes prepared with the use of neat bitumens of 2 grades and 7 types of polymer bitumens have been determined and comparatively analyzed in the work. The bitumens of grades BND 100/130 and BND 130/200 produced by the Pavlodar petrochemical plant have been selected for preparation of the asphalt concretes, polymer bitumens and polymer asphalt concretes. 7 types of the polymers (Elvaloy 4170, Elvaloy AM, Kraton D 1192A, Calprene 501, SBS L 30-01 A, KUMHO KTR, Butonal NS 198) have been selected for the modification of the bitumens. Short procedure has been represented for the preparation of the polymer bitumens. 29 types of the asphalt and the polymer asphalt concretes have been prepared with the use of the above bitumens and polymer bitumens (asphalt concrete of type A - 7, asphalt concrete of type B - 15, stone mastic asphalt concrete SMA-15 - 1, stone mastic asphalt concrete SMA-20 - 6).

The following main indicators of quality have been determined for the asphalt concretes and polymer asphalt concretes by testing in relevant laboratory devices: 1) rut depth at the temperature of 60 °C after 10 000 passages of the wheel (ST RK EN 12697-22-2012); 2) tensile strength at the temperature of -30 °C (pr. EN 12697-46-2012); 3) compression strength at the temperature of 50 °C (ST RK 1218-2003); 4) water saturation (ST RK 1218-2003).

It is found out that the modification of the bitumens with the polymers increases essentially the main standard indicators of the asphalt concretes: rutting resistance, strength at high temperatures and low temperatures, resistance to the cyclic freezing and thawing (frost resistance). The reactive polymers Elvaloy 4170 and Elvaloy AM are the most efficient among the used ones.

Key words: Bitumens, polymers, asphalt concretes, polymer asphalt concretes, standard indicators.

1. Introduction. At present in Kazakhstan, as well as in many countries of the world, quality of road bitumens and asphalt concretes is evaluated separately in accordance with the requirements of the current standard and technical base [1, 2]. Meanwhile, it is important to bear in mind that an asphalt concrete rather than a bitumen is a final material used in a road structure. The bitumen is one of the components of the asphalt concrete. However, preliminary evaluation of quality of the bitumen and other used materials facilitated essentially the design of the optimal composition of the asphalt concrete – a final product.

It follows from the above that the problem of efficiency for the use of bitumens and polymers should be finally solved only after determination and analysis of the indicators of quality for the relevant asphalt concretes and polymer asphalt concretes.

This work determines and analyzes comparatively the main standard indicators of 29 types of the asphalt concretes and polymer asphalt concretes prepared with the use of neat bitumens of 2 grades and 7 types of polymer bitumens.

2. Materials

2.1. Bitumens. The bitumens of grades BND 100/130 and BND 130/200 produced by the Pavlodar petrochemical plant have been selected for preparation of asphalt concretes, polymer bitumens and polymer asphalt concretes. The indicators of quality for these bitumens satisfy the requirements of the standard ST RK 1373-2013 [1].

2.2. Polymers. 7 types of polymer compositions belonging to two different groups have been selected for modification of bitumens (table 1).

Table 1 – Polymer compositions

Description	Group	Producer	Country
Elvaloy 4170 Elvaloy AM	Elastomeric copolymer	Dow Corporate	USA
Kraton D 1192A	Linear block copolymer	USA Headquarters	USA
Calprene 501	Linear block copolymer	Dynasol Group	USA
SBS L 30-01 A	Linear block copolymer	SIBUR	Russia
KUMHO KTR	Linear block copolymer	Kumho Petrochemical Co. LTD	South Korea
Butonal NS 198	Cation water dispersion copolymer	BASF Trading Company GmbH	Germany

2.3. Polymer bitumen preparation. Preparation of polymer bitumens with the use of the neat bitumens produced by the plants has been performed in the laboratory of Kazakhstan Highway Research Institute (KazdorNII). Mixer of model IKAEUROSTAR 20 DIGITAL has been used for this purpose the paddle of which is rotating with the constant rate of 2000 rotations per minute.

The preparation of the polymer bitumens has been performed in the following technological order:

1) neat bitumen was heated up to the temperature of 175-180 °C in the mixer;

2) an amount of polymer selected before was added gradually and regularly into a heated neat bitumen;

3) the mixture of bitumen and polymer has been mixed in a continuous manner and regularly for 2 hours.

As for the polymers Elvaloy 4170 and Elvaloy AM, the obtained homogeneous mix of the bitumen and the polymer for the following 12 hours has been at the constant temperature of 175-180 °C for complete carrying-out of chemical reactions between components of the bitumen and the polymers of grade Elvaloy.

The indicators of quality for the prepared polymer bitumens satisfy the requirements of the standard ST RK 2534-2014 [4].

2.4. Polymer asphalt concretes. 29 types of the asphalt concrete and polymer asphalt concrete (asphalt concrete of type A – 7, asphalt concrete of type B – 15, stone mastic asphalt concrete SMA-15 – 1, stone mastic asphalt concrete SMA-20 - 6) have been prepared with the use of the above bitumens and polymer bitumens. The data regarding the prepared and tested asphalt concretes and polymer asphalt concretes are represented in table 2.

The indicators of quality for the prepared asphalt concretes and polymer asphalt concretes satisfy the requirements of the standards ST RK 1225-2019 [2], ST RK 1223-2019 [4], GOST 31015-2002 [5] and ST RK 2373-2019 [6].

Table 2 – Data regarding the prepared and tested asphalt concretes and polymer asphalt concretes

No	Type of asphalt concrete	Bitumen grade	Description of modifier	Amount of modifier, %	Contracted notation
1	Asphalt concrete fine-grained type B	BND 100/130	–	–	PNHZ_100-130_B
2		BND 100/130	Elvaloy 4170	1.4	PNHZ_100-130_B+Elvaloy1
3		BND 100/130	Elvaloy AM	2.0	PNHZ_100-130_B +Elvaloy2
4		BND 100/130	Kraton	4.0	PNHZ_100-130_B +Kraton
5		BND 100/130	Calprene 501	4.0	PNHZ_100-130_B +Calprene
6		BND 100/130	Butonal NS 198	3.0	PNHZ_100-130_B +Butonal
7		BND 100/130	SBSL 30-01 A	3.0	PNHZ_100-130_B +SBS
8		BND 100/130	KUMHO KTP	3.0	PNHZ_100-130_B +KUMHO1
9		BND 100/130	KUMHO KTP	6.0	PNHZ_100-130_B +KUMHO2
10		BND 130/200	Elvaloy 4170	1.8	PNHZ_130-200_B +Elvaloy1
11		BND 130/200	Elvaloy AM	2.2	PNHZ_130-200_B +Elvaloy2
12		BND 130/200	Kraton	6.0	PNHZ_130-200_B +Kraton
13		BND 130/200	Calprene 501	6.0	PNHZ_130-200_B +Calprene
14		BND 130/200	Butonal NS 198	3.5	PNHZ_130-200_B +Butonal
15		BND 130/200	SBSL 30-01 A	5.0	PNHZ_130-200_B +SBS
16	Asphalt concrete fine-grained type A	BND 100/130	–	–	PNHZ_100-130_A
17		BND 130/200	Elvaloy 4170	1.6	PNHZ_130-200_A +Elvaloy1
18		BND 130/200	Elvaloy AM	2.2	PNHZ_ 130-200_A +Elvaloy2
19		BND 130/200	Kraton	4.0	PNHZ_130-200_A+Kraton
20		BND 130/200	Calprene 501	5.0	PNHZ_130-200_A+Calprene
21		BND 130/200	Butonal NS 198	3.5	PNHZ_130-200_A +Butonal
22		BND 130/200	SBSL 30-01 A	4.0	PNHZ_130-200_A +SBS
23	Asphalt concrete stone mastic SMA-15	BND 100/130	–	–	PNHZ_100-130_SMA15
24	Asphalt concrete stone mastic SMA-20	BND 100/130	–	–	PNHZ_100-130_SMA20
25		BND 130/200	Elvaloy 4170	1.7	PNHZ_130-200_SMA20+Elvaloy1
26		BND 130/200	Calprene 501	5.0	PNHZ_130-200_SMA20+Calprene
27		BND 130/200	SBSL 30-01 A	5.0	PNHZ_130-200_SMA20+SBS
28		BND 130/200	Butonal NS 198	3.5	PNHZ_130-200_SMA20+Butonal
29		BND 130/200	Kraton	5.0	PNHZ_130-200_SMA20+Kraton

3.Methods

3.1. Rut depth at the temperature of 60 °C after 10 000 wheel passages. It is determined under the standard ST RK EN 12697-22-2012 [7] in the device ‘Hamburg wheel”. It characterizes the resistance of asphalt concretes to the rutting in a hot season of the year at the frequent repeated passages of heavy trucks. The less the rut size is the more resistant this type of the asphalt concrete is considered to be. Comparison of the rut sizes obtained for a number of the asphalt concretes gives an opportunity to determine the most resistant ones to the rutting among them.

3.2. Tensile strength at the temperature of -30 °C. This indicator is determined under the standard pr. EN 12697-46-2012 [8] and it characterizes the strength of asphalt concretes at low temperatures. In other words, this indicator gives an opportunity to perform the comparative evaluation for the resistance to the low temperature cracking in asphalt concrete pavements in cold regions.

3.3. Compression strength at the temperature of 50 °C. This indicator is determined under the standard ST RK 1218-2003 [9] and it characterizes the strength of asphalt concretes at high temperatures.

3.4. Water saturation. It is determined under the standard ST RK 1218-2003 [9]. It is considered that the asphalt concretes with the lower value of water saturation are more resistant to the cyclic freezing and thawing.

4. Results and discussion

4.1. Rut depth at the temperature of 60 °C after 10 000 wheel passages. It is clearly seen from Figure 1 that, as a rule, non-modified (neat) bitumens are the weakest resistant to rutting. Modification of bitumens decreases essentially the size of the rut. Big (by several times) increase of the rutting resistance for the asphalt concretes occurs in cases of bitumen modifications with the polymers Elvaloy 4170 and Elvaloy AM. For example, the decrease of the rut size for the asphalt concretes with the polymers Elvaloy 4170 and Elvaloy AM for the asphalt concretes of types A and B was by 3-5 and 2-3 times respectively.

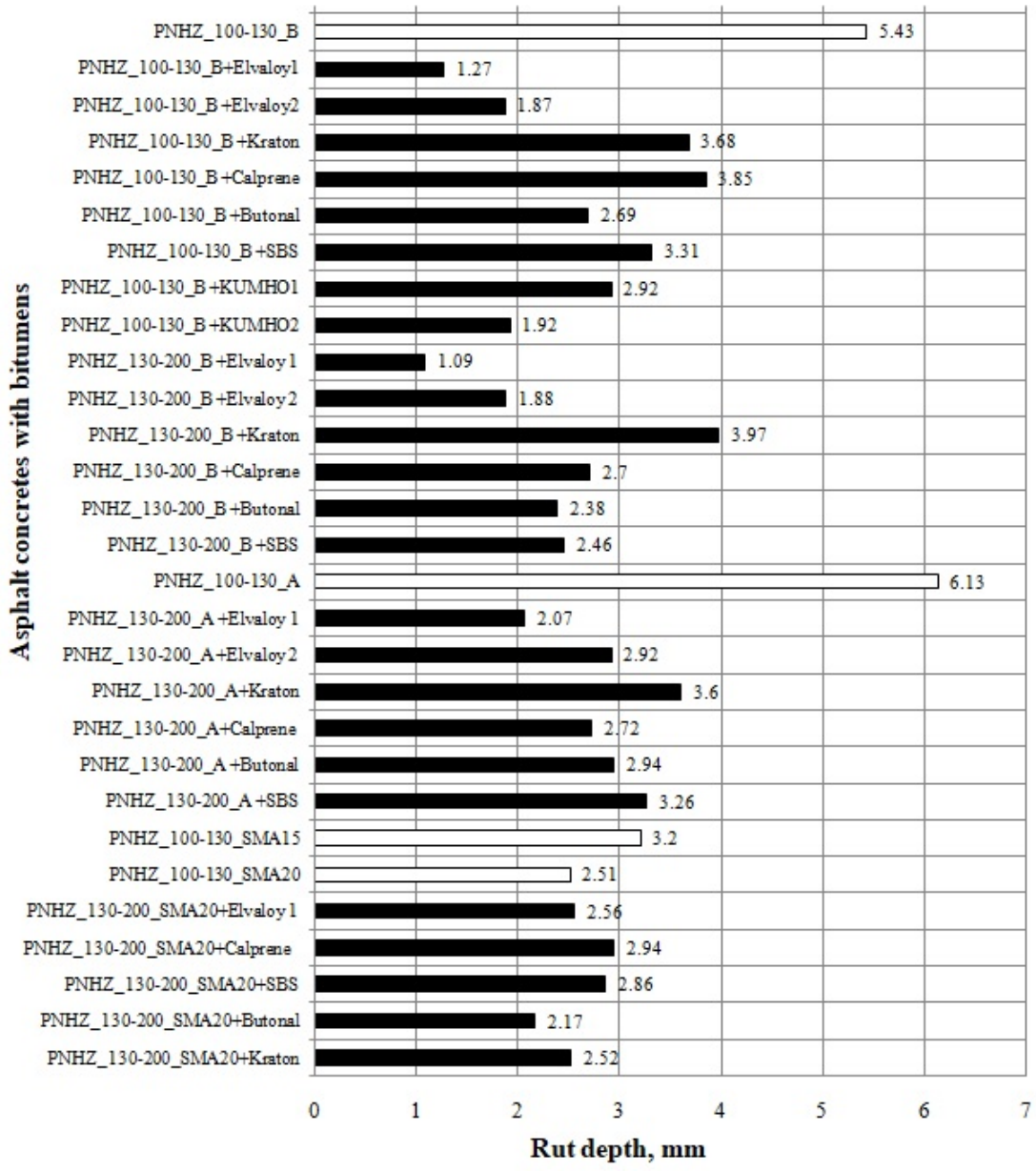

Figure 1 – Rut depth on the asphalt concrete samples at 60 °C after 10 000 wheel passages

4.2. Tensile strength at the temperature of -30 °C. As it is seen from figure 2, the modification of the bitumens with the polymers increases its low temperature strength. Meanwhile, the asphalt concretes with the polymers Elvaloy 4170, Elvaloy AM and KUMHO (3%) have the largest effect. For example, the strength of the asphalt concrete of type B with the bitumen of grade BND 130/200 and the polymer Elvaloy AM has been increased by 2.09 times compared with the conventional asphalt concrete of type B with the bitumen of grade BND 100/130. And the strength increase of the asphalt concrete of type B with the bitumen of grade BND 100/130 with this polymer has been 1.73 times. The addition of the polymer KUMHO (3%) into the bitumen of grade BND 100/130 specified the increase of the low temperature strength for the asphalt concrete of type B by 1.84 times.

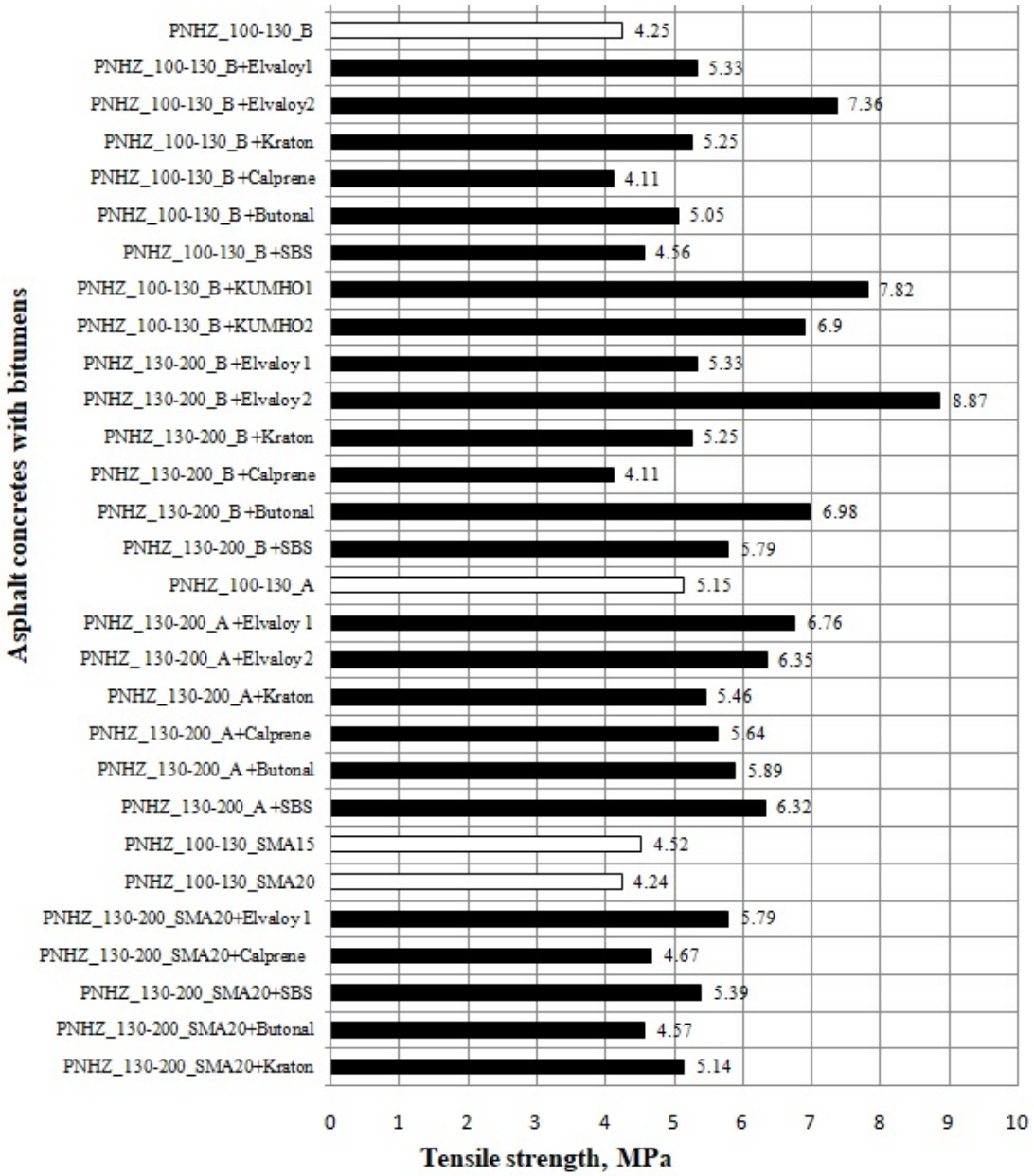

Figure 2 – Tensile strength of the asphalt concretes at the temperature of -30 °C

4.3. Compression strength at the temperature of 50 °C. It is found out that the modification of the bitumens with the polymers increases essentially the high temperature (at +50°C) compression strength of the asphalt concretes as well (figure 3). The polymers Elvaloy 4170, Elvaloy AM, Calprene 501 and

KUMHO (6 %) have proved to be the most efficient for the asphalt concretes of type B, and Elvaloy 4170 and Elvaloy AM proved to be the most efficient for the asphalt concretes of type A. The strength increases for the asphalt concretes of types A and B, the stone mastic asphalt concretes were 47.5- 96.7 %, 44.9-88.4 % and 60.6-97.2 % respectively.

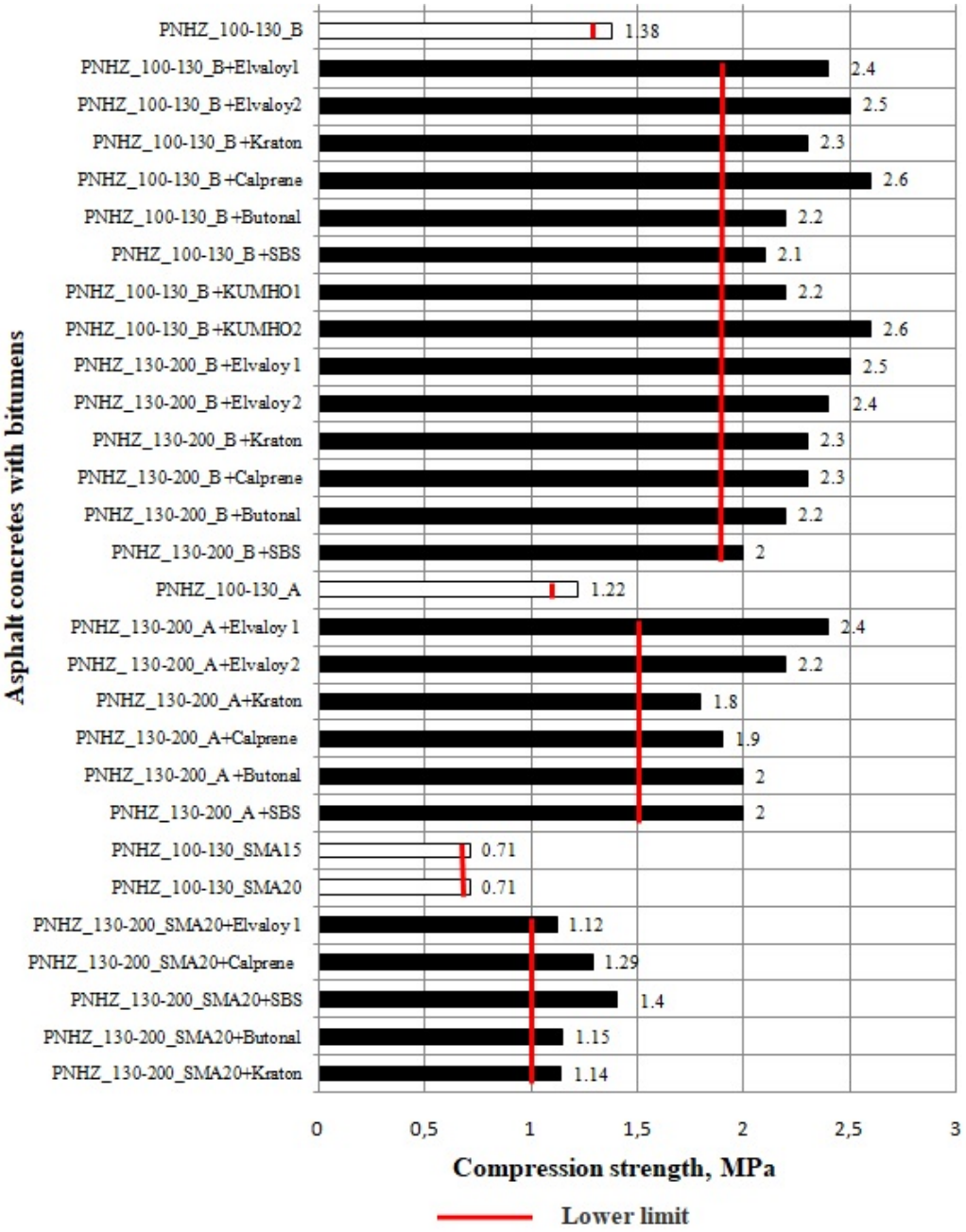

Figure 3 – Compression strength of the asphalt concretes at the temperature of 50 °C

4.4. Water saturation. Test results have shown (figure 4) water saturation of the asphalt concretes is essentially improved practically in all the considered cases for the modification of the bitumens. Meanwhile, as it is seen, some differences occur depending on the type of the asphalt concrete. For example, the water saturation decreases for the asphalt concretes of types B and A, stone mastic asphalt concrete SMA-20 were 1.3-2.3; 1.14-1.32 and 1.39-2.13 times.

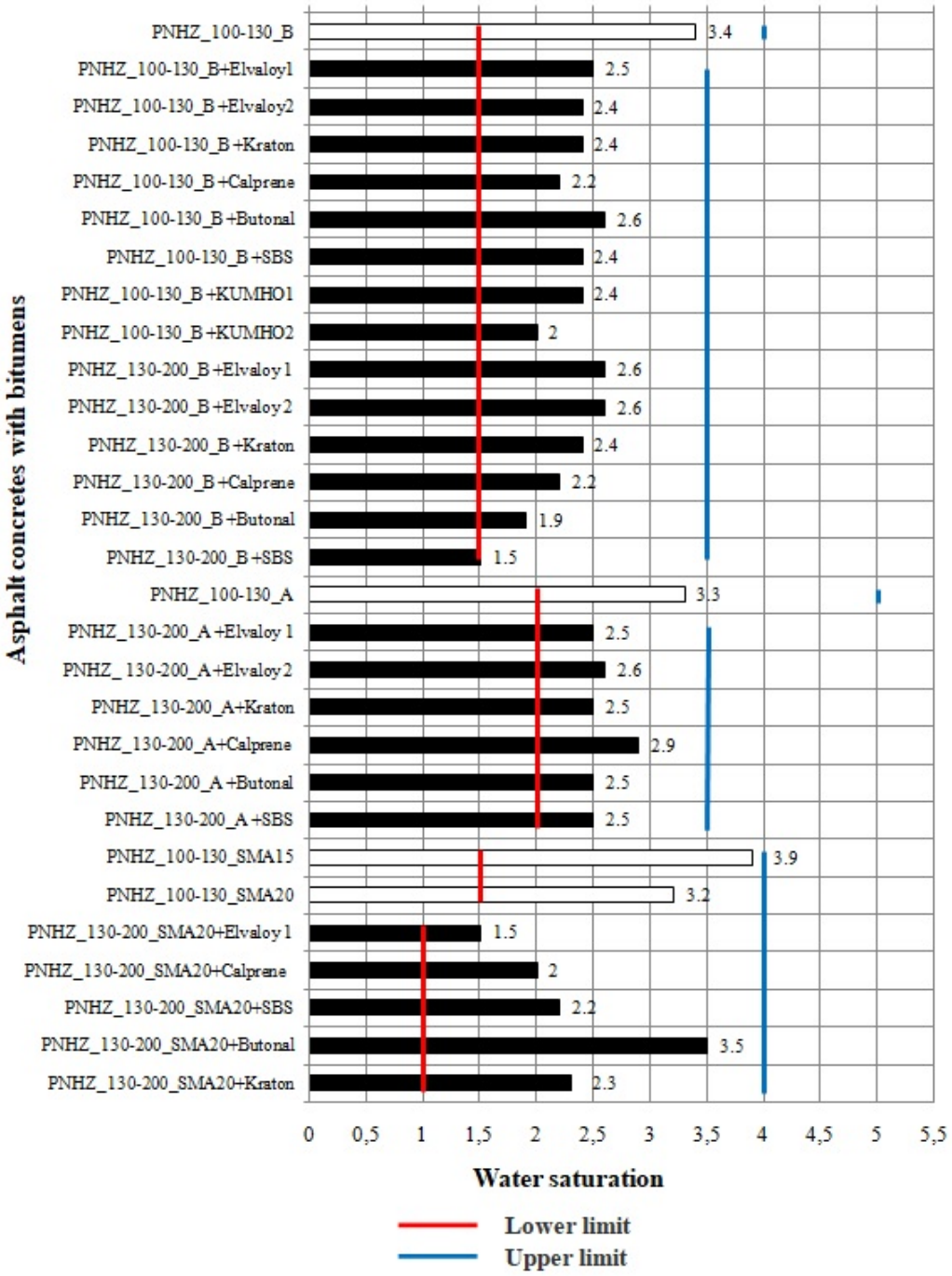

Figure 4 – Water saturation of the asphalt concretes

Conclusion. Based on the results of the comparative analysis for the main standard indicators of the tested asphalt concretes and polymer asphalt concretes one can draw the following conclusions:

1. The modification of the bitumens with the polymers increases essentially the main standard indicators of the asphalt concretes: rutting resistance, strength at high and low temperatures, resistance to cyclic freezing and thawing (frost resistance).

2. The reactive polymers Elvaloy 4170 and Elvaloy AM are the most efficient among the used ones.

М. Ж. Жұрынов[1], Б. Б. Телтаев[2], Е. Д. Әмірбаев[2]

[1]«Д. В. Сокольский атындағы жанармай, катализ және электрохимия институты» АҚ, Алматы, Қазақстан;
[2]«Қазақстан жол ғылыми-зерттеу институты» АҚ, Алматы, Қазақстан,

ПОЛИМЕРАСФАЛЬТОБЕТОНДАРДЫҢ НЕГІЗГІ СТАНДАРТТЫҚ КӨРСЕТКІШТЕРІ

Аннотация. Бұл жұмыста 2 маркалы таза битум және полимербитумдардың 7 түрін қолдана отырып дайындалған асфальтбетондар мен полимерасфальтобетондардың 29 түрінің негізгі стандарттық көрсеткіштері анықталды және салыстырмалы түрде талданды. Асфальтбетондар, полимербитумдар және полимерасфальтбетондарды дайындау үшін Павлодар мұнай-химия зауытында (ПМХЗ) өндірілген МЖБ 100/130 және МЖБ 130/200 маркалы битумдар таңдалды. Таңдалған битумдардың сапа көрсеткіштері ҚР СТ 1373-2013 стандартының талаптарын қанағаттандырады. Битумды модификациялау үшін полимерлердің 7 түрі таңдалды (Elvaloy 4170, Elvaloy AM, Kraton D 1192A, Calprene 501, SBS L 30-01 A, KUMHO KTR, Butonal NS 198). Зертханалық жағдайда полимербитумдарды дайындаудың қысқаша әдістемесі келтірілген. Аталған битумдар мен полимербитумдарды қолдану арқылы асфальтбетон мен полимерасфальтобетонның 29 түрі (А типті асфальтбетон - 7, Б типті асфальтбетон - 15, шағыл тасты мастикалық асфальтбетон ШМА-15 - 1, шағыл тасты мастикалық асфальтбетон ШМА-20 - 6) дайындалды. Асфальтбетондар мен полимерасфальтобетондар сапасының көрсеткіштері ҚР СТ 1225-2019, ҚР СТ 1223-2019, МЕМСТ 31015-2002, ҚР СТ 2373-2019 стандарттарының талаптарын қанағаттандырады.

Тиісті зертханалық қондырғыларда сынау арқылы асфальтбетондар мен полимерасфальтобетондар сапасының мынадай негізгі көрсеткіштері анықталды: 1) 60 °С температурада доңғалақтың 10 000 рет жүріп өтуінен кейін пайда болған сораптың тереңдігі (ҚР СТ EN 12697-22-2012); 2) -30 °С температурада созылудағы беріктік (pr. EN 12697-46-2012); 3) 50 °С температурада сығудағы беріктік (ҚР СТ 1218-2003); 4) сумен қанығу (ҚР СТ 1218-2003).

Битумдарды полимерлермен модификациялау асфальтбетондардың негізгі стандарттық көрсеткіштерін едәуір арттыратыны анықталды: сораптарға төзімділік, жоғары және төмен температуралардағы беріктік, циклдік тоңу және еруге төзімділік (аязға төзімділік). Пайдаланылғандардың ішінде ең тиімдісі - Elvaloy 4170 және Elvaloy AM реактивтік полимерлері.

Түйін сөздер: Битумдар, полимерлер, асфальтобетондар, полимерасфальтобетондар, стандарттық көрсеткіштер.

М. Ж. Журинов[1], Б. Б. Телтаев[2], Е. Д. Амирбаев[2]

[1]“Институт топлива, катализа и электрохимии им. Д. В. Сокольского”, Алматы, Казахстан;
[2]“Казахстанский дорожный научно-исследовательский институт”, Алматы, Казахстан

ОСНОВНЫЕ СТАНДАРТНЫЕ ПОКАЗАТЕЛИ ПОЛИМЕРАСФАЛЬТОБЕТОНОВ

Аннотация. В настоящей работе определены и сравнительно проанализированы основные стандартные показатели 29-и видов асфальтобетонов и полимерасфальтобетонов, приготовленных с применением чистых битумов 2-х марок и 7-и видов полимербитумов. Для приготовления асфальтобетонов, полимербитумов и полимерасфальтобетонов были выбраны битумы марок БНД 100/130 и БНД 130/200, произведенные Павлодарским нефтехимическим заводом (ПНХЗ). Показатели качества выбранных битумов удовлетворяют требованиям стандарта СТ РК 1373-2013. Для модифицирования битумов были выбраны 7 видов полимеров (Elvaloy 4170, Elvaloy AM, Kraton D 1192A, Calprene 501, SBS L 30-01 A, KUMHO KTR, Butonal NS 198). Изложена краткая методика приготовления полимербитумов в лабораторных условиях. С применением указанных битумов и полимербитумов было приготовлено 29 видов асфальтобетона и полимерасфальтобетона (асфальтобетон типа А – 7, асфальтобетон типа Б – 15, щебеночно-мастичный асфальтобетон ЩМА-15 – 1, щебеночно-мастичный асфальтобетон ЩМА-20 – 6). Показатели качества асфальтобетонов и полимерасфальтобетонов удовлетворяют требованиям стандартов СТ РК СТ РК 1225-2019, СТ РК 1223-2019, ГОСТ 31015-2002, СТ РК 2373-2019.

Путем испытания в соответствующих лабораторных установках были определены следующие основные показатели качества асфальтобетонов и полимерасфальтобетонов: 1) глубина колеи при температуре 60 °С после 10 000 проходов колеса (СТ РК EN 12697-22-2012); 2) прочность при растяжении при температуре -30 °С (pr. EN 12697-46-2012); 3) прочность при сжатии при температуре 50 °С (СТ РК 1218-2003); 4) водонасыщение (СТ РК 1218-2003).

Установлено, что модификация битумов полимерами существенно повышает основные стандартные показатели асфальтобетонов: колееустойчивость, прочность при высоких и низких температурах, устойчивость к циклическим замораживаниям и оттаиваниям (морозостойкость). Среди использованных наиболее эффективными являются реактивные полимеры Elvaloy 4170 и Elvaloy AM.

Ключевые слова: битумы, полимеры, асфальтобетоны, полимерасфальтобетоны, стандартные показатели.

Information about authors:

Zhurinov M.Zh., Doctor of Chemical Sciences, Professor, Academician, President of NAS RK; nanrk.mzh@mail.ru, https://orcid.org/0000-0001-5314-1219

Teltayev B.B., Doctor of Technical Sciences, Corresponding Member of NAS RK, Professor, President of JSC "Kazakhstan Highway Research Institute"; bagdatbt@yahoo.com, https://orcid.org/0000-0002-8463-9965

Amirbayev Ye.D.,Chief of Road Construction Materials Division of JSC "Kazakhstan Highway Research Institute"; https://orcid.otg/0000-0001-8508-8803

REFERENCES

[1] ST RK 1373-2013. Bitumens and bituminous binders. Oil road viscous bitumens. Technical specifications. Astana, 2013.

[2] ST RK 1225-2019. Road airfield asphalt concrete mixes and asphalt concrete. Technical specifications. Astana, 2019.

[3] ST RK 2534-2014. Bitumens and bituminous binders. Oil road modified bitumens. Technical specifications. Astana, 2014.

[4] ST RK 1223-2019. Road airfield polymer asphalt concrete mixes and polymer asphalt concrete. Technical specifications. Astana, 2019.

[5] GOST 31015-2002. Asphalt concrete mixes and stone mastic asphalt concrete. Technical specifications. M., 2002.

[6] ST RK 2373-2019. Airfield stone mastic polymer asphalt concrete mixes and stone mastic polymer asphalt concrete. Technical specifications. Astana, 2019.

[7] ST RK EN 12697-22-2012. Bitumen mixes. Test method for hot asphalt concrete mixes. Part 22. Determination of forming rut depth on asphalt concrete samples. Astana, 2012.

[8] pr. EN 12697-46-2012. Asphalt concrete mixes. Test method for hot asphalt concrete mixes. Part 46: Determination of low temperature cracking and properties by uniaxial tension tests. Astana, 2012.

[9] ST RK 1218-2003. Materials on the basis of organic binders for road and airfield construction. Test methods. Astana, 2003.

МАЗМҰНЫ – СОДЕРЖАНИЕ – CONTENTS

Publication Ethics and Publication Malpractice
in the journals of the National Academy of Sciences of the Republic of Kazakhstan

For information on Ethics in publishing and Ethical guidelines for journal publication see http://www.elsevier.com/publishingethics and http://www.elsevier.com/journal-authors/ethics.

Submission of an article to the National Academy of Sciences of the Republic of Kazakhstan implies that the described work has not been published previously (except in the form of an abstract or as part of a published lecture or academic thesis or as an electronic preprint, see http://www.elsevier.com/postingpolicy), that it is not under consideration for publication elsewhere, that its publication is approved by all authors and tacitly or explicitly by the responsible authorities where the work was carried out, and that, if accepted, it will not be published elsewhere in the same form, in English or in any other language, including electronically without the written consent of the copyright-holder. In particular, translations into English of papers already published in another language are not accepted.

No other forms of scientific misconduct are allowed, such as plagiarism, falsification, fraudulent data, incorrect interpretation of other works, incorrect citations, etc. The National Academy of Sciences of the Republic of Kazakhstan follows the Code of Conduct of the Committee on Publication Ethics (COPE), and follows the COPE Flowcharts for Resolving Cases of Suspected Misconduct (http://publicationethics.org/files/u2/New_Code.pdf). To verify originality, your article may be checked by the Cross Check originality detection service http://www.elsevier.com/editors/plagdetect.

The authors are obliged to participate in peer review process and be ready to provide corrections, clarifications, retractions and apologies when needed. All authors of a paper should have significantly contributed to the research.

The reviewers should provide objective judgments and should point out relevant published works which are not yet cited. Reviewed articles should be treated confidentially. The reviewers will be chosen in such a way that there is no conflict of interests with respect to the research, the authors and/or the research funders.

The editors have complete responsibility and authority to reject or accept a paper, and they will only accept a paper when reasonably certain. They will preserve anonymity of reviewers and promote publication of corrections, clarifications, retractions and apologies when needed. The acceptance of a paper automatically implies the copyright transfer to the National Academy of Sciences of the Republic of Kazakhstan.

The Editorial Board of the National Academy of Sciences of the Republic of Kazakhstan will monitor and safeguard publishing ethics.

Правила оформления статьи для публикации в журнале смотреть на сайте:

www:nauka-nanrk.kz

ISSN 2518-170X (Online), ISSN 2224-5278 (Print)

http://www.geolog-technical.kz/index.php/en/

Редакторы *М. С. Ахметова, Д. С. Аленов, А. Ахметова*
Верстка *Д. А. Абдрахимовой*

Подписано в печать 01.02.2021.
Формат 70x881/8. Бумага офсетная. Печать – ризограф.
12,75 п.л. Тираж 300. Заказ 1.

Национальная академия наук РК
050010, Алматы, ул. Шевченко 28, т. 272-13-19, 272-13-18